



UNIVERSITY OF  
BIRMINGHAM

# **The role of NM23-H1/H2 proteins in diffuse large B-cell lymphoma**

By

**Maiss Kasem Al-Amere**

A thesis submitted to the  
University of Birmingham  
For the degree of  
DOCTOR OF PHILOSOPHY

School of Biosciences  
College of Life and Environmental Sciences  
University of Birmingham  
June 2019

UNIVERSITY OF  
BIRMINGHAM

**University of Birmingham Research Archive**

**e-theses repository**

This unpublished thesis/dissertation is copyright of the author and/or third parties. The intellectual property rights of the author or third parties in respect of this work are as defined by The Copyright Designs and Patents Act 1988 or as modified by any successor legislation.

Any use made of information contained in this thesis/dissertation must be in accordance with that legislation and must be properly acknowledged. Further distribution or reproduction in any format is prohibited without the permission of the copyright holder.

## **Abstract**

There is increasing evidence that NM23-H1 plays important roles in normal cell development, differentiation and in cancer progression. It was found in previous studies that high expression of NM23-H1 protein is associated with poor prognosis and worse outcomes in diffuse large B-cell lymphoma (DLBCL). One possible approach is to study the role of NM23-H1 in DLBCL is to use cell line models.

The expression of NM23-H1 and related NM23-H2 was investigated in a panel of DLBCL cell lines (Farage, HT, U2932, SUDHL4, SUDHL5, SUDHL6, OCILY1, OCILY3 and OCILY7) by Western blotting and quantitative RT-PCR. These approaches confirmed high expression of NM23-H1 and -H2 indicating that DLBCL cell lines are appropriate models to investigate the role of these proteins in DLBCL. Western blotting identified for the first time that DLBCL cells release NM23-H1 into their extracellular environment whilst NM23-H2 is not released. In contrast KG1a acute myeloid leukaemia cells did not secrete NM23-H1. To investigate possible autocrine signalling by NM23-H1, DLBCL cell lines were tested for endogenous binding of NM23-H1 and binding of exogenously added fluorescently labelled NM23-H1. Neither approach suggested strong binding by DLBCL cells. Together these results supported the hypothesis that the elevated NM23-H1 serum levels detected in DLBCL patients is derived, at least partially, from tumour cell clone and that NM23-H1 protein is secreted from DLBCL cells not to act on tumour clone directly but by acting upon other cells in the host and tumour microenvironment.

The CRISPR/Cas9 approach was used to generate NM23-H1 KO clones of the HT DLBCL cell line. HT NM23-H1 KO cells grew normally and maintained high viability when cultured in either normoxic or hypoxic conditions. Furthermore, their growth and viability was not altered when provided with recombinant NM23-H1. These findings indicated that NM23-H1 is not crucial for DLBCL cell survival and that the impact of NM23-H1 on DLBCL prognosis is most likely mediated via an extrinsic cellular mechanism affecting the tumour microenvironment.

Our lab has previously identified that monocytes stained positively when exposed to exogenous recombinant NM23-H1. Given the relationships between monocytes/macrophage infiltration in lymph nodes and monocytes/lymphocytes ratios on

patients' outcomes in DLBCL this study focused on a possible interaction of DLBCL cells with monocytes via the release of NM23-H1. HT NM23-H1 knockout cells were acclimatised to serum free culture and co-cultured with peripheral blood monocytes from normal donors purified by negative selection. Monocytes survived poorly as monocultures in serum free cultures but their survival was very much enhanced in the presence of HT WT and HT NM23-H1 KO cells and also WT and NM23-H1 KO KG1a cells. The levels of 27 cytokines were measured in the supernatants of co-cultures via Luminex multiplex technology. Whilst many cytokines showed no variation in levels, IL-1 $\beta$ , IL-6, IL-8, MIP-1 $\alpha$  and MIP-1 $\beta$  were elevated in co-cultures of WT HT cells and monocytes compared to HT KO cells, KG1a WT or KO cells. Elevated secretion of these cytokines did not require cell-cell contact between HT cells and monocytes. The commonality between HT KO, KG1a WT and KG1a KO cells is that unlike HT WT cells they do not secrete NM23-H1. Thus it is possible that secreted NM23-H1 drove the elevated secretion of IL-1 $\beta$ , IL-6, IL-8, MIP-1 $\alpha$  and MIP-1 $\beta$ . To test this recombinant Nm23-H1 was added HT KO cell/monocyte co-cultures. Addition of NM23-H1 enhanced the secretion of IL-6 and IL-1 $\beta$  and to a lesser degree IL-8. However, the addition of recombinant NM23-H1 had a negligible effect on MIP-1 $\beta$  and MIP-1 $\alpha$ . In summary the experiments provided here demonstrate the mechanistic relationship between elevated serum NM23-H1 in DLBCL patients and provide evidence that the prognostic relationship relates to modification of the cytokine milieu via released NM23-H1 interaction with other cells including monocyte/macrophages.

## **Acknowledgment**

First of all, I would like to thank Dr. Farhat Khanim for her amazing support throughout this PhD. She has helped me to become a much better researcher and scientist. Her enthusiasm and hard work are inspiration to me and everyone in our laboratory. Thank you for being an awesome, unique supervisor in laboratory and life. Thank you for the cake, chocolate lovely presents and surprises. You made my day at many occasions. Thank you for every single hug, for being a good friend and even a mom many times, despite being only a few years older than me. Thank you for your everyday magic words: Focus, listen and think!! I am also very thankful to my second supervisor Prof Chris Bunce for the support, help, advice, understanding nice notes and comments. I will keep your nice words till the rest of my life. Other than smiling flowers in our office every morning, special thanks for them. They are really amazing. Thank you both my wonderful supervisors for giving me the chance to be a member of the FK and CB group, suggesting an extremely impressive project, your enthusiasm and belief that I could do it, without you both nothing could happen. Big thank you to my awesome internal examiner, ever smiling, Dr. Melissa Grant, you are my PhD sunshine and my idol. The words cannot express your impressive role during my long journey. You were always the shiny light source in my PhD. I would like to thank everyone at FK and CB Lab who helped during my research, in particular the very nice previous and current postdocs, Sandro, Anna Maria, Yao, Shazia and Christina. They showed great support and patience in helping me day by day to get through this PhD. We are all trying very hard to provide a better life for patients with hematological malignancies. Thank you to all of my lovely friends at the 8th floor, Diaa, Sue, Noor, Israa, Elis, Zuhail, Bader, Connie, Rhian, Varvara, Angelos, Sanjana, Justina and Ally for being super lovely and life time friends. I would like to thank my funding sources Iraqi ministry of Higher Education and Scientific Research, without whom I would have been unable to achieve this research. I would like to thank Prof Mark Dryson, Dr. Ilaria and Recce in the Institute of Immunology and Immunotherapy who have been supportive throughout my project. I would like to thank my brilliant husband Atheer (MTC), my two lovely boys Ahmed (Dode) and Mustafa (Tofe) who have put up with a lot over the last five years. Their understanding in allowing me to spend long hours away from them being a student again has meant huge sacrifices on their behalf and I will forever be appreciative and thankful in every way to them, especially to you Atheer, my soulmate, you are the centre of my world, the inspiration behind my passion, and the reason I strive to be a better woman, mum, scientist and Maiss!!! A big thanks from Birmingham to Bagdad for my happiness reason and my soulmates, my lovely, nice,

amazing and kind family especially Dad and Mom who taught me that the price of success is first of all believe in Allah and keep asking for his support, then dedication, hard work and unremitting devotion to the things you want to see them happen. To my handsome and awesome brothers Ali, Mohammed, Amro and my wonderful gorgeous sister and daughter at the same time Raneem. My nice sisters in law, Abeer and Aseel. Thank you my brilliant friends without your lovely words and continues support nothing could happen: Nada, Janna, Abeer, Hala and Dina. You always believe that I could do it. Love you all more than the words can say. Thank you to all, whom I loved, with your lovely presence I am happy every day and forever.

*Maiss*

# Table of Contents

<b>1</b>	<b>General Introduction .....</b>	<b>1</b>
1.1	Blood components.....	1
1.2	Immune system.....	4
1.2.1	The innate immune system .....	4
1.2.2	The adaptive immune system .....	5
1.2.3	T cell development .....	6
1.2.4	Normal B-cell development.....	9
1.3	Lymphomas.....	12
1.3.1	Hodgkin's lymphoma (HL) .....	12
1.3.2	Non-Hodgkin's lymphoma (NHL).....	13
1.4	Diffuse Large B-Cell Lymphoma (DLBCL) .....	14
1.4.1	Molecular classification of DLBCL.....	16
1.4.2	DLBCL treatment.....	19
1.4.2.1	Standard therapies in DLBCL.....	19
1.4.2.2	Novel therapies in DLBCL.....	20
1.4.3	Tumour infiltrating Lymphocytes (TIL) .....	21
1.5	The NM23 protein family.....	23
1.5.1	Structure and classification .....	23
1.5.2	NM23 potential function in normal development.....	24
1.5.3	The biochemical activity of NM23.....	25
1.5.4	NM23-H1 in haemopoiesis .....	25
1.5.5	NM23 proteins in cancer .....	27
1.5.6	NM23-H1 in haematological malignancies.....	28
1.5.6.1	NM23-H1 in AML .....	28
1.5.6.2	NM23-H1 in DLBCL.....	29
<b>2</b>	<b>Materials and methods.....</b>	<b>34</b>
2.1	Cell Culture.....	34
2.1.1	Maintenance of cell lines.....	34
2.1.2	Serum-free (ITS+) cultures of DLBCL cell lines.....	34
2.1.3	Long-term storage of cells in liquid nitrogen .....	36

2.1.4	Recovery of cell lines from liquid nitrogen.....	36
2.1.5	Purification of normal donor peripheral blood mononuclear cells (PBMCs).....	36
2.1.6	Magnetic sorting of cells .....	37
2.1.7	Maintenance and treatment of CD40L expressing L3-L cells.....	38
2.1.8	Mitomycin C treatment of CD40L-L cells.....	38
2.1.9	Expansion of CD19+ B cells on CD40L-L cells.....	38
2.1.10	Preparing conditioned media (CM) from DLBCL cell lines .....	39
2.1.11	Culturing normal donor cells in Conditioned media (CM) .....	39
2.1.12	Co-Culture of normal donor monocytes with HT/KG1a cells.....	39
2.1.13	Culturing of normal donor monocytes with HT/KG1a cells in transwell.....	39
2.2	Flow cytometry assays .....	40
2.2.1	Cell surface staining and flow cytometry for immunophenotyping .....	40
2.2.2	Direct staining and flow cytometry for surface bound Nm23-H1 staining .....	41
2.2.3	Flow cytometry for detecting intracellular NM23-H1 protein.....	42
2.2.4	Measuring cell counts using flow cytometry.....	42
2.3	Protein Analysis.....	44
2.3.1	Recombinant NM23-H1 (rNM23-H1) production .....	44
2.3.1.1	pET-15b-NM23-H1 vector construct.....	44
2.3.1.2	Transformation of BL21 (DE3) E.coli bacterial cells.....	45
2.3.1.3	Purification of recombinant NM23-H1 protein .....	45
2.3.1.4	Determination of rNm23-H1 concentration.....	46
2.3.2	Analysis of DLBCL extracellular NM23-H1 protein .....	46
2.3.3	DLBCL protein sample preparation .....	47
2.3.4	Protein determination .....	47
2.3.5	Protein sample preparation for western blotting .....	47
2.3.6	Sodium dodecyl sulphate –polyacrylamide gel electrophoresis (SDS-PAGE) ....	48
2.3.7	Semi-dry protein transfer .....	48
2.3.8	Immunodetection of proteins .....	48
2.3.9	Coomassie blue staining.....	49
2.4	Quantitative real-time polymerase chain reaction (QRT-PCR).....	50
2.4.1	RNA extraction.....	50
2.4.2	Reverse transcription. ....	50



2.4.3	$\beta$ -actin PCR.....	51
2.4.4	QRT-PCR for NM23-H1 .....	52
2.4.5	QRT-PCR data analysis .....	52
2.5	CRISPR/Cas9 knock out (KO) of NM23-H1 in DLBCL cells .....	53
2.5.1	CRISPR Overview .....	53
2.5.2	sgRNA primer design .....	53
2.5.3	Plasmid DNA preparation (Miniprep).....	54
2.5.4	Annealing and dephosphorylation reaction.....	56
2.5.5	Restriction digest of pSpCas9(BB)-2A-Puro .....	56
2.5.6	Ligation reactions and bacterial transformations .....	57
2.5.7	Selection of positive colonies .....	57
2.5.8	Large-scale plasmid DNA preparation (Maxipreps) .....	57
2.6	Transfection and clonal selection of DLBCL cell lines .....	58
2.6.1	Determination of Puromycin sensitivity of DLBCL cell lines.....	58
2.6.2	Optimisation and electroporation of DLBCL cell lines.....	59
2.6.3	Puromycin enrichment of transfected cells .....	59
2.6.4	Clonal Selection and expansion of NM23-H1 knockout (KO) cells.....	60
2.6.5	Screening of clones for knockout of NM23-H1 .....	60
2.7	Genomic analysis of NM23-H1 KO HT cells .....	60
2.8	Nested PCR AMPLIFICATION of the NME1 gene locus .....	61
2.9	Analysis of cytokines in conditioned media.....	63
2.9.1	Harvesting conditioned media for cytokine analysis .....	63
2.9.2	BioPlex 27-plex cytokine assay .....	63
2.10	Statistical Analyses.....	65
<b>3</b>	<b>Intracellular and extracellular detection of NM23-H1/H2 in DLBCL .....</b>	<b>66</b>
3.1	<i>NME1</i> expression in DLBCL cell lines .....	66
3.2	Intracellular NM23-H1 and NM23-H2 expression in human DLBCL cell lines. ....	67
3.3	Intracellular NM23-H1/H2 expression in human DLBCL cell lines in comparison to LCL cell lines and B-cells.....	69
3.4	Analysis Intracellular NM23-H1 expression in human DLBCL cell lines by flow cytometry.....	71
3.5	Extracellular expression of NM23-H1/NM23-H2 in human DLBCL cell lines.....	73

3.6	Detection of extracellular NM23-H1/NM23-H2 in LCLs and healthy donor CD19+ B-cells. ....	75
3.7	Human DLBCL cell lines binding status to recombinant NM23-H1 fluorescently labelled using Alexa 647 .....	75
3.8	Summary .....	78
<b>4</b>	<b>Generation and characterisation of NM23-H1 CRISPR Knock-Out Cell Lines.....</b>	<b>79</b>
4.1	CRISPR gene editing .....	79
4.2	Cloning NME1 sgRNA primers into the CRISPR-Cas9 expression vector .....	81
4.3	Puromycin dose response .....	81
4.4	Determination of transfection efficiency. ....	83
4.5	Generation of NM23-H1 KO clones .....	84
4.6	Intracellular expression of NM23-H2 is maintained in NM23-H1-KO clones. ....	86
4.7	Sequencing of NM23-H1-KO clones.....	87
4.8	Growth rate of HT WT and HT NM23-KO clones .....	89
4.9	Investigation of the effect of hypoxia vs normoxia on proliferation of HT WT, HT NM23-KO and KG1a cells .....	90
4.10	Summary .....	94
<b>5</b>	<b>DLBCL influence cytokine secretion by monocytes via release of NM23-H1 .....</b>	<b>95</b>
5.1	NM23-H1 intracellular expression in DLBCL cell lines acclimatised to growth in serum free cultures.....	95
5.2	NM23-H1 extracellular expression in DLBCL cell lines acclimatised to growth in serum free cultures.....	96
5.3	QRT-PCR analysis of <i>NME1</i> expression in ITS+ maintained HT WT and NM23-H1 KO clones (ITS+) versus HT WT and NM23-KO growing in complete media.....	98
5.4	Response of peripheral blood mononuclear cells to extracellular NM23-H1 and recombinant NM23-H1. ....	98
5.5	Characterising viable PBMCs sup-populations by Immunophenotyping. ....	101
5.6	Measuring the impact of conditioned media on T-cells (CD3 positive cells) .....	101
5.7	T-cell subsets response to extracellular NM23-H and exogenous recombinant NM23-H1.....	102

5.8	Monocyte response to extracellular NM23-H and exogenous recombinant NM23-H1 .....	104
5.9	Response of B-cells to extracellular NM23-H and exogenous recombinant NM23-H1. ....	105
5.10	Immunophenotyping and purification assessment of monocyte fractions negatively selected from normal donor PBMCs. ....	107
5.11	Exogenous recombinant NM23-H1 promotes CD14+ monocyte survival.....	108
5.12	Exogenous recombinant NM23-H1 enhances the survival of KG1a cells in serum-free media.....	113
5.13	Cultures treated with recombinant NM23-H1 displayed adherent cell clusters ....	116
5.14	Monocytes respond to extracellular NM23-H1 and recombinant NM23-H1 in the presence or absence of cell to cell interaction .....	118
5.15	CD14+ monocytes from normal donors do not require direct cell to cell contact for improved survival in co-cultures.....	119
5.16	Addition of exogenous rNM23-H1 promotes survival of CD14+ monocytes in transwell culture conditions. ....	120
5.17	Co-culture of monocytes with HT WT and HT KO cells differentially stimulates the production of certain pro-inflammatory cytokines .....	122
5.18	KG1a WT cells do not recapitulate the effect of HT WT cells in co-culture with monocytes on pro-inflammatory cytokines. ....	125
5.19	Exogenously added recombinant NM23-H1 promotes the induction of some pro-inflammatory cytokines .....	128
5.21	Summary.....	132
<b>6</b>	<b>General discussion.....</b>	<b>133</b>
	<b>Future work .....</b>	<b>140</b>
	<b>References .....</b>	<b>141</b>
	Appendix A: Recipes and buffers.....	154
	Appendix B: Supplementary figures .....	158
	Appendix C: Publications .....	163

## List of Figures

Figure 1.1 Haematopoiesis model	3
Figure 1.2 Overview of human T-cell development	6
Figure 1.3 T cell and APC interactions	7
Figure 1.4 T cell lineage specification	8
Figure 1.5 Summary of B cell development	9
Figure 1.6 Basic immunoglobulin structure	10
Figure 1.7 Characteristic immunophenotype markers of B-cell malignancies	12
Figure 1.8 Cytomorphological features of four types of DLBCL	15
Figure 1.9 Key oncogenic pathways in DLBCL	18
Figure 1.10 Nm23-H1 promotes the AML blasts survival of through an indirect mechanism	29
Figure 1.11 Serum NM23-H1 and DLBCL survival	30
Figure 1.12 Serum NM23-H1 and survival in DLBCL	30
Figure 1.13 Surface NM23-H1 expression and correlation with poorer survival in aggressive lymphomas	31
Figure 1.14 Cytoplasmic NM23-H1 levels and DLBCL prognosis	32
Figure 2.1 pET15b expression vector	44
Figure 2.2 Schematic of the RNA-guided Cas9 nuclease	53
Figure 2.3 CRISPR/Cas9 vector pSpCas9(BB)-2A-Puro(PX459) V2.0	55
Figure 3.1 NME1 mRNA expression in DLBCL cell lines	67
Figure 3.2 Analysis of NM23-H1 and NM23-H2 protein expression in DLBCL cell lines	68

Figure 3.3 Analysis of NM23-H2 and NM23-H1 protein expression in DLBCL cell lines, LCLs and normal donor CD19+ B-cells	70
Figure 3.4 Intracellular Nm23-H1 expression in DLBCL and KG1a	72
Figure 3.5 Analysis of extracellular NM23-H1 and NM23-H2 protein expression in cultures of DLBCL cell lines	74
Figure 3.6 Analysis of extracellular NM23-H1 and NM23-H2 protein expression in HT cell line, LCL and normal donor CD19+ B-cells	75
Figure 3.7 rNM23-H1- Alexa 647 differentially binds DLBCL cell lines and KG1a	77
Figure 4.1 NME1 gene structure and transcript variants	80
Figure 4.2 Experimental overview of CRISPR-Cas9-mediated NME1 Knock out plasmid construction	82
Figure 4.3 Puromycin dose responses of DLBCL cell lines	83
Figure 4.4 Determination of transfection efficiency	84
Figure 4.5 Generation of Nm23-H1 Knockout (KO) clones	86
Figure 4.6 Nm23-H1 intracellular expression in exponentially growing Nm23-H1-KO clones	87
Figure 4.7 Sequencing of NM23-H1 knockout clone 1 (KO1)	88
Figure 4.8 Sequencing of NM23-H1-KO clones KO2, KO3 and KO4	89
Figure 4.9 Growth rate of HT WT and HT NM23-KO clones	90
Figure 4.10 Hypoxia vs normoxia effect on cell viability	90
Figure 4.11 Cell growth rate for HT cell line in normoxic and hypoxic conditions	92
Figure 4.12 Hypoxia vs normoxia effect on cell growth rate for KG1a cell line	93
Figure 5.1 comparison of NM23-H1 intracellular expression in cell lines cultured in	96

media containing FBS and ITS+

Figure 5.2 NM23-H1 extracellular expression in serum free acclimatised DLBCL cell lines	97
Figure 5.3 NME1 mRNA expression in HT WT and NM23-KO clones grown in FBS and serum-free (ITS+) conditions	98
Figure 5.4 Response of normal donor PBMCs to conditioned media and rNM23-H1	100
Figure 5.5 Determination of T-cells (CD3+ cells) within primary blood samples	101
Figure 5.6 T-cell subsets response to extracellular NM23-H and exogenous rNM23-H1	103
Figure 5.7 Response of CD14+ monocytes to extracellular NM23-H1 and exogenous rNM23-H1	104
Figure 5.8 Proportions of viable B-cells (CD19+) in response to extracellular NM23-H1 and rNM23-H1	106
Figure 5.9 Monocyte immunophenotyping	108
Figure 5.10 Exogenous NM23-H1 and rNM23-H1 enhances monocytes differentiation and supports the survival of CD11b+, CD14+ and CD11b+CD14+ cells	110
Figure 5.11 CD14+ monocyte cell numbers increase marginally in serum-free media when supplemented with rNM23-H1	111
Figure 5.12 CD14+ monocyte survive better in co-culture	111
Figure 5.13 Survival of CD14+ monocytes grown in co-culture with HT WT and NM23-H1 KO cells	112
Figure 5.14 Survival index for CD14+ monocytes co-cultured with KG1a WT and NM23-H1 KO clone	113
Figure 5.15A Exogenous rNM23-H1 supports the survival of KG1a not HT cells in	114

serum-free media	
Figure 5.15B Exogenous rNM23-H1 supports the survival of KG1a not HT cells in serum-free media	115
Figure 5.16 Cell micrograph of WT and Nm23-KO cells for both HT (Secreted NM23-H1) and KG1a (Non-Secreted NM23-H1)	116
Figure 5.17 Cell population were consistently more adherent and clustered in rNM23-H1 treated monocytes and Monocytes + HT WT or HT Nm23-KO co-cultures	117
Figure 5.18 Cell micrographs of rNM23-H1 treated co-cultures at 48hrs in rNM23-H1 treated monocytes and monocytes + HT KG1a or KG1a Nm23-KO co-cultures	118
Figure 5.19 Assessment of HT (WT and Nm23-KO) cells after 48hrs incubation in transwell cell culture	119
Figure 5.20 CD11b+, CD14 and CD11b+ CD14+population response to extracellular NM23-H1	120
Figure 5.21 CD11b+, CD14 and CD11b+ CD14+population response to exogenous rNM23-H1	121
Figure 5.22 Monocyte - HT cell line co-culture stimulates the production of some pro-inflammatory cytokines	123
Figure 5.23 Cytokines not modulated in monocyte co-cultures by knockout of NM23-H1 in HT cells	124
Figure 5.24 Monocyte–KG1a WT cells co-culture do not recapitulate Monocyte–HT WT cells stimulation effect on pro-inflammatory cytokines	126
Figure 5.25 Cytokines not modulated in monocyte co-cultures by knockout of NM23-H1 in KG1a cells.	127

Figure 5.26 Recombinant NM23-H1 protein modulates cytokine expression for some cytokines in co-culture experiments	129
Figure 5.27 Cytokines not modulated in monocyte co-cultures in presence of recombinant NM23-H1 protein	130
Figure 5.28 Cytokines not modulated in monocyte co-cultures in presence of recombinant NM23-H1 protein	131



## List of Tables

Table 1.1 Characteristics and function of the major blood cells	2
Table 1.2 NHL subtypes proportion and expected UK cases per year	14
Table 1.3 Characteristics of Newly Defined DLBCL based on shared genetic aberrancies	17
Table 1.4 Current DLBCL drugs and their functions	20
Table 1.5 NM23 Proteins family classification	24
Table 2.1 Summary of cell lines used in this study	35
Table 2.2 Antibodies used for cell type identification by flow cytometry	41
Table 2.3 Antibodies used for NM23-H1 surface staining of cell lines	42
Table 2.4 of antibodies used in western blotting	49
Table 2.5 Sequence of primers and probes used for NM23-H1 QRT-PCR	52
Table 2.6 sgRNA sequences used for targeting NM23-H1	54
Table 2.7 Primer sequences for nested PCR of the NME gene locus	61
Table 4.1 Selected CRISPR/Cas9 sgRNA designed to target the NME1 gene	80

## Abbreviations

ABC	Activated B cell-like
ALC	Absolute lymphocyte count
AMC	Absolute monocyte count
AML	Acute myeloid leukemia
APC	Antigen presenting cells
ATP	Adenosine triphosphate
AWD	Abnormal wing disks
BL	Burkitt's Lymphoma
BCR	B cell receptor
BSA	Bovine serum albumin
BTK	Bruton's tyrosine kinase
CD	Cluster of differentiation
cDNA	Complementary DNA
CLL	Chronic lymphocytic leukemia
CLP	Common lymphoid progenitor
CM	Conditioned media
CMP	Common myeloid progenitor
CRISPR	Clustered regularly interspaced short palindromic repeats
CRP	C-reactive protein
CTLs	Cytotoxic T-lymphocytes
DCs	Dendritic cells
DLBCL	Diffuse large B-cell lymphoma
DN	Double negative
DNA	Deoxyribonucleic acid
DP	Double positive
EB	Elution buffer
EDTA	Ethylenediaminetetraacetic acid
ErP	Erythrocyte precursor
FACS	Fluorescence activated cell sorting
FBS	Foetal bovine serum
FL	Follicular lymphoma
FSC	Forward scatter
GCB	Germinal centre B cell-like
G-CSF	Granulocyte colony stimulating factor
GEP	Gene expression profiling
GFP	Green fluorescent protein
GM-CSF	Granulocyte monocyte colony stimulating factor
GMP	Granulocyte/macrophage precursor
GTP	Guanosine triphosphate
HL	Hodgkin's lymphoma
HSC	Haematopoietic stem cell
IFN- $\gamma$	Interferon- $\gamma$
Ig	Immunoglobulin

IL	Interleukin
IMDM	Iscoe's modified Dulbecco's medium
IPTG	Isopropyl $\beta$ -D-1-thiogalactopyranoside
ITS	Insulin-Transferrin-Selenium
KO	Knockout
Kpn	killer of prune
LCLs	Lymphoblastoid cell lines
LPS	Lipopolysaccharide
LSC	Leukemic stem cell
LT-HSC	Long term haematopoietic stem cell
LT-SRC	Long term SCID repopulating cell
MACs	Magnetic activated cell sorting
MBL	Mannose binding lectin
MC	Mitomyocin C
MCL	Mantle cell lymphoma
MCP-1	Monocyte chemoattractant protein 1
MEP	Megakaryocyte/erythrocyte precursor
MHC	Major histocompatibility complex
MIP-1	Macrophage inflammatory protein-1
MKP	Megakaryocyte precursor
MM	Master mix
mRNA	Messenger RNA
MZL	Marginal zone lymphoma
NDK	Nucleoside diphosphate kinases
NDPs	Nucleoside diphosphates
NEB	Nuclear extraction buffer
NHE	Non-homologous end joining
NHL	Non-Hodgkin's lymphoma
NK	Natural killer cell
NM23	Non-metastatic 23
NTP	Nucleoside triphosphate
O/N	Overnight
OD	Optical density
OS	Overall survival
PAM	Protospacer adjacent motif
PAMPs	Pathogen-associated molecular patterns
PBMCs	Peripheral blood mononuclear cells
PBS	Phosphate buffered saline
PCR	Polymerase chain reaction
PFS	Progression free survival
PRRs	Pattern recognition receptors
PVDF	Polyvinylidene fluoride
QRT-PCR	Quantitative real time PCR
RBCs	Red blood cells
RIPA	Radioimmunoprecipitation assay buffer
RNA	Ribonucleic acid

RT	Room temperature
SDS	Sodium dodecyl sulphate
SDS-PAGE	Sodium dodecyl sulphate polyacrylamide gel electrophoresis
S.E.M.	Standard error mean
sgRNA	Single guide RNA
SLL	Small lymphocytic lymphoma
SLOs	Secondary lymphoid organs
SOC	Super optimal broth with carbon catabolite repression
SP	Single positive
SSC	Side scatter
STAT	Signal transducer and activator of transcription
ST-HSC	Short term haematopoietic stem cell
ST-SRC	Short term SCID repopulating cell
TBS	Tris-Buffered Saline
TCR	T cell receptor
TGF- $\beta$	Transforming growth factor beta
Th	T helper
TIL	Tumour infiltrating Lymphocytes
TL	T-cell lymphoma
TLRs	Toll-like receptors
TNF- $\alpha$	Tumour necrosis factor-alpha
T-regs	Regulatory T cells
TV	Transcript variant
WBCs	White blood cells
WHO	World health organisation
WT	Wild-type
XLA	X-linked agammaglobulinaemia

**CHAPTER ONE**

**GENERAL**

**INTRODUCTION**

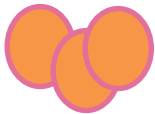


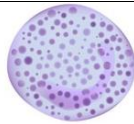
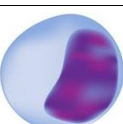

# **1 General Introduction**

## **1.1 Blood components**

Human blood is a body fluid and connective tissue made up of blood cells, platelets and plasma. Plasma contains dissolved protein, carbohydrates, such as glucose, and ions that function together in defence, haemostasis and transport. There are two major blood cell classes, red (erythrocytes) and white (leukocytes) blood cells.

Red blood cells (RBCs), described in Table 1.1, are the most abundant cellular blood component giving blood its characteristic colour. Red cells transport oxygen to the body's tissues and return carbon dioxide to lungs (Delves et al., 2017). Erythrocytes arise from HSCs by a process termed erythropoiesis. Via a process of progressive lineage restriction, progenitor cells become committed to the erythroid lineage and develop into erythroblasts (the earliest cell identifiable by its morphology to be committed to erythroid differentiation) that differentiate into reticulocytes, then into mature RBCs before being released into blood circulation.

The white blood cells (WBCs) have five major subtypes as described in Table 1.1 and function in immune responses and fighting infection. Leukocytes reside not only in blood stream, but are also present in lymphatic and interstitial fluids (Mackay et al., 2000). All blood cells are derived from a common pool of multipotent haematopoietic stem cells (HSCs) (Figure 1.1) (Reece et al., 2011).

	Cell subtype		Cell number per $\mu\text{l}$ of blood	Description	Function	Half life
Erythrocytes Red blood cells (RBCs)			4.5-6 million	Diameter 7-8 $\mu\text{m}$ , no nuclei, biconcave shape	Transport oxygen and carbon dioxide in the blood	120 days
Leukocytes White blood cells (WBCs)			5000-10000	Densely staining granules, dark stained and nucleus	Defence function	Few hours to years
	Granular Leukocytes(neutrophils, eosinophils and basophils)		1500-9900	Multilobed nucleus	Innate immunity	Few hours to few days
	Neutrophils		3000-7000	Diameter 12-14 $\mu\text{m}$ , multilobed nucleus	Pathogen engulfment by phagocytosis, cytotoxic activity against tumour	8hours to 5days
	Eosinophils		30-350	Diameter 12-15 $\mu\text{m}$ , bilobed nucleus	Phagocytosis and release inflammation mediators	Few minutes to few days
	Basophils		20-50	Diameter 10-14 $\mu\text{m}$ , bilobed nucleus	Releasing heparin and histamine	Few hours to few days
	A granular Leukocytes		1500-4900	Nucleus with simple shape	Body defence	Few hours to years
	Lymphocytes		1500-3000	Diameter 5-17 $\mu\text{m}$ , spherical nucleus	Adaptive and humoral immunity	Few hours to years
	Monocytes		200-900	Diameter 14-24 $\mu\text{m}$ , kidney or U-shaped nucleus	Antigen presenting cells, phagocytosis	Months

**Table 1.1 Characteristics and function of the major blood cells.** The cellular components of human blood are shown. Red blood cells which deliver oxygen to the body and remove carbon dioxide. White blood cells (neutrophils, monocytes, lymphocytes, eosinophils, and basophils) which involved in the immune response, adapted from (Tortora and Nielsen, 1992)

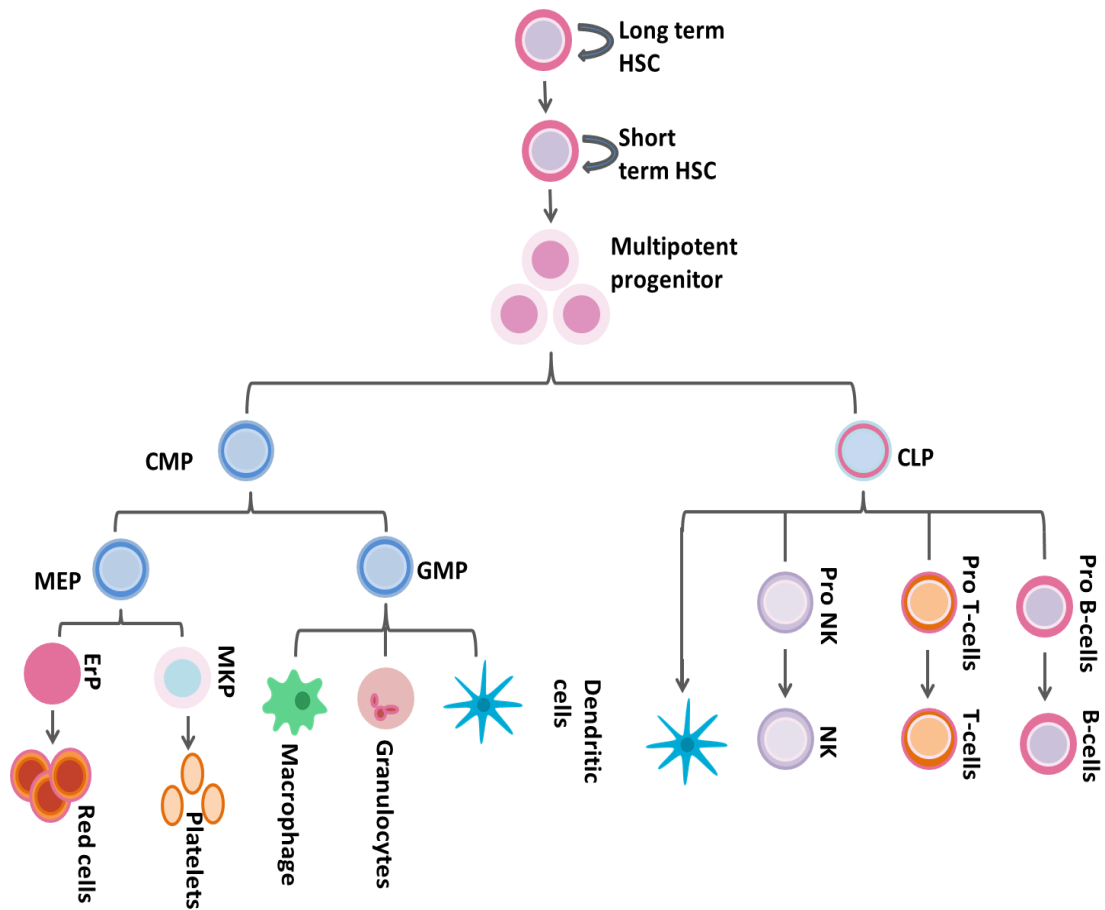


**Figure 1.1 Haematopoiesis model.** The cells with long-term capacity (LT-HSCs) produce short-term capacity (ST-HSCs). ST-HSCs, in turn produce, multipotent progenitors with no self-renewal capacity, but which are highly proliferative. Continuous, further lineages of these cells generate mature blood cells with different shapes and functions. **HSCs** = haematopoietic stem cells, **CLP** = common lymphoid progenitor, **CMP** = common myeloid progenitor, **NK** = natural killer, **GMP** = granulocyte/macrophage precursor, **MEP** = megakaryocyte/erythrocyte precursor, **MKP** = megakaryocyte precursor, **ErP** = erythrocyte precursor. Adapted from (Reya et al., 2001).



## **1.2 Immune system**

The human body coexists in a world filled with infectious organisms. The immune system is a specialised group of cells, tissues and organs that are organised to protect the body against such infections (Mackay et al., 2000). Immune cells are all produced from bone marrow HSCs. Then they either move to secondary lymphoid tissue for extra development or keep circulating in the blood stream or lymph to identify external pathogenic threats, as well as monitoring internal processes e.g. anti-tumour immune responses (Munhoz and Postow, 2016). The immune system cells of vertebrates are composed of the innate and adaptive immune systems (Delves et al., 2017).

### **1.2.1 The innate immune system**

The innate immunity is classified as a first line protection against foreign attacks since it can be initiated without previous exposure to the threat. It includes the orchestrated activities of different cell types and soluble factors. Macrophages, monocytes, granulocytes, natural killer(NK) cells and dendritic cells (DCs) all possess essential roles in innate immunity (Delves et al., 2017). Soluble factors involved in innate responses include acute phase proteins, for example mannose binding lectin (MBL) (Auriti et al., 2017) and C-reactive protein (CRP) (Rao and Gopal, 2015). The cytokines secreted by macrophage (like tumour necrosis factor- $\alpha$  (TNF- $\alpha$ ), Interlukin-1 (IL-1), Interlukin-6 (IL-6)) enhance the secretion of MBL and CRP proteins by hepatocytes. When infectious bacteria and other microorganisms cause infections or penetrate the body's epithelia or mucosa, this activates the innate immune system cellular components which can use their pattern recognition receptors (PRRs) to identify common structures of different pathogens (pathogen-associated molecular patterns (PAMPs)) (Boller and Felix, 2009, Nürnberger and Brunner, 2002). C type lectin receptors and toll-like receptors (TLRs) are important examples of membrane-bound PRRs (Akira and Hemmi, 2003). The recognition of PAMPs by PRRs on phagocytic cells (macrophage, monocytes, neutrophil granulocytes and DCs) initiates the phagocytosis of the PAMP bearing structure (Mackay et al., 2000). These interactions also enhance chemokine and inflammatory cytokine secretion as well as help macrophage and DCs process proteins into peptides which are then presented to major histocompatibility complex (MHC) molecules (Kawai and Akira, 2010). This process initiates an essential cross-talk between the

innate and adaptive immune responses. DCs, cells by their role as antigen presenting cells (APC), contribute professionally in innate and adaptive immunity cross talk (Mackay et al., 2000).

### **1.2.2 The adaptive immune system**

The production of the two major components of the adaptive immune system, B cells and T cells, begins in the bone marrow. B cells mature into naive B-cells within the bone marrow whereas T-cell progenitor cells migrate to thymus before maturing and entering into the circulation as naive T cells (Schmitt and Zúñiga-Pflücker, 2002). Naive B and T cells express immature pathogen receptors on their surface, B cell receptor (BCR), as well as T cells and which express T cell receptor (TCR), both receptors generated randomly (Market and Papavasiliou, 2003, LeBien and Tedder, 2008). The majority of B cells and T cells will die during the development processes by failing either positive selection or negative selection. Some B or T cells will have receptors responding correctly to the specific pathogen-derived epitope. Interaction with pathogen epitopes triggers clonal expansion of the T or B cell and maturation of the receptor (Starr et al., 2003, LeBien and Tedder, 2008). This process takes some time and results in a delay prior to production of fully functioning effectors. An efficient immune system involves the T lymphocytes selection expressing receptors which are restricted via major histocompatibility complex (MHC) but at the same time self-antigens tolerant. This selection happens mainly in the thymus, when lymphocyte precursors express their first surface receptor. T cells primarily arise from haematopoietic stem cells which migrate to the thymus. T cells development demands signals from non-hematopoietic stromal cells comprising numerous types of mesenchymal fibroblasts and thymic epithelial cells (TECs) (Anderson and Jenkinson, 2001). T cells differentiation is identified by the temporal expression of cell surface markers (CD4, CD8, CD44, and CD25) on the thymocyte. When the cells enter the thymus, the precursors will lack their expression of CD4 and CD8 and they are called double negative (DN). DN T cells express TCR  $\beta$  chain only, however  $\alpha$  locus rearrangement initiation will start immediately after pre-TCR signalling. Nevertheless,  $\alpha$  locus rearrangement full-scale will not happen until the cell becomes a quiescent double positive (DP) cell (Starr et al., 2003). The whole process, called positive selection, is introduced in cortical DP thymocytes and finalized in several days. Remarkably,

evidence proposes that the TCR need to continue its engagement and maintain signalling for the period of this process (Wilkinson et al., 1995).

### 1.2.3 T cell development

T cells undergo a series of developmental steps (Figure 1.2) regulated by antigen presentation, local extracellular signals (cytokines), receptor-receptor interactions. T cells

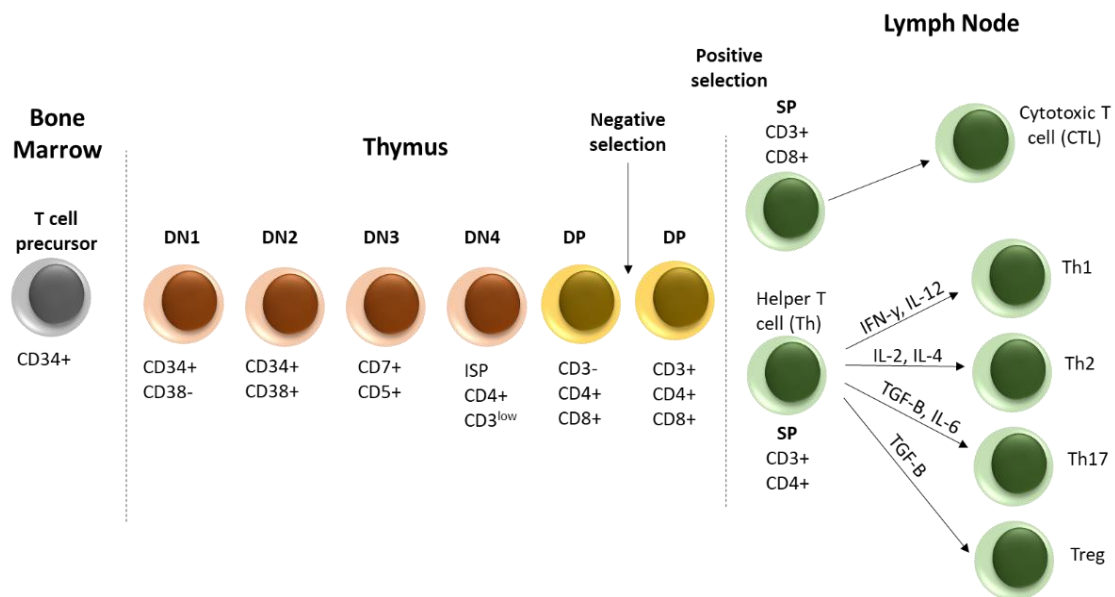


**Figure 1.2 Overview of human T-cell development.** T cell precursors from the bone marrow migrate to the thymus where they undergo multiple stages of development stimulated by local signal. The vast majority of cells (~98%) will die during negative selection and the remaining 2% will go onto positive selection to produce either cytotoxic T cells or T helper cells. **DN**: double negative, **DP**: Double positive, **ISP**: immature single positive; **SP**: single positive, **IFN-γ**: interferon gamma, **IL-12/2/4/6**: interleukin, **TGF-β**: transforming growth factor beta.

recognise antigenic peptide when it has been presented by MHC receptors on antigen presenting cells (APCs) (Figure 1.3) (McBlane et al., 1995). CD4 co-receptor binds to peptide presented in MHC class II on APCs whereas CD8 co-receptor binds to peptides presented by MHC class I on APCs (Figure 1.3) (Delves et al., 2017). CD8+ develops into cytotoxic T-lymphocytes (CTLs) following activation and are the cells responsible for cytotoxic activity.

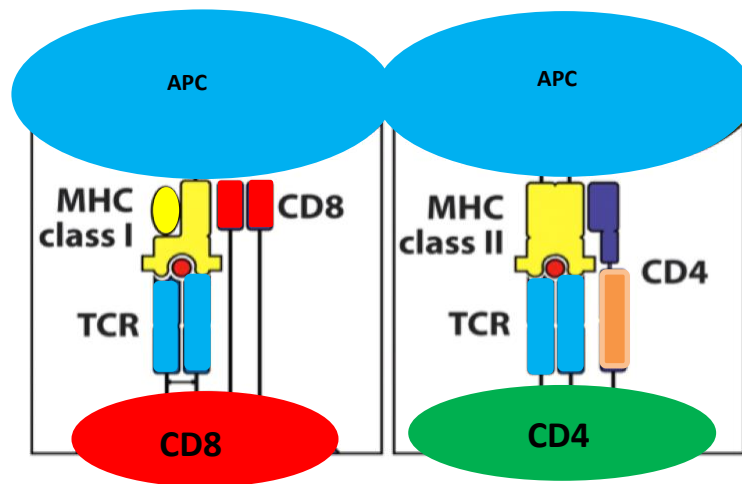


**Figure 1.3. T cell and APC interactions.** CD8<sup>+</sup> T cells recognise antigenic peptide presented in the context of major histocompatibility complex I (MHC I) receptors on Antigen presenting cells (APCs) whereas CD4<sup>+</sup> T cells recognise antigen bound to MHC class II on APC.

The local cytokine expression during CD4<sup>+</sup> activation is determining CD4<sup>+</sup> expansion into Th1, Th2, Th17 or T regulatory T cells (T-regs) cells (Figure 1.2 and 1.4). IL-2 and interferon gamma (IFN- $\gamma$ )/or IL-18 enhance Th1 generation that activate macrophages to boost pathogen intracellular killing. Whilst IL-4 that producing by Th2 cells which stimulates B-cell development and antibody production as well as activating macrophages to expel extracellular parasites e.g. worms. Stimulation with transforming growth factor beta (TGF- $\beta$ ) and IL-6 induces Th17 production that target extracellular parasites through antimicrobial peptide production and recruitment and activation of neutrophils. T-regs are responsible for long-term humoral immunity.

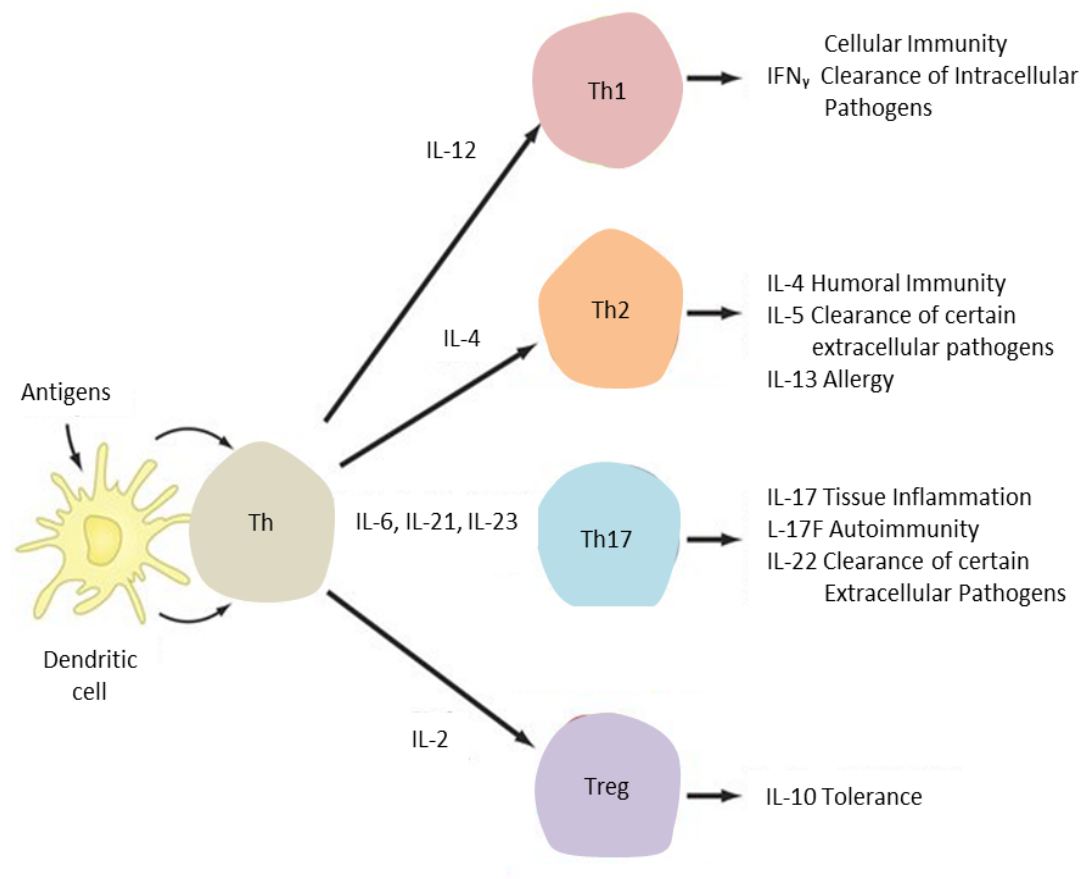


**Figure 1.4. T cell lineage specification.** Dendritic cells can interact with uncommitted CD4<sup>+</sup> T helper cells (Th) to initiate differentiation into a number of CD4<sup>+</sup> T cell lineages including T helper (Th) 1, Th2 and Th17 cells, as well as T regulatory (Treg) cells. Distinct signalling cascades, cytokines and transcription factors are activated during the differentiation into these different effector cells, which subsequently results in the activation of further cyto/chemokines and their respective receptors which may play roles in positive/negative feedback loops. Each type of effector cell is characterised by its specific immune-regulatory function and synthesis of particular cytokines as indicated on the right adapted from (Jetten, 2009).

### 1.2.4 Normal B-cell development

In mammals, B cells development initiates in the bone marrow with development of the common lymphoid progenitor (CLP) cells from HSCs. CLPs are responsible for generating B cells, T-cells, NK cells or dendritic cells (Cedar and Bergman, 2011). From the bone marrow, B cells migrate to secondary lymphoid organs (SLOs) e.g. spleen, where they continue development through defined stages. Each stage is characterised by distinct gene expression patterns and immunoglobulin heavy (H) chain and light (L) chain gene loci arrangements which arise from B cells undergoing V(D)J recombination (Market and

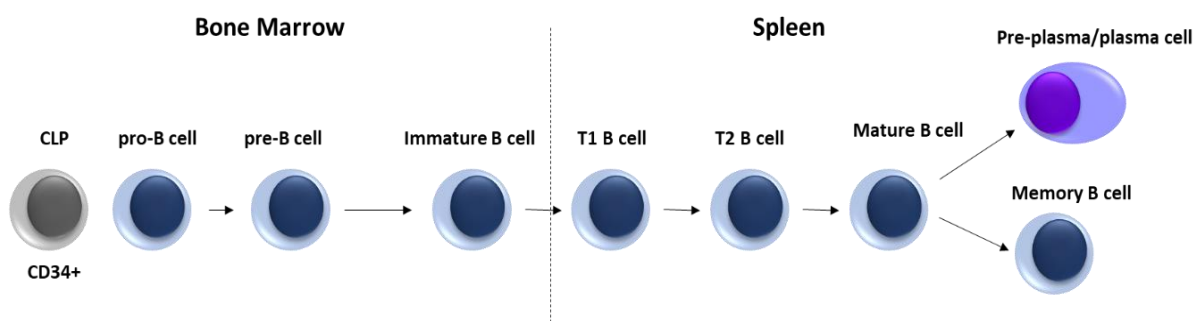


**Figure 1.5. Summary of B cell development.** The figure summarises the main stages of B cell development. Immature B cells exit the bone marrow and transit via the blood to secondary lymphoid organs e.g. spleen, as transitional B cells which undergo further maturation.

Papavasiliou, 2003). Figure 1.5 summarises the key stages of B cell development and differentiation. In the bone marrow, B cells undergo positive and negative selection. Positive selection in the bone marrow is antigen-independent and involves signalling through both the pre-BCR and the BCR which is required to allow continued B cell development. Negative selection occurs through the binding of self-antigen with the BCR resulting in clonal deletion, receptor editing, anergy, or ignorance (B cell ignores signal and continues development) (Krammer, 2000). This negative selection process is essential to establish self-tolerance and to prevent development of autoreactive B cells. Immature B cells migrate from the bone marrow into the spleen as transitional B cells. During transit and until entry into the spleen, B cells are called T1 B cells. Within the spleen, T1 cells transition into T2 B cells (Isnardi et al., 2008).

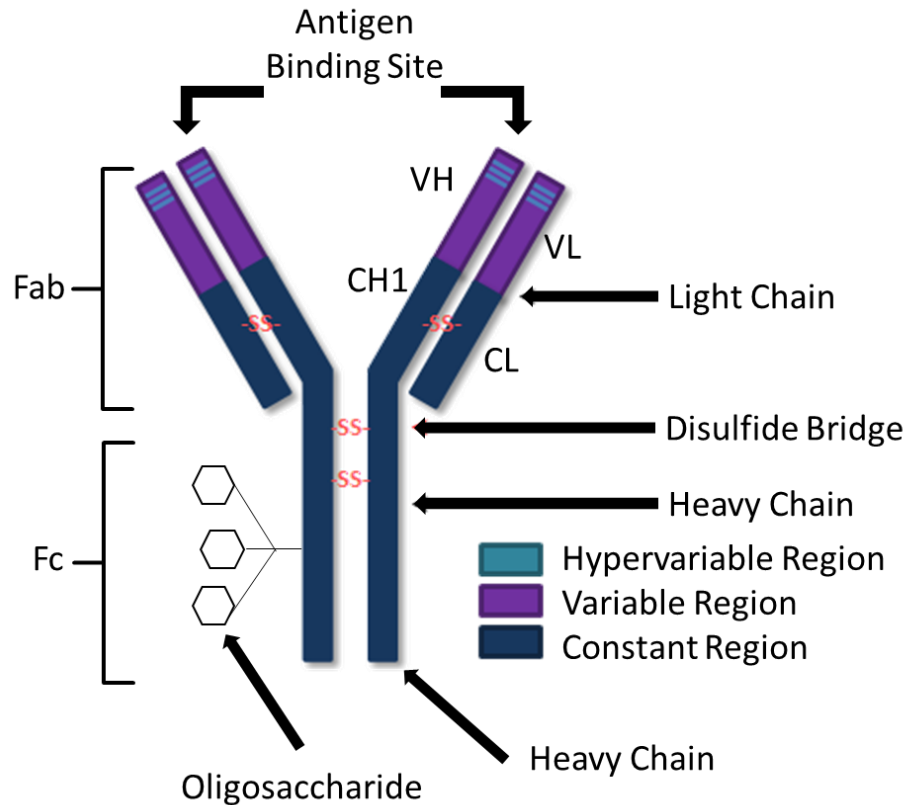


**Figure 1.6. Basic immunoglobulin structure.** Fab: Fragment, antigen-binding, Fc: Fragment, crystalizable. CL: Constant domain, Light chain. CH: Constant domain, heavy chain. VL: Variable domain, Light chain. VH: Variable domain, heavy chain. Adapted from (Kumar and Clark, 2012)

B cell development occurs in distinctive differential steps which are categorised by the BCR specific structure. The BCR consisting of two identical heavy chain and two identical light-chain immunoglobulin (Ig) polypeptides linked covalently with a disulphide bridges. Other BCR components are the CD79A and CD79B molecules. BCR crosslinking is activated the intracellular signalling components including some tyrosine kinases (Küppers, 2005).

The earlier stages in B cell development are distinguished by successive rearrangement of heavy- and light-chain immunoglobulin (Ig) genes to produce mature Ig molecules (Figure 1.6). This process, called VDJ rearrangement, is a highly controlled series of genetic events (Küppers, 2005). Upon B-cell differentiation stage that recognizes an antigen plus other B cell surface receptors activation that modulating BCR signalling, there will be extra proliferation induction and /or more differentiation steps (Rajewsky, 1996). In bone marrow, where early B cell development occurs bone marrow and it supported by functional surface antigen receptor. B cells with functional BCR leave the bone marrow and

differentiate into mature naive B cells, whilst those B cell precursors which fail in expressing BCR will undergo apoptosis. Once antigens bind to BCR that will activate mature naive B cells to participate in immune responses (Küppers, 2005). BCR expression is essential for B-cell development and survival in peripheral blood (Lam et al., 1997).

The pro-B cells are derived from HSC and identified by their cell-surface proteins e.g. CD10 and CD19. CD19 is generally expressed by all B- cell lineages and plays a role in amplifying activity of Src-family kinases that regulate intracellular signal transduction. CD20 is another marker for mature B-cells. CD20 functions as a membrane embedded  $\text{Ca}^{2+}$  channel. CD21 function is as an Epstein-Barr virus receptor which works alongside CD19 to produce transmembrane signals. The CD19/CD21 complex is a very important co-receptor for B-cells, co-operatively enhancing signalling via B cell receptor (Fujimoto et al., 2000). This enhancing process occurs in response to complement-tagged antigens and T cell dependent activation. CD19/CD21 is not targeting complement-tagged antigens directly for processing, however it influencing B cell antigens processing via its signalling function (Cherukuri et al., 2001). CD23 is expressed on activated B-cells as low-affinity IgE receptor that regulates IgE production. CD40 is one of the essential survival factors (Messina et al., 1991).

These immunophenotyping markers can be used as essential components for the diagnostic and classification of a variety of cancerous and non-cancerous disorders and can help to guide therapy or draw a clinical outcome prediction. Figure 1.7 shows some characteristic immunophenotype markers of B-cell malignancies.



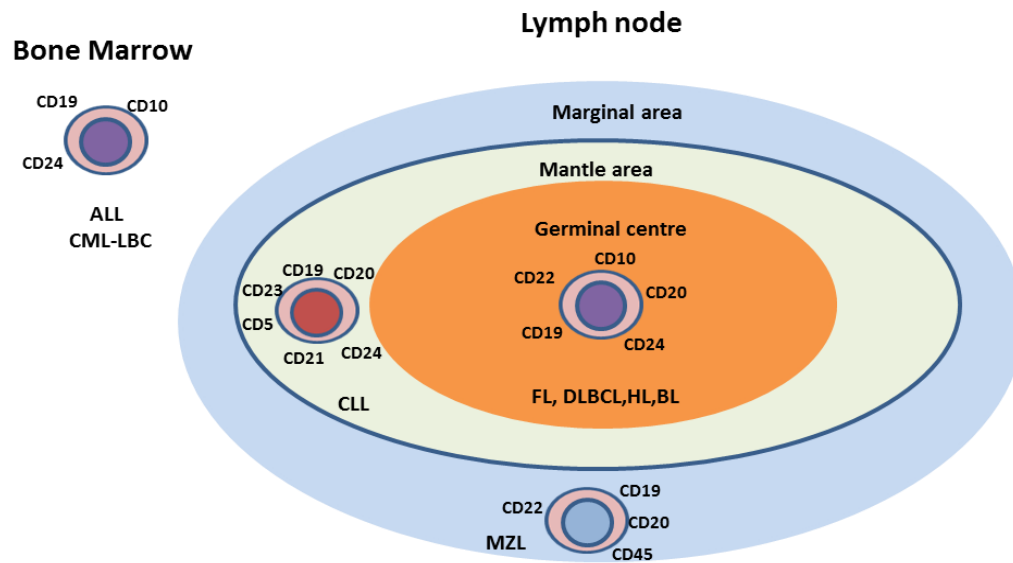


**Figure 1.7. Characteristic immunophenotype markers of B-cell malignancies.** Selected Immunophenotype markers (Cell surfaces, cytoplasmic and nuclear) expressed during normal B cell development and malignancies. **ALL** refers to acute lymphoblastic leukaemia; **CML-LBC**, chronic myelocytic leukaemia lymphoid blast crisis; **CLL**, chronic lymphocytic leukaemia; **FL**, follicular lymphoma; **DLBCL**, diffuse large B cell lymphoma; **HL**, Hodgkin's lymphoma and **BL**, Burkitt's lymphoma; **MZL** marginal zone lymphoma. Adapted from (LeBien and Tedder, 2008).

### 1.3 Lymphomas

Lymphomas are cancers of the lymphatic system characterised by the accumulation of malignant lymphocytes in lymph nodes leading to lymphadenopathy. They start due to the accumulation of genetic aberrations, that influence growth and survival (Hoffbrand and Moss, 2011, Hoffman et al., 2009). There are two main categories of lymphoma. They are called Hodgkin's lymphoma (HL) and non-Hodgkin's lymphoma (NHL).

#### 1.3.1 Hodgkin's lymphoma (HL)

The first descriptions of Hodgkin's disease date back to 1832, when it was described by the British pathologist Thomas Hodgkin who defined an autopsy case series was taken from patients with lymphadenopathy and splenic enlargement (Alizadeh et al., 2000, Hoffman et al., 2009).

Then in 1898, Dorothy Reed and Carl Sternberg identified characteristic large mononuclear cells or multinucleate giant cells that were always found to be associated with HL tumours which came to be called Reed-Sternberg cells (Jaffe, 2009, Kanzler et al., 1996). Until the late 1990s, Hodgkin lymphoma (HL) was thought to be a malignancy arising from either germinal or post-germinal centre B cells. Typically, the tumour cells comprise only a small proportion of the tumour mass which is surrounded by a reactive inflammatory locale consisting of eosinophils, neutrophils, lymphocytes, plasma cells and histiocytes (Thomas et al., 2004). HL incidence in the UK and USA is 2.7- 2.8 per 100,000 per year, with ~1700 new cases diagnosed in the UK annually (CRUK). It can start at any age but is more common in young people <40 years and in those older than 60 (Townsend and Linch, 2012). It is estimated that HL accounts for approximately 10% of newly diagnosed lymphoma cases in the United States (8260 of 80,500 cases) and 0.5% of all new cancer diagnoses. Of the approximately 21,210 deaths due to lymphoma each year in the US, around 1070 (or 5%) are from HL, which is almost 0.2% of all cancer deaths (Siegel et al., 2017).

### **1.3.2 Non-Hodgkin's lymphoma (NHL)**

NHL is a heterogeneous group of malignancies arising from T or B lymphocytes and at various stages of their differentiation (Swerdlow et al., 2016). Around 60-70% of NHL cases either present or occur in bone marrow, spleen or lymph node, however it can develop almost in any other tissue (Shankland et al., 2012). NHL is the sixth most common cancer diagnosis in both men and women in the UK (Ferlay et al., 2013). It is more common in people aged over 65 years. Broadly speaking there are 6 different subtypes of NHL (Table 1.2) of which follicular lymphoma (FL) and diffuse large B-cell lymphoma (DLBCL) are the most common subtypes (Shankland et al., 2012). NHL incidence differs extensively between various histological types (Table 2). FL is the most common low-grade lymphoma which grows very slow. Despite this slow growth rate, FL is difficult to cure and is commonly retained under control with intermittent continued treatment (Tsang and Gospodarowicz, 2007). In contrast, high grade lymphomas like DLBCL grow faster and are clinically more aggressive (Niitsu et al., 2001a).

NHL Subtype	NHL Proportion	Expected UK cases per year
Marginal zone lymphoma (MZL)	19.9%	2050
Mantle cell lymphoma (MCL)	5.0%	510
Follicular lymphoma (FL)	18.1%	1860
Diffuse large B-cell lymphoma (DLBCL)	48.5%	4990
Burkitt's Lymphoma (BL)	2.0%	210
T-cell lymphoma (TL)	6.3%	650
All Lymphomas		10,280

**Table 1.2 NHL subtypes proportion and expected UK cases per year adapted from (Ferlay et al., 2013).**

#### **1.4 Diffuse Large B-Cell Lymphoma (DLBCL)**

DLBCL is a heterogeneous tumour group and can occur in nodal (lymphoid) or extra nodal sites including bone, lung and testis. It is classified as the most common aggressive NHL subtype and comprises 40% of NHL patients (Swerdlow et al., 2016). It is most common in adults in their seventh decade but can arise in children as well (Garber, 2001). Individuals with primary or acquired immunodeficiency including human Immunodeficiency virus (HIV) infection patients and those on immunosuppressant therapy following solid organ transplants are more susceptible to developing DLBCL (Gucalp and Noy, 2010, Carbone and Gaidano, 2001). DLBCL occurs usually as a de novo tumour; however Follicular lymphoma can transform into DLBCL. In Richter's transformation, chronic lymphocytic leukaemia/small lymphocytic lymphoma (CLL/SLL) transform to DLBCL (Rossi and Gaidano, 2009). In other cases, marginal zone lymphoma (MZL) or nodular lymphocytic predominant Hodgkin lymphoma (NLPHL) (Lee and LaCasce, 2009) and Follicular lymphoma (FL) (Martinez et al., 2008, De Jong et al., 2009) can also transform into DLBCL. DLBCL patients can present clinically with painless adenopathy or abdominal pain related to tumour bulk. Patients can complain from what are called 'B-Symptoms' that include unexplained fever, weight loss of more than 5% or night sweats (Tai et al., 2011). Investigation of a DLBCL biopsy patient can

show that lymph node architecture is completely disturbed with diffuse proliferation of large centroblast like cells or immunoblastic cells in some cases (Swerdlow et al., 2016) (Figure 1.8). Upon immunophenotyping, DLBCL cells characteristically express CD10/19/20/22/24 (Colomo et al., 2003, Craig and Foon, 2008). The proliferation marker (Ki-67) typically varies between 40-90% in DLBCL patients identifying that a large proportion of the tumour cells are in cell cycle and hence the aggressive nature of the disease. Cases expressing Ki-67 in higher than 90% of cells often carry a *MYC* gene translocation meaning that the tumour will be classified as intermediate between Burkitt's lymphoma and DLBCL (Perry et al., 2013). Overall, *MYC* gene rearrangements are seen in ~10% of DLBCL cases and generally associates with poor outcome (Savage et al., 2009).

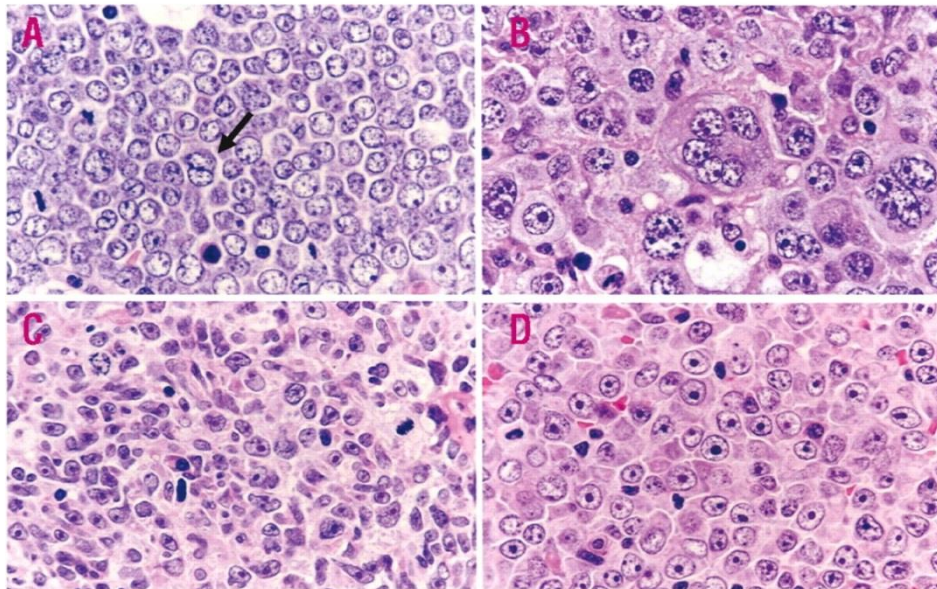


**Figure 1.8. Cytomorphological features of four types of DLBCL.** The cells size is variable from medium to large, homologous, with amphophilic or a pale basophilic cytoplasm. (A) Common type (monomorphic) or what called centroblastic type, easy detected with bi-nucleated cells. (Arrow). (B) Giant cell-rich type. (C) Polymorphic type, identified with medium and large-sized cells. (D) The immunoblastic type. Adapted from (Yamaguchi et al., 2008).

### **1.4.1 Molecular classification of DLBCL**

Three main subtypes of DLBCL have been identified with underlying obvious biologic, clinical and genetic differences (Lenz and Staudt, 2010, Alizadeh et al., 2000, Savage et al., 2003) (Table 3):

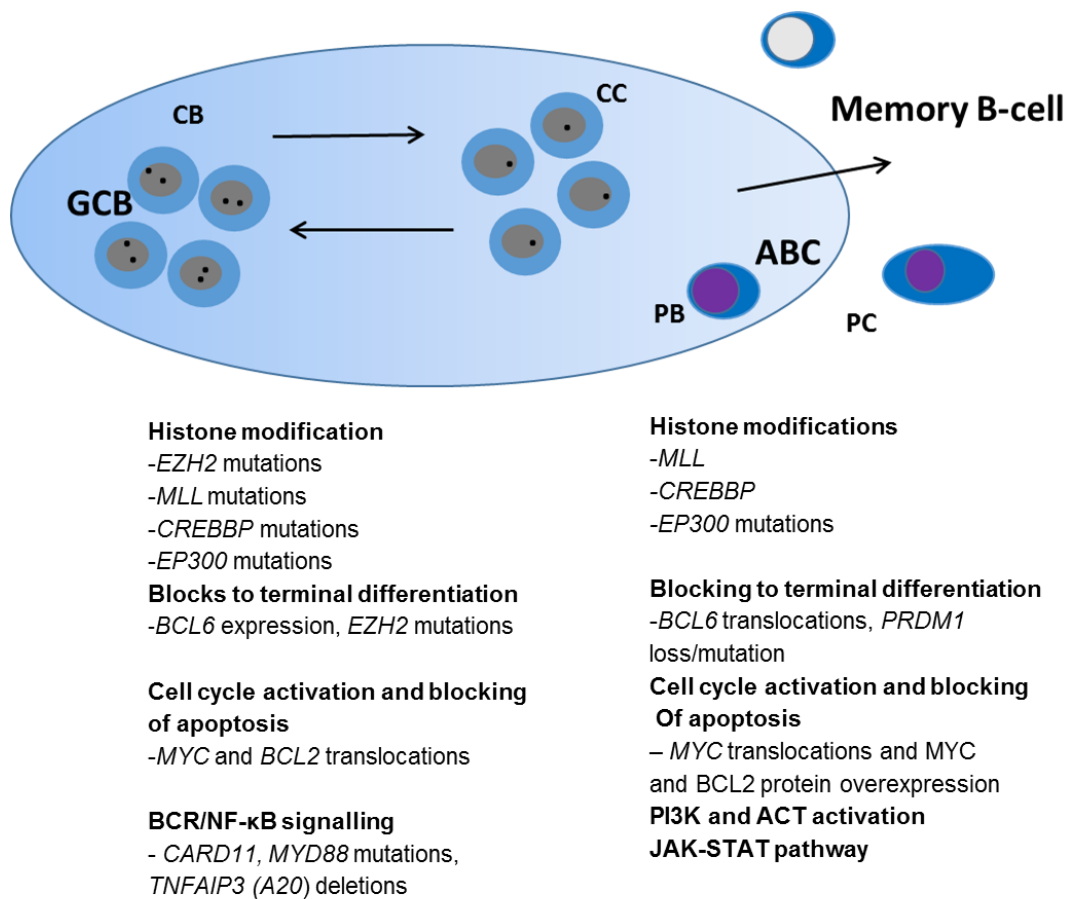
1. germinal centre B cell-like (GCB) DLBCL, expressing normal germinal centre B cells hallmarks
2. activated B cell-like (ABC) DLBCL, that do not express germinal centre B cell-restricted genes and are produced from post-germinal centre B cells;
3. primary mediastinal B cell lymphoma (PMBCL), which may be derived from thymic B cells and express genes that are usually expressed in Hodgkin Reed-Sternberg cells (Rodriguez-Abreu et al., 2007).

Figure 1.9 shows the differences between ABC and GCB DLBCLs. Gene expression profiling (GEP) analysis has provided a better understanding of molecular mechanisms involved in DLBCL disease development, as well as discovery of expression characteristics related to poor clinical outcome (Lenz and Staudt, 2010, Alizadeh et al., 2000, Rosenwald et al., 2002).

Genetic Subtype/Cluster	Genetic Abnormalities	Cell of origin	5-years Overall Survival
<b>MCD</b>	<i>MYD88</i> L265 mutations <i>CD79B</i> mutations	ABC	26%
<b>BN2</b>	<i>BCL6</i> fusions <i>NOTCH1</i> mutations	ABC, GCB, and unclassified	36%
<b>N1</b>	<i>NOTCH1</i> mutations	ABC	65%
<b>EZB</b>	<i>EZH2</i> mutations <i>BCL2</i> translocations	GCB	68%
<b>Cluster 1</b>	<i>BCL6</i> structural variants <i>NOTCH2</i> signalling	ABC	79%
<b>Cluster 2</b>	Biallelic inactivation of <i>TP53</i> , <i>17p</i> loss	ABC and GCB	62%
<b>Cluster 3</b>	<i>BCL2</i> , <i>KMT2D</i> , <i>CREBBP</i> , <i>EZH2</i> mutations	GCB	57%
<b>Cluster 4</b>	BCR/PI3K signalling, NF-κB and RAS/JAK/STAT pathways	GCB	72%
<b>Cluster 5</b>	<i>18q</i> gain, <i>BCL2</i> and <i>MALT1</i> expression	ABC	54%
<b>Cluster 0</b>	No cohesive alterations	NA	100%

**Table 1.3. Characteristics of Newly Defined DLBCL based on shared genetic aberrancies.**

ABC = Activated B-cell-like; BCR = receptor; GCB = germinal B-cell-like; NA = not available; NFκB = nuclear factor kappa B; PI3K = phospho-inositol 3-kinase.



**Figure 1.9. Key oncogenic pathways in DLBCL.** Two major molecular DLBCL subtypes are shown: the GCB and the ABC type. Both tumours rise from stages of differentiation reminiscent of germinal centre B cells. The GCB subtype rises from centroblasts, whilst the ABC subtype rises from a plasmablastic cell just prior to germinal centre exit. The main oncogenic pathways are listed, as well as the recurrent mutations, gains and losses of genetic material. **CB**, centroblast; **CC**, centrocyte; **PB**, plasmablast; **PC**, plasma cell.

## **1.4.2 DLBCL treatment**

### **1.4.2.1 Standard therapies in DLBCL**

DLBCL, the most common lymphoid malignancy that advance quickly, needs immediate treatment. Rituximab or Rituxan (chemotherapy and monoclonal antibody combination) is usually used to treat DLBCL in combination with the chemotherapy regime R-CHOP (rituximab, cyclophosphamide, doxorubicin, vincristine, and prednisone) which is used to treat 60-70% of patients. In some cases, R-CHOP is used after stem cell transplantation. Another effective regime includes rituximab, doxorubicin, cyclophosphamide, vindesine, bleomycin, and prednisone, followed with high dose methotrexate, ifosfamide and cytarabine (Bachy and Salles, 2015, Récher et al., 2011). Another effective treatment in DLBCL is DA-EPOCH which consists of continuous infusion with adjusted doses of etoposide, prednisone, vincristine, cyclophosphamide and doxorubicin with rituximab (Bachy and Salles, 2015, García-Suárez et al., 2013, García-Suárez et al., 2007). However, R-CHOP is the essential therapeutic choice for most DLBCL patients (Sehn and Gascoyne, 2015).

In recent times, DLBCL therapeutic effects have been amended because the treatment choices have expanded to include high-dose chemotherapy in combination with peripheral blood stem cell transplantation, mini-transplantation, allogeneic bone marrow transplantation (Niitsu et al., 2004) and antibody treatment with ibritumomab or rituximab since rituximab is a chimeric antibody, so the entire humanised antibodies that produces against the drug need to eliminate, like IMMU-106 (hA20), when these antibodies enhance the infusion reactions and remove the human antibodies development against the drug. Table 1.4 shows some other current DLBCL drugs with their functions (Fanale and Younes, 2007).



Therapy	Function
Rituximab	Induces apoptosis of CD20+ cells
Cyclophosphamide	DNA duplication inhibitor
Doxorubicin	Macromolecular biosynthesis inhibitor
Vincristine	Microtubule formation inhibitor
Prednisone	DNA synthesis inhibitor
Enzastaurin	PKC $\beta$ inhibitor
Everolimus	mTOR inhibitor
Lenalidomide	Immunomodulator and antiangiogenic
Ibritumomab tiuxetan	Radioimmunotherapy
Bendamustine	Alkylating agent
Bortezomib	Proteasome inhibitor
Epratuzumab	rhCD22 mAb
Fostamatinib	Syk kinase inhibitor

**Table 1.4. Current DLBCL drugs and their functions.**

#### **1.4.2.2 Novel therapies in DLBCL**

In the past few years, novel therapies have been introduced that take into consideration DLBCL molecular subtypes and are designed to target specific pathways controlling the pathogenesis of this disease. These new drugs are most suitable for ABC DLBCL because they target B-cell receptor signalling or NF- $\kappa$ B pathway which are continuously active in this subtype (Sehn and Gascoyne, 2015). Bruton's tyrosine kinase (BTK) has emerged as a replacement therapeutic target in some malignancies. Ibrutinib, the most clinically advanced molecular inhibitor of BTK, has demonstrated excellent tolerability and activity in a variety of B-cell cancers that led to its approval for relapsed mantle cell lymphoma and chronic leukaemia (Maas and Hendriks, 2001, Dunleavy et al., 2018). BTK plays a major role in B-cell development and may be a distinctive therapeutic target in B-cell malignancies. In humans, loss of function mutations in BTK leads to X-linked agammaglobulinaemia (XLA) that is characterised by low peripheral blood B cells, low/negligible levels of immunoglobulin, and continuous infections (Aalipour and Advani, 2014). This clinical phenotype highlights the essential role of BTK in B-cell development and immunoglobulin production (Maas and Hendriks, 2001). Ibrutinib (BTK inhibitor) achieved an acceptable response in just 5% GC DLBCL patients compared to 41% of ABC DLBCL patients (Sehn and Gascoyne, 2015, Aalipour and Advani, 2014). Bortezomib is a proteasome inhibitor that has been used for treating ABC DLBCL in combination with DA-EPOCH for relapsed patients (Sehn and Gascoyne, 2015, Dunleavy et al., 2009). New trials are ongoing using a combination of bortezomib and R-CHOP in previously untreated patients (Furman et al.,

2010). Another promising study is aiming to target multiple components based on the fact that activating phosphatidylinositol 3-kinase (PI3K)/AKT/mammalian target of rapamycin (mTOR) signalling pathway is involved in cellular metabolism and growth. This pathway can be activated in B cell lymphomas by variety of mechanisms (Janku et al., 2013). Phosphatase and tensin homolog PTEN (a gene with tumor suppressing activity) deletion can affect this pathway. PTEN loss of expression has been detected in 55% of GCB DLBCL in comparison to only 14% of non-GCB cases (Roschewski et al., 2014). Another combination of R-CHOP therapy with lenalidomide (an immunomodulatory drug with antiangiogenic activity and inhibitory effect on NF- $\kappa$ B pathway) has recently been tested (Thieblemont et al., 2012).

#### **1.4.3 Tumour infiltrating Lymphocytes (TIL)**

It has been identified in many lymphomas and solid cancers that tumours are infiltrated by non-malignant T cells (TILs). The importance of identification of particular T cell subsets: CD4 T helper cells (Th cells), CD4 T regulatory cells (T reg cells) and CD8 cytotoxic cells. These subsets have been suggested as a prognostic factor for survival prediction in B cell lymphoma patients (Xu et al., 2001, Lee et al., 2006a). Not just T cell type but also T cell numbers are important. A high level of CD4+ T cells is associated in many malignancies with a better outcome (Fridman et al., 2012). Also, the impact of differing T cell subsets is context specific. For example Treg cells are associated with poor outcome in epithelial cancers and a better outcome in some B cell lymphomas (Carreras et al., 2006). One explanation may be due to the direct negative impact of Treg on B cell proliferation (Yang et al., 2006). The other effective subset of CD4+ cells is Th cells which can subdivide into two subgroups. T helper cells 1 subtype (Th1) cells produce tumour necrosis factor- $\alpha$  (TNF- $\alpha$ ) and Interferon-  $\gamma$  (IFN- $\gamma$ ). These cells are associated with a better outcome in malignancies due to their association with immunological clearance within the tumour. T helper cells 2 subtype (Th2) subtype CD4+ T cells produce IL4,5,10 and 13 and have immunosuppressive functions (Fridman et al., 2012, Haabeth et al., 2011). The variation even within CD4 subset (Th1 and Th2) might cause different outcomes. Besides cell number and subset variations, location of the infiltrating cells within the tumour may be relevant to disease progression and response to therapy. For example, whether they are in the tumour stroma, tumour edge or tumour centre (Mei et al., 2014, Seo et al., 2013). In melanoma, the *in vitro* culture and reinfusion of

tumour infiltrating lymphocytes (lymphocytes removed from patients tumour site) resulted in better treatment response for 50% of those patients (Besser et al., 2013, Dudley et al., 2008). Thus, immune cell infiltration parameters have been used in DLBCL outcome prediction (Lenz et al., 2008b, Phipps-Yonas et al., 2013).

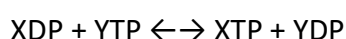
Another important prognostic parameter for NHL is the circulating absolute monocyte count (AMC) and absolute lymphocyte count (ALC), that has been used as a surrogate marker for host immune-effector in outcome prediction (Wilcox et al., 2011, Li et al., 2012). AMC and ALC are routinely applied as they are easy to measure. Another study investigated the correlation between T cell activation within the tumour microenvironment and outcome in DLBCL cohorts (Alizadeh et al., 2011). It simply explained that adding an agonist antibody to CD137 (CD137 is one of the tumor necrosis factor (TNF) receptor family, exist in immune cells like monocytes and activated B and T lymphocytes (Kienzle and von Kempis, 2000) could result in immune response improvement against the lymphoma (Houot et al., 2009). Research using animal models emphasised the role of CD4+ T cells in generating an anti-tumour microenvironment (Ding et al., 2012). Antigen presentation improvement was identified as an effective survival determinant in DLBCL patients (Ott et al., 2010, Rimsza et al., 2004, Pasqualucci et al., 2011, Higashi et al., 2016). The animal models in these studies explained the role of TH1 secreted cytokines, like IL1, IFN- $\gamma$  and TNF- $\alpha$  in stimulating macrophages which mediated malignant B cell clearance. The mouse model identified PD1, a cell surface receptor and one of immunoglobulin superfamily usually expressed on pro-B cells and T cells, expression on 27% of DLBCL cases. The histiocytes surrounding DLBCL tumour were positive for PD1 in 38% of DLBCL cases where the tumour cells did not express PD1 (Andorsky et al., 2011). PD1 is a CD28 superfamily member, delivering negative signals via interaction with its two ligands, PD-L1 or PD-L2 (Jin et al., 2010). Binding of PD1 with its ligands e.g. PD-L1, expressed on antigen-presenting cells or tumor cells leading to down-regulation of effector T cell function (Gatalica et al., 2015). PD1 represents an effective mechanism of immune evasion by a number of lymphomas and solid tumours (Gatalica et al., 2015). One of the explanations could be that PD1 is responsible for CD4+ T cells down regulation in DLBCL patients. There are successful trials in solid tumours targeting PD1 (Topalian et al., 2012, Brahmer et al., 2012) and parallel trials have been conducted in B cell

lymphomas (Berger et al., 2008). The treatment with anti-PD1 antibody resulted in T cells and NK cells function enhancement in follicular lymphoma (Westin et al., 2014).

## **1.5 The NM23 protein family**

### **1.5.1 Structure and classification**

The human NM23 protein family are nucleoside diphosphate kinases (NDKs or NDPKs) (Postel et al., 2009). NDKs catalyse terminal phosphate exchange transphosphorylation reactions between nucleoside diphosphates (NDPs) and nucleoside triphosphates (NTPs),



(Gilles et al., 1991). All NM23 family protein contain one or more conserved NDK (either completed or truncated) domains (Boissan et al., 2009). The 10 members of the human NM23 protein family can be divided into two subgroups based on their phylogenetic characteristics (Bilitou et al., 2009). NM23 family members are involved in major cellular activities such as differentiation, proliferation, signal transduction and apoptosis (Bilitou et al., 2009, Postel, 2003). A summary of NM23 protein family biological and molecular characteristics are listed in Table 5. The group I members (NM23-H1, H2, H3, H4) have a conserved active site for NDPK activity (Bilitou et al., 2009). They all show identity at gene sequence level by 58-88% NDK activity. They show identical three dimensional structure (Boissan et al., 2009).

The most studied proteins are NM23-H1 and NM23-H2 which in humans are responsible for the majority of NDK activity (Postel et al., 2009). Despite the similarity between NM23-H1 and NM23-H2 being 88%, they are very different in their isoelectric points. The explanation is that many of the acidic amino acids residues in NM23-H1 are substituted by basic amino acids in NM23-H2 (Véron et al., 1995). The predominant form of NM23-H1 is hexameric, but it can exist also as monomers, dimer or trimer (Kim et al., 2003, Min et al., 2002).

Group II members (NM23- H5, H6, H7, H8, H9, H10) show more divergence within the group, and have only 25-45% identity (Lacombe et al., 2000b).

Group	NM23	Synonym	Chromosome Locus	Molecular Weight (kD)	Expression	Subcellular Localisation	NDK Activity
I	H1	A	17q21.3	17.1	Ubiquitous (brain, intestine, kidney, liver)	Cytoplasm, nuclei	+
I	H2	B	17q21.3	17.3	Ubiquitous (heart, kidney, liver, pancreas)	Cytoplasm, nuclei	+
I	H3	C	16p13.3	18.9	Ubiquitous (adrenal gland, cerebellum, pituitary gland)	Cytoplasm, mitochondria	+
I	H4	D	16p13.3	20.7	Ubiquitous (heart, liver, prostate)	Mitochondria	+
II	H5		7p14.1	67.3	Spermatozoa flagella (testes), cilia (nasal, trachea)	?	-
II	H6		3q22.3	36.9	Spermatozoa flagella (testes), cilia (lung)	Microtubule	+
II	H7		5q31.1	24.2	Spermatozoa flagella (testes), cilia	Microtubule	-
II	H8	TXNDC3	3p21.3	21.1	Ubiquitous (heart, kidney, skeletal muscle, spleen)	Cytoplasm, mitochondria	+/-
II	H9	TXNDC6	1q24	42.5	Spermatozoa flagella (testes), cilia	?	-
II	H10	RP2	Xp11.1	39.6	Ubiquitous	Cell membrane	+

**Table 1.5. NM23 Proteins family classification.** Adapted from (Lacombe et al., 2000a, Boissan et al., 2009, Desvignes et al., 2009).

### 1.5.2 NM23 potential function in normal development

Various lines of evidence implicate roles for NM23/NDPK proteins in cell differentiation and development. In the Gram-negative bacterium, *Myxococcus xanthus*, it has been shown that NDK is an essential requirement for cell division (Lombardi et al., 2000). It has been shown in drosophila that the abnormal wing disks (awd) gene encoding Drosophila NDPK is expressed in wide range of tissues during different developmental stages and therefore the protein is crucial for traditional development (Dearolf et al., 1988). Homozygous mutations that have an effect on the kinase activity of the enzyme resulted in developmental abnormalities of the brain, wing imaginal disks and ovaries, and lead to morbidity at the late larval/puparium stage (Dearolf et al., 1988, Xu et al., 1996). In addition, the killer-of-prune

(K-pn) mutation is lethal in an exceedingly dominant manner once combined with a null mutation of the prune eye colour gene, leading to tumor-like defects and death throughout early development (Timmons and Shearn, 1997).

### **1.5.3 The biochemical activities of NM23**

NM23 biochemical activity was initially described by Paul Berge and Hans Kreps (Steeg et al., 1988). NM23 was demonstrated to add the terminal gamma phosphate to nucleoside diphosphate (NDP) after removing it from a donor nucleoside triphosphate (NTP) (Steeg et al., 1988). After that, the enzyme gained its correct chemical name, which is NTP/NDP transphosphorylase. Subsequently NM23 was identified as a multifunctional protein that can mediate many enzymatic reactions including: G-protein signalling, mutational susceptibility, nucleoside pool and microtubule dynamics (Kim et al., 2009, Lee and Lee, 1999, MacDonald et al., 1995). NM23 protein was shown to be involved in Guanosine-5'-triphosphate (GTP) synthesis and Guanine nucleotide-binding proteins (G-protein) activation (Veluthakal et al., 2009). This process regulates the cellular basal cAMP levels. It is mediated by alpha subunit phosphorylation which involves membrane interaction between G-protein  $\beta$ ,  $\gamma$  dimers and NM23-H2 (Cuello et al., 2003, Hippe et al., 2007). They are involved also in regulation of various aspects of DNA metabolism such as DNA binding, transcription and modulating factors (Postel, 2003). As well as 3' – 5' exonucleases and DNA repair (Kaetzel et al., 2006). Another protein kinase activity exhibited by NM23 family is histidine phosphorylation or serine phosphorylation, which involves histidine residue (His118) auto phosphorylation by ATP (Engel et al., 1995, Steeg et al., 2011).

### **1.5.4 NM23-H1 in haematopoiesis**

NM23-H1 and NM23-H2 are detectable in CD34+ hematopoietic stem and progenitors cells (HSPCs) with CD34+ cells expressing the highest intracellular levels of NM23-H1 (Willems et al., 1998). Haematopoietic cell maturation is inversely correlated to NM23 expression with minimal intracellular expression found in peripheral blood leukocytes (Willems et al., 2002). NM23-H1 is also found extracellularly in bone marrow plasma, umbilical cord blood plasma and normal peripheral blood plasma (Willems et al., 1998). The correlation between haemoglobin levels and NDPK level suggested that the presence in of NM23 in plasma was a consequence of red blood cell lysis (Willems et al., 2002). Considering

that erythropoiesis was enhanced *in vitro* by NM23, it might be that haemolysis of red blood releases NM23 as an alarm signal to stimulate erythropoiesis (Willems et al., 2002). Furthermore, this activity was present even with the H118F kinase-dead mutant indicating that the kinase function is not needed for promotion of erythropoiesis. An experiment investigating the impact of adding NM23 to assays with CD34<sup>++</sup>CD38<sup>-</sup> haematopoietic progenitors demonstrated that NM23 seems to have an impact on the terminal stages of haematopoietic maturation, inhibiting monocytic differentiation and therefore promoting erythropoiesis (Willems et al., 1998, Willems et al., 2002). This revealed a feedback mechanism, in which NM23 released from lysed red blood cells skews the differentiation of haematopoietic progenitors in order to preserve erythroid cell numbers. Mice that lacked both Two Isotypes of Murine NM23/Nucleoside Diphosphate Kinase, *NM23-M1* and *NM23-M2* genes were stunted in growth and died perinatally (Postel et al., 2009). These double knockout mice also displayed a severe impaired haematological phenotype including severe anaemia, abnormal erythroid cell development, loss of the iron transport receptor molecule TfR1, and reduced iron uptake by Nme1 ( -/- ) /Nme2 ( -/- ) erythroid cells (Willems et al., 2001, Aalipour and Advani, 2014).

Whilst the above studies promote a model based on release of NM23 from lysed cells, it has also been demonstrated that NM23-H1 is released from CD34<sup>+</sup> HSPCs and not as a lysis product (Lilly et al., 2011). NM23-H1 recombinant protein was able to promote the survival and expansion of CD34<sup>+</sup> HSPCs from umbilical cord blood (Personal communication with Prof Chris Bunce). Okabe-Kato et al demonstrated that the provision of exogenous recombinant NM23-H1 (recombinant NM23-H1) to normal peripheral blood mononuclear cells (PBMC) can inhibit their survival and stimulated the secreting of inflammatory cytokines and chemokines, including IL-1 $\beta$ , IL-6, IL-8, MCP-1 and GM-CSF (Okabe-Kado et al., 2009a).

### **1.5.5 NM23 proteins in cancer**

The human NDPK, NM23, which stands for non-metastatic clone 23, was classified as the first metastasis suppressor gene when the lack of this gene was linked to metastasis of tumour cells (De La Rosa et al., 1995). NM23 was identified for the first time from differential hybridization experiments using murine K-1735 melanoma cell line clones with

variable metastatic potential (Steeg et al., 1988). Further work verified the ability of NM23 to reduce the metastatic potential of melanoma cell lines after the transfection of murine NM23-H1 cDNA into these cell lines resulted in suppression of several cancer associated properties in murine melanoma cells, including tumour incidence and metastasis and cytokine responsiveness (Leone et al., 1991). The incidence of primary tumour formation reduced significantly and independently of growth rate. The histidine protein kinase (Freije et al., 1997) and 3'-5'exonuclease activities in NM23 has been linked to its metastasis suppressive effect since mutant NM23-H1 lacking both the NDPK and histidine kinase, but retaining the 3'-5 exonuclease, exhibited compromised tumour-suppressor activity.

It was demonstrated for the first time that the importance of the 3'-5' exonuclease activity of NM23-H1 is metastasis suppressor function and there is cooperatively in the three enzymatic activities of NM23-H1 in suppressing the metastatic process (Zhang et al., 2011). A second NM23 gene designated NME2 was identified in 1991 (Stahl et al., 1991). The NME2 gene encodes the NM23-H2 protein which is 88% similar to NM23-H1. It has been determined that NM23 complexes in human erythrocytes are hetero-hexamers made up of NM23-H1 and H2 in varying proportions to form the erythrocyte NDP kinase (Gilles et al., 1991). NM23-H1 expression was inversely correlated with metastatic potential in experimental rodent cells and various human tumours such as breast, cervical, ovarian, pancreatic, gastric and bladder cancer, melanomas and hepatocellular carcinoma (MacDonald et al., 1995, Marino et al., 2012). The overexpression of exogenous NM23-H1 decreases the metastatic potential in multiple cancer cells and suppresses the tumour cell invasion and motility (Horak et al., 2007). NM23-H1 was identified as metastasis suppressor in various human cancers and its overexpression predicts better prognosis in patients (Lacombe et al., 1991, Leone et al., 1991, Ura et al., 1996, Chow et al., 2000, Nesi et al., 2001, Dursun et al., 2002, Boissan and Lacombe, 2006, Marino et al., 2012). In these cancers, the accumulation of intracellular NM23-H1 has been demonstrated via immunohistochemical studies (Marino et al., 2012).

#### **1.5.6 NM23-H1 in haematological malignancies**

High cytoplasmic expression of NM23-H1 and elevated serum NM23-H1 was correlated with more aggressive disease and poor treatment response in various haematological



malignancies including AML, Hodgkin's and non-Hodgkin's lymphoma (Okabe-Kado et al., 2012, Niitsu et al., 2003b, Niitsu et al., 2001a, Niitsu et al., 2004, Niitsu et al., 2011a, Niitsu et al., 1999, Niitsu et al., 2003c).

#### **1.5.6.1 NM23-H1 in AML**

NM23-H1 is overexpressed in various haematological neoplasms including AML, acute lymphoblastic leukaemia, myelodysplastic syndrome, and chronic myelogenous leukaemia (CML) in blast crisis (Yokoyama et al., 1998). The normal serum concentration of NM23-H1 in peripheral blood is < 10ng/ml whilst concentrations in AML patients' serum have been shown to reach up to 250ng/ml (Niitsu et al., 2000). NM23-H1 promoted AML cell survival via an indirect mechanism facilitated by a more mature population of progenitor cells (Figure 1.10)(Lilly et al., 2011). The immature CD34+ve leukemic stem cells (LSCs) overexpressing and secreting NM23-H1 are likely to be responsible for high serum NM23-H1 level(Willems et al., 1998, Lilly et al., 2011). The secreted NM23-H1 then binds to the more mature progenitor cells which respond by secreting cytokines and growth factors, e.g. interleukin 6 (IL6), IL1 $\beta$ , GCSF (Granulocyte colony stimulating factor), that promote the survival and proliferation of the LSCs(Lilly et al., 2011).The release of IL-6, IL-1 $\beta$  indicated a role for inflammation in NM23-H1 promotion of leukaemogenesis. Therefore, NM23-H1 is a potential target for AML treatment if we can identify mechanisms to inhibit extracellular NM23-H1 function in AML.

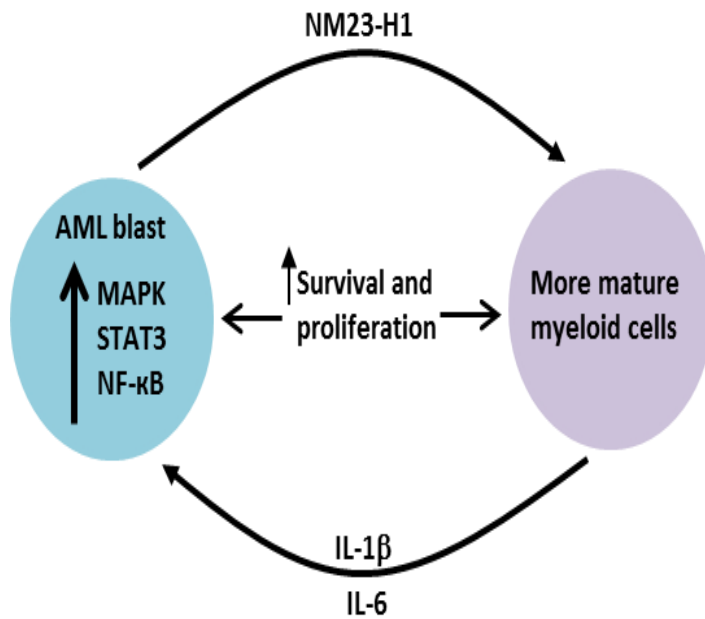


**Figure 1.10: Nm23-H1 promotes the AML blasts survival of through an indirect mechanism.** Nm23-H1 is released by AML blasts which bind to the more mature population of myeloid cells. This stimulates pro-inflammatory cytokine array secretion, from which IL-1 $\beta$  and IL-6 feedback to the immature AML cells promoting survival and proliferation via activating signalling pathways like MAPK, STAT3 and NF- $\kappa$ B. Adapted from (Lilly et al., 2015).

#### 1.5.6.2 NM23-H1 in DLBCL

As for AML, there is also strong evidence identifying a correlation between high NM23-H1 (>75ng/ml) in the plasma of patients with malignant NHL, low-grade and high-grade HL with worse prognosis (Niitsu et al., 1999, Niitsu et al., 2000, Niitsu et al., 2003b, Niitsu et al., 2004, Niitsu et al., 2006, Niitsu et al., 2011a, Bircan et al., 2008). Serum NM23 levels, cytoplasmic NM23 and/or cell surface NM23 were postulated to promote escape from apoptosis and treatment resistance due to its correlation with treatment responsiveness and prognosis (Niitsu et al., 2004).

Several studies have demonstrated that elevated NM23-H1 is associated with poor response to treatment and consequently poor prognosis (Niitsu et al., 1999, Niitsu et al., 2000, Niitsu et al., 2001a, Niitsu et al., 2004, Niitsu et al., 2011a). Univariate and multivariate analysis of known prognostic factors in aggressive lymphoma confirmed that the strongest independent factor-predicting prognosis was plasma/serum NM23-H1 levels, and it could be useful in prediction of overall survival (OS) and progression free survival (PFS) (Figures 1.11and 1.12) (Niitsu et al., 2004).

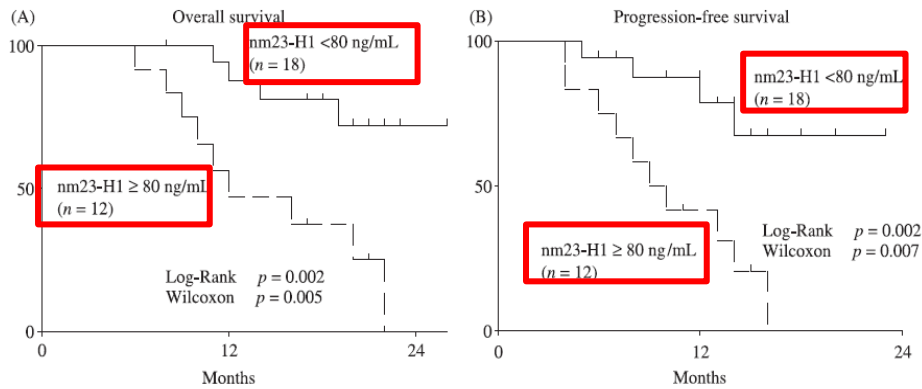


**Figure 1.11 Serum NM23-H1 and DLBCL survival.** (A) Overall survival and (B) Progression free survival (PFS) curves of elderly patients with relapsed DLBCL with high or low NM23-H1. The patients with a high level of NM23-H1 ( $\geq 80 \text{ ng/mL}$ ;  $n=12$ ) had a worse prognosis than patients with low level of NM23-H1 ( $\leq 80 \text{ ng/mL}$ ;  $n=18$ ) adapted from (Niitsu et al., 2006).

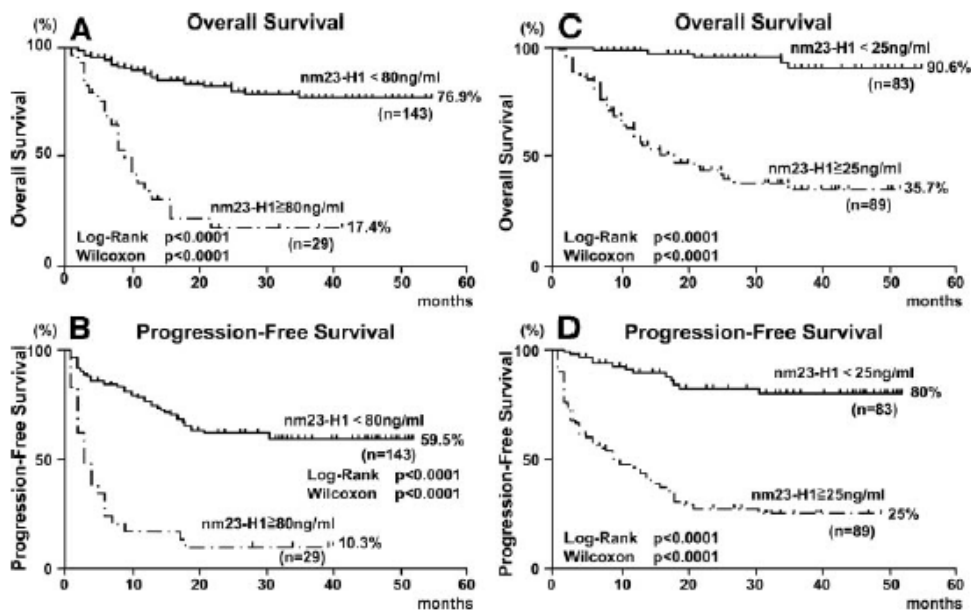


**Figure 1.12 Serum NM23-H1 and survival in DLBCL.** Overall survival curves (A and C) and progression-free survival curves (B and D) of patients with DLBCL. The patients were divided into high and low serum NM23-H1 levels by two cut-off values, i.e. 80 ng/mL (A and B) and 25 ng/mL (C and D). In both cut-off values, high NM23-H1 patients had shorter overall and progression-free survival periods than low NM23-H1 patients (Niitsu et al., 2004).

The higher cytoplasmic NM23-H1 expression in lymphoma cells is correlated with poor prognosis in patients who received RCycLOBEAP therapy. Patients with high cytoplasmic NM23-H1 required more aggressive treatments regimes than those with low cytoplasmic NM23-H1 expression (Niitsu et al., 2011b). Surface expression of NM23-H1 was also correlated to worse overall survival and progression-free survival in patients with aggressive lymphoma (Figure 1.13) (Niitsu et al., 2003a).

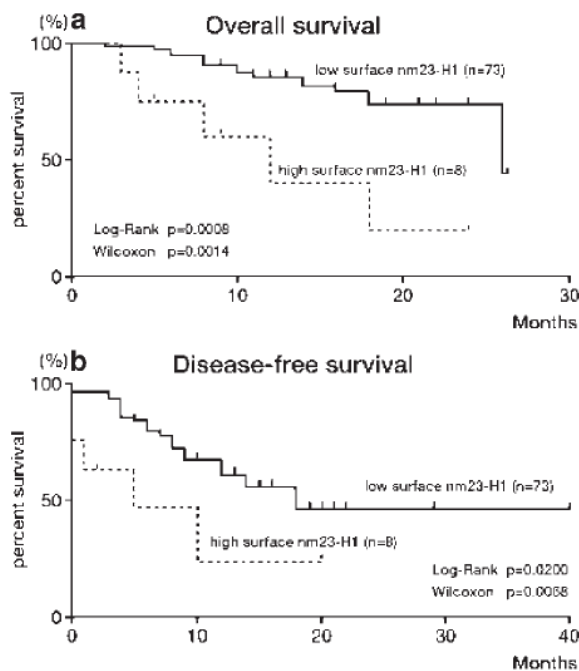


**Figure 1.13 Surface NM23-H1 expression and correlation with poorer survival in aggressive lymphomas.** Overall survival curves (A) and progression-free survival curves (B) of patients with aggressive lymphoma. The eight patients with high surface NM23-H1 had a worse prognosis than the 73 patients with low surface NM23-H1 expression. (Niitsu et al., 2003a)

Multivariate analysis also suggested that both cytoplasmic NM23-H1 and serum NM23-H1 could be a significant prognostic factor for DLBCL. However, higher serum NM23-H1 has been shown to correlate more strongly than cytoplasmic NM23-H1 levels with prognosis and is therefore a more useful prognostic factor (Figure 1.14) (Niitsu et al., 2004). Taken together, these studies suggest that higher levels of extracellular and/or intracellular NM23-H1 is associated with and possibly causative of a poor prognosis in lymphoma (Niitsu et al., 2001a, Niitsu et al., 2003a, Niitsu et al., 2011a, Lee et al., 2006b).

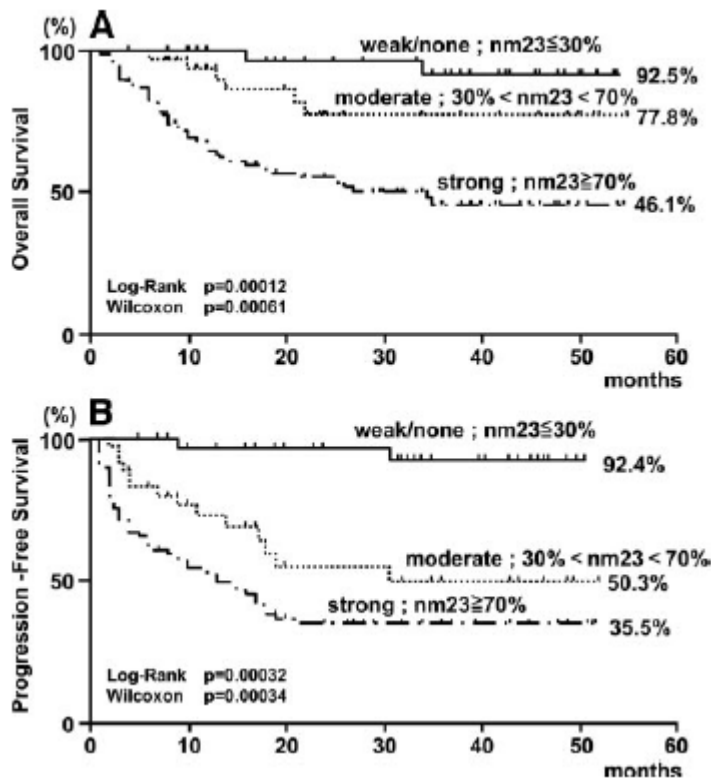


**Figure 1.14 Cytoplasmic NM23-H1 levels and DLBCL prognosis.** (A) Overall survival and (B) Progression free survival (PFS) curves of DLBCL patients DLBCL with strong, moderate or weak (none) NM23-H1 cytoplasmic expression. The patients with strong NM23-H1 cytoplasmic expression had a worse prognosis than patients with moderate or weak NM23-H1 cytoplasmic expression adapted from (Niitsu et al., 2004)

All of these data and studies measuring NM23-H1 in serum and in the tumour tissue of DLBCL patients confirm a positive correlation between elevated cytoplasmic expression of NM23-H1 and high serum concentrations (Niitsu et al., 2004). However, there is no mechanism known for how the NM23-H1 may be entering the plasma. Furthermore, there is no direct evidence that the serum NM23-H1 is derived solely from the lymphoma cells or whether other cells may secrete NM23-H1 in response to the tumour. It should be noted that in very few studies, were the levels of NM23-H2 studied. This may in part be due to lack of suitable antibodies and assays.

## The aim of this study

Our group have previously shown that human and bacterial NDK proteins are able to promote survival and proliferation of leukaemia cells (Lilly et al., 2011) and that this was mediated indirectly through cross-talk between the NM23-H1 producing CD34+ leukemic cells and more committed CD11b monocytic progenitors. Survival of the CD34+ cells was promoted through production of cytokines such as IL-6 and IL-1 $\beta$ .

The evidence is clear that NM23-H1 expression in tumour tissue and in the serum of DLBCL patients is associated with poor prognosis, however all these studies are correlative. Therefore, using a panel of DLBCL cell lines as a model system, the aims of this study were to:

1. Characterise NM23-H1 and NM23-H2 intracellular and extracellular expression at the mRNA and protein level. This includes determining whether DLBCL cells are able to bind extracellular NM23-H1 and take it up.
2. Generate CRISPR/Cas9 knockout (KO) models of NM23-H1 in the DLBCL cell lines and characterise the impact of the KO on DLBCL survival and proliferation *in vitro*.
3. Using the wild-type (WT) and NM23-H1 KO DLBCLs, determine whether the extracellular NM23-H1 produced by DLBCL cells is able to signal to other blood cells either in monoculture with conditioned media from DLBCL cell lines and also in co-culture experiments.
4. Study the impact of WT and NM23-H1 KO DLBCL cells on cytokine production by normal donor PBMCs and purified monocyte populations.

# **CHAPTER TWO**

## **MATERIALS AND**

## **METHODS**

## **2 Materials and methods**

### **2.1 Cell Culture**

#### **2.1.1 Maintenance of cell lines**

A panel of DLBCL and AML cell lines were used in these studies. The characteristics of the cell lines are summarised in Table 2.1. The cell lines are divided into two groups: the first group includes Farage, HT, U2932, SUDHL4, SUDHL5, SUDHL6 and KG1a which are maintained in RPMI 1640 (Invitrogen Gibco), supplemented with 10% v/v foetal bovine serum (FBS), 100 U/ml penicillin and 100U/ml streptomycin (complete media) (all Invitrogen Gibco). The second group includes OCILY1, OCILY3 and OCILY7 which are maintained in Iscove's modified Dulbecco's medium (IMDM) supplemented with 20% FBS, 100 U/ml penicillin and 100U/ml streptomycin (All Invitrogen Gibco). The cultures were incubated 37°C with 5% CO<sub>2</sub> in a humidified incubator. Cells were maintained in exponential phase i.e. cell density between 0.5-1.5x10<sup>6</sup> cells/ml, by passaging 1:3 every three days.

#### **2.1.2 Serum-free (ITS+) cultures of DLBCL cell lines**

For some of the experiments, DLBCL cell lines needed to be incubated in serum-free conditions. DLBCL cell lines were acclimatised to growth in serum-free conditions by gradually replacing FBS containing media with media (RPMI 1640 or IMDM) supplemented with 1% v/v ITS+ (Thermo Fisher) and 100 U/ml penicillin and 100U/ml streptomycin (All Invitrogen Gibco). This was done by taking cultures of cells in FBS containing complete media and feeding them with ITS+ media with each passage.



Cell line	ABC/GCB	Medium	Subculture	Doubling time	Harvest	Morphology	Immunology	Viruses	Year of origin	Disease
HT	GCB	85-90% RPMI 1640 + 10-15% FBS	Split ratio 1:3 to 1:5 every 3-4 days; seed out at ca. 0.3-0.5 x 10 <sup>6</sup> cells/ml; maintain at 0.5-1.5 x 10 <sup>6</sup> cells/ml	ca. 30-40 hours	ca. 1 x 10 <sup>6</sup> cells/ml	Small round cells growing as clumps in suspension	CD3 -, CD10 +, CD13 -, CD19 +, CD20 +, CD37 +, CD38 +, cyCD79a +, CD138 -, HLA-DR +	PCR: EBV -, HBV -, HCV -, HIV -, HTLV-I/II -, SMRV -	1983	Diffuse mixed lymphoma
U-2932	ABC	90% RPMI 1640 + 10% FBS	Split ratio 1:4 twice a week; seed out at ca. 0.5 x 10 <sup>6</sup> cells/ml; maintain at 1-1.5 x 10 <sup>6</sup> cells/ml	ca. 50 hours	ca. 2 x 10 <sup>6</sup> cells/ml	Small round cells growing singly and in clusters in suspension	CD3 -, CD10 +, CD13 -, CD19 +, CD20 +, CD37 +, CD38 +, cyCD79a +, CD80 +, CD138 +, HLA-DR +	PCR: EBV -, HBV -, HCV -, HIV -, HTLV-I/II -, SMRV -	1984	Non-Hodgkin's B cell lymphoma
FARAGE		90% RPMI 1640 + 10% FBS	Split ratio 1:3 every 2-3 days; maintain at 0.3-3 x 10 <sup>6</sup> cells/ml	ca. 24-36 hours	ca. 1.5 x 10 <sup>6</sup> cells/ml	Small round cells growing in clumps in suspension	CD10 +/-; CD11a +; CD19 +; CD20 +; CD21 +; CD22 +; CD23 +; CD29 +; CD38 +; CD39 +; CD40 +; CD44 +; CD54 +; CD58; CD23 -; HLA DR+	PCR: HBV -, HCV -, HIV -	1990	Non-Hodgkin's B cell lymphoma
OCILY1	GCB	80% Iscove's MDM + 20% FBS	Split ratio 1:2 every 2-3 days; seed out at ca. 0.5 x 10 <sup>6</sup> cells/ml; maintain at 0.5-2 x 10 <sup>6</sup> cells/ml	ca. 50-60 hours	ca. 2.5 x 10 <sup>6</sup> cells/ml	Small round to polymorph cells growing singly in suspension	CD3 -, CD10 +, CD13 -, CD19 +, CD20 +, CD34 -, CD37 +, CD38 +, CD80 +, CD138 -, HLA-DR -	PCR: EBV -, HBV -, HCV -, HIV -, HTLV-I/-II -	1983	B-cell non-Hodgkin lymphoma (B-NHL; diffuse large cell.
OCILY3	ABC	80% Iscove's MDM + 20% FBS	Split ratio 1:3 to 1:5 every 2-3 days; seed out at ca. 0.1-0.2 x 10 <sup>6</sup> cells/ml	ca. 24 hours	ca. 0.9 x 10 <sup>6</sup> cells/ml	Small round cells growing singly or in clumps in suspension	CD3 -, CD10 -, CD13 -, CD19 -, CD20 +, CD34 -, CD37 +, CD38 +, cyCD79a +, CD80 +, CD138 -, HLA-DR +	PCR: HBV -, HCV -, HIV -	1983	B-cell non-Hodgkin lymphoma (B-NHL; diffuse large cell.
OCILY7	GCB	80% Iscove's MDM + 20% FBS	Split ratio 1:3 every 2 days; maintain at 0.5-3 x 10 <sup>6</sup> cells/ml; seed out at ca. 0.3-3 0.5 x 10 <sup>6</sup> cells/ml	ca. 15 hours	ca. 3.5 x 10 <sup>6</sup> cells/ml	Small round to polymorph cells growing singly or in clusters in suspension	CD3 -, CD10 +, CD13 -, CD19 +, CD20 +, CD34 -, CD38 +, CD80 +, CD138 -, HLA-DR -	PCR: HBV -, HCV -, HIV -	1984	B-cell non-Hodgkin lymphoma (B-NHL; diffuse large cell.
SUDHL4	GCB	80-90% RPMI 1640 + 10-20% FBS	Split ratio 1:2 to 1:3 every 2 days; seed out at ca. 0.5 x 10 <sup>6</sup> cells/ml; maintain at 0.5-1.8 x 10 <sup>6</sup> cells/ml	ca. 40 hours	ca. 1.0-1.5 x 10 <sup>6</sup> cells/ml	single round cells growing singly in suspension	CD3 -, CD10 +, CD13 -, CD19 +, CD20 +, CD34 -, CD37 +, CD38 +, cyCD79a +, CD138 -, HLA-DR +	PCR: EBV -, HBV -, HCV -, HIV -, HTLV-I/II -, SMRV -	1976	Non-Hodgkin's B cell lymphoma
SUDHL5	GCB	80-90% RPMI 1640 + 10-20% FBS	Split ratio 1:2 to 1:5 every 2-3 days; seed out at ca. 0.5 x 10 <sup>6</sup> cells/ml; maintain at 0.1-1.0 x 10 <sup>6</sup> cells/ml	ca. 40 hours	ca. 1.5 x 10 <sup>6</sup> cells/ml	round to polymorph cells growing in clumps	CD3 -, CD10 +, CD13 -, CD19 +, CD20 +, CD37 +, cyCD79a +, CD80 -, HLA-DR +	PCR: EBV -, HBV -, HCV -, HIV -, HTLV-I/II -	1978	large cell lymphoma; diffuse mixed histiocytic and lymphoma
SUDHL6	GCB	80-85% RPMI 1640 + 15-20% FBS	Split ratio 1:2 to 1:3 every 3 days; seed out at ca. 0.8 x 10 <sup>6</sup> cells/ml; maintain at 0.4-1.0 x 10 <sup>6</sup> cells/ml	ca. 35-40 hours	1.5-2.0 x 10 <sup>6</sup> cells/ml	small single cells growing singly or in clusters in suspension	CD3 -, CD10 +, CD13 -, CD19 +, CD20 +, CD34 -, CD37 +, CD38 +, CD80 +, CD138 -, HLA-DR+	PCR: EBV -, HBV -, HCV -, HIV -, HTLV-I/II -, SMRV -	1977	large cell lymphoma; diffuse mixed histiocytic and lymphocytic lymphoma; follicular B cell lymphoma

**Table 2.1: Summary of cell lines used in this study.**

### **2.1.3 Long-term storage of cells in liquid nitrogen**

To store cells long-term,  $1 \times 10^7$  cells were centrifuged at 230xg for 5 minutes (FALCON 6/300, MSE, London, U.K.) and the cell pellet resuspended in 1ml freezing mix (see Appendix A) The cell suspension was pipetted into labelled 1.8ml cryovials (Nunc) and frozen down slowly by placing vials in a sealed polystyrene container which was stored at -20°C for 60 minutes, then -80°C overnight and liquid nitrogen the next day. For short-term storage, vials were stored at -80°C.

### **2.1.4 Recovery of cell lines from liquid nitrogen**

Frozen vials were rapidly thawed by placing in a 37°C water bath for 1-2mins. The cell suspension was transferred to a 30ml universal tube and 1.0ml of cold complete media added gradually drop by drop with gentle agitation. The cell suspension was allowed to stand for 1 minute before adding a further with 1ml, 2ml and 10ml. This gradually dilutes the freezing mix and prevents cellular osmotic shock and cell death. After addition of media, the cells were pelleted by centrifugation at 230xg for 5 minutes and the supernatant discarded. The cell pellet was resuspended in 2ml cold complete media and transferred to 24 well plates. Cells were incubated at 37°C with 5% CO<sub>2</sub> until the cells had recovered sufficiently to be transferred into a 25cm<sup>2</sup> flask.

### **2.1.5 Purification of normal donor peripheral blood mononuclear cells (PBMCs)**

Normal donor blood (20-100ml) was donated by normal healthy adult donors after informed consent with ethical approval (University of Birmingham, ERN\_17-0065). Donors' age was between (18-60) years, both male and female. At the date of collecting blood samples, the donors did not use any medications or anti-inflammatories. Blood samples were collected into 50ml polypropylene tubes containing 9ml sodium citrate/45ml blood as an anticoagulant and allowed to stand at room temperature for >30mins. They were diluted 1:1 with RPMI 1640 supplemented with 100U/ml penicillin, 100µg/ml streptomycin (Wash media). 15ml Ficoll-Paque Plus (Amersham) was pipetted into 50ml tubes and the diluted blood carefully layered on top. After centrifugation at 400xg for 40 minutes at room temperature without the brake, peripheral blood mononuclear cells (PBMCs) were visible as

a white band just above the Ficoll-Paque layer. Some of the plasma was removed to gain easier access and the PBMC layer carefully pipetted off into a clean 50ml tube. PBMCs were washed with 3x volume Wash Media and centrifugation at 200xg for 10mins. The wash was repeated 3 times using at least 25mls Wash Media each time to remove platelets. The PBMCs were resuspended in 20ml Wash Media and counted using a haemocytometer.

#### **2.1.6 Magnetic sorting of cells**

For some of the experiments, specific blood cells were needed. Miltenyi Biotec MACS magnetic sorting was used to purify the populations. This involves labelling cells with antibodies conjugated to magnetic beads and then separating them from non-labelled cells in a magnetic field. A CD19+ positive selection kit was used to purify B cells which were used as normal controls for DLBCLs. Monocytes were purified using a Pan-Monocyte negative selection kit (MACS Miltenyi Biotec/ Pan monocyte isolation kit-Human). The protocol for B cells and monocytes was initially similar.  $2 \times 10^7$  PBMCs were washed in 10ml cold MACS buffer (see Appendix A) and centrifuged at 374xg for 5mins. The cell pellet was resuspended in 320 $\mu$ l cold MACS buffer, 80 $\mu$ l antibody-bead conjugates added and incubated at 4°C for 15 minutes. The cells were washed with 0.5ml MACS buffer, centrifuged and then resuspended in 0.5ml cold MACS buffer. In the meantime, MACS LS columns (Miltenyi Biotec) were placed in the magnetic field of a MACS separator magnet (Miltenyi Biotec) and washed using 0.5ml cold MACS buffer. Once the MACS buffer had dripped through, the cell suspension was pipetted into the column. For negative pan-monocyte purification, the flow-through (negative fraction) which contains the monocytes was collected into a 30ml universal tube. The column was washed with 3x 1ml MACS buffer and the flow-through collected. Cells were pelleted by centrifugation at 374xg for 5mins, washed with 5ml complete RPMI 1640 media (Wash media) and centrifuged again. The final cell pellet was resuspended in RPMI 1640 media and counted using a haemocytometer. For CD19+ B cells which are positively selected, the flow-through (negative fraction) and 3 x 1ml MACS buffer washes were discarded. The column was then removed from the magnet, 5ml MACS buffer added, the column plunger firmly inserted, and the positive fraction collected in a 15ml tube.

The positive fraction was counted, and the cells pelleted before resuspending in required media.

#### **2.1.7 Maintenance and treatment of CD40L expressing on murine L fibroblasts**

CD19<sup>+</sup> B cells were stimulated into cell cycle and proliferation using a combination of CD40L expressed on murine L fibroblasts and interleukin-4 (IL-4). Murine L cells had previously been stably transfected with plasmids encoding CD40 ligand (CD40L-L cells) (Gagro et al., 2000) (kind gift from Professor John Gordon). CD40L-L cells were grown in T75 flasks in RPMI 1640 supplemented with 100U/ml penicillin, 100µg/ml streptomycin and 10% v/v foetal bovine serum (complete media) (all Invitrogen Gibco). Cultures were maintained in humidified incubators at 37°C with 5% CO<sub>2</sub>. When cultures were ~80% confluent, the media was removed, cells washed with 10ml warm PBS and 2ml 1xTrypsin EDTA added (Gibco). Following incubation at 37°C with 5% CO<sub>2</sub> for 3-5mins, 8 ml of complete media was added and pipetted vigorously several times to produce a single cell suspension. 1ml of this cell suspension was left in the flask and 10ml fresh RPMI complete media added.

#### **2.1.8 Mitomycin C treatment of CD40L-L cells**

In order to arrest proliferation, CD40L- L cells were treated with mitomycin C (MC) (Sigma). CD40L-L cells were grown to 100% confluence in T75 flasks. The media was replaced with 10ml RPMI complete media supplemented with 20µg/ml mitomycin C and cells incubated for 3 hours at 37°C with 5% CO<sub>2</sub>. The monolayer was washed 3 times with 10ml warm PBS, trypsinised as described in section 2.1.7 and counted. Aliquots of 5x10<sup>6</sup> cells were frozen down at -80°C as described above, to destroy any residual mitomycin C.

#### **2.1.9 Expansion of CD19<sup>+</sup> B cells on CD40L-L cells**

Frozen CD40L-L cells were thawed from -80°C as described in section 2.1.4 and resuspended at 1x10<sup>5</sup> cells/ml in RPMI complete media in 24 well plates, allowing 1ml per well. Cells were allowed to attach over night at 37°C with 5% CO<sub>2</sub>. The next day, the media was removed and 1ml of CD19<sup>+</sup> cells diluted to 1x10<sup>6</sup> cells/ml in RPMI complete media, with the addition of 1ng/ml IL-4 (R&D systems) added to the stromal L-cells. Cells were maintained and grown for 8 days, with fresh media added at day 3-4.

#### **2.1.10 Preparing conditioned media (CM) from DLBCL cell lines**

For some experiments, conditioned media from DLBCL cell lines was used for culturing normal donor cells. To prepare the CM,  $5 \times 10^6$  exponentially growing DLBCL cells were centrifuged at 230xg for 5mins at room temperature. The supernatant was discarded (to remove any NM23-H1 already present) and cell pellets resuspended in 10ml warm complete media before incubating for 96hrs at 37°C with 5% CO<sub>2</sub> in a humidified incubator. The cultures were then harvested into 15ml polypropylene tubes and centrifuged at 260g for 5mins. The supernatant was filtered through a 0.2µm syringe filter (Acrodisc, Pall) and stored at 4°C until used. Conditioned media was prepared fresh when needed and used within 24hrs of preparation.

#### **2.1.11 Culturing normal donor cells in Conditioned media (CM)**

Purified PBMCs or monocytes were resuspended in conditioned media from DLBCL cells (with or without recombinant NM23-H1 protein) at a concentration of  $1 \times 10^6$  cells/ml. Experiment volumes and day of analysis varied between the different experiments and is described in the relevant sections. For experiments in 96 well plates, 200µl of resuspended cells were added per well.

#### **2.1.12 Co-Culture of normal donor monocytes with HT/KG1a cells**

Purified PBMCs or monocytes were resuspended in ITS+ media alone or in combination with wild-type (WT) or NM23-H1 knockout (KO) cells in 1:1 ratio at a concentration of  $1 \times 10^6$  cells/ml in 200µl per well of 96 well plates. In some cases, exogenous recombinant NM23-H1 (rNM23-H1) was added at 2µg/ml.

#### **2.1.13 Culturing of normal donor monocytes with HT/KG1a cells in transwell**

Purified PBMCs or monocytes were resuspended in ITS+ media at a concentration of  $1 \times 10^6$  cells/ml. In parallel, WT or NM23-H1 KO cells HT/KG1a cells were resuspended at  $1 \times 10^6$  cells/ml with or without exogenous recombinant NM23-H1 (rNM23-H1) at 2µg/ml. Using Transwell (Millicell/Cell culture inserts) 24 well plates, 600µl of HT cell suspension were pipetted in the bottom of each well. The cells were incubated for 6 hours before the addition

of monocytes to the transwell, to allow the secretion of Nm23-H1. The transwell insert was carefully placed in each well carefully and 200µl of PBMCs/monocytes cell suspension pipetted into the transwell. Cultures were incubated at 37°C with 5% CO<sub>2</sub> in a humidified incubator.

## **2.2 Flow cytometry assays**

A range of flow cytometry assays were used. Samples were collected in FACS tubes (Sarstedt, 5ml 75x12mm) and analysed using a Becton Dickinson (BD) FACSCalibur using BD CellQuest Pro Software.

### **2.2.1 Cell surface staining and flow cytometry for immunophenotyping**

PBMCS and Monocytes were immunophenotyped at the point of purification and also after incubation in the different experiments e.g. co-culture or in the presence of rNM23-H1. In general, 100µl of cell suspension was pipetted into a FACS tube and immunophenotyping antibody or matched isotype control antibodies added together with FCR block (5µl) (MACS Miltenyi Biotech). Antibodies and their matched isotypes control are shown in Table 2.2. After mixing well, samples were incubated at room temperature for 10mins in the dark. To remove unbound antibody, 2ml cold PBS was added and samples centrifuged at 230xg for 5mins and the supernatant poured off. The remaining cell suspension was mixed briefly. 200µl FACS Fix (see Appendix A) was added and samples were stored at 4°C wrapped in foil to protect from light. To enumerate cell numbers, 10µl fluorescent microsphere Counting beads (BD Biosciences) were added to each sample before analysing. Forward scatter and side scatter were used to define the viable cell population. Isotype control antibody stained samples were used as negative controls to define gates for positive staining.

Cell type	Antibody	Fluorophore	Matched isotype control	Volume per FACS tube
KG1a cells	CD34	APC	Ms. IgG2b	2 $\mu$ L
B-cells, granulocytes and monocytes.	CD19	APC	Ms. IgG2b	2 $\mu$ L
	CD19	FITC	Ms. IgG1	2 $\mu$ L
	CD11b	PE	Ms. IgG2a	2 $\mu$ L
	CD14	FITC	Ms. IgG1	2 $\mu$ L
	CD16	APC	Ms. IgG2b	2 $\mu$ L
T cells	CD3	PE	Ms. IgG2a	2 $\mu$ L
	CD3	FITC	Ms. IgG1	2 $\mu$ L
	CD8	FITC	Ms. IgG1	2 $\mu$ L
	CD4	APC	Ms. IgG2b	2 $\mu$ L

**Table 2.2 Antibodies used for cell type identification by flow cytometry.** *Ms.* = Mouse, *APC*= Allophycocyanin, *PE*= Phycoerythrin and *FITC*= Fluorescein Isothiocyanate.

### 2.2.2 Direct staining and flow cytometry for surface bound NM23-H1 staining

Exponentially growing cells (100 $\mu$ L) from each cell line were aliquoted into 2 separate labelled FACS tubes and 2 $\mu$ L of fluorophore-conjugated anti-NM23-H1 monoclonal antibody (Table 2.3) or matched isotype added. After incubating at room temperature for 20mins in the dark place, cells were washed with 2mL cold PBS and the cell pellet resuspended in 300  $\mu$ L FACS fix (see Appendix A). Samples were stored wrapped in foil at 4°C until analysis.

Primary Antibody	Matched Isotype Control	Volume per FACS Tube
<b>NM23-H1 (37.6) FITC-conjugated (GeneTEX)</b>	Ms IgG1 (BD Biosciences)	2µL
<b>NM23-H1 (C-20) FITC conjugated (Santa Cruz Biotech)</b>	Ms IgG1 (BD Biosciences)	2µL

***Table 2.3: Antibodies used for NM23-H1 surface staining of cell lines***

### **2.2.3 Flow cytometry for detecting intracellular NM23-H1 protein**

In order to analyse intracellular NM23-H1 protein expression, cells were permeabilised and fixed (Cell Permeabilization kit) (Life technologies). A volume of 100µl containing  $1 \times 10^6$  cells was pipetted into FACS tubes. To the tube, 100µl of Reagent A (Fixation Medium) was added and incubated for 15 minutes in the dark at room temperature. Cells were washed once with 3 mL wash medium (PBS + 5% FBS) and centrifuged for 5 minutes at 200xg. The supernatant was poured off and cells resuspended in the residual liquid by vortexing. 100µl Reagent B (Permeabilisation Medium) was added to the tubes together with anti- NM23-H1 antibody (C-20, Santa Cruz Biotech) or corresponding isotype control (Ms IgG1), mixed by vortexing for 1–2 seconds and incubated for 20 minutes in the dark at room temperature. Samples were washed once with 3 mL wash medium (PBS + 5% FBS), centrifuged for 5 minutes at 300xg and the supernatant poured off. Cells were fixed with 200µl FACS Fix and analysed by flow cytometry within 18hrs.

### **2.2.4 Measuring cell counts using flow cytometry**

Cell cultures were set up based upon the required experimental design. At defined timepoints a fixed volume of cell suspension (100-200µl) was collected into a FACS tube. In some instances, cells were stained with immunophenotyping antibodies and FACS Fix added (see Appendix A). For measurement of cumulative cell growth, 300µl of cells were placed in a FACS tube, washed with 2mL cold PBS Cells were resuspended in 300µL FACS fix (see Appendix A). Fluorescent microsphere Cyto Cal Counting beads (BD Biosciences: 1,019 beads



per  $\mu\text{l}$ ) (10 $\mu\text{L}$ ) were added to every tube before analysis. Dotplots of Forward Scatter and Side Scatter were used to gate on viable cells (R1) and on the beads (R2). Collection was stopped when 20,000 events had been collected in the viable gate. The cell density per ml was calculated using the following formula:

$$\left( \frac{\text{Total viable cells counted (R1)}}{(\text{Beads in R2}/10,190 \text{ (total beads added)}) \times \text{vol of cells } (\mu\text{l})} \right) \times 1000 = \text{cells/ml}$$

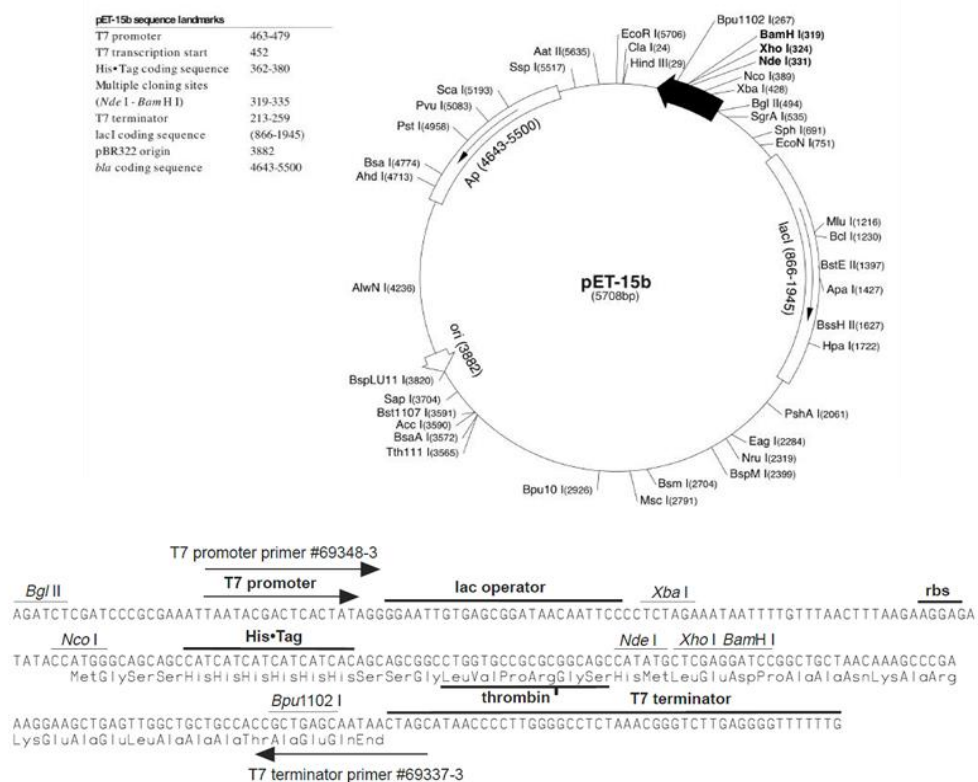
Where volume of cells is the volume added to the FACS tube (100-200 $\mu\text{l}$ ). To calculate cumulative cell count, the viable cell density was multiplied by culture volume (ml) at the start of the experiment and dilution factor for each passage, i.e. for a 1:3 dilution then multiply by 3.

## 2.3 Protein Analysis

### 2.3.1 Recombinant NM23-H1 (rNM23-H1) production

#### 2.3.1.1 pET-15b-NM23-H1 vector construct

Recombinant NM23-H1 was expressed from the pET-15b expression vector (Novagen, Merck Chemicals Ltd) (Figure 2.1). The NM23-H1 protein coding region had been cloned into the Nde1 and BamH1 restriction sites downstream and in-frame of a 6xHis tag so that it produced an N-terminal His-tagged protein (construct created by Q.T. Luong, 2007). Expression of recombinant protein from the T7 promoter was induced using isopropyl  $\beta$ -D-1-thiogalactopyranoside (IPTG).



#### pET-15b cloning/expression region

**Figure 2.1 pET15b expression vector.** The NM23-H1 open reading frame was cloned between the NdeI and BamHI sites to be in-frame with the 6xHis tag. Ampicillin resistance is encoded by the beta-lactamase gene (Ap). LacI encodes the lac repressor which suppresses expression by binding to the lac operator. Addition of isopropyl  $\beta$ -D-1-thiogalactopyranoside (IPTG) overcomes repression and induces expression from the T7 promoter. Addgene (published plasmid map).

### **2.3.1.2 Transformation of BL21 (DE3) *E.coli* bacterial cells**

The pET-15b-NM23-H1 vector construct was transformed into competent *E. coli* BL21 (DE3) (Bioline) cells. BL21 (DE3) *E.coli* cells express an IPTG inducible T7 RNA polymerase gene and not expresses the Lon and OmpT bacterial proteases. Competent cells (50µl) were thawed on ice, 50ng of pET-15b-NM23-H1 vector construct added and the DNA allowed binding to cells by incubation on ice for 5 minutes. Cells were heat-shocked at 42°C for 30secs in a water bath and then returned to ice for 2mins. 250µl of SOC medium (Sigma) was added and the reactions incubated at 37°C for 1 hour with shaking at 220rpm. To select for transformants, 200µl of transformation mix was spread on to LB plates (see Appendix A) supplemented with 100µg/ml ampicillin (+amp) (Sigma) and incubated at 37°C overnight. Single colonies were picked the following day and used to inoculate 5ml LB broth + amp (See Appendix A) before incubating overnight at 37°C with shaking at 220rpm. The next day glycerol stocks were made by adding 200µl of 100% glycerol to 800µl of cells and stored at -80°C until use.

### **2.3.1.3 Purification of recombinant NM23-H1 protein**

Streaks from frozen glycerol stocks of BL21 (DE3):pET15b-NM23-H1 cells were used to inoculate 5ml LB +amp and cultures incubated overnight at 37°C with shaking at 220rpm. The following morning, the cultures were diluted 1:50 in 200ml LB +amp and incubated with shaking at 37°C until the cultures reached an OD<sub>600nm</sub> of 0.6. Then 1mM IPTG (Sigma) was added to induce NM23-H1 expression and cultures incubated at 37°C with shaking for 3hrs. Bacteria from the 200ml cultures were pelleted by centrifuging at 6000×g at 4°C for 15 minutes and the supernatant discarded. The wet weight of the pellet was measured and 5ml of BugBuster™ containing 1µl/ml benzonase (Novagen) added per mg of wet weight. Bacteria were completely resuspended and mixed at room temperature for 20 minutes before centrifugation at 6000×g at 4°C for 20 minutes to pellet the membranes. The supernatant containing soluble protein was purified using the Bugbuster Ni-NTA His-Bind Purification kit (Novagen) according to manufacturer's instructions. Briefly, 1ml of His-Bind Resin was added to a chromatography column and the storage buffer allowed passing through the column. The resin was washed with 1.5ml sterile dH<sub>2</sub>O, 2.5ml 1xCharge Buffer,

followed by 1.5ml 1x Binding Buffer. Bacterial cell extract was pipetted into the column and allowed to drip through under gravity flow before washing with 5ml 1x Binding Buffer followed by 3ml 1xWash Buffer. Protein was eluted with Elution Buffer (EB) in 3 separate 1ml fractions. The purity of the recombinant NM23-H1 protein was assessed by SDS-PAGE and Coomassie blue staining (see section 2.3.9) of 30µl of eluted protein. The protein was labelled with Alexa647 by another student in the lab (Joy Harris-Folb in January 2016 the and the recombinant protein samples was fluorescent labelled by using the molecular Probes' Alexa Fluor 647 labelling kit according to manufacturer's instructions).

#### **2.3.1.4 Determination of rNm23-H1 concentration**

Protein concentration was determined using a Bio-Rad Protein Assay (Bio-Rad Laboratories, Hemel Hempstead, UK) according to manufacturer's instructions. Briefly, 0, 2.5, 5, 7.5, 10, and 15µl of BSA protein standards at 100µg/ml were pipetted in duplicate wells of a 96 well plate and made up to 160µl with distilled water. Eluted rNm23-H1 protein was diluted 1:5 in elution buffer (EB) and 1µl of this was added to 159µl of distilled water in duplicate wells. Bio-Rad reagent (40µl) was added to all wells, mixed and incubated at room temperature for 5 minutes. Optical density (OD) was read at 595nm, and the protein concentration of the rNm23-H1 elution fractions calculated from a standard curve of OD<sub>595nm</sub> against protein concentration of BSA standards.

#### **2.3.2 Analysis of DLBCL extracellular NM23-H1 protein**

From each exponentially growing cell line,  $4.5 \times 10^6$  cells were aliquoted into universal tubes, and centrifuged at 230xg for 5 minutes. The supernatant was poured off and the cell pellet resuspended in 4.5ml fresh media. 1ml of cell suspension was pipetted into each of 4 wells of 48 well plates. 1 ml PBS was added into all the wells around the edge of 48 well plates. After overnight incubation 3 x 1ml of cell suspension was harvested into 3 eppendorf tubes (3 repeat per cell line) and the samples centrifuged at 6000xg for 10 seconds. Supernatants were transferred into fresh Eppendorf and stored at -20°C.

### **2.3.3 DLBCL protein sample preparation**

From exponentially growing cell lines,  $1-5 \times 10^6$  cells were aliquoted into eppendorf tubes and washed with 1 ml cold PBS. Cell pellets were resuspended in 200  $\mu$ L RIPA buffer (see Appendix A) supplemented with 1X EDTA-free protease inhibitor cocktail (Sigma) and incubated on ice for 30mins before freezing at  $-20^{\circ}\text{C}$  overnight to allow lysis to complete. Samples were centrifuged at 6000xg for 10 minutes and the supernatant collected and stored at  $-20^{\circ}\text{C}$ .

### **2.3.4 Protein determination**

Protein concentration was measured using the Bio-Rad Dc Protein Assay (Bio-Rad). 2 $\mu$ L BSA standards (0, 0.625, 1.25, 2.5, 5 and 10mg/ml) and 2 $\mu$ L protein sample were added to duplicate wells in a 96 well plate. Following addition of 25 $\mu$ L of solution 'A' (made by adding 20 $\mu$ L reagent S to each 1ml of reagent A) to each well, 200 $\mu$ L of reagent B was added to all the wells before mixing by pipetting gently up and down. After 15 minutes incubation, plates were read in a spectrophotometer (Perkin-Elmer Victor X3 plate reader) at 690 nm. A standard curve was plotted of BSA standards against fluorescence and the equation of the line used to calculate the concentrations of protein samples.

### **2.3.5 Protein sample preparation for western blotting**

*For cell lysates:* 20 $\mu$ g protein was mixed with 5 $\mu$ L 4x SDS gel loading buffer (see Appendix A) to a final volume of 20 $\mu$ L in a 0.2ml tube, heated to  $70^{\circ}\text{C}$  for 10 minutes in a PCR machine and centrifuged briefly to collect the sample.

*For conditioned media:* 24 $\mu$ L of conditioned media and 8 $\mu$ L 4x SDS gel loading buffer (see Appendix A) were mixed together in a 0.2ml tube, heated to  $70^{\circ}\text{C}$  for 10 minutes in a PCR machine and centrifuged briefly to collect the sample. 20 $\mu$ L were used for SDS-PAGE.

*For recombinant NM23-H1:* 5 $\mu$ L of eluted protein from each elution fraction was mixed with 5 $\mu$ L 4x SDS gel loading buffer (see Appendix A) to a final volume of 20 $\mu$ L in a 0.2ml tube, heated to  $70^{\circ}\text{C}$  for 10 minutes in a PCR machine and centrifuged briefly to collect the sample.

### **2.3.6 Sodium dodecyl sulphate –polyacrylamide gel electrophoresis (SDS-PAGE)**

Discontinuous 1.5mm SDS-polyacrylamide gels were prepared with 12.5% acrylamide (see Appendix A) using the Mini-Protean 3 gel system (Bio-Rad). After incubation at room temperature for 30 minutes to fully polymerise the acrylamide, stacking gel solution (see Appendix A) was added and 10 well 1.5mm combs inserted. Once completely set, gels were clipped into the mini-Protean 3 gel electrophoresis frame and the tank filled with 1x SDS-PAGE running buffer (see Appendix A). Prepared protein samples/conditioned media and 5µl BLUEye Prestained Protein Ladder (Geneflow Ltd) were loaded onto the gel and electrophoresed at 120V with 1x SDS gel running buffer (see Appendix A) for 60-70 minutes.

### **2.3.7 Semi-dry protein transfer**

Polyvinylidene fluoride (PVDF) membrane (Millipore, Watford, U.K.) cut to 7cm x 9cm was soaked in methanol (Fisher) for 10 seconds, dH<sub>2</sub>O for 10 seconds and equilibrated in 1x transfer buffer (see Appendix A) for 5 minutes. Semi-dry transfer was carried out by placing 6 pieces of 3mm filter paper (10x8cm) soaked in 1x transfer buffer onto the anode plate of a Bio-Rad Semi-Dry Transfer cassette (Bio-Rad). The equilibrated PVDF membrane was layered onto the filter paper followed by the gel and a further 6 pieces of 3MM filter paper soaked in 1x transfer buffer. Transfer was carried out at 25V for 1 hour.

### **2.3.8 Immunodetection of proteins**

After transfer, the membrane was blocked for 15 minutes at RT in 5% w/v skimmed milk powder in Tris-Buffered Saline (TBS) with Tween 20 (TBS-T) (5% blocking solution) (see Appendix A). Primary antibody (Table 2.4) was diluted in 5% blocking solution and the membrane incubated overnight at 4°C with rocking. After overnight incubation, membranes were washed 3 times for 5 minutes in TBS-T with rocking at 70rpm on a gyro-rocker (Scientific laboratory supplies). The membrane was incubated for 1 hour at RT with IRDye® 800CW anti-Rabbit IgG and/or IRDye® 700LT anti-Mouse IgG antibodies (both LI-COR) diluted 1:10000 in 5% blocking solution before 3 washes in TBS-T with 0.01% Sodium dodecyl sulphate (SDS) and a further wash in TBS (see appendix A). All washes were 5 minutes at RT with rocking at 70rpm. Protein bands were visualised and quantified using LI-COR Odyssey®

CLx Infrared Imaging System and Image J software. Protein levels were normalised for loading using the  $\beta$ -actin signal.

Primary Antibody	Dilution for WB	Secondary Antibody	Dilution
NM23-H1 (C20) antibody rabbit polyclonal (Santa Cruz Biotech)	1:1000	IRDye® 800 Anti-Rabbit IgG LI-COR GmbH	1:10000
Anti-NM23A antibody mouse monoclonal [AT5F4] to NM23A (Abcam Biotechnology company)	1:1000	IRDye® 700 Anti-Mouse IgG LI-COR GmbH	1:10000
NM23-H2 (I-15) antibody goat polyclonal (Santa Cruz Biotech)	1:1000	IRDye® 800 Anti-Goat IgG LI-COR GmbH	1:10000
Anti-NME2 antibody rabbit monoclonal [EPR8351] to NME2 (Abcam Biotechnology company)	1:1000	IRDye® 800 Anti-Rabbit IgG LI-COR GmbH	1:10000

***Table 2.4 of antibodies used in western blotting***

### **2.3.9 Coomassie blue staining**

For analysis of purity of rNM23-H1, after completion of electrophoresis, gels were covered with Coomassie blue stain (see Appendix A) and incubated at room temperature with gentle mixing for a minimum of 3hrs. Non-specific staining was removed by replacing the stain with Destain solution (see Appendix A) and incubating overnight with gentle rocking. The proteins on the gel were visualised using a GeneFlash transilluminator (GeneFlow).

## **2.4 Quantitative real-time polymerase chain reaction (QRT-PCR)**

### **2.4.1 RNA extraction**

A PBS-washed pellet of  $1-5 \times 10^6$  cells was used to extract RNA using a Qiagen RNeasy mini kit (Qiagen, Crawley, U.K.) according to the manufacturer's instructions. Cell pellets were

resuspended in 350µl buffer RLT. The lysed samples were centrifuged through a QIAshredder spin column to homogenise samples. One volume of ethanol 70% (Fisher Loughborough, U.K.) was added to the samples and the entire mixture (700µl) added to an RNeasy mini column. The column was centrifuged for 15 seconds at 3300xg in a microfuge, the supernatant was poured off. The column was washed with addition of 350µl buffer RW1 and the column centrifuged for 15 seconds at 3300xg in a microfuge. To remove DNA from the sample, 10 µl of DNase I stock solution was added to 70 µl of buffer RDD (Qiagen) and 80µl of this DNase solution added to the column and incubated for 15 minutes at RT. 350µl buffer RW1 was added to the column and the column centrifuged for 15 seconds at 3300xg. The flowthrough was discarded. Buffer RPE (500µl) was added to the column and centrifuged for 15 seconds at 3300xg in a microfuge and the flowthrough was discarded. The columns were centrifuged for 1min at 3300xg in a microfuge without adding anything to remove any residual buffer. The RNeasy column was transferred to a clean 1.5ml collection tube, RNA eluted with the addition of 50µl RNase-free water and centrifugation for 1 minute at 3300xg. RNA was stored at -20°C. RNA quantification was done using Nanophotometer (Geneflow) at 260nm.

#### **2.4.2 Reverse transcription.**

1µg RNA was used to produce cDNA by reverse transcription. Superscript II reverse transcriptase was obtained from Invitrogen (Paisley, U.K.) and the reaction carried out as follows: 1µl of both random Hexamer (250ng) (Promega) and dNTPs (10µmoles) (Bioline, London, U.K.) were added to 1µg of RNA, the volume made up to 12µl with DNase RNase free water (Invitrogen Gibco), and the mix heated to 65°C for 5mins. The samples were centrifuged for 15 seconds at 3300xg in a microfuge and transferred to ice. A master mix was made as 1 x mix of the following: 1x First-Strand buffer, 25mM DTT, RNaseIn (Promega) and 1µl (200units) SuperScript® II Reverse Transcriptase (RT). 8µl of master mix was added to the RNA, primer, dNTP mix. The mix was incubated at 25 °C for 10 minutes, 42 ° C for 90 minutes and 70°C for 15 minutes in a thermocycler.



### 2.4.3 $\beta$ -actin PCR.

To assess that the reverse transcriptase reaction had worked, PCR reactions for  $\beta$ -actin were performed using the following primers:

$\beta$ -actin Forward: 5'GTCACCAACTGGGACGACA 3'

$\beta$ -actin Reverse: 5'TGGCCATCTCTTGCTCGAA 3'

cDNA samples were diluted 1:2 by adding 20 $\mu$ l DNase/ RNase free water. A 1x master mix (MM) was prepared allowing the following per sample: 5.0 $\mu$ l 10X BioTaq buffer (Bioline), 1.5 $\mu$ l MgCl<sub>2</sub> (50mM), 1.0 $\mu$ l dNTP mix (10mM), 1.0 $\mu$ l  $\beta$ -actin primer mix (10 $\mu$ M), and 0.75 $\mu$ l BioTaq polymerase (Bioline). Sufficient MM was prepared for all the samples and 2 negative (no cDNA) PCR controls. The MM was mixed well by vortexing and centrifuged for 15 seconds at 6000xg. 49 $\mu$ l of MM was aliquoted into each PCR tube (0.2ml) allowing 2 extra tubes as PCR negative controls. Then 1 $\mu$ l of cDNA was added to each tube. The tubes were placed in PCR machine (Perkin Elmer ABI2200) and cycles using the following cycle conditions:

	94°C -30sec	} x38 cycles > 72°C 10min > 4°C hold (8°C O/N)
94°C for 5 min >>	55°C- 30sec	
	72°C- 30sec	

Subsequently, 12.5 $\mu$ l 4x DNA gel loading buffer (Bioline) was added to the 50 $\mu$ l PCR reaction. 30 $\mu$ l of the samples mixture and 5 $\mu$ l of Hyperladder I (Bioline) were loaded onto a 1% w/v agarose gel (prepared with 1xTBE) and electrophoresed in 1xTBE buffer (see appendix A) at 40V for 45 minutes.  $\beta$ -actin PCR products (453bp) were visualised under UV transillumination.

### 2.4.4 QRT-PCR for NM23-H1

NM23-H1 primers/probes were previously designed and optimised by the group (Table 2.5). Gene specific primers were synthesised by Sigma Genosys (Sigma) and probes were synthesised by Eurogentec.

Primer / probe	Sequence (5'-3')
Nm23-H1 forward	5' GGCCTGGTGAAATACATGCA 3'
Nm23-H1 reverse	5' GGCCCGTCTTCACCACAT 3'
Nm23-H1 probe	5' CTCCCAGACCATGGCAACTACCGG 3'
18S forward	5' GCCGCTAGAGGTGAAATTCTTG 3'
18S reverse	5' CATTCTTGGCAAATGCTTTCG 3'
18S probe	5' TCTGGTCCGTCTTGCGCCGG 3'

**Table 2.5 Sequence of primers and probes used for NM23-H1 QRT-PCR**

Each QRT-PCR reaction contained: 18pmoles of gene specific 5' and 3' primers, 1× pre-optimised Mastermix (consisting of MgCl<sub>2</sub>, dNTPs and buffer; Eurogentec), 2.5 pmoles of gene specific probe (5' 6-FAM-, 3'- TAMRA labelled), cDNA (1µl), in a total reaction volume of 20µl with dH<sub>2</sub>O. As an internal control 18S ribosomal RNA expression was analysed using the same mix as above, but with 18s specific primers and probes (5'-VIC, 3'-TAMRA labelled). Each sample was set up in triplicate in a 96 well optical quality plate, which was sealed with optical quality film, and the reactions were run on an ABI Prism 7700 Sequence Detector (Applied Biosystems) (see section 2.9.4.4. for QRT-PCR analysis).

#### **2.4.5 QRT-PCR data analysis**

After completion of the run, QRT-PCR data was analysed using ABI Prism 7700 Sequence System software (Applied Biosystems). Cycle threshold (Ct) values were calculated by setting the threshold line through the exponential phase of the PCR profiles for both the gene of interest and the 18S internal control gene. The Ct values for the 18S internal control gene was subtracted from the Ct values for the gene of interest to give  $\Delta$ Ct values. The control sample  $\Delta$ Ct values were averaged across the triplicate wells and this control  $\Delta$ Ct average subtracted from all the test  $\Delta$ Ct values to give  $\Delta\Delta$ Ct values. For each sample, the average  $\Delta\Delta$ Ct values was calculated and fold difference in gene expression between the control sample and test samples calculated using the formula:  $2^{-\Delta\Delta Ct}$ . Experiments were repeated a minimum of N=3 for cell lines and average data calculated +/- SEM. Statistical analysis was performed on the  $\Delta$ Ct values.

## 2.5 CRISPR/Cas9 knock out (KO) of NM23-H1 in DLBCL cells

### 2.5.1 CRISPR Overview

When cells are transfected with the Cas9 DNA nuclease and a synthetic guide RNA (sgRNA) (Figure 2.2), the sgRNA complexes with the Cas9 enzyme and targets the Cas9 to the specific genome locus where the Cas9 nicks the DNA 4bp upstream of the protospacer adjacent motif (PAM) sequence. The cell then uses non-homologous end joining (NHEJ) DNA damage repair to repair the nicks however NHEJ is error-prone often resulting in deletions or insertions which can result in loss of gene expression due to frame-shifts.

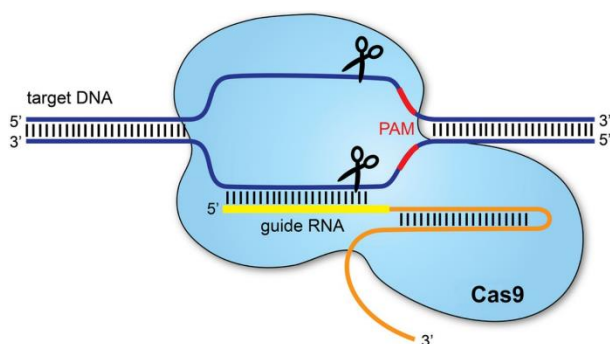


**Figure 2.2: Schematic of the RNA-guided Cas9 nuclease.** The Cas9n nuclease from *S. pyogenes* (in yellow) is targeted to genomic DNA by a synthetic guide RNA (sgRNA) consisting of a 20-nt guide sequence (blue) and a crRNA (red). The guide sequence pairs with the DNA target, directly upstream of a requisite 5'-NGG adjacent motif (PAM; pink). Cas9n mediates a single strand break (SSB) 3-4 bp upstream of the PAM (red triangle) which is repaired by the cell. Figure taken from (Redman et al., 2016).

### 2.5.2 sgRNA primer design

Primers single guide RNA (sgRNA) were designed using an online tool available at the Sanger Institute ([https://www.sanger.ac.uk/htgt/wge/find\\_crisprs](https://www.sanger.ac.uk/htgt/wge/find_crisprs)). NCBI RefSeq data was used as sequencing reference. Primers for the sgRNA were designed around the start codon for NM23-H1. Primers specificity was checked using BLAST ([ncbi.nlm.nih.gov/tools/primers-blast](https://ncbi.nlm.nih.gov/tools/primers-blast), NCBI) and only those specific to NM23-H1 and not NM23-H2 or other non-specific genes were selected. The restriction sites of BbsI restriction enzyme were added to sgRNA for cloning purposes. A Guanine nucleotide was added if the sgRNA did not start with G and a C residue to the end of the complementary sgRNA to assist during restriction digest. Primers were ordered from Sigma-Aldrich. Table 2.6 summarises the sgRNA selected to target NM23-H1.

Oligos ID (abbreviation)	Exon	Restriction site (BbsI)	sgRNA NM23-H1 sequence	PAM	Strand
1148934541(4541)	2	CACCG	TAGACAGTAGCACCATCTCT	TGG	-
		AAAC	AGAGATGGTGCTACTGTCTAC		
1148934544(4541)	2	CACCG	ACTTTAGGGATCGTCTTTCA	AGG	+
		AAAC	TGAAAGACGATCCCTAAAAGT		
1148934717(4544)	3	CACCG	ATCTGGTTTGATCGCAATGA	AGG	-
		AAAC	TCATTGCGATCAAACCAGAT		
1148934716(4544)	3	CACCG	AATGAAGGTACGCTCACAGT	TGG	-
		AAAC	ACTGTGAGCGTACCTTCATT		

**Table 2.6 sgRNA sequences used for targeting NM23-H1.** Target sequences were selected using the Sanger Institute CRISPR sgRNA tool.  
([https://www.sanger.ac.uk/htgt/wqe/find\\_crisprs](https://www.sanger.ac.uk/htgt/wqe/find_crisprs))

### 2.5.3 Plasmid DNA preparation (Miniprep)

A glycerol stock of plasmid pSp-Cas9 (BB)-2A-Puro (PX459) (Figure 2.3) was kindly provided by Dr. Michael Tomlinson (UoB). Bacteria were streaked onto agar plates contain ampicillin (amp, 100µg/ml) and incubated at 37°C O/N. A single colony was picked and used to inoculate a 10ml Luria broth (LB) + amp culture and grown overnight at 37°C with shaking (220rpm).

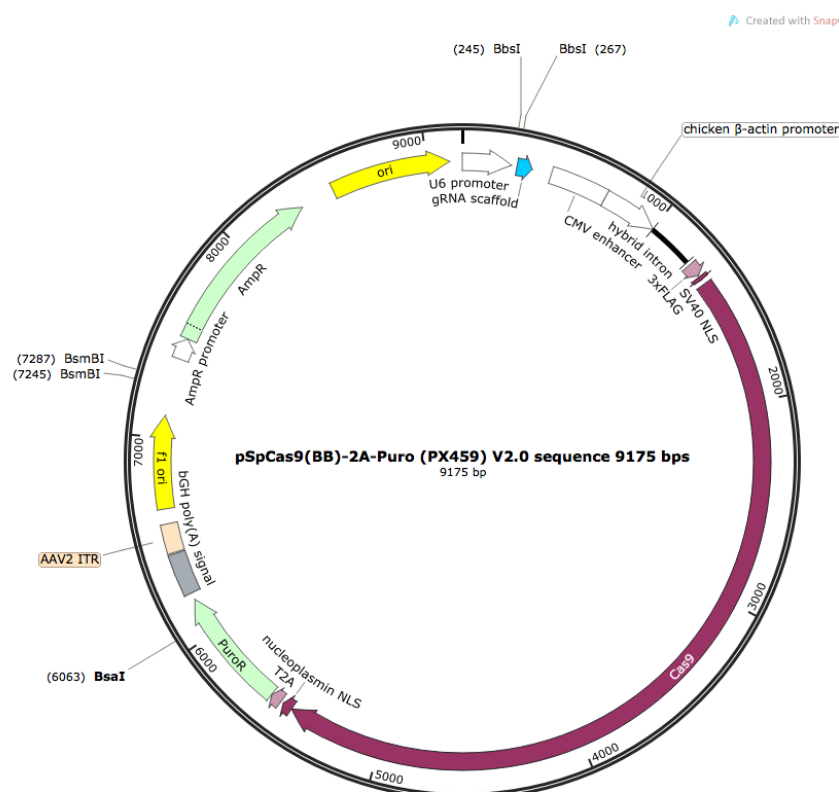


**Figure 2.3 CRISPR/Cas9 vector pSpCas9(BB)-2A-Puro(PX459) V2.0.** This vector (from Addgene) was used in this study (Ran et al., 2013). The plasmid expresses ampicillin resistance (AmpR) for selection in bacteria, the Cas9 nuclease and puromycin resistance gene for eukaryotic cell selection. The sgRNA were cloned into the BbsI site.

(<https://www.addgene.org/62988/>)

To prepare plasmid DNA for cloning, plasmid DNA was extracted using the Qiagen Miniprep Plasmid DNA extraction kit according to manufacturer's instructions (Qiagen). Briefly, bacterial cells were harvested by centrifuging for 30s at 7200xg. The supernatant was discarded and the cell pellet was resuspended in 250µl of Resuspension Buffer P1 before vortexing to mix the cells well. 250µl of Lysis Buffer P2 was added to cell mixture and mixed gently by inverting tube 6-8 times. The reaction was incubated at room temperature for up to 5 min or until the lysate had become clear. 300µl Neutralization Buffer P3 was added and mixed thoroughly by inversion. Precipitated protein and genomic DNA was removed by centrifuging for 5 min at 7200xg at RT. A maximum of 750µl of clarified sample supernatant was pipetted onto the plasmid mini spin column and centrifuged for 1 min at 7200xg before discarding flow-through. The spin column was washed with 600µl Wash Buffer PW2 (supplemented with ethanol) and centrifuging for 1 min at 7200xg. The spin columns were centrifuged for 2min at 7200xg to remove residual ethanol. To elute plasmid DNA from the column, 50µl of dH<sub>2</sub>O was added directly onto the centre of the spin column, incubated at room temperature for 1 min before centrifuging for 1min at 7200xg. Plasmid DNA concentration was quantified using a nanophotometer and 5µl plasmid DNA mixed with 2µl 5xDNA gel loading buffer blue (bromophenol blue) (Bioline), and 3µl of deionized water before agarose gel electrophoresis. 10µl of the prepared plasmid DNA mixture was run alongside 5µl of Hyperladder I (1 kb) (Bioline quantitative DNA marker) on a 1% (m/v) agarose gel in 1xTBE (see Appendix I) at 60V for 50 minutes. The gel was visualised by UV transillumination.

#### **2.5.4 Annealing and dephosphorylation reaction**

Annealing reaction was undertaken in 10 µl reaction mixture. 1µl of forward sgRNA primer (100 µM), 1µl of reverse sgRNA primer (100 µM), 1µl of T4 ligation buffer (10x, Bioline), 1 µl T4 polynucleotide kinase (PNK, Bioline) with 6µl deionized water. The reaction was incubated at 37°C for 30 minutes, 95°C for 5 minutes before cooling to 25°C at a rate of 5°C per minute. Annealed primers were diluted 1:200 in dH<sub>2</sub>O to a concentration of 50nM. The annealed primers were electrophoresed alongside 5µl of Hyperladder I (Bioline) on a 2% agarose gel in 1xTBE buffer at 60V for 30 minutes, to check efficiency of annealing. The gel was visualised under UV transillumination.

### **2.5.5 Restriction digest of pSpCas9(BB)-2A-Puro**

The vector pSpCas9(BB)-2A-Puro was digested with BbsI in a 20µl reaction containing 1x Buffer (New England Biolabs, NEB), 1µl BbsI and 1µg plasmid miniprep DNA. The reaction was incubated for 3 hours at 37°C and digestion verified by electrophoresing digested and non-digested DNA on a 1% agarose gel at 60V for 50 minutes. Digested plasmid DNA was excised from the gel and purified using Qiagen QIAquick Gel Extraction Kit according to manufacturer's instructions. Briefly, the gel slice was weighed and 3 volumes (100mg gel = 100µl) QG buffer added. After incubating at 50°C for 10 min (or until the gel slice had completely dissolved), 1 gel volume isopropanol was added to the sample and mixed by shaking. The sample was pipetted into a QIAquick spin column in a 2 ml collection tube and centrifuged for 1 min at 7200xg. The flow-through was discarded and the column washed with 500µl Buffer QG and centrifuged for 1 min at 7200xg. The column was then washed with 750µl Buffer PE and the QIAquick column placed into a clean 1.5 ml microcentrifuge tube. Plasmid DNA was eluted with 50µl water, incubation at room temperature for 4 min and centrifugation for 1 min at 7200xg. Plasmid DNA was stored at -20°C.

### **2.5.6 Ligation reactions and bacterial transformations**

BbsI digested pSpCas9(BB)-2A-Puro plasmid DNA and annealed sgRNAs were ligated in a 20µl reaction containing 1µl BbsI digested plasmid (100ng), 2µl annealed sgRNA oligos (100nmoles), 1x T4 DNA ligase buffer and 1µl T4 DNA. The ligation reaction was incubated at RT for 60 minutes. A vial of competent DH5α E.coli (Bioline) were removed from -80°C and thawed on wet ice. The cells were gently mixed by lightly flicking the tubes and 50µl of competent bacteria pipetted into a pre-chilled Eppendorf together with 5µl of the ligation reaction before incubating on ice for 30 minutes. The bacteria were heat shocked in a water bath at 42°C for 30 seconds and then returned to ice for 2 minutes. 1 ml of 950µl super optimal broth with carbon catabolite repression SOC medium (Invitrogen) was added and Eppendorfs incubated at 37°C for 60 minutes with shaking at 200rpm. Then 100µl of the transformation mix was spread on L agar plate containing 100µg/ml ampicillin using a sterile spreader and incubated at 37°C overnight.

### **2.5.7 Selection of positive colonies**

Colonies were picked, re-streaked onto fresh L agar + amp plates and also used to inoculate 5ml LB+amp cultures which were grown overnight at 37°C with shaking at 220rpm. Miniprep plasmid DNA was extracted as described in Section 2.7.2. Miniprep DNA (250ng) was sequenced using 3.3pmoles U6 promotor primer (GAT ACA AGG CTG TTA GAG AGA T) through the Biosciences Genomics facility using dideoxy Big Dye chemistry. Chromatograms were analysed using Chromas v2.6.5 software. Colonies with successful insertion of the sgRNA were then expanded for large-scale plasmid purification for transfections.

### **2.5.8 Large-scale plasmid DNA preparation (Maxipreps)**

Plasmid DNA was extracted using the Qiagen Maxi kit (Qiagen). Bacterial cultures of 250ml LB + ampicillin (100µg/ml) were incubated overnight at 37°C with shaking at 220rpm. Bacteria were pelleted by centrifugation at 400xg for 10mins at 4°C and the cell pellet resuspended thoroughly in 10ml P1 buffer in 50ml polypropylene tubes. After addition of 10ml Buffer P2, samples were mixed vigorously by inversion 4-6 times. This process was repeated after adding 10ml Buffer P3. Samples were centrifuged for 30mins at 800xg at 4°C. A Qiagen-tip 500 column was equilibrated by adding 10 ml Buffer QBT and letting this flow through by gravity. The supernatant from the bacterial lysis was pipetted onto the equilibrated Qiagen Tip 500 and the samples allowed flowing through by gravity. The column was washed twice with 30 ml Buffer QC. Plasmid DNA was eluted with 15ml Buffer QF into a clean 50ml polypropylene tube and then precipitated by addition of 10.5ml room temperature isopropanol and stored on ice for 30mins. The samples were centrifuged at 800xg for 30mins at 4°C, supernatant poured off and the DNA pellet washed twice with 5ml room temperature 70% ethanol and centrifugation at 800xg for 10mins at 4°C. After the wash step, the DNA pellet was air-dried and resuspended in 500µl TE buffer (see Appendix A).

## **2.6 Transfection and clonal selection of DLBCL cell lines**

### **2.6.1 Determination of Puromycin sensitivity of DLBCL cell lines**

In order to enrich for cells transfected with the pSpCas9 (BB)-2A-Puro plasmids, short-term treatment with puromycin was used to kill off non-transfected cells. Hence, DLBCL cell lines were plated out at  $2 \times 10^4$  cells/well in 150  $\mu$ l in complete media to the internal 60 wells of 96 well plates. PBS (200  $\mu$ l) was pipetted into the outer wells as a humidity barrier. A 4x puromycin (10mg/ml stock, Sigma) dose titration of 0.8-80  $\mu$ g/ml was prepared and 50  $\mu$ l pipetted per well with triplicates at each concentration. This gave a final puromycin concentration in the wells of 0, 0.2, 0.5, 1.0, 2.5, 5.0, 7.5, 10.0 and 20.0  $\mu$ g/ml in 200  $\mu$ l. Control wells with 200ml media, with no cells or antibiotics were included in the plates. After 72hrs incubation at 37°C and 5%CO<sub>2</sub> in a humidified incubator, media was carefully removed and replaced with fresh complete media before placing back into the incubator. After 72 hours, 15  $\mu$ l of Cell Titre Blue (Promega) was added, incubated for 3-6 hours or until colour in control untreated cells wells had changed to a purple/pink. Fluorescence was read in a Perkin Elmer Victor X3 plate reader using excitation wavelength of 560nm and emission of 590nm (560<sub>ex</sub>/590<sub>em</sub>). Readings from media alone (no cells) was subtracted from all wells as background. Cell viability was calculated as a percentage of untreated (0  $\mu$ g/ml puromycin) wells.

### **2.6.2 Optimisation and electroporation of DLBCL cell lines**

DLBCL cell lines were passaged and fed each day for 2 days before transfection to keep cells in exponential phase ( $0.5$ - $1.0 \times 10^6$  cells/ml). Allowing  $5 \times 10^6$  cells per transfection, cells sufficient for the number of transfections were transferred into a 30ml universal tube and centrifuged at 200xg for 5mins at RT. Supernatant was discarded and the cell pellet washed with 5mls warm PBS and centrifugation at 200xg for 5mins at RT. After removing all the PBS, the cell pellet was resuspended in Mirus Ingenio electroporation reagent (Geneflow) allowing 100  $\mu$ l per transfection. Into a 0.2cm electroporation cuvettes, 100  $\mu$ l of cell suspension ( $5 \times 10^6$  cells) and 2.5  $\mu$ g plasmid DNA in less than 20  $\mu$ l volume was mixed together and electroporated using AMAXA Nucleofector I and program X-01. Using fine-



tipped sterile pasteurs, 500µl preheated (37°C) complete media was added to the cuvette before transferring everything into one well of a 6-well plate. The volume was made up to 3mls with warm media and cells allowed to rest overnight.

In order to determine transfection efficiency, the pEF-GFP plasmid was used and transfected cells analysed 24hrs post-transfection by flow cytometry. Briefly, 200µl of non-transfected and GFP transfected cell suspension was pipetted into a FACS tube, 200µl FACS Fix added and the sample analysed by flow cytometry in FL1 on a BD FACS Calibur using BD CellQuest Pro Software and FL1. GFP-positive cells were gated using non-transfected cells as a negative control.

### **2.6.3 Puromycin enrichment of transfected cells**

After electroporation, cells were counted and plated at  $1 \times 10^6$  cells/ml in complete media supplemented with 0.5µg/ml puromycin and incubated at 37°C and 5%CO<sub>2</sub> in a humidified incubator for 3 days. WT and empty vector (Cas9) transfected cells were included as controls. They were then centrifuged at 150xg for 5mins and resuspended in complete media with no puromycin for clonal selection (see section 2.4.6).

### **2.6.4 Clonal Selection and expansion of NM23-H1 knockout (KO) cells**

To select individual clones, cells were counted using haemocytometer, resuspended at ~5 cells/ml and 200µl plated per well in 96 well round-bottomed plates. Four plates were prepared for each transfectant and the remaining cells cultured in a flask. After 2-3 weeks at 37°C and 5%CO<sub>2</sub> in a humidified incubator, colonies could be seen some of the wells. 50µl of media was replaced with fresh complete media every 2 days and the clones transferred to 48 well plates when the 96 wells were confluent. Media was used from the clones growing in 48 well plates for measuring extracellular NM23-H1 levels by western blotting to identify NM23-H1 KO clones. Those clones that had no/little NM23-H1 protein in the media were expanded into flasks and frozen down in liquid nitrogen. Clones from the Cas9 and WT cells were used as NM23-H1 expressing controls.

### **2.6.5 Screening of clones for knockout of NM23-H1**

As clones began to grow in the 48 well plates and the media turned yellow, 100µl of media was collected from the wells without disturbing the cells. The samples were centrifuged at 7200xg for 2mins to remove any cells and the supernatant transferred to clean Eppendorfs before adding 4xSDS gel-loading buffer and denaturing at 70°C for 10mins. 24µl of this denatured media sample was analysed by western blotting for NM23-H1 protein, using HT cell lysates as positive control on the westerns. Only those clones demonstrating a reduction or loss of NM23-H1 protein in the media were expanded, and frozen down.

### **2.7 Genomic analysis of NM23-H1 KO HT cells**

In order to determine the mutations in the NM23-H1 locus giving rise to KO, genomic DNA was extracted from  $5 \times 10^6$  cells for HT wild-type (WT) and KO cell clones using RNA/DNA/Protein purification kit (NORGEN BIOTEK CORPORATION). Cell suspension samples were transferred to an RNase-free tube and were centrifuged at 200xg for 10 minutes to pellet the cells. The supernatant discarded carefully to ensure that the pellet is not dislodged. The cell pellet was washed 1ml of PBS, Centrifuge at 200xg for another 5 minutes. The supernatant was carefully discarded. A few µL of PBS might left behind with the pellet to ensure that the pellet is not dislodged. 300 µL of Buffer SKP was added to the pellet. The cells were lysed by vortexing for 15 seconds to ensure that the entire pellet is completely dissolved before proceeding to the next step. gDNA Purification Column was assemble with one of the provided collection tubes. 600 µL of the prepared lysate was applied onto the column and centrifuged at 3300xg for 1 minute. If the entire lysate volume has not passed through into the collection tube, the samples need to spin for an additional minute 4600xg. The flowthrough was retained for RNA Purification, and stored at -20°C. The spin column was reassembled with the collection tube. 500 µL of wash solution was applied to the column and centrifuge at 3000xg for 1 minute. The flowthrough was discarded. 500 µL of wash solution was applied to the column and centrifuge at 3000xg for 1 minute. The flowthrough was discarded. The column was centrifuged at 4600xg for 2 minutes in order to dry the resin thoroughly. The collection tube was discarded. The column was placed into a fresh 1.7 mL elution tube which provided with the kit. 100 µL of elution buffer was added to

the column and let stand for 2 minutes at room temperature, centrifuged for 2 minutes at 4600xg, followed by an extra 1 minute at 4600xg. The purified DNA sample need to store at 4°C for a few days. For long term storage, it was recommended by the manufacture to store the samples at –20°C.

## 2.8 Nested PCR AMPLIFICATION of the NME1 gene locus

Genomic DNA was amplified in two stages using nested primers in the second round of PCR. The primer sequences used are shown in Table 2.7

Primer	Sequence (5'-3')
Nested PCR Forward 1	CGATTCTCCGCAGTCTTTGG
Nested PCR Reverse 1	GGTTTTGGTCGTAAGGGTT
Nested PCR Forward 2	CTGGACAATTTATGCTTGCC
Nested PCR Reverse 2	CACCGTTTATTGGCTAGTCA

**Table 2.7 Primer sequences for nested PCR of the NME gene locus**

PCR reagents (Accuzyme 10x PCR buffer (Bioline), 10mM dNTP mix and 100µM primers) were thawed on ice and centrifuged briefly. Mastermixes containing water, buffer, dNTPs, primers and Accuzyme DNA polymerase were prepared allowing for the following per reaction:

ddH <sub>2</sub> O	14.5µl
10X buffer	2µl
10 mM dNTP mix	1µl
20 µM Forward Primer	0.5µl
20 µM Reverse Primer	0.5µl
2.5u/µl Accuzyme enzyme	0.5µl

Mastermix (19µl) was aliquoted into 0.2ml thin-walled PCR tubes and 100ng genomic DNA added before cycling in an ABI Perkin Elmer 2200 PCR machine using the following cycling conditions:

94°C for 3mins	} x 35cycles > 72°C for 10mins
94°C for 15sec	
58°C for 15sec	
72°C for 30sec	

The PCR reaction was diluted 1:10 with dH<sub>2</sub>O and the PCR set up again using nested primers X and X and the same PCR reaction conditions as above. PCR cycling parameters for the second round PCR were:

94°C for 3mins	} x 35 cycles > 72°C for 10mins
94°C for 15sec	
58°C for 15sec	
72°C for 20sec	

PCR products were electrophoresed on a 1% agarose 1x TBE gel, PCR products excised from the gels and cleaned up using the Qiagen QIAquick Gel Extraction Kit (section 2.5.6). Sequencing was done by the Genomics DNA Facility (UoB) using the nested PCR primers.

## **2.9 Analysis of cytokines in conditioned media**

Cytokine levels in the CM of cultures were measured using the Bio-Rad Bio-Plex Pro™ assay. This assay uses polystyrene microspheres (beads) of ~6.5µm diameter that have been impregnated with ferrite particles and a mixture of two fluorescent dyes. The relative volumes of the dyes are carefully adjusted to provide up to 100 distinct colours that can be used to fluorescently differentiate the different beads and allows the measurement of up to 100 analytes simultaneously. In the Bio-Rad Bio-Plex Pro Human 27 Cytokine assay, 27 different sets of beads are conjugating to antibodies to 27 human cytokines. Detection of the cytokines is mediated by addition of secondary biotin-tagged antibodies to the 27 different cytokines followed by incubation with streptavidin labelled with phycoerythrin. The streptavidin binds to the biotin on the secondary antibody and the strength of the phycoerythrin signal is proportional to the amount of cytokine. Concentrations of cytokines are determined using cytokine standard curves. The array was selected because it included cytokines that were elevated by NM23-H1 (Okabe-Kado et al., 2009b, Okabe-Kado et al., 2009a).

### **2.9.1 Harvesting conditioned media for cytokine analysis**

Normal donor monocytes were treated with conditioned media from WT or NM23-H1 KO HT cells with or without recombinant NM23-H1. After 48 hours, 200µl of cells was harvested and transferred into Eppendorf tubes. After centrifuging at 200xg for 5mins, the supernatant

was transferred into clean Eppendorfs and the cells analysed by flow cytometry (see section 2.2.1). The supernatant was stored at -20°C before cytokine levels were measured.

### **2.9.2 BioPlex 27-plex cytokine assay**

Cytokine standards were provided lyophilised and were reconstituted with 500µl of standard diluent, vortexed for 1-3 seconds before incubation on ice for 30 minutes. A 4-fold serial dilution of reconstituted cytokine standards was prepared by adding 128µl of standard to 72µl of standard diluent followed by 8 serial 1:4 dilutions (50µl of standards added to 150µl of standard diluent). Bio-Plex magnetic beads and cytokine detection antibodies were mixed by vortexing before diluting 1:10 in assay buffer and antibody diluents, respectively. A 96 well filter plate was first pre-wet with 100 µl assay buffer. Vacuum filtration was used to remove the assay buffer and the plates blotted with clean paper towel. The diluted Bio-Plex magnetic beads were briefly vortexed and 50µl added to each well. The beads were washed by adding 100µl wash buffer per well and then removing the liquid using a vacuum manifold. The wash step was repeated once more. In the meantime, diluted standards and samples were equilibrated to room temperature and mixed by vortexing. 50µl of each standard and samples were pipetted into the appropriate wells of the prepared 96 well plate and incubated on an orbital shaker at 500rpm in the dark at room temperature for 30mins. The plate was washed by adding 100µl wash buffer and removing it using the vacuum manifold. The bottom of the plate was blotted with clean paper towel and the wash repeated twice more. The detection antibodies were briefly vortexed before 25µl was added to each well and the plate incubated on an orbital shaker at 500rpm in the dark at room temperature for 30mins. The wells were washed 3 times with wash buffer as before. Streptavidin-PE was vortexed, diluted 1 in 100 in assay buffer, vortexed again and 50µl added to each well. The plate was incubated with orbital shaking as before for 10 minutes, and the wells washed 3 times with 100µl wash buffer. Assay buffer (125µl) was added to each well, and the plate mixed by shaking at room temperature for 1 minute before plate analysis. Data was acquired with the help of 5 parameter logistic curve on a Luminex-100 instrument (Bio-Plex Systems, BioRad Laboratories, California, USA), using the low reporter 1 (RP1) target value setting and the resulting low photomultiplier tube (PMT) voltage. Data

were analysed using Bio-Plex Manager 4.1.1 software (BioRad). Bead regions were specified for the standard batch, collecting 50 beads per region between doublet discriminator values of 5000 and 25000. A standard curve of median fluorescence intensity against the concentration of cytokine standards was used by the software to determine cytokine concentrations in the conditioned media.

## **2.10 Statistical Analyses**

Results from experiments are presented as means  $\pm$  standard error mean (SEM) Data analysis was performed using the GraphPad Prism version 7 (GraphPad, La Jolla, USA). Differences between samples were analysed using two-tailed paired t-test, one-way ANOVA followed by Tukey's post test or Dunnett's post test. In all cases statistical  $p < 0.05$  were considered statistically significant.

**CHAPTER THREE**  
**INTRACELLULAR AND**  
**EXTRACELLULAR**  
**DETECTION OF NM23-**  
**H1/H2 IN DLBCL**



### 3 Intracellular and extracellular detection of NM23-H1/H2 in DLBCL

#### 3.1 *NME1* expression in DLBCL cell lines

As discussed in chapter 1 there is increasing evidence that NM23-H1 is involved in regulating cell differentiation and normal development. Some studies also suggest a role in cell proliferation as proliferation is inhibited by *NME1* gene down-regulation (Caligo et al., 1995, Cipollini et al., 1997). These proposed characteristics of NM23-H1 corresponded well with studies that implicate NM23 proteins in tumour development and progression in haematological cancers (Zou et al., 1993, Niitsu et al., 2003b). Most relevant to these studies, high expression of NM23-H1 protein has been associated with poor prognosis and worse outcomes in DLBCL (Niitsu et al., 2001a, Okabe-Kado, 2002, Niitsu et al., 2011b). One approach to studying the role of NM23-H1 in DLBCL is to use cell lines as a model. However, to do so requires confirming and characterising NM23-H1 and also NM23-H2 expression in such cells.

Quantitative real-time PCR (QRT-PCR) was used to analyse *NME1* expression in exponentially growing HT, Farage, U2932, SUDHL4, -5, -6 and OCILY1, -3 -7 DLBCL cell lines. The levels of mRNA expression after normalizing to 18S rRNA levels was compared to *NME1* expression in three exponentially growing lymphoblastoid cell lines (LCL; LCL1, LCL2, LCL3) and cycling normal donor CD19<sup>+</sup> B-cells from two healthy donors (ND1, ND2). Normal donor CD19<sup>+</sup> B cells were purified from peripheral blood mononuclear cells (PBMCs) using CD19<sup>+</sup> positive magnetic bead selection and driven into cell cycle by culturing for 8 days on mitomycin C treated murine L-fibroblasts expressing human CD40L in the presence of interleukin 4 (IL-4). Figure 3.1 shows that *NME1* expression was variable between the cells types tested. Farage and U2932 DLBCL cell lines expressed the highest level of *NME1* mRNA, which was 3 fold more than the expression in normal donor B cells. HT, SUDHL5 and OCILY1 also showed significantly greater expression than normal B cells whereas LCL3 expressed significantly less *NME1* mRNA than normal B cells. None of the other differences in levels reached significance.

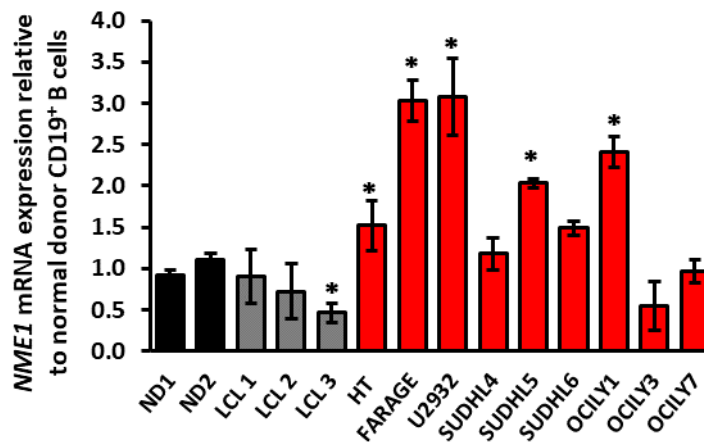


**Figure 3.1 NME1 mRNA expression in DLBCL cell lines.** NME1 mRNA expression was measured by QRT-PCR in exponentially growing DLBCL cell lines (red), lymphoblastoid cell lines (LCL) (grey) and cycling normal donor CD19<sup>+</sup> B-cells from two healthy donors (ND1, ND2) (black). Normal donor CD19<sup>+</sup> B cells were purified from PBMCs using positive magnetic bead selection before culturing for 8 days on mitomycin C treated murine L-fibroblasts expressing human CD40L and in the presence of interleukin 4. NME1 mRNA levels were measured and mRNA expression calculated relative to normal donor B cells. Data shown is average  $\pm$  SEM of a minimum of N=3 samples. \*  $p < 0.05$  (ANOVA with Tukey post-hoc test).

### 3.2 Intracellular NM23-H1 and NM23-H2 expression in human DLBCL cell lines.

Immuno-histological staining of intra-cytoplasmic NM23-H1 correlates with prognosis in DLBCL making stratification of risk more amenable to histopathologists (Niitsu et al., 2004, Lee et al., 2006b). In other B-cell lymphoma settings, NM23-H2 has been shown to drive expression of *NME1* and *c-myc* (Thakur et al., 2008). Therefore, intracellular protein levels of NM23-H1 and NM23-H2 were investigated in HT, Farage, U2932, SUDHL4, SUDHL5, SUDHL6, OCILY1, OCILY3 and OCILY7 DLBCL cell lines using western blotting of total protein lysates.  $\beta$ -actin antibody was used to normalise protein-loading for each lane. Both NM23-H1 (Figure 3.2A) and NM23-H2 (Figure 3.2B) were readily detected in all the DLBCL cells lines tested. Densitometry analysis identified that HT cells contained  $\sim 2.5$  fold more intracellular NM23-H1 than the other cell lines (Figure 3.2C) whereas expression of NM23-H2 appeared more consistent across the cell lines (Figure 3.2D). On first sight, it appears that NM23-H2 protein

levels are lower than NM23-H1 levels (Figure 3.2) however; this cannot be assumed as this could be technical due to different antibody affinities for example. In the western blots for NM23-H2, two bands were detected. However, the antibody used to detect NM23-H2 cross reacts with NM23-H1 and the upper band is most likely NM23-H1 as revealed by data shown later in this thesis.

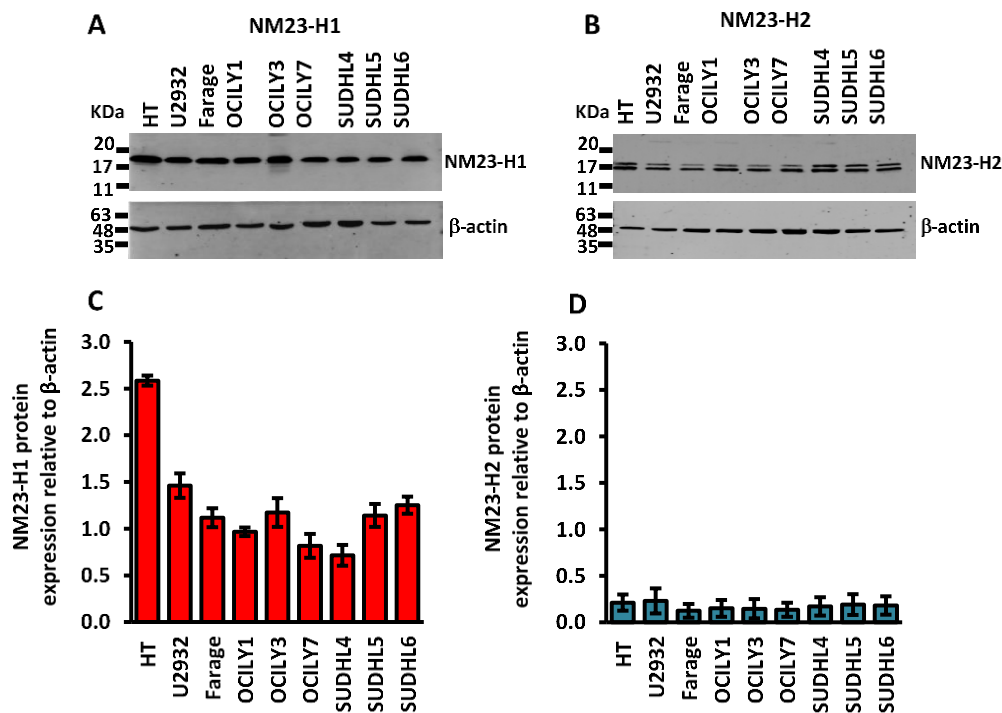


**Figure 3.2 Analysis of NM23-H1 and NM23-H2 protein expression in DLBCL cell lines.** Total protein lysate (20 $\mu$ g) from exponentially growing DLBCL cell lines was separated by SDS-PAGE before immunoblotting for (A) NM23-H1 and (B) NM23-H2 protein.  $\beta$ -actin was used as a loading control. Westerns shown are representative of N=3 replicates. Intracellular NM23-H1/H2 expression was normalised relative to  $\beta$ -actin for (C) NM23-H1 and (D) NM23-H2 protein. Data shown is average  $\pm$  SEM of a minimum of N=3 western from replicate experiments.

### **3.3 Intracellular NM23-H1/H2 expression in human DLBCL cell lines in comparison to LCL cell lines and B-cells.**

The level of NM23-H1 and NM23-H2 intracellular protein expression in two of the DLBCL cell lines (HT and Farage) was compared to three normal donor derived lymphoblastoid cell lines (LCL) LCL1, LCL2, LCL3 cells and normal donor CD19<sup>+</sup> B cells from ND1 and ND2 healthy donors (Figure 3.3A and B). LCLs are generated by immortalising healthy donor peripheral blood B cells with Epstein-Barr Virus (EBV) (Pedersen et al., 2005). Whilst expressing a limited panel of EBV proteins, LCLs represent a model of normal actively proliferating B cells. The normal donor CD19<sup>+</sup> B cells had been driven into cell cycle and proliferation following cell culture for 8 days in the presence of CD40L and IL-4. For comparison with previous data, the acute myeloid leukaemia cell line KG1a, which is known to express NM23-H1 and H2 (Lilly et al., 2015, Willems et al., 1998), was also included in the analysis. NM23-H1 and NM23-H2 intracellular protein levels were normalised to  $\beta$ -actin as a loading control (Figure 3.3C and D).

Whilst the data is N=1 repeat of the westerns due to limited protein availability of normal donor CD19<sup>+</sup> B cell protein, the results show that both HT and Farage expressed higher amounts of both NM23-H1 and NM23-H2 in comparison to LCL cell lines and normal donor CD19<sup>+</sup> B cells. KG1a cells also expressed higher levels but less than the two DLBCL cell lines.

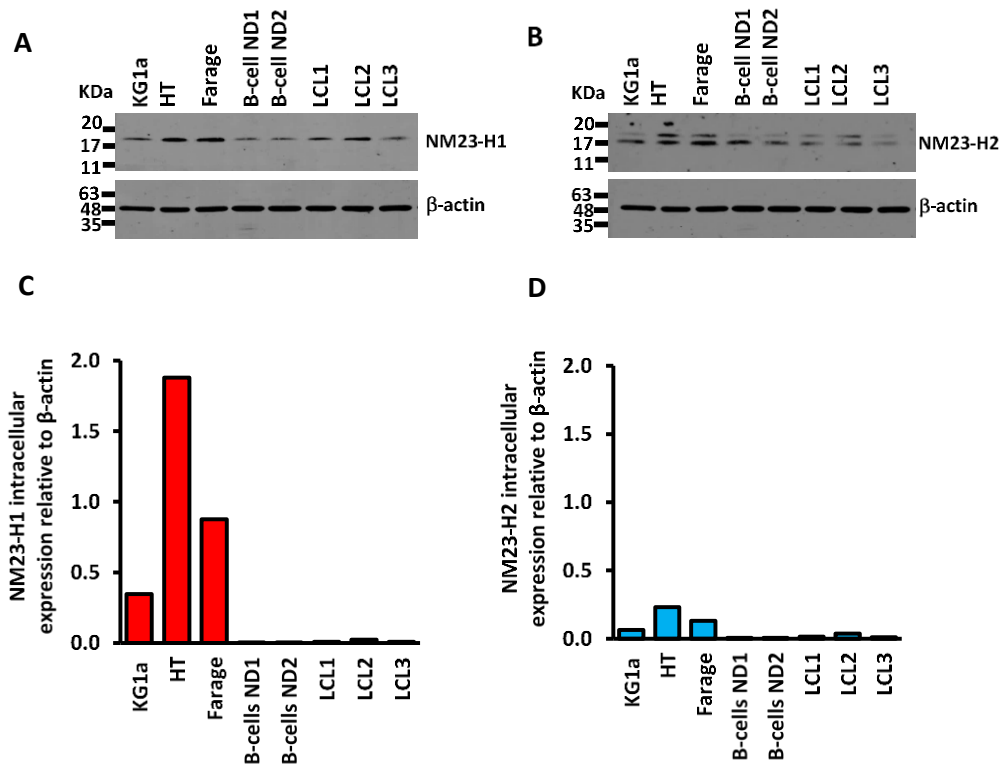


**Figure 3.3 Analysis of NM23-H2 and NM23-H1 protein expression in DLBCL cell lines, LCLs and normal donor CD19<sup>+</sup> B-cells.** Total protein lysate (20 $\mu$ g) from exponentially grown DLBCL cell lines, lymphoblastoid cell lines (LCL) and normal donor B-cells from two healthy donors (ND1, ND2) was separated by SDS-PAGE before immunoblotting for (A) NM23-H1 and (B) NM23-H2 protein.  $\beta$ -actin was used as a loading control. Intracellular expression was calculated relative to  $\beta$ -actin for (C) Nm23-H1 and (D) NM23-H2 protein. Data shown is N=1 repeat of the western. Normal donor B cells were purified from PBMCs using positive magnetic bead selection before culturing for 8 days on mitomycin C treated murine L-fibroblasts expressing human CD40L in the presence of interleukin 4.

Notably in this analysis, HT cells were again found to have particularly high levels of NM23-H1 as previously seen in Figure 3.2A. Together, the data in Figures 3.2 and 3.3 suggest that DLBCL cell lines show relative high expression of NM23-H1 even when compared to AML cells. These findings support the use of these cell lines as *in vitro* models to investigate the role of elevated NM23-H1 expression in DLBCL.

### **3.4 Analysis of Intracellular NM23-H1 expression in human DLBCL cell lines by flow cytometry.**

Flow cytometry was also used to confirm intracellular and surface expression of NM23-H1 protein in the DLBCL cell lines. Exponentially grown cells were permeabilised and fixed before staining using either an isotype-matched control of  $\alpha$ -NM23-H1 – FITC antibody (Santa-Cruz, C20 antibody). Representative dotplots of viable cells (Forward scatter vs side scatter) are shown in Figure 3.4A. Figure 3.4B shows representative histograms of intracellular NM23-H1 expression (white fill) in DLBCL and KG1a cell lines. All DLBCL cell lines presented positive shifts away from the isotype control peak (grey fill) indicating strong NM23-H1 intracellular expression. Farage cell lines displayed a smaller shift from the isotype control peak, indicating less NM23-H1 intracellular expression than the other cell lines. This is in contrast to the western blot results shown in Figure 3.2B where Farage had similar levels to the other DLBCL cell lines, other than HT which had particularly high levels of NM23 H1. The higher level of NM23-H1 in HT cells was not seen by flow cytometry indicated some difference in the sensitivity of the methods. Nonetheless, together the western blotting and flow cytometry analyses indicated that NM23-H1 is readily detected in all DLBCL cell lines used in this study. These data are in agreement with that of immunohistochemical studies (Niitsu et al., 2004, Lee et al., 2006b, Aryee et al., 1996) who identified the higher expression of NM23-H1 in DLBCL.

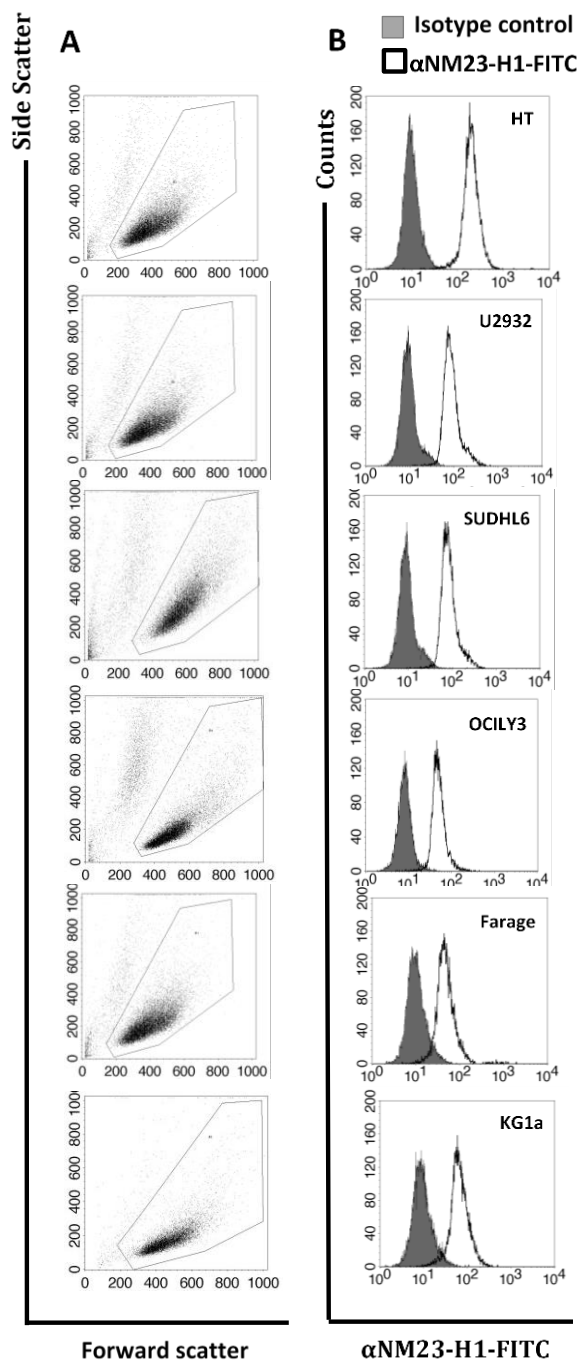


**Figure 3.4 Intracellular Nm23-H1 expression in DLBCL and KG1a.** Intracellular NM23-H1 protein levels were assessed using flow cytometry and  $\alpha$ -NM23-H1-FITC antibody or its matched isotype control (IgG1). The cells were fixed and permeabilised before staining to maintain soluble antigen stability and to permit intracellular access of antibodies. (A) shows the cells side scatter and forward scatter with the gated viable cell population. (B) shows representative histograms of anti-NM23-H1-FITC (Black line) and isotype-FITC control (Grey) stained DLBCLs. (C) shows mean data  $\pm$  SEM of N=3 of the ratio of the geometric mean of the NM23-H1-FITC stained cells relative to the geometric mean of isotype control. (\*) indicates a significant difference between fluorescent NM23-H1 and isotype control ( $p < 0.01$ ) (Two tailed paired T-Test).

### 3.5 Extracellular expression of NM23-H1/NM23-H2 in human DLBCL cell lines.

NM23-H1 plasma levels are elevated in high grade lymphomas and again correlate with poor prognosis, implicating elevated circulating NM23-H1 as a component of the biology driving disease progression (Nesi et al., 2001). In a phase II trial of combination therapy in DLBCL, patients with NM23-H1 serum levels higher than 80ng/ml before the treatment showed significantly poorer prognosis. Following treatment, the serum levels of NM23-H1 fell significantly only in those patients that obtained a complete remission (Niitsu et al., 2006), suggesting that elevated serum NM23-H1 levels in DLBCL come from the malignant clone. However, as yet the role of NM23-H1 in the biology of DLBCL is unknown.

To determine whether or not DLBCL cell lines release NM23 proteins into the extracellular space, extracellular expression of NM23-H1 and NM23-H2 was investigated in the Farage, HT, U2932, SUDHL 4, SUDHL5, SUDHL6, OCILY1, OCILY3 and OCILY7 DLBCL cell lines. Cell culture supernatants were harvested after incubation of  $4.5 \times 10^6$  cells in fresh media for 24 and 96 hours and assessed for the presence of released NM23-H1/NM23-H2 using SDS-PAGE. An NM23-H1 protein band was readily detected after 24 hours and the signal became stronger after 96 hours (Figure 3.5A). The antibody used to detect NM23-H1 was the rabbit polyclonal antibody, anti-NM23-H1 antibody (C20, Santa Cruz Biotech) which may also detect bovine NM23 proteins that could be present in the FBS used in the culture medium of DLBCL cell lines. Therefore, samples of media used to feed DLBCL cell lines (A&C; RPMI1640 with 10% FBS, B; IMDM with 20% FBS) were used as a negative control and no cross reactivity was detected.

NM23-H2 has been identified as *c-Myc* gene trans-activator (Dexheimer et al., 2009). *c-Myc* gene is one of the most activated oncogenes frequently associated with DLBCL pathogenesis (Bogusz et al., 2017). The biological functions of NM23-H2 in oncogenesis are still unclear. However, NM23-H1 and NM23-H2 are often co-expressed so therefore, western blotting for NM23-H2 was performed on the same supernatants in order to determine whether NM23-H2 was released from DLBCLs and may play a role in the disease. However, NM23-H2 was not detected in conditioned medium of any of the DLBCL cell lines even after 96 hours of incubation (Figure 3.5B). Densitometric analysis of extracellular NM23-H1 levels



in DLBCL cell line conditioned supernatants are shown after 24 hours in Figure 3.5C and after 96 hours in Figure 3.5D. These analyses identified that the HT, Farage and U2932 are particularly high secretors of NM23-H1.

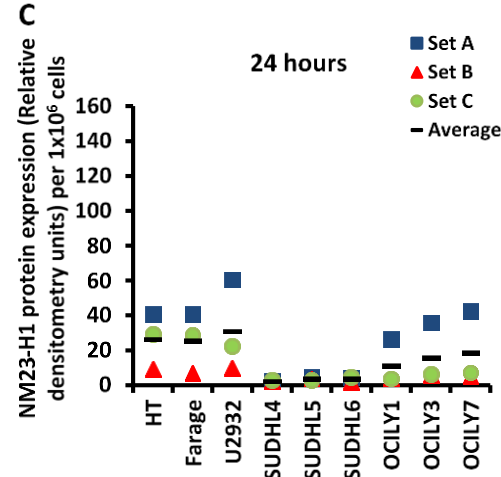
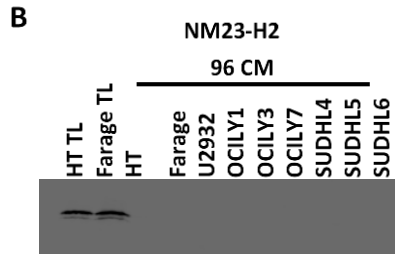
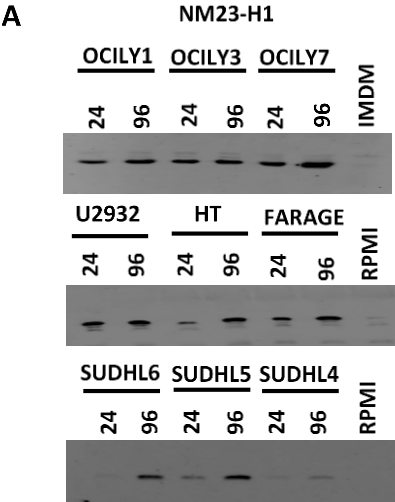
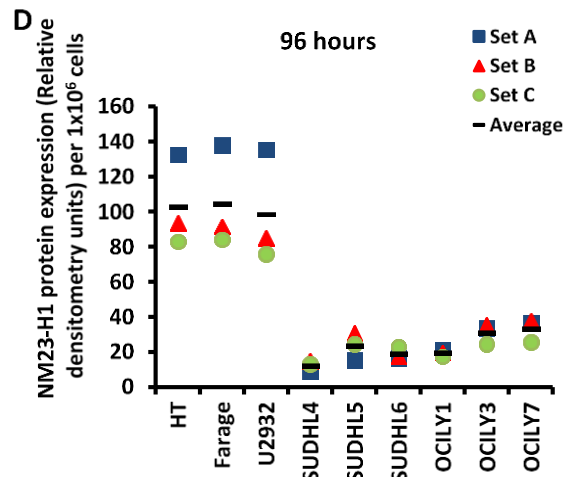


**Figure 3.5 Analysis of extracellular NM23-H1 and NM23-H2 protein expression in cultures of DLBCL cell lines.** Conditioned media (CM) from exponentially grown DLBCL cell lines was harvested after 24 and 96 hours and separated by SDS-PAGE before immunoblotting for (A) NM23-H1 and (B) NM23-H2 protein. Total protein lysate (20 $\mu$ g) from HT and Farage cell lines were used as a positive control. Complete media (RPMI 1640 media with 10% FBS, or IMDM with 20% FBS) was used as negative controls. Westerns shown are representative of N=3 replicates. Extracellular NM23-H1 expression in relative densitometry units are shown after 24 hours in (C) and after 96 hours in (D). Data shown is average  $\pm$  SEM of a minimum of N=3 westerns.



### 3.6 Detection of extracellular NM23-H1/NM23-H2 in LCLs and healthy donor CD19+ B-cells.

Unexpectedly, and in contrast to DLBCL cell lines, NM23-H1 was not observed in the conditioned media of either LCL cell lines or normal B- cell lines (Figure 3.6A). The same was true for NM23-H2, which could not be detected in conditioned media of these cells (Figure 3.6B).

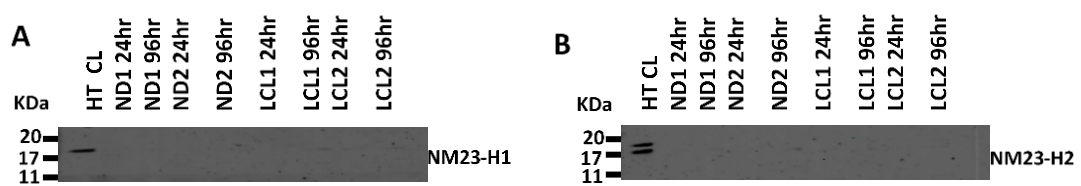
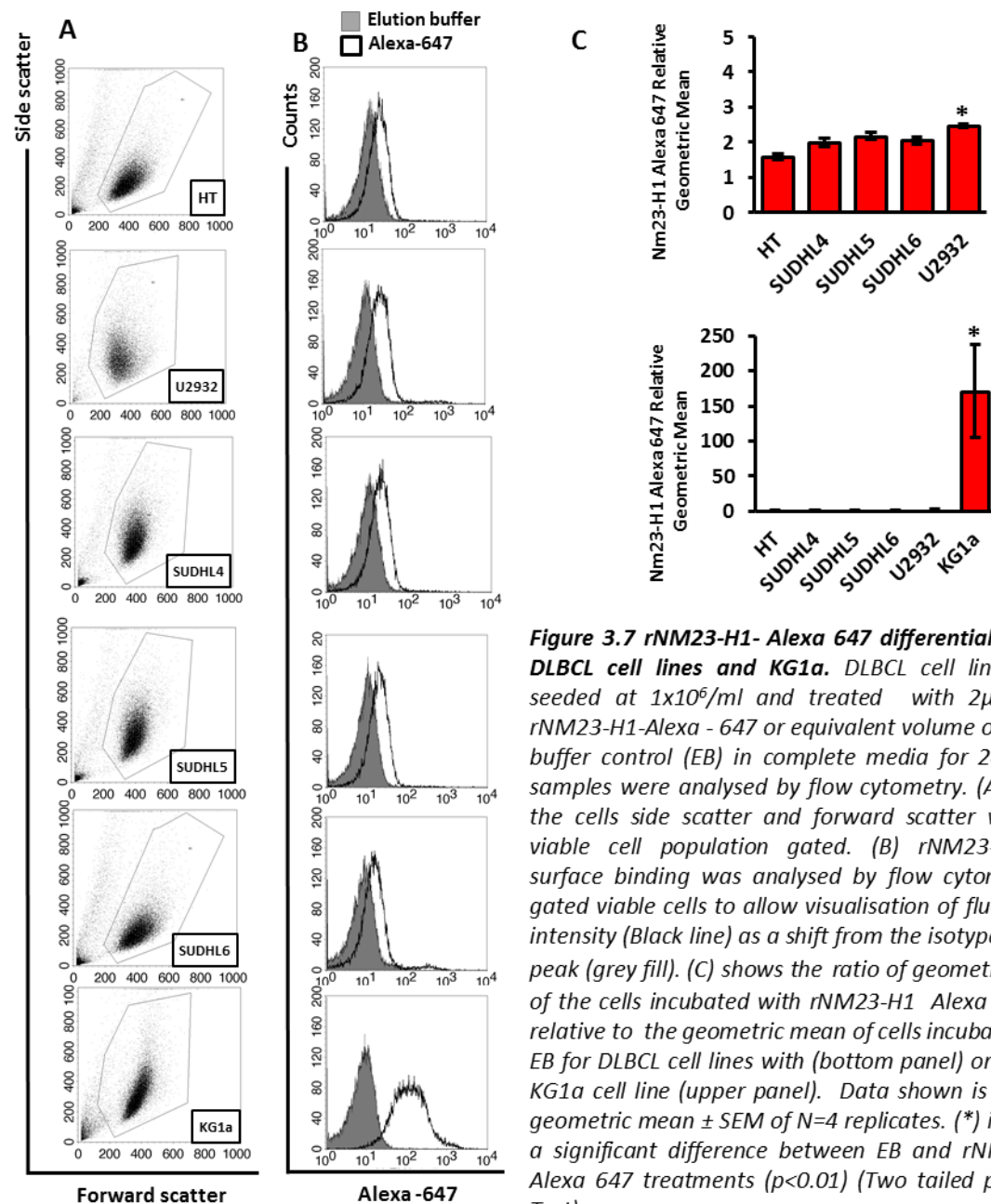


**Figure 3.6 Analysis of extracellular NM23-H1 and NM23-H2 protein expression in HT cell line, LCL and normal donor CD19<sup>+</sup> B-cells.** Conditioned media (CM) harvested after 24 and 96 hours from exponentially growing DLBCL cell lines, lymphoblastoid cell lines (LCL) and cycling normal donor CD19<sup>+</sup> B-cells from two healthy donors (ND1, ND2) was separated by SDS-PAGE before immunoblotting for (A) NM23-H1 and (B) NM23-H2 protein. HT cell lysates (CL) were used as positive controls. Data shown is N=1 repeat of the western. Normal donor B cells were purified from PBMCs using positive magnetic bead selection before culturing for 8 days on mitomycin C treated murine L-fibroblasts expressing human CD40L in the presence of interleukin 4. HT, LCL1, LCL2 and B-cells (ND1 and ND2) were grown in RPMI 1640 media with 10% FBS.

### 3.7 Human DLBCL cell lines binding status to recombinant NM23-H1 fluorescently labelled using Alexa 647.

In a second approach to determine whether DLBCL cells bind NM23-H1 at their surface, recombinant NM23-H1 was directly labelled with Alexa-Fluor 647 to enable the assessment of DLBCL surface binding and or intracellular uptake of NM23-H1. Previous studies identified the enhancing role of NM23-H1 in cell growth and survival in AML cells when its concentration is commensurate with what occurred in patients' serum. The study used 2µg/ml of recombinant NM23-H1 (Okabe-Kado et al., 2009b). Five exponentially growing DLBCL cell lines were therefore treated with final concentration of 2µg/ml of either recombinant NM23-H1-(rNM23-H1) Alexa647 or elution buffer control (EB) in complete media and incubated for 24hrs. Representative forward scatter versus side scatter dotplots with the viable cell population gated for DLBCL cell lines and KG1a are shown in Figure 3.7A. All DLBCL cell lines used in this assay exhibited a small shift in fluorescence intensity from

the EB control peak. In contrast, KG1a AML cells showed a significant positive shift (Figure 3.7B). The histogram shown in Figure 3.7B shows average shifts in geometric mean intensity for n=4 repeats for the DLBCL cell lines and for KG1a. (Figure 3.7C) shows the ratio of geometric mean of the cells incubated with rNM23-H1 Alexa-647 relative to the geometric mean of cells incubated with EB for DLBCL cell lines with (bottom panel) or without KG1a cell line (upper panel). For all the DLBCL cell lines, except U2939, there was no significant binding of the fluorescently tagged rNM23-H1. In contrast to the U2932 DLBCL cells, where an increase of approximately 2 fold in geometric mean was observed, KG1a cells demonstrated a >100 fold increase in fluorescent staining (Figure 3.7 C).



### 3.8 Summary

In this chapter, the aim was to investigate the expression and binding of NM23-H1 and NM23-H2 in DLBCL cell lines (HT, Farage, U2932, SUDHL 4, 5 & 6 and OCILY1, 3 & 7) compared to normal donor B cells. Quantitative RT-PCR and western blotting identified expression of NM23-H1 and western blotting identified intracellular expression of NM23-H2 in all cell lines tested. However, western blotting of supernatant proteins identified the extracellular release of NM23-H1 only and not NM23-H2. Application of exogenous recombinant NM23-H1 to DLBCL cell lines only marginally increased binding to DLBCL cells as measured by flow cytometry. In contrast, exposure of myeloid KG1a cells to rNM23-H1 lead to significant binding and also intracellular uptake of Nm23-H1 protein (subsequent study has done and confocal microscopy confirmed that by viewing a visible bright red signal inside KG1a cell line membrane). These results support the data observed in patients in that the more aggressive and worse prognosis DLBCLs express higher levels of intracellular NM23-H1. Furthermore, these data support the hypothesis that the elevated serum NM23-H1 levels seen in DLBCL patients is, at least in part, be derived from the tumour cell clone. This does not rule out that other cell types also produce extracellular NM23-H1 in those patients with aggressive disease. This data also suggests strongly that the secreted NM23-H1 protein does not act directly on the tumour clone but may instead act upon other cells in the tumour microenvironment and host.

**CHAPTER FOUR**

**GENERATION AND**

**CHARACTERISATION OF**

**NM23-H1 CRISPR**

**KNOCK-OUT CELL LINES**

## 4 Generation and characterisation of NM23-H1 CRISPR Knock-Out Cell Lines

In the previous chapter, the intracellular and extracellular expression of NM23-H1 in DLBCL cell lines (HT, Farage, U2932, SUDHL4, 5, 6, OCILY1, 3 and 7) was characterised. In DLBCL, the relationship with poorer prognosis is associated with both elevated intracellular NM23-H1 as revealed by immunohistology and elevated levels of protein in the blood; raising the possibility that NM23-H1 may affect outcome by either cell intrinsic and/or extrinsic mechanisms. This chapter describes experiments to generate and validate NM23-H1 knock-out (KO) cell lines in order to investigate the impact of NM23-H1 absence on DLBCL cells.

### 4.1 CRISPR gene editing.

The CRISPR/Cas9 technique can be used to generate genetically modified cell lines. In the CRISPR/Cas9 system, a complementary synthetic guide RNA (sgRNA) is used to direct Cas9 nuclease to a specific sequence on the target gene; in this case *NME1*. Each sgRNA carries a C-terminal adjacent Protospacer adjacent motif (PAM) that will target Cas9 nuclease to cleave 4bp upstream of the PAM specific location on *NME1* gene. In the human genome, the *NME1* gene is located on chromosome 17 (Chandrasekharappa et al., 1993) and can encode two transcript variants, 1 and 2 (UCSC genomic browser). The molecular weight prediction of each transcript variant is 17kDa and 18kDa. Full amino acid sequences for both transcription variants of *NME1* gene with sgRNAs positions are shown in Figure 4.1.

For CRISPR/Cas9 knockout of *NME1*, 4 different 20nt *NME1* sgRNAs were designed, 2 sgRNA targeting exon 2 and 2 sgRNA targeting (Table 4.1 and Figure 4.1). sgRNAs were selected using an online tool available on the Sanger Institute CRISPR website (see methods). Predicted sgRNAs were checked for specificity for *NME1* by BLAST alignment analysis and those sgRNA which had the lowest predicted off target were selected (Table 4.1). sgRNA 4541 targets translation start site in transcript variant 1 and sgRNA 4716 the translation start site in transcript variant 2 as shown in Figure 4.1.

Primer name	NME1 gene transcript variant	Exon number	sgRNA sequence	PAM	Strand	Total Off Target
4541	Tv1	Exon 2	TAGACAGTAGCACCATCTCT	TGG	-	89
			AGAGATGGTGCTACTGTCTA			
4544	Tv1	Exon 2	ACTTTAGGGATCGTCTTTCA	AGG	+	65
			TGAAAGACGATCCCTAAAGT			
4717	Tv2	Exon 3	ATCTGGTTTGATCGCAATGA	AGG	-	39
			TCATTGCGATCAAACCAGAT			
4716	Tv2	Exon 3	AATGAAGGTACGCTCACAGT	TGG	-	62
			ACTGTGAGCGTACCTTCATT			

**Table 4.1. Selected CRISPR/Cas9 sgRNA designed to target the NME1 gene.** Synthetic guide RNAs (sgRNAs) for NME1 were designed and comprised of 20nt gene-specific sequence plus protospacer adjacent motif (PAM sequence, AGG/TGG).

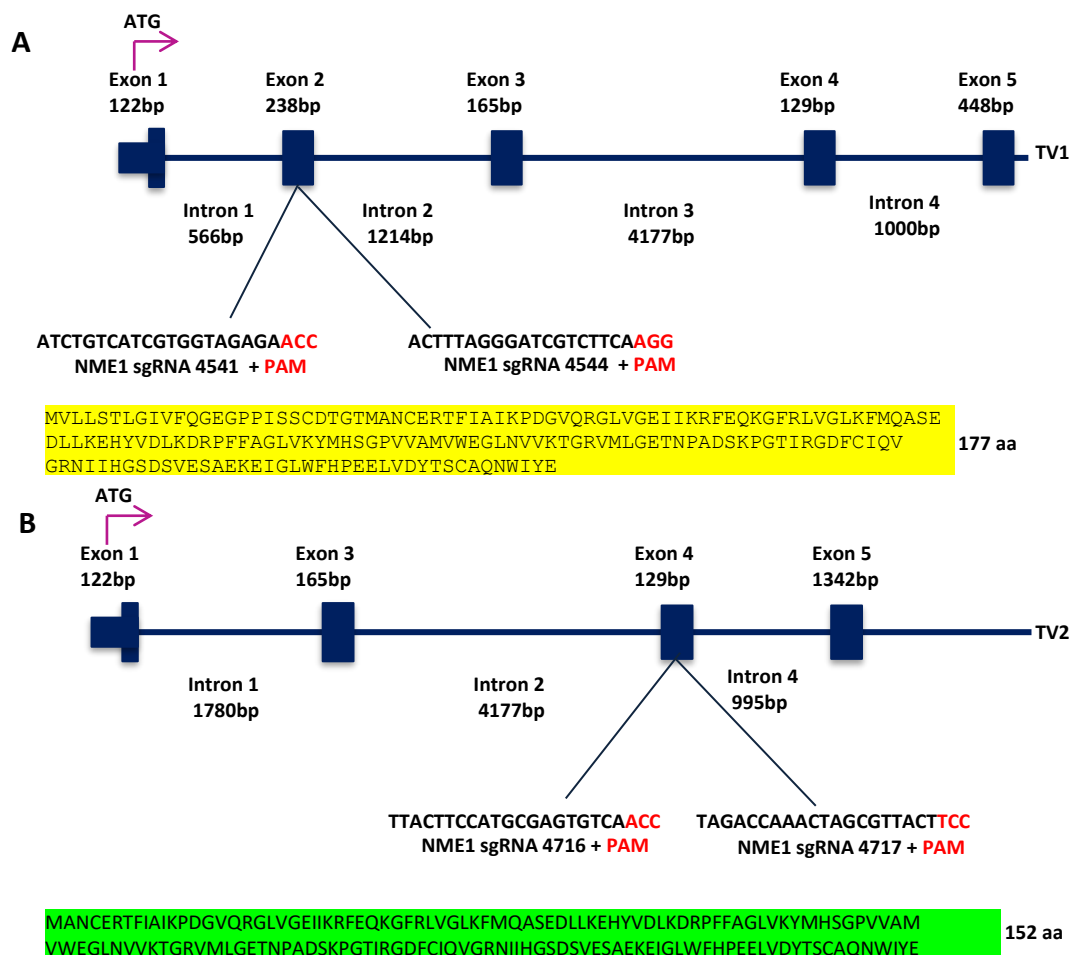


**Figure 4.1. NME1 gene structure and transcript variants.** (A) Transcript variant (TV)1 of NME1 gene, which produces a protein with 177aa and 19kD, both sgRNAs sequences that target NME1 gene translation start site are located in exon two. (B) TV2 of NME1 gene, which produces a protein with 152aa and 17kD. Exons are shown in blue, the translation start site (ATG –Methionine) is shown with the pink arrow. PAM is shown with red. Exon 2 is missing in TV2.



## **4.2 Cloning NME1 sgRNA primers into the CRISPR-Cas9 expression vector**

Complementary oligonucleotide primers were ordered for each sgRNA sequence. These were annealed, creating a short double-stranded DNA segment with overhanging 5' CACC and 3' CAAA BbsI restriction enzyme sites. These dsDNA were ligated into pSpCas9(BB)-2A-Puro(PX459) V2.0 which had been digested with BbsI restriction enzyme (see schematic Figure 4.2). This puts expression of the sgRNA under control of the U6 RNA polymerase III promoter. The sgRNA-ligated-plasmid was transformed into competent DH5 $\alpha$  bacteria and plated on L-agar +ampicillin plates overnight at 37C°. The following day, colonies were picked and grown up in L-broth + ampicillin overnight before extracting plasmid DNA using a Miniprep kit and sequencing using U6 promoter primer. Figure 4.2 shows a schematic of the cloning pipeline and chromatograms for plasmids with the 4544 sgRNA and the 4716 sgRNA successfully cloned into the BbsI site.

## **4.3 Puromycin dose response.**

The CRISPR/Cas9 expression plasmid carries a puromycin resistance gene to permit efficient selection of transfected eukaryotic cells. It was therefore important to characterise the puromycin sensitivity of the DLBCL cell lines. This was performed in a 96 well format. Before performing the puromycin dose responses, seeding cell density for DLBCL cell lines in a 96 well plate assay over 72hrs at 37°C was optimised and found to be  $5 \times 10^3$  cells/well (See Appendix B). Using this cell density, DLBCL cell lines were exposed to a dose response of puromycin (0, 0.1, 0.25, 0.5, 0.75, 1.0 and 2.0  $\mu\text{g}/\text{ml}$ ) for 72hours. Dose responses for the DLBCL cell lines are shown in Figure 4.3A. Figure 4B summarises the calculated IC<sub>50</sub> values measured for all the cell lines to determine the concentration required to kill 50% of non-transfected cells, and the dose that killed >95% non-transfected cells (Figure 4.3C). For all the DLBCL cell lines, except U2932 which was 0.75  $\mu\text{g}/\text{ml}$ , the dose of 0.5  $\mu\text{g}/\text{ml}$  puromycin was used for selection of transfected cells.

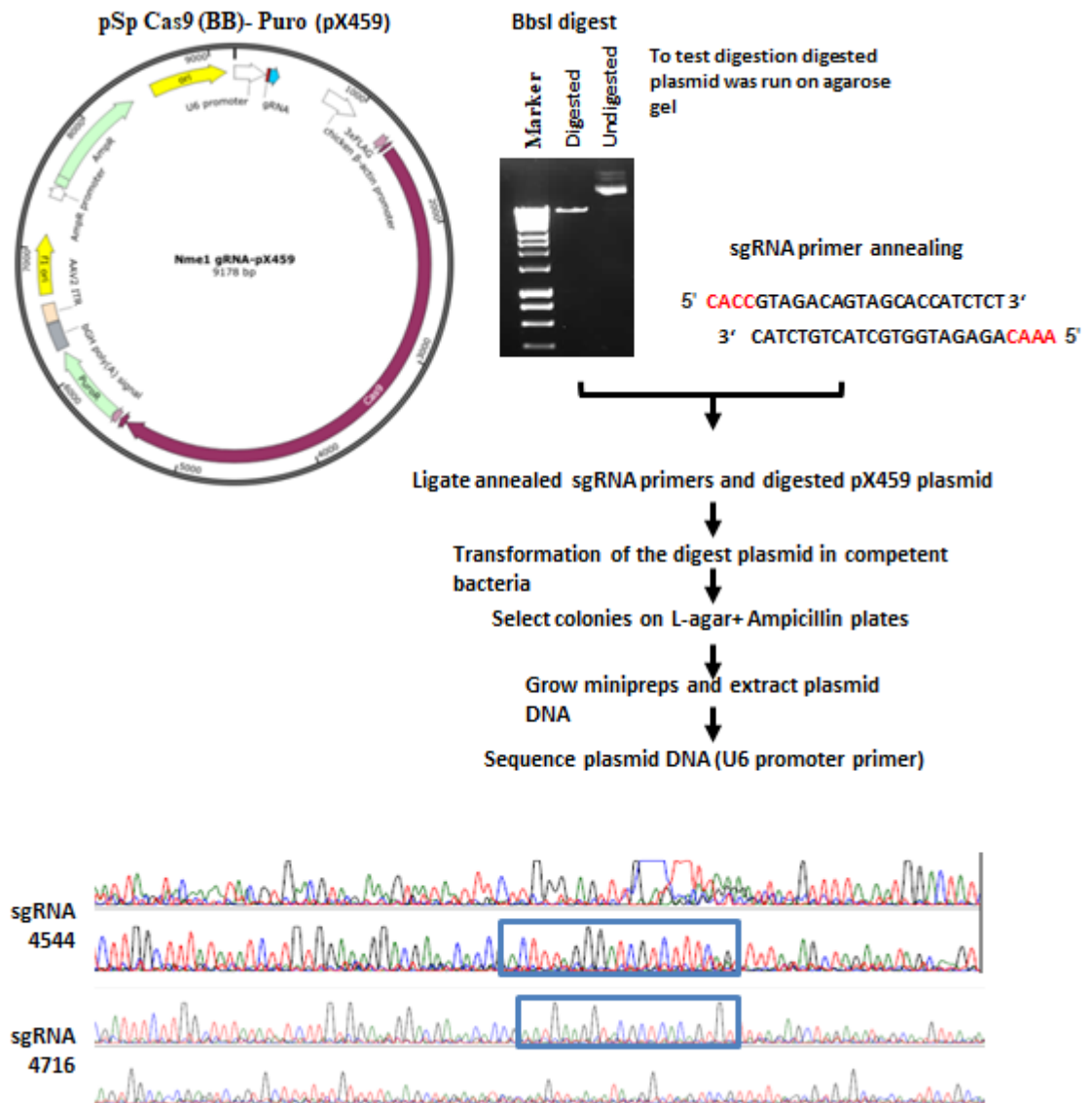


**Figure 4.2 Experimental overview of CRISPR/Cas9-mediated NME1 Knock out plasmid construction.**

sgRNA were designed to target the NME1 gene, the primers were annealed and ligated into pSpCas9(BB)-Puro (pX459) plasmid. A FLAG and nuclear localisation sequence (NLS)-tagged CAS9 cDNA is encoded on the plasmid downstream of the chicken  $\beta$ -actin promoter for expression in eukaryotic cells. Puromycin resistance is conferred by the PuroR gene. The RNA polymerase III U6 promoter is located upstream to drive NME1 sgRNA expression. The annealed sgRNA primers were ligated with the digested plasmid using T4 DNA ligase. The sgRNA-ligated-plasmid was transformed into competent DH5 $\alpha$  E.coli bacteria, plated on L-agar +ampicillin plates overnight at 37Co. The following day, colonies were picked and grown up in L-broth + ampicillin overnight before extracting plasmid DNA using a Miniprep kit and sequencing using U6 promoter primer. The chromatogram shows plasmid sequences with the 4544 and 4716 sgRNAs successfully cloned into the BbsI site.

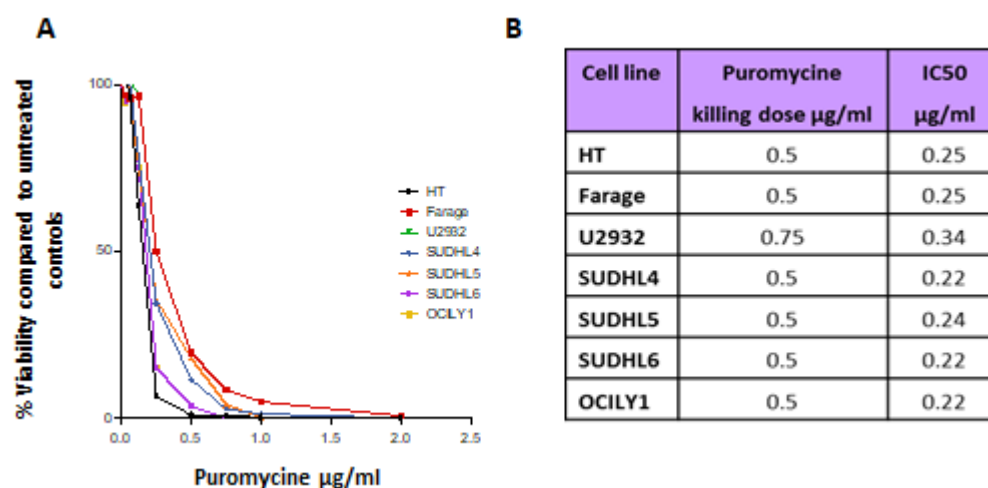


**Figure 4.3 Puromycin dose responses of DLBCL cell lines.** **A.** DLBCL cell lines were subjected to increasing amounts of puromycin in 96-well plates and cultured for 72 hours at 37°C. CellTiter-Blue® Reagent (10µl/well) was added and cells were incubated for 3 hour before recording fluorescence (560Ex/590Em) using a FLUO star Omega plate reader. Data shown is average geometric mean  $\pm$  SEM of N= 4 replicates. Viability was calculated as a percentage of control untreated cells. **B.** Summary for puromycin IC50 doses for all DLBCL cell lines tested and the killing dose used for selection of PuroR transfected cells.

#### 4.4 Determination of transfection efficiency.

Since DLBCL cell lines had previously not been transfected in our laboratory, a control transfection experiment with GFP-expressing plasmid was performed. Exponentially growing DLBCL cell lines ( $5 \times 10^6$  cells) were transfected by electroporation with 5µg of a control GFP expressing (pEF-GFP) plasmid using the Nucleofector I system (Figure 4.4A). After 24hrs post-transfection, fluorescence microscopy demonstrated good numbers of GFP-positive cells (Figure 4.4B). The percentage of GFP positivity cells was assessed quantitatively using flow cytometry (Figure 4.4C and 4.4D) using mock-transfected cells as a negative control. Transfection efficiencies between 10-40% were achieved in the DLBCL cell lines.

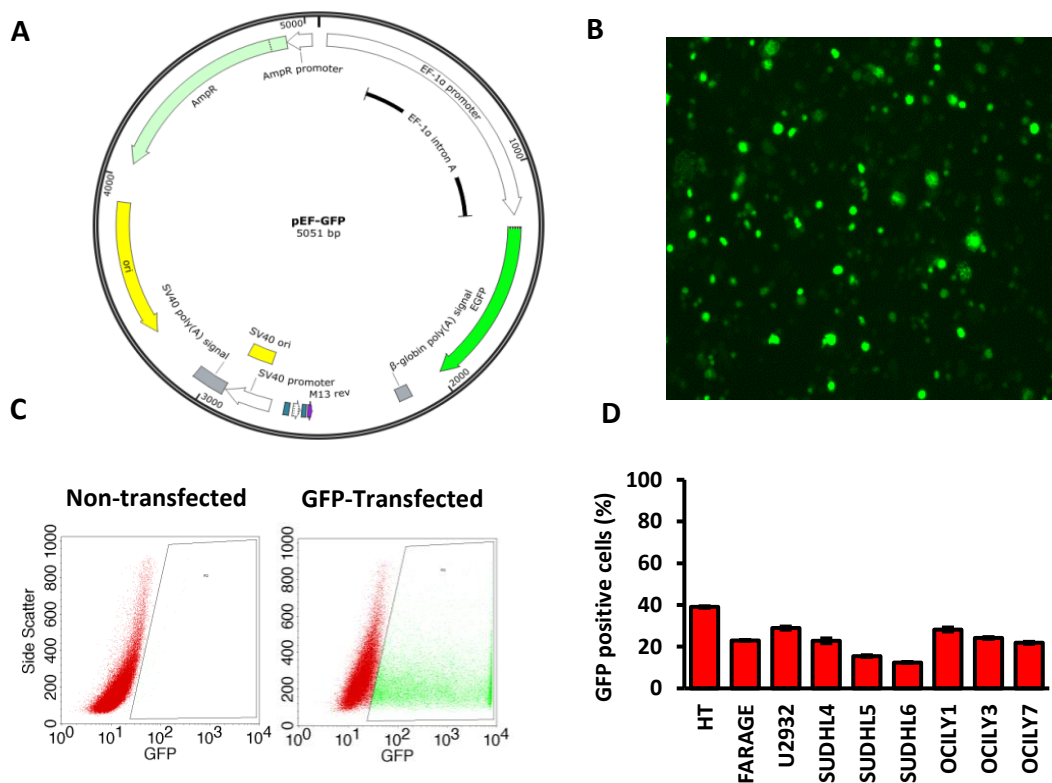


**Figure 4.4 Determination of transfection efficiency.** DLBCL cells were transfected with pEF-GFP plasmid using electroporation and analysed using flow cytometry. (A) pEF-GFP plasmid map. (B) A representative image of GFP-transfected cells obtained using fluorescence microscopy. (C) Representative dotplots of GFP-transfected cells and non-transfected cells, showing side scatter and GFP positive cells (green). (D) The percentage of GFP positive cells for nine DLBCL cell lines used in this study. Data shown is average geometric mean  $\pm$  SEM of N=4 replicates.

## 4.5 Generation of NM23-H1 KO clones

Having established conditions for transfection and puromycin selection, HT, Farage, U2932, SUDHL4, SUDHL5, SUDHL6, OCILY1, OCILY3 and OCILY7 DLBCL cell lines were transfected with the pSp-Cas9(BB)-Puro-(PX459)-NM23-H1-sgRNA vectors. After 24hours, transfected DLBCL cells were incubated with puromycin (0.5 $\mu$ g/ml or 0.75 $\mu$ g/ml) for 3 days before plating the remaining viable cells out in limiting dilution for single colony selection. Over a period of 2-6 weeks of culturing, the conditioned media from growing colonies was tested for NM23-H1 secretion by western blotting. Of more than 100 clones screened for each of the nine DLBCL cell lines transfected (~900 clones screened), only six clones from HT cell line were successful NM23-H1 knockouts/knockdowns. Figure 4.5A shows the original identification of these clones by western blotting of culture supernatant. One of these

isolates started re-expressing NM23-H1 later in time, probably indicating that this culture was not a true clone started from a single cell. The remaining clones were renamed KO1, KO2, KO3 and KO4 and are referred to as such hereafter. These clones were expanded and Figure 4.5B shows a representative western blot of total lysates from these clones probed for NM23-H1 and  $\beta$ -actin as a loading control. HT wild type cells and Cas9 control vector transfected cells (HT cells transfected with plasmid encoding Cas9 alone with no *NME1* sgRNA) were used as a positive control for NM23-H1 protein expression. NM23-H1 expression normalised to  $\beta$ -actin expression was performed on n=3 analyses and the mean data is shown in Figure 4.5C. As seen from this analysis, small levels of expression remained detectable in HT KO1 and KO2. In contrast, no extracellular expression of NM23-H1 was detected for all of the four HT KO clones irrespective of the low levels of intracellular protein observed in KO1 and KO2 (Figure 4.5D and E).

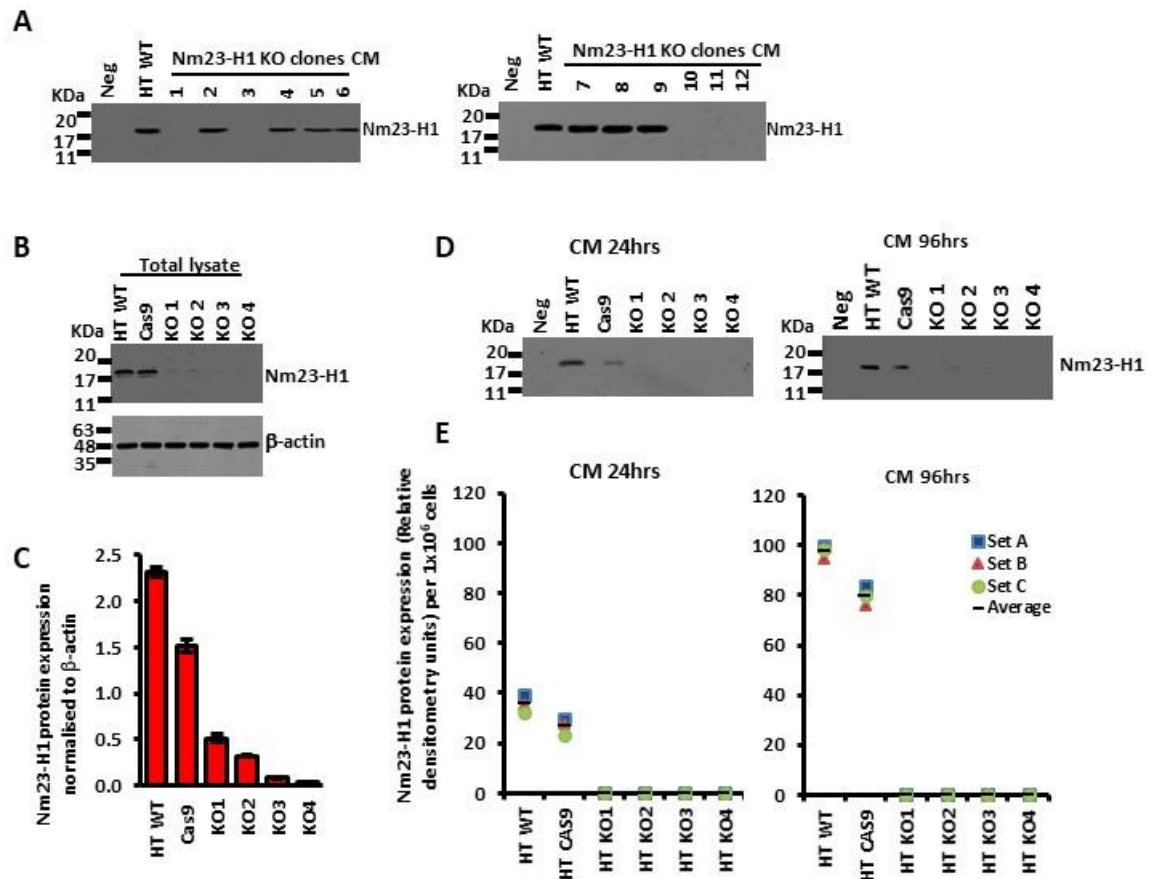


**Figure 4.5 Generation of Nm23-H1 Knockout (KO) clones.** CRISPR/CAS9 construct carrying sgRNA targeting the NME1 gene was transfected into HT DLBCL cells and selected with 0.5µg/mL puromycin over a course of three days. Identification of puromycin-resistant clones was performed manually by scanning the clones using light microscopy. (A) shows the initial screen of HT clones: the conditioned media from growing clones was analysed by immunoblotting for secreted Nm23-H1. KO denotes NME1 knockout cells. Neg is the control media negative control. (B) Total protein lysate (20µg) from exponentially grown DLBCL WT and NME1 KO cells were analysed by immunoblotting for NM23-H1 with β-actin as a loading control. HT wild type and Cas9 were used as a positive control. (C) shows quantitation of western blots for Nm23-H1 protein expression levels normalised to B-actin in NM23-H1 KO clones. (D) Conditioned media (24µl) from exponentially Nm23-H1 KO clones was harvested after 24 and 96 hours and assessed by western blotting for Nm23-H1 protein, HT wild type and Cas9 were used as a positive control. Extracellular Nm23-H1 expression in relative densitometry units are shown after 24 hours and after 96 hours in (E). Data shown is average ± SEM of a minimum of N=3 westerns of extracellular NM23-H1 protein levels.

#### 4.6 Intracellular expression of NM23-H2 is maintained in NM23-H1-KO clones.

In chapter 3, probing of DLBCL cell lysates for NM23-H2 gave two bands at approximately 17 and 19 KDa. As shown in Figure 4.6A, this doublet was again seen in both HT WT and Cas9 lysates but not in HT KO clones in which only the 17KDa band was detected. The antibody used to probe for NM23-H2 in this experiment was the anti-NME2 antibody [EPR8351]

(ab131329) antibody which is known to have some cross reactivity with NM23-H1. The loss of the upper band therefore confirms NM23-H1 knockout in the HT KO clones using a second antibody and at the same time identifies that knockout of NM23-H1 in these clones did not affect NM23-H2 expression. Densitometric analysis of n=2 westerns demonstrated similar levels of NM23 H2 expression in HT WT and KO cells Figure 4.6B.

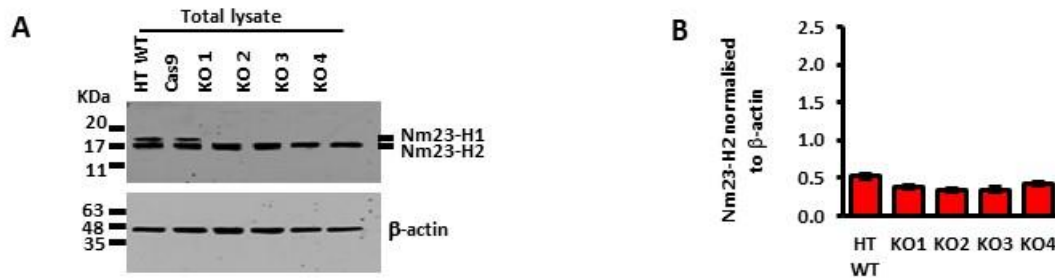


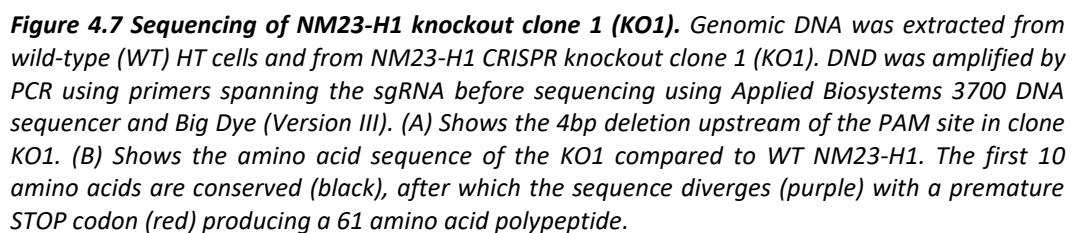
**Figure 4.6 Nm23-H1 intracellular expression in exponentially growing Nm23-H1-KO clones.** Total protein lysate (20µg) from exponentially grown Nm23-H1-KO clones was separated by SDS-PAGE before immunoblotting for Nm23-H2, β-actin was used as a loading control. (A).Nm23-H2 intracellular expression in exponentially growing Nm23-H1-KO clones, HT wild type and Cas9 were used as a positive control. (B) Intracellular Nm23-H2 expression levels quantitation in Nm23-H1 KO clones.

#### 4.7 Sequencing of NM23-H1-KO clones.

Sequencing was performed in the attempt to identify the deletion in the NM23-H1 gene in the CRISPR/Cas9 knockout of HT KO cell lines. Genomic DNA was extracted, and PCR performed to amplify the targeted region of *NME1* as described in Chapter 2. The PCR products were run on 1% agarose gels to check their purity before using for sequencing. Sequencing was performed using Applied BioSystems 3700 DNA sequencer and Big Dye (Version III) in the Functional Genomics Laboratory at the University of Birmingham. In the case of clone KO1, sequencing identified that CRISPR/Cas9 editing resulted in a 4bp deletion 2bp upstream of PAM sites (Figure 4.7A). This resulted in a frameshift generating a polypeptide of 61 amino acids length with only the first 10 amino acids conserved with the wild-type (WT) protein (Figure 4.7).

Unfortunately, sequencing with these primers did not identify mutations in clones KO2, KO3 and KO4. In order to get better DNA sequencing results, nested PCR was used to

**A**





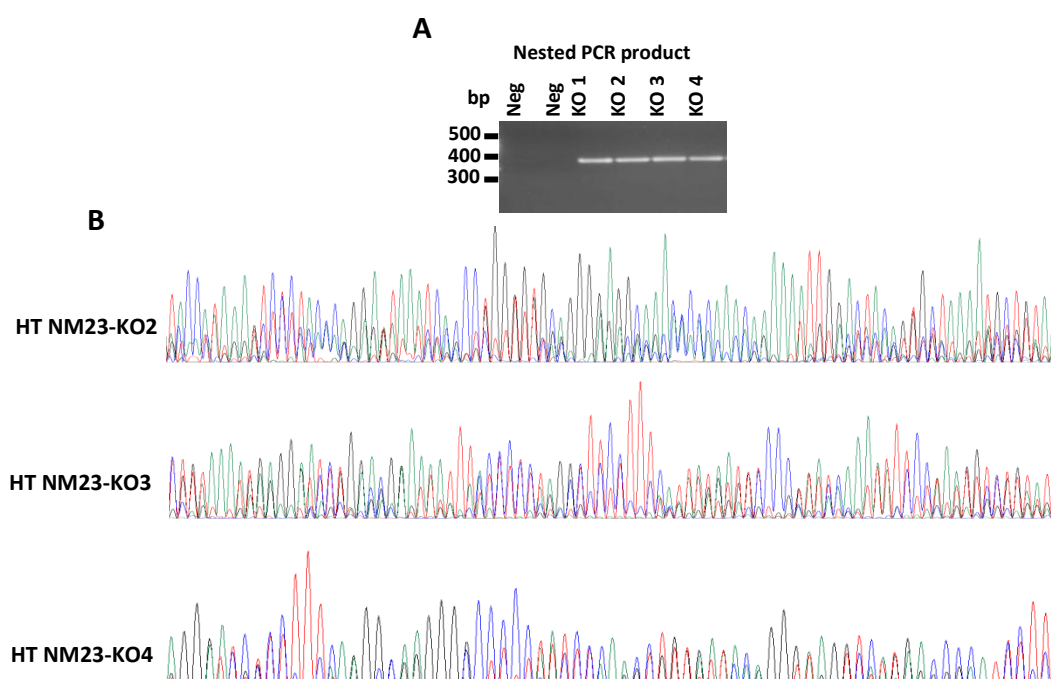


**Figure 4.8 Sequencing of NM23-H1-KO clones KO2, KO3 and KO4.** In order to get better genomic DNA sequencing results, nested PCR was used to improve sensitivity and specificity of PCR products. (A) The nested PCR products were separated on 1% agarose gel to check their purity before using for sequencing. Two nested PCR master mix samples with no DNA were run as a negative control. (B) Nm23-KO clones sequencing, showing the poor sequencing of the clones KO2,3 and 4. It was again a poor sequencing with multiple peaks.

#### 4.8 Growth rate of HT WT and HT NM23-KO clones

NM23-H1 expression is associated with cell proliferation in several human tumours, such as prostate carcinoma (Igawa et al., 1994), neuroblastoma (Hailat et al., 1991) and leukaemia (Keim et al., 1992). Proliferation activity in human mammary tumour (Caligo et al., 1995) has been correlated directly to *NME1* gene expression. Hence, it was crucial to determine if there were any changes in cell proliferation rate or any important phenotypic consequences after knocking out *NME1* gene expression in HT DLBCL cells. HT WT, HT Cas9 and HT NM23-KO1-4 cells were seeded at  $1 \times 10^6$  cells/ml, monitored day by day and counted with flow cytometry for 7 days, being fed as necessary. Figure 4.9 shows cumulative cell numbers over 7 days. As can be seen, there was no difference between WT or NM23-H1 KO cells in their growth and survival.

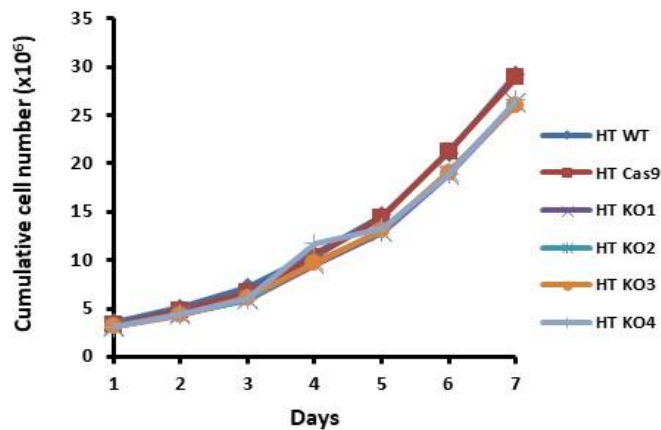


**Figure 4.9 Growth rate of HT WT and HT NM23-KO clones.** HT WT, HT Cas9, HT NM23-KO1-4 were plated at  $1 \times 10^6$  cells/ml, monitored day by day and counted with flow cytometry for seven days. Data is plotted as days versus cumulative cell number. N= 3 replicates.

#### 4.9 Investigation of the effect of hypoxia vs normoxia on proliferation of HT WT, HT NM23-KO and KG1a cells.

Since the NM23-H1 KO HT cells grew similarly to the WT cells under normal conditions i.e.  $37^\circ\text{C}$  in 5%  $\text{CO}_2$  and 21%  $\text{O}_2$ . Many lymphomas will have areas of hypoxia, hence the growth of WT and NM23-KO HT cells in hypoxic conditions (1%  $\text{O}_2$ ) was determined and compared to growth in normoxia (21%  $\text{O}_2$ ). HT WT, HT Cas9 and NM23-KO1-4 were plated at a concentration of  $0.5 \times 10^6$  cells/ml and KG1a WT, KG1a Cas9 and NM-KO at  $0.25 \times 10^6$  cells/ml

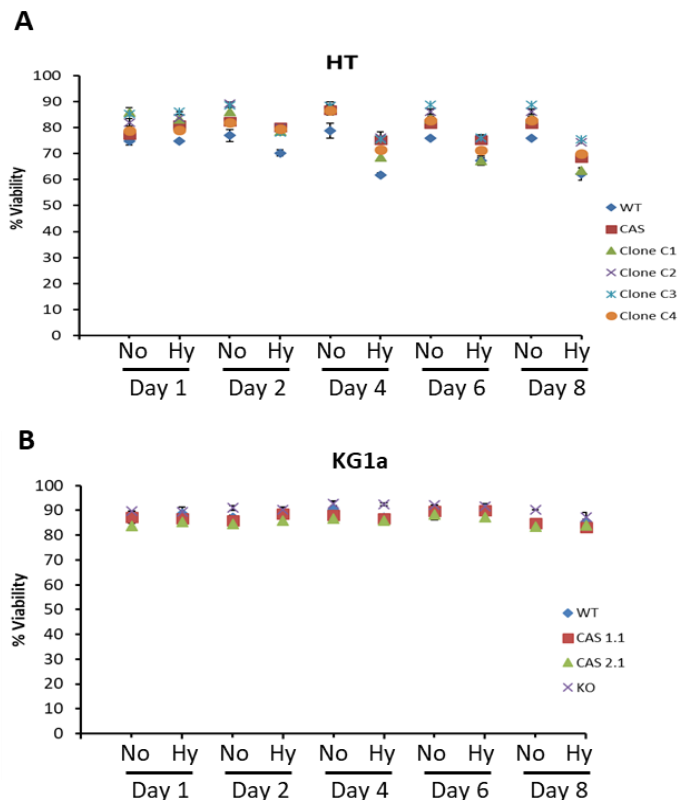


**Figure 4.10 Hypoxia vs normoxia effect on cell viability.** Cells were grown in complete RPMI 1640 media with 10%FBS. HT cells were plated at  $0.5 \times 10^6$  cells/ml, and KG1a cells at  $0.25 \times 10^6$  cells/ml. Parallel cultures were incubated in normal oxygen conditions- 20% (normoxia-No), or under hypoxia at 1%  $\text{O}_2$  (hypoxia- Hy). Cell viability was assessed by flow cytometry over 8 days and cells passaged as needed. (A) shows the % viability of HT cells (B) show the viability of the KG1A cells for 8 days. Data shown is average  $\pm$  SEM of N=3. (\*  $p < 0.05$ ) (ANOVA with Tukey post-hoc test).

in 4mls. Cell number and viability was measured by flow cytometry every day and cultures passaged (1:2 or 1:3) every 2 days as required. Figure 4.10A shows the viability of the HT cells over 8 days, Figure 4.10B show the viability of the KG1a cells (KG1a NM23-H1 KO cells were generated by Dr. Sandro Trova, School of Biosciences) for 8 days. As can be seen, there was no difference in the viability of the NM23-H1 KO cells compared to WT or Cas9 control cells indicating that NM23-H1 is not essential for cell viability either in normoxia or under hypoxic conditions.

Cell number was also assessed over the 8 days and Figure 4.11A shows the growth rates of HT WT, HT Cas9, HT-NM23-KO1-4 when grown in 21% O<sub>2</sub>. The doubling time for these cells was calculated and was found to be ~28hrs (Figure 4.11B). There was no significant difference between WT HT cells or any of the NM23-H1 KO clones. Cell viability after 8 days was also comparable between WT HT cells and the NM23-H1 clones (Figure 4.11C). No differences were observed between HT WT and NM23-H1 cells when they were cultured under hypoxia however the doubling time increased to ~37hrs (Figure 4.11D, E and F).

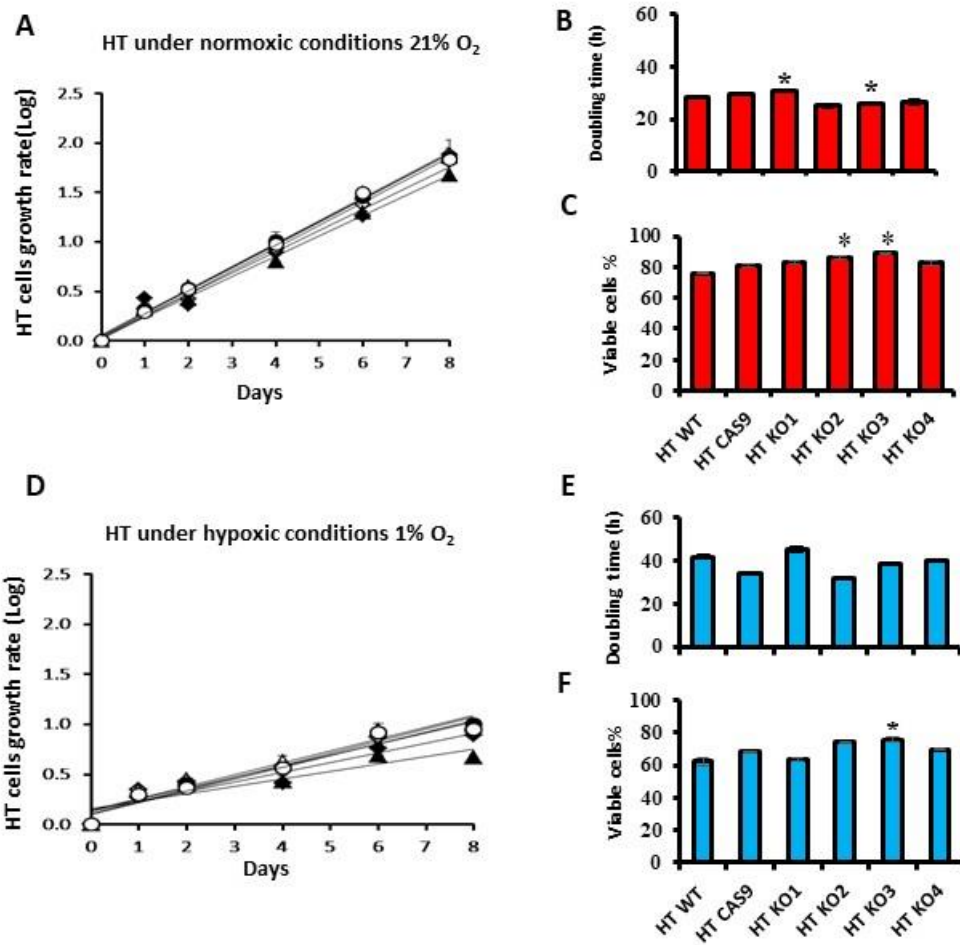


**Figure 4.11 Cell growth rate for HT cell line in normoxic and hypoxic conditions.** HT WT, HT Cas9 and NM23-KO1-4 were plated at a  $0.5 \times 10^6$  cells/ml and incubated either at 21% or 1 % O<sub>2</sub>. Cells were counted via flow cytometry every day and split 1:2 or 1:3 as required. The experiment was set for 8 days with one plate for each day. (A) Logarithmic cell growth rate of HT cells over 8 days in normoxic conditions. (B) Doubling time of the HT cells over 8 days in normoxic conditions. (C) Percentage of viable cells in normoxic conditions at day 8. (D) Logarithmic cell growth rate of HT cells within 8 days in hypoxia conditions. (E) Doubling time of the HT cells within 8 days in hypoxic conditions. (F) Shows the percentage of viable cells in hypoxic conditions. Data shown is average  $\pm$  SEM of N=3. (\*  $p < 0.05$ ) (ANOVA with Tukey post-hoc test).

Similar to the HT cells, no significant differences were observed between WT and NM23-H1 KO KG1a cells. The growth rates in 21% O<sub>2</sub> of KG1a WT, KG1a Cas9 1, KG1a Cas9 2 and KG1a-KO cells are shown in 4.12 A. The doubling time for these cells was calculated and shown in 4.12 B. Cell viability is shown in 4.12C. Figure 4.12 D, E and F show the same parameters for the same cells under hypoxic conditions.

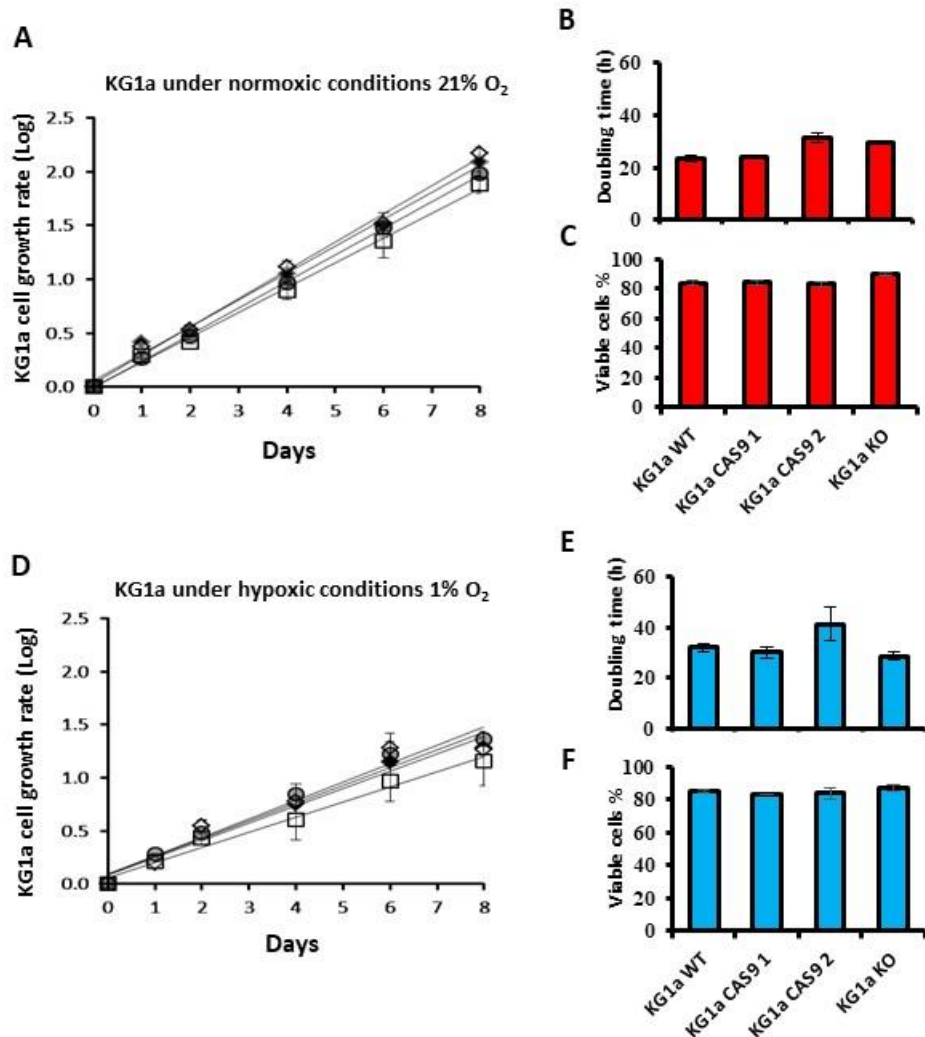


**Figure 4.12 Hypoxia vs normoxia effect on cell growth rate for KG1a cell line.** The cells were exponentially growing in complete RPMI 1640 media with 10%FBS. KG1a WT, KG1a Cas9 and NM-KO plated at  $0.25 \times 10^6$  cells/ml and incubated either at 21% or 1 % O<sub>2</sub>. Cells were counted by flow cytometry every day and split 1:2 or 1:3 as required. The experiment was set for 8 days with one plate for each day. (A) Logarithmic cell growth rate of HT cells over 8 days in normoxic conditions. (B) Doubling time of the HT cells over 8 days in normoxic conditions. (C) Percentage viable cells in normoxic conditions. (D) Logarithmic cell growth rate of HT cells over 8 days in hypoxia conditions. (E) Doubling time of KG1a cells over 8 days in hypoxic conditions. (F) Percentage viable cells in hypoxic conditions. Data shown is average  $\pm$  SEM of N=3. (\*  $p < 0.05$ ) (ANOVA with Tukey post-hoc test).

#### 4.10 Summary

In this chapter stable knockout (KO) in the *NME1* gene in DLBCL cell lines were generated. To do this, CRISPR/Cas9 vectors were constructed with sgRNAs targeting exons 2 or 3 of the *NME1* gene. Of the 9 DLBCL cell lines transfected, and >900 clones analysed; only one cell line HT, gave rise to 4 *NME1* KO clones. In parallel, KG1a AML cells were also transfected with the CRISPR/Cas9 vectors and of the >100 clones screened, only 1 *NME1* KO clone was identified. Of the 4 HT clones, 2 demonstrated very low levels of intracellular NM23-H1 compared to HT WT and HT Cas9 control transfected cells. The remaining 2 KO clones had no detectable NM23-H1 protein. No protein was detected in the KG1a KO clone. All *NME1* KO clones, both HT and KG1a, had no detectable NM23-H1 protein in the media indicating that even the very low levels of NM23-H1 protein seen in HT KO1 and KO2 was not being secreted. Importantly, NM23-H2 expression was not altered in any of the KO clones demonstrating the specificity of the knockout. CRISPR/Cas9 knockout of NM23-H1 in either HT or KG1a cells had no impact on cell growth, viability or immunophenotype indicating that NM23-H1 is not essential for growth and survival under the conditions tested. These data suggest that the impact of NM23-H1 on prognosis is mediated through paracrine cell extrinsic mechanisms affecting the tumour microenvironment.

**CHAPTER FIVE**

**DLBCL INFLUENCES**

**CYTOKINE SECRETION**

**BY MONOCYTES VIA**

**RELEASE OF NM23-H1**

## **5 DLBCL influences cytokine secretion by monocytes via release of NM23-H1**

In the previous chapter it was identified that knocking out NM23-H1 had no impact on viability, cell growth or immuno-phenotype of HT-KO clones. Thus, it appears that NM23-H1 expression and release may be not directly important for DLBCL cells. Thus, the reported impact of NM23-H1 levels on DLBCL prognosis could be due to actions of released NM23-H1 on the tumor microenvironment and potentially mediated by extrinsic cellular mechanisms. The experiments presented in this chapter, investigated the possible cross-talk between released NM23-H1 and other immune cells. It was felt important for these experiments to establish cell cultures under serum-free conditions (see chapter 2). Serum components can degrade, bind or interact with cellular secretions and this may have influenced results. Furthermore, FBS used in experiments is likely to contain bovine NM23 that could potentially impact on NM23-H1 released in culture. DLBCL cell lines were gradually acclimatised to growth in serum free conditions (media supplemented with 1% ITS+ instead of 10% FBS) by feeding with ITS+ media at each passaging until the cells were growing in serum-free media. There was an initial slowing down of the cells after which they continued to grow normally.

### **5.1 NM23-H1 intracellular expression in DLBCL cell lines acclimatised to growth in serum free cultures.**

When maintained in FBS, DLBCL cell lines demonstrated high intracellular expression of NM23-H1 (Chapter 3). Figure 5.1 compares the expression of NM23-H1 by HT, Farage, U2932, SUDHL4, SUDHL5, SUDHL6, OCILY1, OCILY3 and OCILY7 cells when maintained in complete medium (RPMI media +10% FBS for HT, Farage, U2932, SUDHL4, SUDHL5 and SUDHL6: IMDM media +20% FBS for OCILY1, OCILY3 and OCILY7) or when acclimatised to growth in media substituted with 1% ITS+ in place of FBS. The western blotting results demonstrated that these cell lines exhibited markedly similar levels of NM23-H1 protein in either condition.



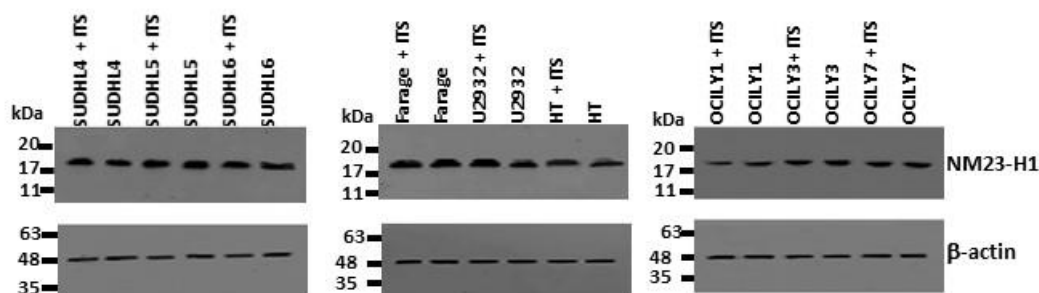


**Figure 5.1 comparison of NM23-H1 intracellular expression in cell lines cultured in media containing FBS and ITS+.** Lysate from exponentially growing DLBCL cell lines (20ug) in FBS (10% FBS for HT, Farage, U2932, SUDHL4, -5, -6 and 20% FBS for OCILY1, -3, -7) or DLBCL cell lines growing in ITS+ (1%) media were separated by SDS-PAGE and probed for NM23-H1 expression and  $\beta$ -actin as a loading control. Detection was performed using fluorescent secondary antibodies.

## 5.2 NM23-H1 extracellular expression in DLBCL cell lines acclimatised to growth in serum free cultures.

Extracellular expression of NM23-H1 was also investigated in the nine DLBCL cell lines acclimatised to growing in serum free conditions. Culture supernatants were harvested and assessed for NM23-H1/NM23-H2 secretion using SDS-PAGE. Western blotting was performed after incubating DLBCL cell lines in fresh media for 24 and 96 hours. The cells were either incubated in complete media with 20% FBS (For OCILY1, -3 and -7), 10% FBS (For HT, U2932, Farage, SUDHL4, -5 and -6) or in media supported with 1% ITS+. NM23-H1 protein was observed after 24 hours with a stronger signal after 96 hours, Figure 5.2A. Feeding media (30 $\mu$ l) was used as a negative control, to ensure no cross-reaction between the media components and anti-NM23 H1 antibody (C20, Santa Cruz Biotech) that was used to probe the examined membranes. Serial dilutions of recombinant NM23-H1 were loaded onto and separated by SDS-PAGE and probed for NM23-H1 expression in order to quantify NM23-H1 secretion DLBCL cell lines grown in FBS media and ITS+, Figure 5.2 B, C. It was crucial to check cell viability for cell lines used to detect NM23-H1 secretion was not coming from dying cells Figure 5.2 D.

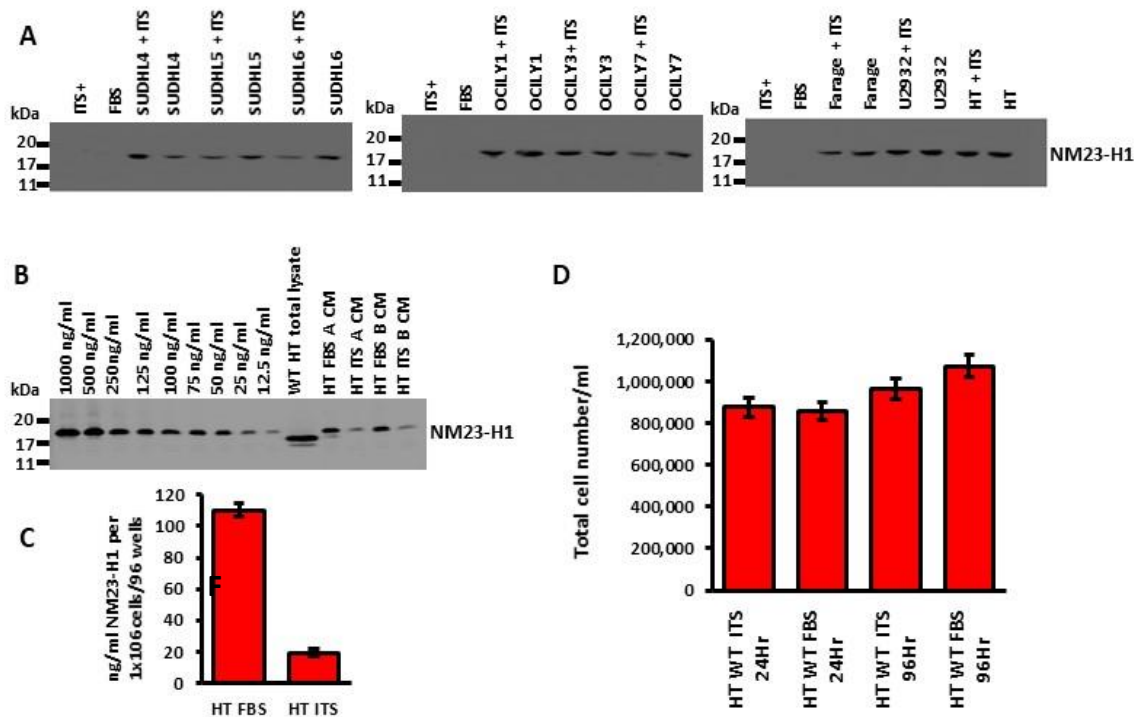


**Figure 5.2 NM23-H1 extracellular expression in serum free acclimatised DLBCL cell lines.** (A)Conditioned media (CM) (24 $\mu$ l) from exponentially growing DLBCL cell lines in FBS or ITS+ media were separated by SDS-PAGE and probed for NM23-H1 expression. Detection was performed using fluorescent secondary antibodies. As a negative control, (24 $\mu$ l) of media (RPMI1640/IMDM) either with ITS+ or FBS were loaded in the first two lanes on each gel. (B) A serial dilution of rNM23-H1 samples was made to get 1000, 500, 250, 125, 100, 75, 50, 25 and 12.5 ng/ml. 24 $\mu$ l of rNM23-H1 protein or CM was mixed with 8  $\mu$ l 4xSDS-gel loading buffer and 30 $\mu$ l of each sample separated by SDS-PAGE and probed for NM23-H1 expression. (C) Levels of NM23-H1 in the CM was calculated from a standard curve of the rNM23-H1 serial as NM23-H1 ng/ml per 1x10<sup>6</sup> cells. (D) Total cell number/ml for HT WT cultures was measured at the time of harvesting of CM. Data shown is mean  $\pm$  SEM of N=4 experiments.

### 5.3 QRT-PCR analysis of *NME1* expression in ITS+ maintained HT WT and NM23-H1 KO clones (ITS+) versus HT WT and NM23-KO growing in complete media.

QRT-PCR was used to analyse *NME1* mRNA expression in exponentially growing HT WT and NM23-KO (KO3 and KO4) clones maintained in ITS+ versus, HT WT and NM23- KO (KO1, KO2, KO3 and KO4) growing in complete media. *NME1* mRNA expression was normalised to 18S and then calculated as expression relative to WT HT cells grown in FBS media (complete media) (Figure 5.3). The results show that HT WT maintained in ITS+ media expressed only ~20% of the *NME1* mRNA expressed when the same cells were grown in FBS containing media. In both serum conditions and in ITS+, the NM23-H1 KO clones expressed <10% compared to WT HT cells, and for clone KO4, the levels were at the limits of detection.

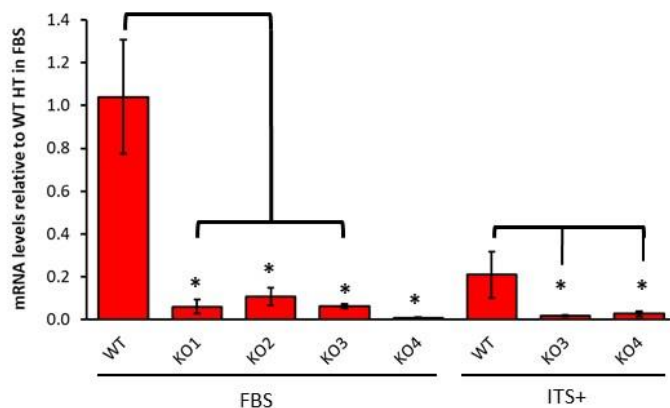


**Figure 5.3 *NME1* mRNA expression in HT WT and NM23-KO clones grown in FBS and serum-free (ITS+) conditions.** *NME1* mRNA expression was measured by QRT-PCR in exponentially growing FBS HT, WT and NM23-KO clones and ITS+ HT, WT and NM23-KO clones. *NME1* mRNA levels were calculated relative to HT WT grown in FBS. Data shown is average  $\pm$  SEM of a minimum of N=3 samples. \*  $p < 0.05$  (ANOVA with Tukey post-hoc test).

### 5.4 Response of peripheral blood mononuclear cells to extracellular NM23-H1 and recombinant NM23-H1.

Data from this project indicate that DLBCL cells do not bind NM23-H1. If NM23-H1 is in fact not taken up by DLBCL cells, then the premise must be that the extracellular NM23-H1 is signaling to other components of the tumour microenvironment or to systemic components. A previous student in the lab (unpublished data) investigated the NM23-H1 binding ability of cells present in normal peripheral blood. The result showed that approximately 50% CD3+ T

cells, almost all monocytes and granulocytes and approximately 50% of B cells bound NM23-H1.

The current experiments investigated the binding and effect of NM23-H1 secreted by HT WT cells on peripheral blood mononuclear cells (PBMCs). Blood samples collected from four healthy volunteers were used to isolate PBMCs by density centrifugation. Purified PBMCs were seeded at  $0.5 \times 10^6$  cells/ml in either complete media supplemented with rNM23-H1 ( $2 \mu\text{g/ml}$ ), conditioned medium (CM) from 96hr cultures of HT WT, HT Cas9, NM23-KO clones (KO1-KO4) or in WT HT CM supplemented with rNM23-H1 ( $2 \mu\text{g/ml}$ ). The viability of PBMC cultures was measured after 96hrs by flow cytometry counting beads. A gate (R1) was drawn around viable cells and the counting beads (R2) used to determine the viable cell numbers (Figure 5.4).

In cultures where extracellular NM23-H1 was present, i.e. CM from HT WT and HT Cas9, Media plus exogenous rNM23-H1 ( $2 \mu\text{g/ml}$ ) or HT WT CM plus exogenous recombinant NM23-H1 ( $2 \mu\text{g/ml}$ ), there was a small increase in cell number/ml from  $0.5 \times 10^6$  cells/ml to  $0.6-0.65 \times 10^6$ . However, this increase was not significant across the four donors. In contrast, in the absence of NM23-H1 (CM from NM23-KO clones KO1-KO4), there was a decrease in cell number per ml from  $0.5 \times 10^6$  cells/ml to  $0.45 \times 10^6$  cells/ml or even to  $0.4 \times 10^6$  cells/ml which was consistent across donors but did not reach statistical significance (Figure 5.4B). These data indicate that NM23-H1 is able to support PBMC survival.

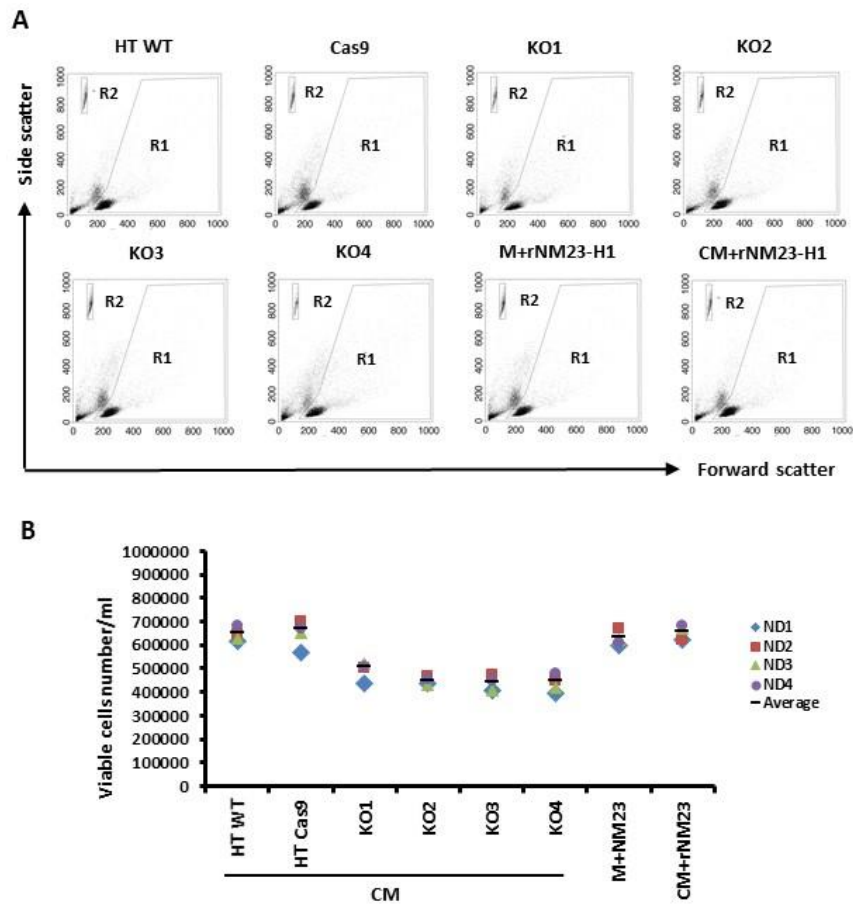


**Figure 5.4 Response of normal donor PBMCs to conditioned media and rNM23-H1.** Samples of normal peripheral blood taken from 4 donors (ND1, ND2, ND3 and ND4). Peripheral blood mononuclear cells (PBMCs) were purified by density centrifugation. Cells were cultured at  $0.5 \times 10^6$  cells/ml with conditioned medium of HT WT, NM23-KO clones, RPMI 1640 FBS+ media plus ( $2 \mu\text{g/ml}$ ) or WT HT conditioned media plus ( $2 \mu\text{g/ml}$ ) for 6 days. The samples analysed by flow cytometry and the viable number were determined using the viable gate (R1) and (R2) which gated the counted beads. **A.** Representative flow cytometry dot plots showing side scatter and forward scatter from one donor depicting viable cells. **B.** A graph showing the total cell number per 1 ml for the eight treatments for four donors. Data is presented as mean  $\pm$  SEM. (N=3). KO1:NM23-KO1, KO2:NM23-KO2, KO3:NM23-KO3 and KO4:NM23-KO4. \*  $p < 0.05$  (ANOVA with Dunnett's test). N=5 replicates.

## 5.5 Characterising viable PBMCs sup-populations by Immunophenotyping.

Immunophenotyping was used to characterise different viable PBMCs populations following treatments. Specific fluorescent antibodies to cell surface markers were used to identify T cells (CD3, CD4, CD8), monocytes (CD14), granulocytes (CD11b) and B cells (CD19).

## 5.6 Measuring the impact of conditioned media on T-cells (CD3 positive cells)

CD3 is a T cell co-receptor cell surface marker used to identify all T-cells. CD4 identifies T helper cells and CD8 cytotoxic T cells. T cells were identified in the treated samples by staining with anti-CD3-PE or an isotype control and analyzed by flow cytometry. Representative side scatter/forward scatter dot plots for one donor are shown in Figure 5.5 A. Two gates are shown; (R3) which identified viable lymphocytes in the total viable cells samples and (R2) that gated the counting beads. CD3-positive cells accounted 60% to 70% of the surviving PBMCs across the four normal donors. Gate (R4) was applied to R2 gated cells to identify CD3 positive cells within the lymphocyte population and is illustrated as a representative forward scatter/CD3 dot plot for one donor (Figure 5.5B).

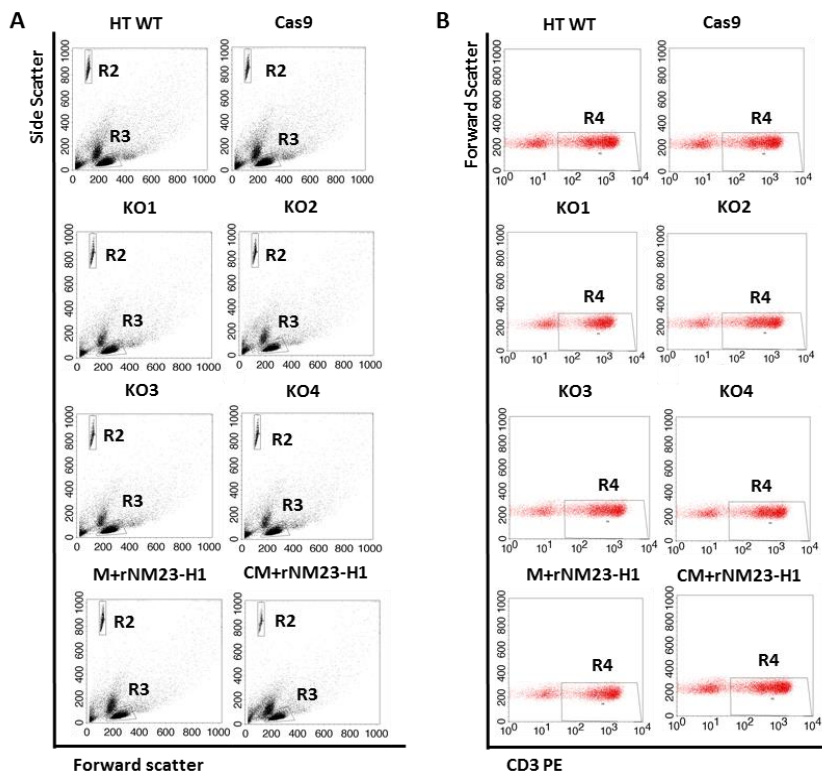


**Figure 5.5 Determination of T-cells (CD3+ cells) in normal donor PBMC samples.** Density centrifugation used to purify PBMCs, cells were cultured at  $0.5 \times 10^6$  cells/ml and treated with conditioned medium of HT WT, NM23-KO clones, RPMI 1640 FBS+ media plus (2 $\mu$ g/ml) exogenous rNM23-H1 or conditioned media of WT HT plus (2 $\mu$ g/ml) exogenous rNM23-H1 for 6 days. (A) Representative dot plots for one sample are shown, the viable gate (R3) applied in to identifying the lymphocytes in the total PBMCs viable cells and (R2) which gated the counted beads. (B) PBMCs cells were stained with CD3-PE or its isotype control (IgG1) and analyzed by flow cytometry. Viable lymphocyte was analyzed for CD3 expression (R4). N=5 replicates.

## **5.7 T-cell subsets response to extracellular NM23-H and exogenous recombinant NM23-H1.**

A mix of FITC-conjugated CD8 and APC-conjugated CD4 antibodies were used in determining viable T-cell sub-populations. Representative CD4/CD8 dot plots for one donor are shown in Figure 5.6A. There were differences in numbers of viable CD4+ cells identified in the presence of either extracellular NM23-H1 (HT WT and HT Cas9 supernatants) or exogenous recombinant NM23-H1 compared treatment with HT KO supernatants which lack Nm23-H1 (Fig 5.6 B). In general, cultures exposed to either extracellular or rNM23-H1 had tendencies towards a modest increase in numbers CD4+ viable cells whereas in cultures treated with HT KO supernatants had a modest decrease in CD4+ cell numbers. However, these differences did not reach statistical significance. In the same way, CD8+ T-cells modestly increased at day 6 in response to CM from HT WT, HT Cas9 or exogenous recombinant NM23-H1 treatment. Whereas there were modest decreases in CD8+ T cells after 6 days in cultures treated with HT KO supernatants. However, these differences did not reach statistical significance.

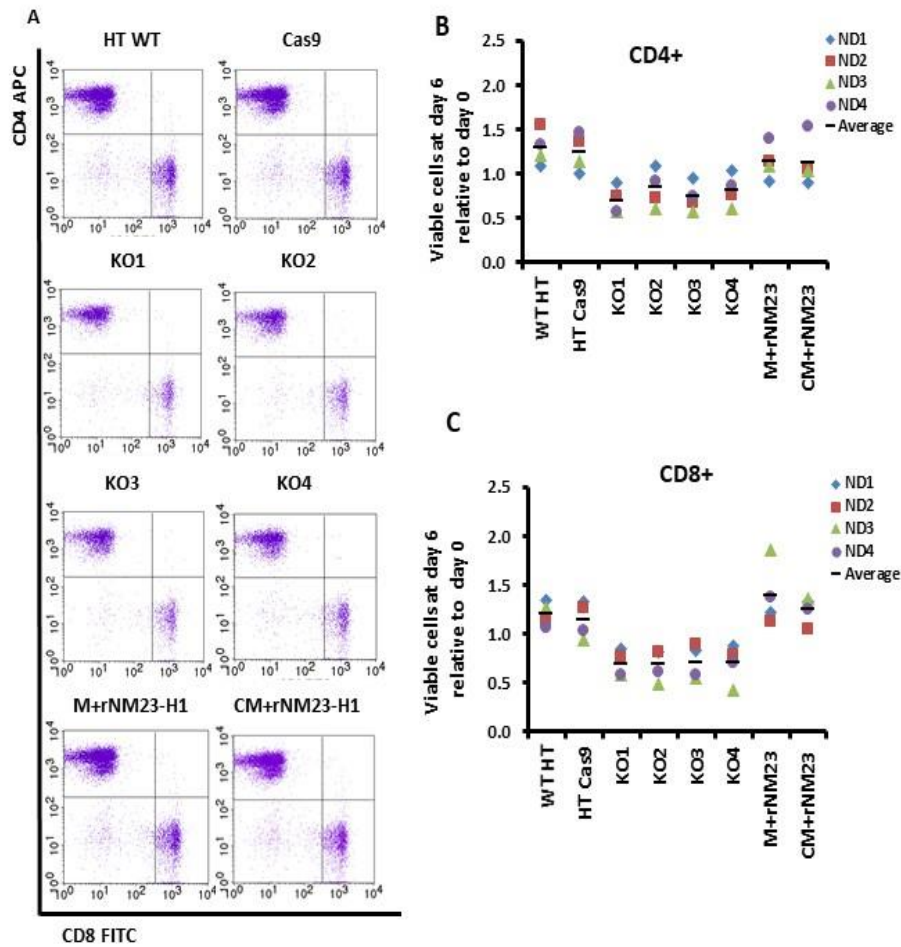


**Figure 5.6 T-cell subsets response to extracellular NM23-H and exogenous rNM23-H1.** PBMCs were purified using density centrifugation and cultured at  $0.5 \times 10^6$  cells/ml with conditioned medium from HT WT, HT Cas9, NM23-KO clones, RPMI 1640 FBS+ media plus  $2 \mu\text{g/ml}$  exogenous rNM23-H1 or WT HT conditioned media plus  $2 \mu\text{g/ml}$  exogenous rNM23-H1. Cells were harvested at day 6 and stained using anti-CD4 APC and anti-CD8 FITC before analysis by flow cytometry. (A) Representative CD8/CD4 dot plots from (B) fold change in CD4+ cell number relative to purified untreated PBMCs on day 0. (C) CD8 fold change in comparison to purified untreated PBMCs on day 0. Data is presented as mean  $\pm$  SEM. (N=3). \*  $p < 0.05$  (ANOVA)



## 5.8 Monocyte response to extracellular NM23-H and exogenous recombinant NM23-H1.

The presence of monocytes in PBMCs cultures was investigated using antibody to CD14 which is strongly expressed on monocytes and macrophages, however, it is negative or weakly expressed on pro-monocytes. Figure 5.7A shows representative CD11b/CD14 dot plots for one donor (for the remaining donors see Appendix B). In these plots CD14<sup>+</sup> cells are in gates R6 (CD14<sup>+</sup>/CD11b<sup>+</sup>) and R7 (CD14<sup>+</sup>/CD11b<sup>-</sup>). Figure 5.7B shows cumulative data for survival of total CD14<sup>+</sup> monocytes from all donors tested. Similar to the data for T-cell subsets (Figure 5.6), there was a modest increase in total CD14<sup>+</sup> cells at day 6 in response to CM from HT WT, HT Cas9 or exogenous rNM23-H1 treatment. Whereas there were modest decreases in CD8<sup>+</sup> T cells after 6 days in cultures treated with HT KO supernatants (a flow diagram in Appendix B explaining the experiments details). The majority of these differences did not reach significance with the exception of PBMCs grown in CM from NM23-KO1 and NM23-KO4 where the numbers of CD14<sup>+</sup> monocytes decreased (\*p<0.05) (Figure 5.7B).

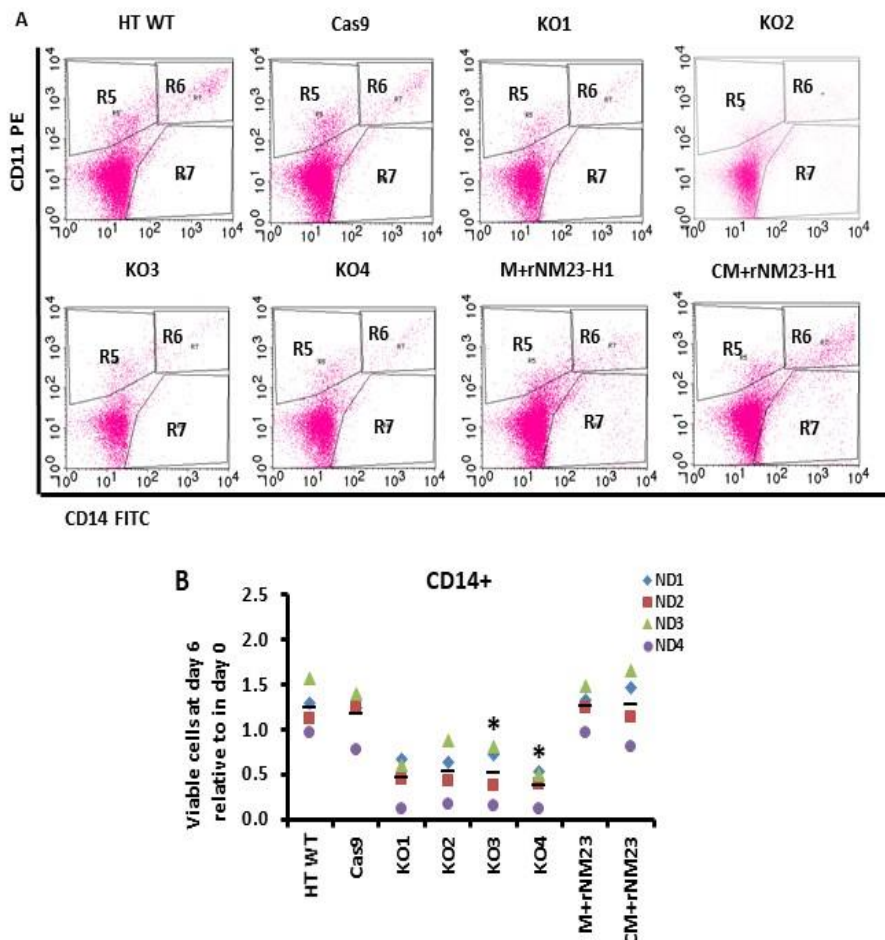


**Figure 5.7 Response of CD14<sup>+</sup> monocytes to extracellular NM23-H1 and exogenous rNM23-H1.** PBMCs were purified using density centrifugation and seeded at  $0.5 \times 10^6$  cells/ml in conditioned medium from HT WT, HT Cas9, NM23-KO clones, RPMI 1640 FBS+ media plus 2  $\mu$ g/ml exogenous rNM23-H1 or WT HT conditioned media plus 2  $\mu$ g/ml exogenous rNM23-H1. Cells were harvested at day 6 and stained with anti-CD14 FITC and anti-CD11b PE antibodies before analysis by flow cytometry. (A) Representative CD14/CD11b dot plots from ND1 show CD11b<sup>+</sup> cells (R5). CD14<sup>+</sup> cells (R7). CD14<sup>+</sup> CD11b<sup>+</sup> (R6). (B) CD14 fold change in comparison to purified untreated PMNCs in day 0. Data is presented as mean  $\pm$  SEM. (N=3). Dunnett's test).

## **5.9 Response of B-cells to extracellular NM23-H and exogenous recombinant NM23-H1.**

APC-conjugated CD19 antibody was used to identify viable CD19<sup>+</sup> B-cells at day 6 in treated PBMCs. Representative CD19 dot plots/forward scatter for one donor are shown in Figure 5.8A. As with the other cell types, extracellular NM23-H1 and exogenous rNM23-H1 treatments increased the proportion of CD19<sup>+</sup> B-cells in PBMCs cultures compared to day 0 (Figure 5.8 B). In samples treated with HT WT CM plus exogenous recombinant NM23-H1 this increase was statistically significant. In cultures treated with CM from HT KO cells there was a fall in numbers of CD19<sup>+</sup> cells at day 6 which reached significance for NM23-KO1, KO3 and KO4.

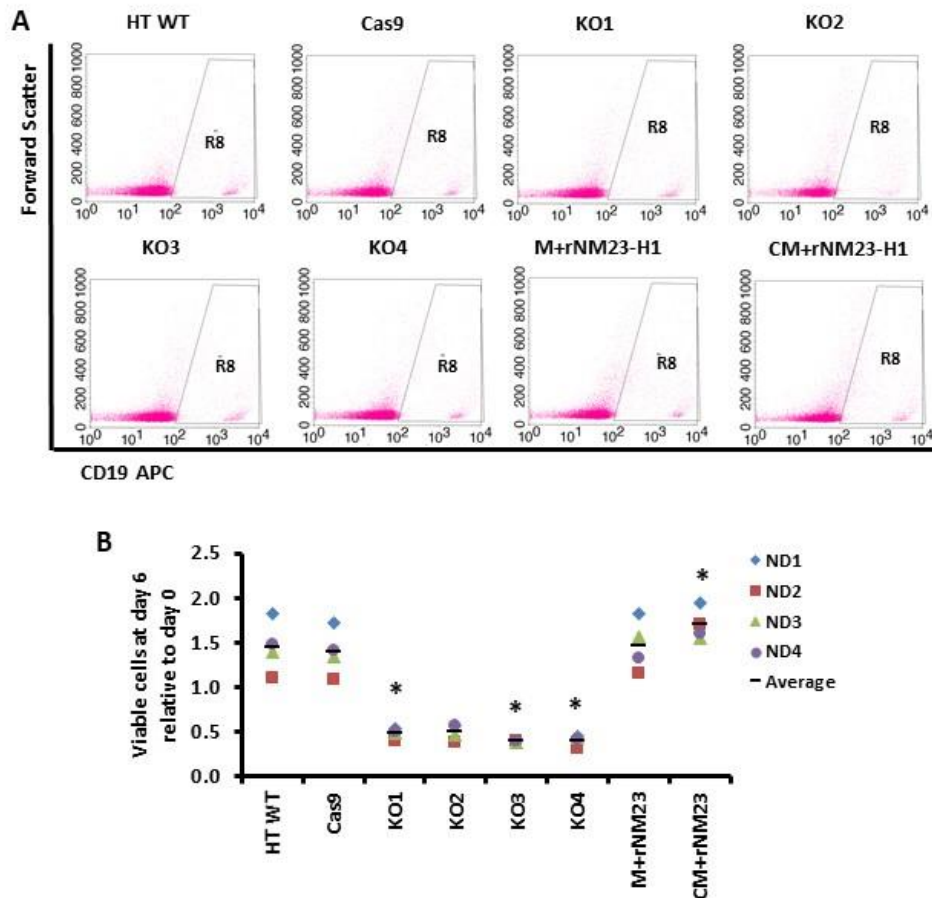


**Figure 5.8 Proportions of viable B-cells (CD19+) in response to extracellular NM23-H1 and rNM23-H1.** PBMCs were seeded at  $0.5 \times 10^6$  cells/ml, treated with conditioned medium of HT WT, HT Cas9, NM23-KO clones, RPMI 1640 FBS+ media plus  $2 \mu\text{g/ml}$  exogenous rNM23-H1 or WT HT conditioned media plus  $2 \mu\text{g/ml}$  exogenous rNM23-H1. Harvested at day 6 and stained using anti-CD19 APC antibody, analysed by flow cytometry. (A) Representative Side scatter/CD19 dot plots from ND1 show CD19+ cells (CD19+ in R8). (B) Fold change in CD19+ B cells relative to purified untreated PBMCs on day 0. Data is presented as mean  $\pm$  SEM. (N=3). \* $p < 0.05$  (ANOVA with Dunnett's test).

### **5.10 Immunophenotyping and purification assessment of monocyte fractions negatively selected from normal donor PBMCs.**

Previous results identified that expression and release of NM23-H1 is not directly necessary for DLBCL cells, suggesting that the impact of NM23-H1 on prognosis may be mediated by cell extrinsic mechanisms affecting the tumour microenvironment. A previous student in our lab, (unpublished data) identified that almost all monocytes present in normal peripheral blood bind rNM23-H1. The earlier results in this chapter demonstrated a greater proportion of CD14+ in PBMCs samples treated with extracellular NM23-H1 and exogenous rNM23-H1, in comparison to PBMCs samples treated with CM of NM23-KO clones. This suggests that NM23-H1 might positively affect monocytes viability, survival and potentially differentiation. Whereas CD14 is the main marker for human monocytes (Ginhoux and Jung, 2014, Qu et al., 2014, Murphy, 2012) they can be subdivided into three subtypes based on relative expression of CD14 and CD16. CD16 is also expressed on macrophage during their involvement in clearing and uptake antibody-opsonized pathogens(Murphy, 2012). Classical monocytes express strong CD14 positivity and are negative for CD16 (CD14++CD16-). Non-classical monocytes have weaker CD14 expression and strong CD16 positivity (CD14+CD16++). However, a subset of monocytes has intermediate expression (CD14++CD16+), (see Appendix B).

Monocytes were isolated from purified PBMCs from five normal donors by using negative selection as described in chapter 2. A mix of FITC-conjugated CD14 and APC-conjugated CD16 antibodies were used to characterise the viable monocytes in these preparations and to assess monocyte purification efficiency. Flow cytometry was used to assess single positive CD16, single positive CD14 and double positive CD14 CD16 cells. Side scatter/forward scatter and CD14/CD16 dot plots for the five donors are shown in Figure 5.9A-B. Each immunophenotype as a percentage of total cells percentage is illustrated in Figure 5.9C. Figure 5.9D shows that the purity of the cultures was between 86 %-96 % monocytes.

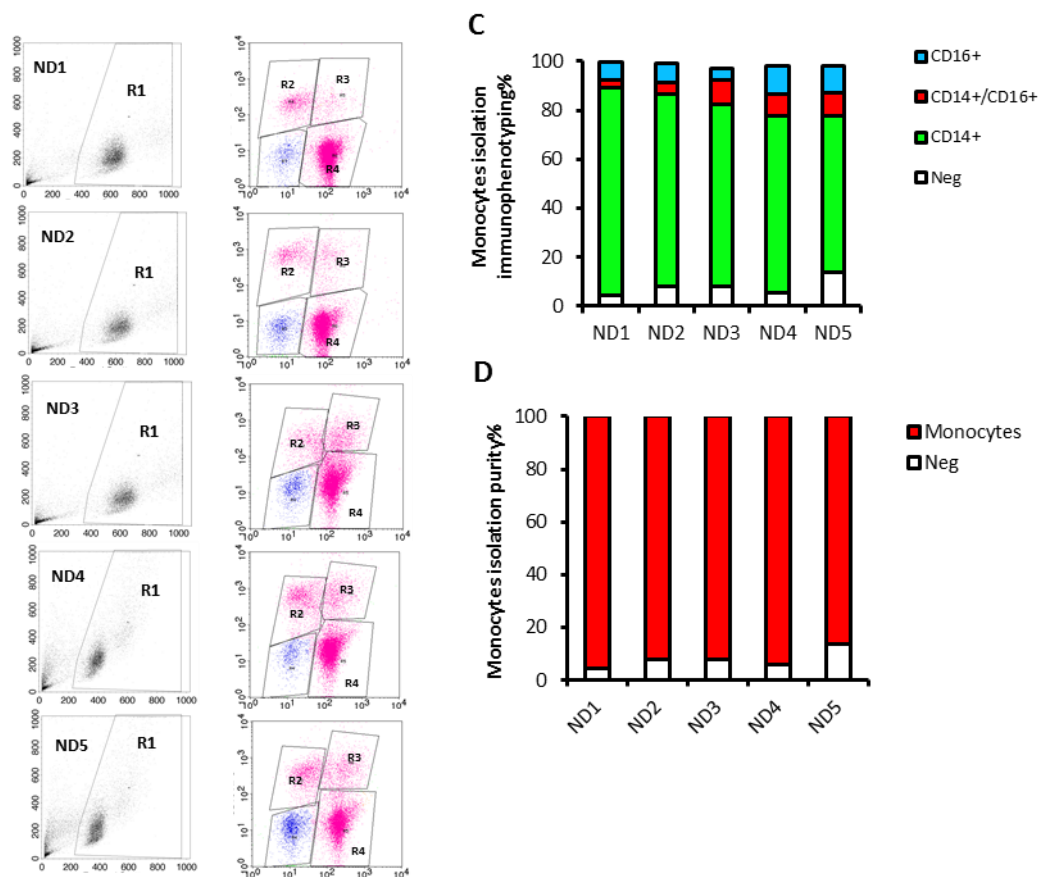


**Figure 5.9 Monocyte immunophenotyping.** Monocytes were purified from PBMCs by negative selection, before staining with FITC-conjugated CD14 and APC-conjugated CD16 antibodies and analysing using flow cytometry based. (A) Forward scatter/Side scatter dotplots of the five donors with gate R1 identifying the viable cells. (B) CD16/CD14 dot plot of the five samples are shown, (R2) which gated CD16+, (R3) gated CD14+CD16+, (R4) gated CD14+. (C) Proportion of each phenotype for each donor expressed as % of total viable cells. (D) Monocyte purity for each donor expressed as % of total viable cells. Normal Donor 1-5: ND1, ND2, ND3, ND4 and ND5.

### 5.11 Exogenous recombinant NM23-H1 promotes CD14+ monocyte survival

Alteration of host immunity is one of the most important and integral part of lymphoma pathogenesis (Rachinel and Salles, 2009, Nogai et al., 2011). It was previously identified that CD14+ cells can compose more than 30% of lymphoma tumours (Zhang et al., 2015); this close spatial connection between CD14+ cells and lymphoma cells suggests important cell to cell crosstalk. Thus, the association between higher NM23-H1 in DLBCL poor prognosis might be mediated by crosstalk between tumour cells and monocyte/macrophages in the tumour environment or beyond.

To test the impact of NM23-H1 on monocytes, purified primary monocytes from 5 healthy donors were cultured alone or co-cultured with HT WT cell line (NM23-H1 secretor) and KG1a AML cell line (non NM23-H1 secretor) at  $0.5 \times 10^6$  cells/ml in a 1:1 ratio, in the presence or absence of  $2 \mu\text{g/ml}$  recombinant NM23-H1, for 48 hours. Where exogenous recombinant NM23-H1 was not added an equivalent volume of EB was added as a control. The experiment was conducted in serum-free conditions (ITS+ media). Flow cytometry was used to determine any impact of the different culture conditions on monocyte viability and cell numbers. Representative side scatter/forward scatter plots and CD11b/CD14 dot plots of the six treatments for one donor at 48 hours are shown in Figure 5.10. An 'exogenous rNM23-H1 survival index' was used to evaluate monocyte responses to recombinant NM23-H1 using the following formula:

$$\frac{\text{Viable cells per ml with rNM23-H1}}{\text{Viable cells per ml with EB control for relative treatment}}$$

Viability indices of  $<1.0$  represented "negative" cell survival below EB control and those  $>1.0$  represented "positive" cell survival above EB control.

As can be seen in Figure 5.10, monocytes grown as monocultures in ITS+ with either elution buffer (EB) or even after the addition of rNM23-H1 have very low survival (bottom four dotplots). Cells were seeded at  $0.5 \times 10^6$  cells/ml at day 0, however 48hrs later there were between 2,000-11,000 cells/ml left in media with EB. Analysis of the cell numbers showed that in all 5 donors, there was improved survival with the addition of rNM23-H1 in all donor samples with cell numbers increasing to 3000-29000 cells/ml. Responses varied significantly between monocytes from the different donors (Figure 5.11). Analysis of the survival index for monocytes grown in ITS+ was between 1.2-6.1 fold. This data did not reach significance due to the small sample numbers.

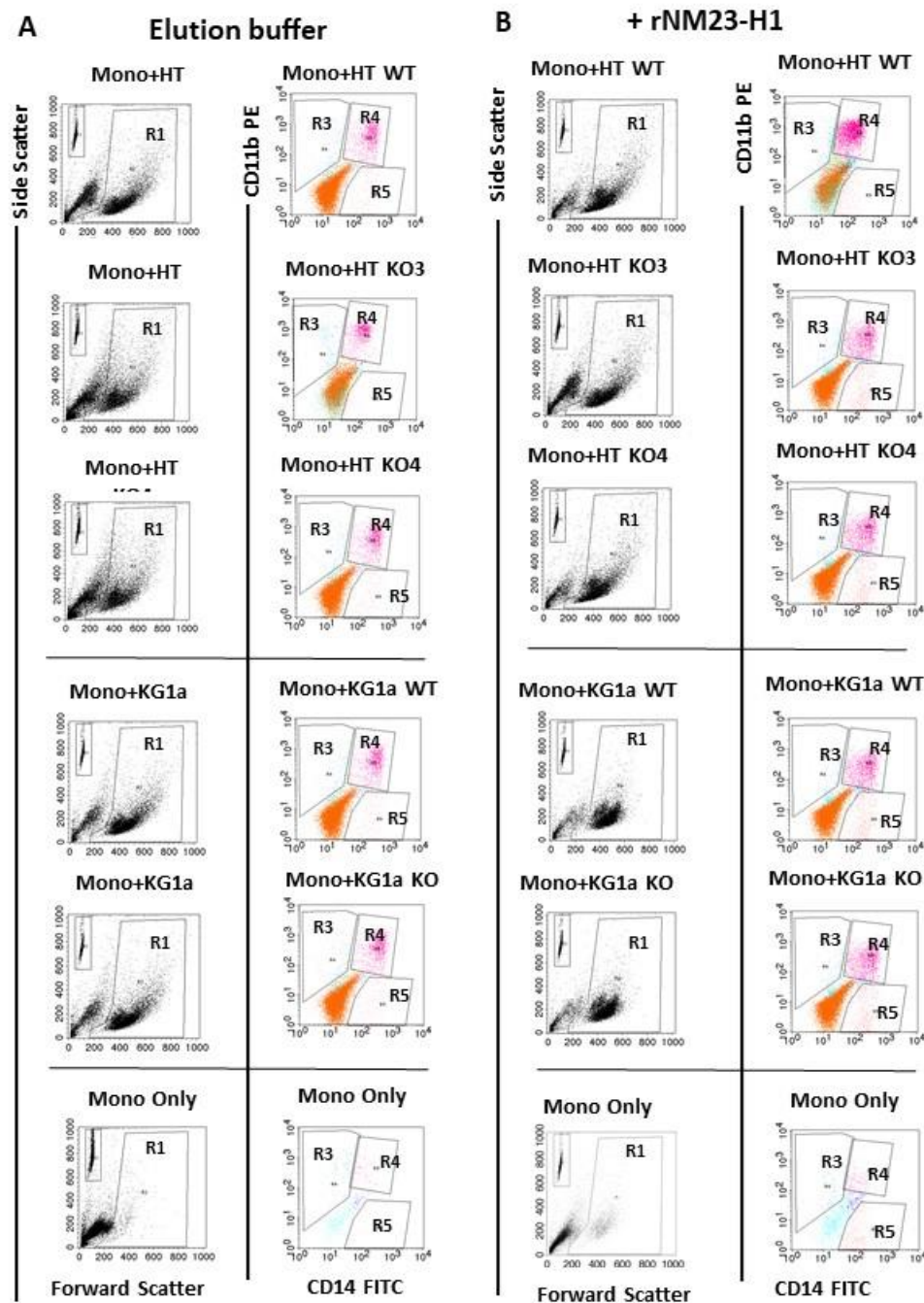


**Figure 5.10 Exogenous rNm23-H1 enhances monocytes and lymphoma cells growth.** Monocytes were purified from PMNCs by negative selection from five healthy donors, seeded at  $0.5 \times 10^6$  cell/m, cultured alone or in combination with HT WT, HT Nm23-KO3, HT Nm23-KO4, KG1a WT and KG1a Nm23-KO with either  $2 \mu\text{g/ml}$  of exogenous rNm23-H1 or elution buffer as a negative control. All cells were harvested after 48hrs before and analysed via flow cytometry. Only monocytes culture was used as a positive control. **A.** Representative side scatter/forward scatter dot plots of the six treatments for one donor are shown, the viable gate (R1) applied to identifying the viable cells in the total purified monocytes. (R2) applied on counted beads. **B.** Representative CD11b/CD14 dot plots of the six treatments for one donor are shown, (R3) applied to identifying CD11b+ viable cells, (R4) applied to identifying CD14+ viable cells and (R5) applied to identifying CD11b+CD14+ viable cells in the total purified monocytes. (R2) applied on counted beads. KO1:Nm23-KO1, KO2:Nm23-KO2, KO3:Nm23-KO3 and KO4:Nm23-KO4. M and Mono: Monocytes.



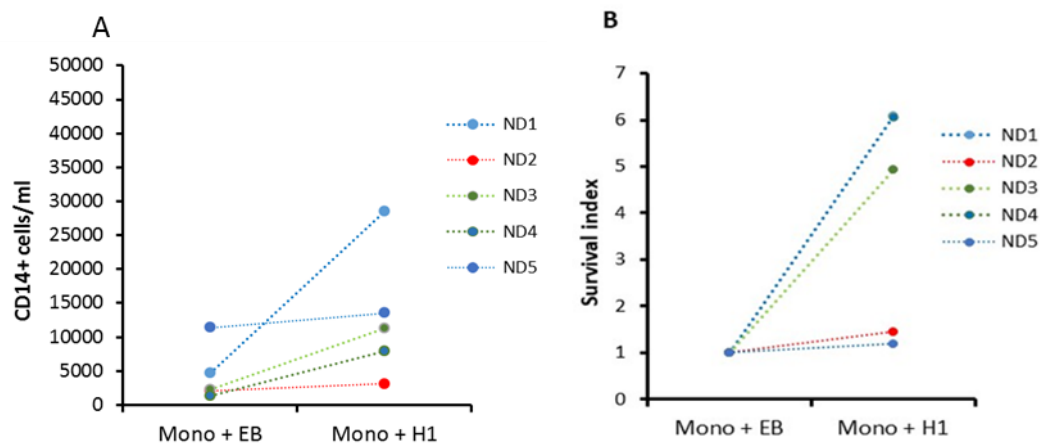


**Figure 5.11 CD14+ monocyte cell numbers increase marginally in serum-free media when supplemented with rNM23-H1.** Purified monocytes were cultured at  $0.5 \times 10^6$  cells/ml in serum free media (1%ITS+, RPMI 1640 +pen/strep) in the presence of either elution buffer (EB) control or  $2 \mu\text{g/ml}$  rNM23-H1. Cell number was quantitated after 48hours using anti-CD14-FITC antibody, fluorescent counting beads and flow cytometry. Data is presented as (A) cells/ml and as (B) survival index (cell numbers in EB/cell numbers in rNM23-H1). Dotted line links the samples for each donor. ND: Normal donor, Mono: monocytes, EB: elution buffer, H1: rNM23-H1.

Co-culturing monocytes with wild-type (WT) HT cells and also KG1a cells significantly improved monocyte survival (Figure 5.12) with increases in cell number to  $\sim 55,000$  cells/ml with HT and 155,000 cells/ml with KG1a. These numbers are still significantly below the original plating density of 500,000 cells/ml.

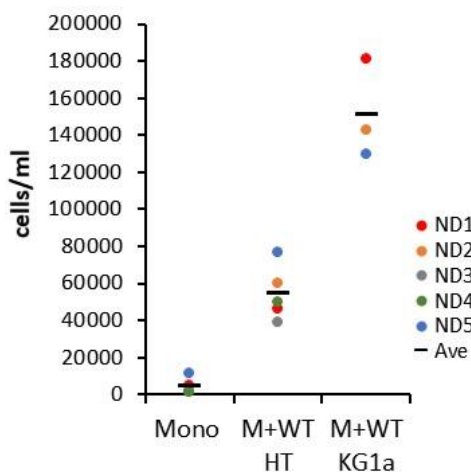


**Figure 5.12 CD14+ monocyte survive better in co-culture.** Purified monocytes were cultured at  $0.5 \times 10^6$  cells/ml in serum free media (1%ITS+, RPMI 1640 +pen/strep) with either HT cells or KG1a cells at  $0.5 \times 10^6$  cells/ml. Viable cell number was quantified after 48hours using anti-CD14-FITC antibody, fluorescent counting beads and flow cytometry. Data is presented as cells/ml. Dotted line links the samples for each donor. ND: Normal donor, Mono: monocytes.



Co-culturing monocytes with any of the HT or KG1a cells, WT or NM23-H1 KO clones, improved cell survival indicating that co-culturing itself promotes survival of monocytes (Figures 5.10, 5.13 and 5.14). The NM23-KO clones did not demonstrate significantly worsened or improved survival relative to WT cells for both HT lymphoma cells, and the KG1a cell lines.

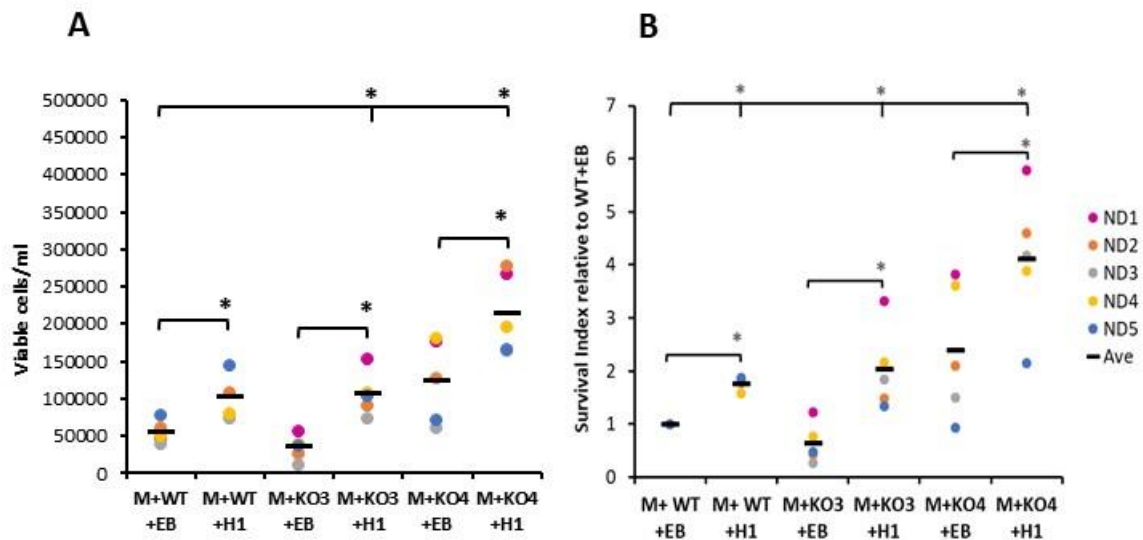


**Figure 5.13 Survival of CD14+ monocytes grown in co-culture with HT WT and NM23-H1 KO cells.** Purified monocytes were co-cultured in a 1:1 ratio with either HT WT or NM23-H1 KO cells in the presence of either elution buffer (EB) control or 2 $\mu$ g/ml rNM23-H1. Viability was assessed at 48hrs using flow cytometry and fluorescent counting beads and cells/ml calculated. Data is presented as (A) viable cells/ml and (B) survival index of all CD14+ cells i.e. number of cells in treatments/KO compared to monocytes cultured with WT+EB. \* $p$ <0.05 (ANOVA with Dunnett's test). ND: Normal donor, M: monocytes, WT: Wild-type cells, KO3/KO4: NM23-H1 knockout clones, EB: elution buffer, H1: rNM23-H1.

The addition of rNM23-H1 (2 $\mu$ g/ml) to the HT co-cultures significantly ( $p$ <0.01) enhanced survival of monocytes in all the HT cultures (WT and NM23-H1 KO) relative to their own EB control and also to WT HT cells supplemented with EB (Figure 5.13). It should be noted however that viable cell numbers still did not reach the original plating density of 500,000 cells/ml (Figure 5.13A). It cannot be determined from this assay whether the cells remaining at 48hrs are the original plated monocytes that survived for the duration of the assay or whether there has been some cell proliferation combined with cell death. Similar to the HT cells, the NM23-H1 KO cells did not differ in their ability to promote monocyte survival

(Figure 5.14) however, in contrast to the HT cells, the addition of rNM23-H1 did not enhance the survival (Figure 5.14).

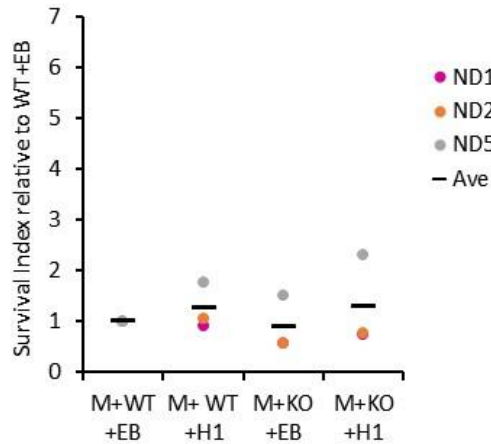


**Figure 5.14 Survival index for CD14+ monocytes co-cultured with KG1a WT and NM23-H1 KO clone.** Purified monocytes were co-cultured in a 1:1 ratio with KG1a WT, KG1a NM23-H1 KO, in the presence of either elution buffer (EB) control or 2µg/ml rNM23-H1. Viability was assessed at 48hrs using flow cytometry and fluorescent counting beads and cells/ml calculated. Data is presented as survival index of all CD14+ cells i.e. number of cells in treatments/KO compared to monocytes cultured with KG1a WT+EB. ND: Normal donor, M: monocytes, WT: KG1a WT cells, KO: KG1a NM23-H1 knockout clone, EB: elution buffer, H1: rNM23-H1. \* $p < 0.05$  (ANOVA with

## 5.12 Exogenous recombinant NM23-H1 enhances the survival of KG1a cells in serum-free media.

In addition to looking at the survival of monocytes in the co-cultures, viability of the HT and KG1a cells was also determined. The use of CD19 staining on the co-cultured cells identified HT cells (WT and KO) within the cultures. An anti-CD34 antibody was used to follow the fate of KG1a WT and KO cells in the cultures. The proportion of CD19+ viable HT cells remained relatively constant across all the co-culture treatments irrespective of whether the HT cells were WT or NM23-H1 knockouts (Figure 5.15A-B). The addition of recombinant NM23-H1 to the cultures enhanced HT cell numbers slightly but this was not significant. In contrast, the addition of recombinant NM23-H1 did enhance the survival of CD34+ KG1a cells (KG1a) (Figure 5.15C-D). The numbers of KG1a cells in co-cultures with monocytes from all five donors was significantly higher in the presence of rNM23-H1 compared to EB control after 48hrs ( $p < 0.01$ ) as can be visualised by the density of the CD34+cloud (R6) in recombinant NM23-H1 treatment co-cultures (Figure 5.15 D). This observation is particularly interesting since we know that KG1a cells can bind exogenously added NM23-H1 whereas HT cells do not (Chapter 3).

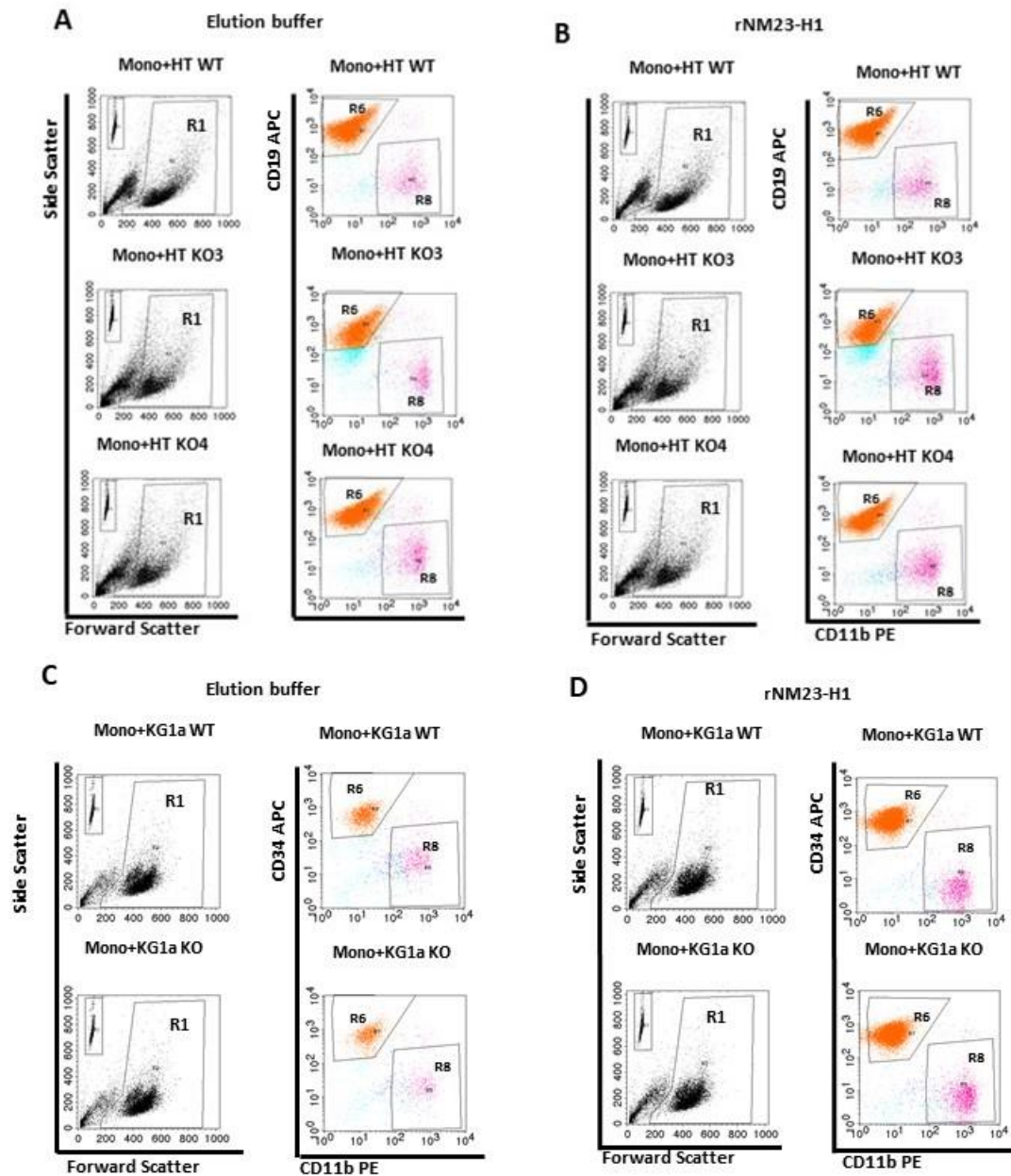


**Figure 5.15A Exogenous rNM23-H1 supports the survival of KG1a not HT cells in serum-free media.** Purified monocytes were co-cultured with either HT or KG1a WT/KO clones with all cells at  $0.5 \times 10^6$  cell/ml, in the presence of  $2 \mu\text{g/ml}$  of exogenous rNM23-H1 or equivalent amount elution buffer (EB) as a negative control. Representative Forward scatter/side scatter dot plots are shown for one donor for HT cells (A) and KG1a (C). Representative CD11b-PE vs CD19-APC are shown for HT-co-culture (B) and CCD11b+PE versus CD34 APC for KG1a co-cultures (D). Mono: Monocytes, WT: wild-type cells, KO: Nm23-H1 knockout cells .N=3.

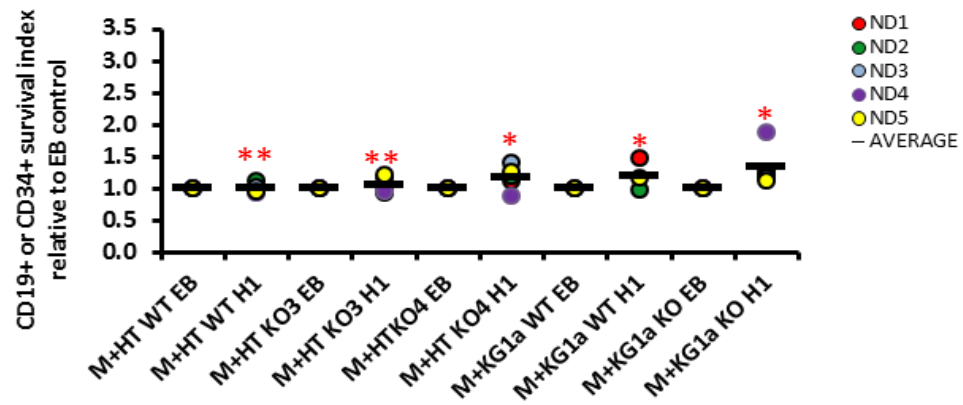


**Figure 5.15B Exogenous rNM23-H1 supports the survival of KG1a not HT cells in serum-free media.**

Purified monocytes were co-cultured with either HT or KG1a WT/KO clones with all cells at  $0.5 \times 10^6$  cell/ml, in the presence of  $2 \mu\text{g/ml}$  of exogenous rNM23-H1 or equivalent amount elution buffer (EB) as a negative control. A graph illustrated the survival index fold change in CD19+ or CD34+ in rNm23-H1 treatment relative to elution buffer control across the five donors. Data is presented as mean  $\pm$  SEM. Paired t-test has been applied. \*  $p < 0.05$ , \*\*  $p < 0.01$ . KO3:Nm23-KO3 and KO4:Nm23-KO4, M: Monocytes, WT: WT cells, KO: NM23-H1 knockout clone, EB: elution buffer and H1: rNM23-H1.

### 5.13 Cultures treated with recombinant NM23-H1 displayed adherent cell clusters

Representative micrographs of HT cells and KG1a cells cultures in Figure 5.16. are shown the appearance of non-treated cells in culture.

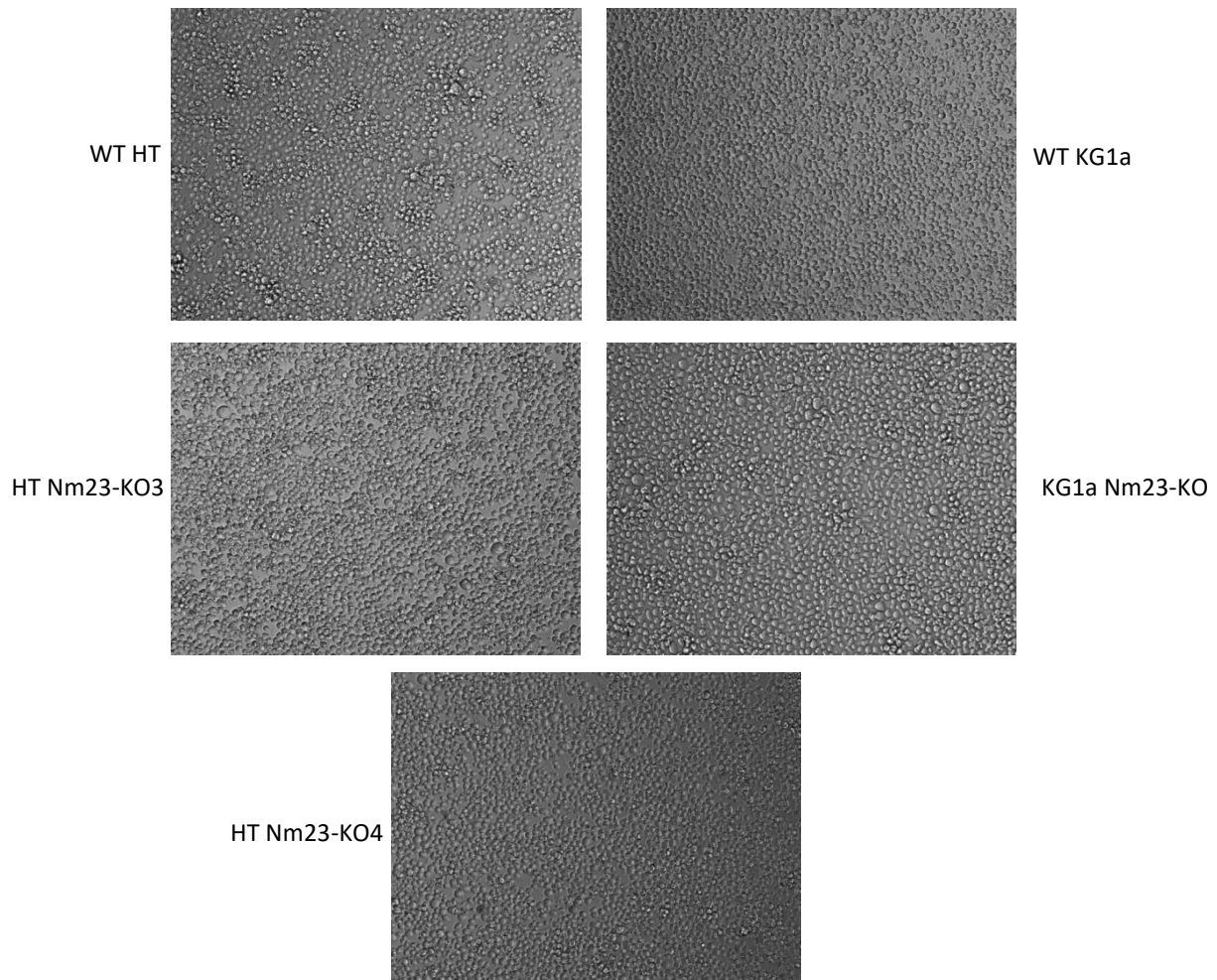


**Figure 5.16 Cell micrograph of WT and Nm23-KO cells for both HT (Secreted NM23-H1) and KG1a (Non-Secreted NM23-H1).** Cell micrographs from representative normal growing in ITS+ media, non-treated WT and NM23-KO cells for both HT and KG1a. Cell micrograph of direct survival assay was acquired at 40x magnification. N=3.

Figure 5.17 shows the poor survival of monocytes when cultured alone in ITS+ supplemented media (top left panel) and that survival is improved when rNM23-H1 is present (top right panel). These rNM23-H1 treated monocytes displayed consistent adherent cell populations. To varying degrees HT WT and KO cells cultured in combination with monocytes were clustered around these adherent monocytes.

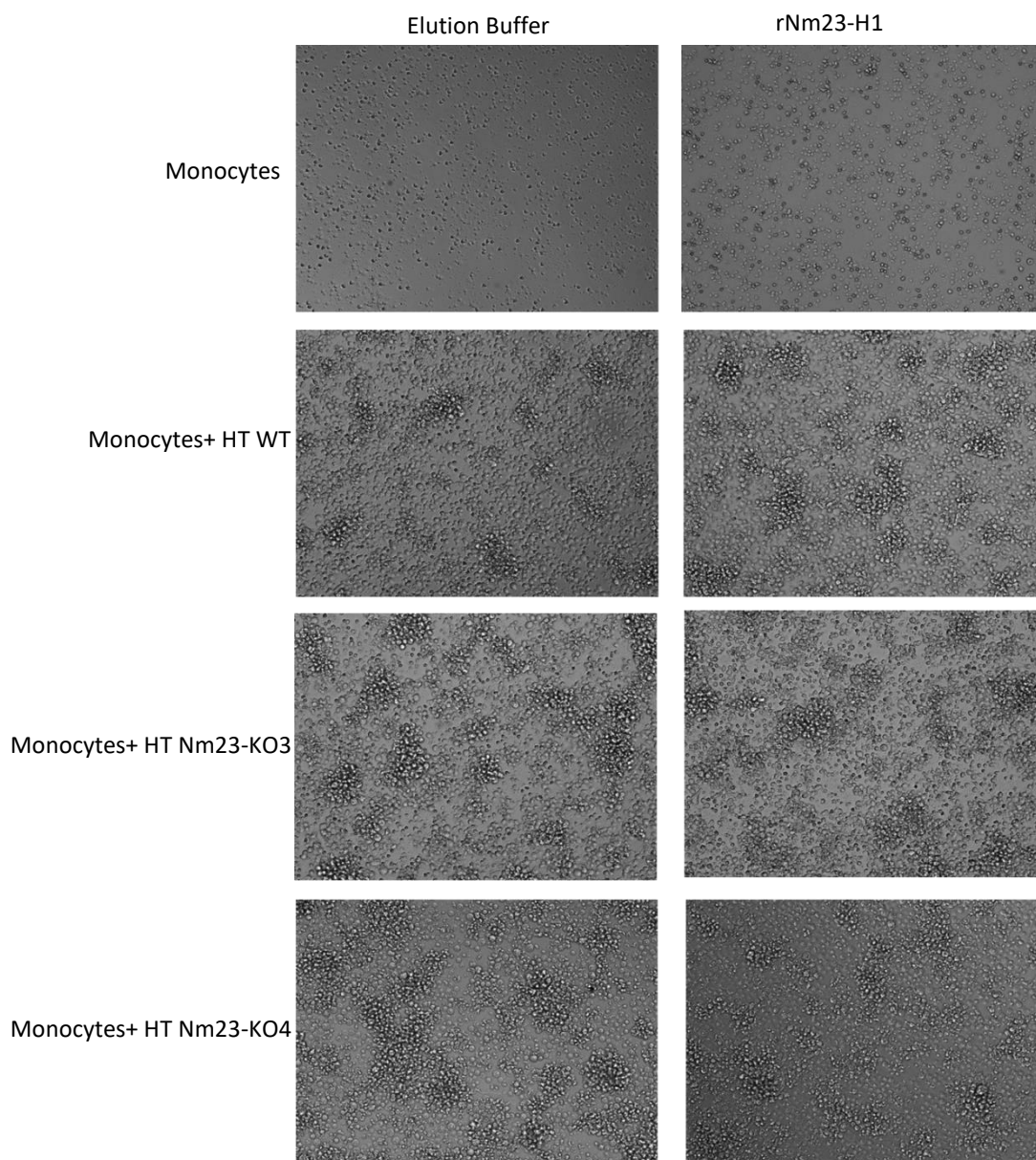


**Figure 5.17 Cell population were consistently more adherent and clustered in rNM23-H1 treated monocytes and Monocytes + HT WT or HT Nm23-KO co-cultures.**

*Cell micrographs from treated co-cultures of representative rNM23-H1 treatments and EB control at after 48hrs. The cells are growing in ITS+ media. 40 x magnifications were used in direct survival assay cultures acquirement of cell micrograph. N=3.*

As shown in Figure 5.18 KG1a WT cells clustered around monocytes more than KG1a KO cells. The addition of rNM23-H1 appeared to accentuate this with the greatest clustering appearing when KG1a WT cells and rNM23-H1 were combined.



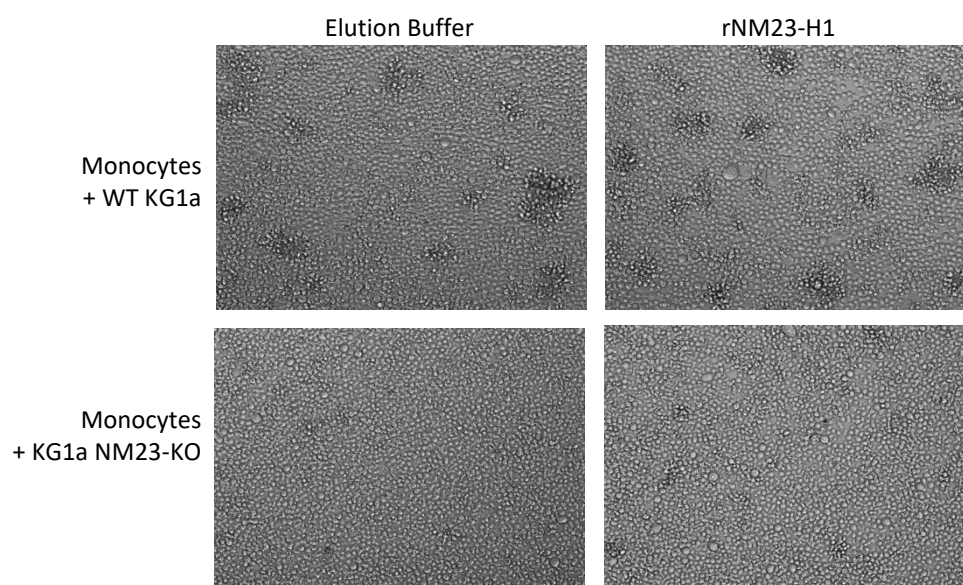


**Figure 5.18 Cell micrographs of rNM23-H1 treated co-cultures at 48hrs in rNM23-H1 treated monocytes and monocytes + HT KG1a or KG1a Nm23-KO co-cultures.**  
*Cell micrographs from treated co-cultures of representative rNM23-H1 treatments and EB control after 48hrs (40x magnification). N=3.*

#### **5.14 Monocytes respond to extracellular NM23-H1 and recombinant NM23-H1 in the presence or absence of cell to cell interaction**

The clustering observed the co-culture experiments, and its co-occurrence with culture conditions that had promoted survival of normal donors suggested that cell-cell contact may contribute to the actions of NM23-H1. To test if cell-cell contact was needed, transwell co-cultures were used. In this case, the cells are cultured together in the same well but separated by a membrane which allows diffusible factors to travel between the two cell populations but inhibits cell-cell contact. Purified primary monocytes from two were donors split in half. One half were co-cultured as previously with HT WT or KO cells in a 1:1 ratio, in presence or absence of 2  $\mu\text{g/ml}$  recombinant NM23-H1, for 48 hours in ITS+ media. The monocytes and HT cells were each cultured at  $0.5 \times 10^6$  cells/ml. The remaining monocytes were plated at  $0.5 \times 10^6$  cells/ml into transwell cell culture inserts (24 well plates) (transwell permeable supports) in wells containing HT cells (WT or NM23-KO) in the lower half also seeded at  $0.5 \times 10^6$  cell/ml.

A mix of APC-conjugated CD19 and APC-conjugated CD14 antibodies were used confirm that monocytes in the transwell cell cultures had not migrated through to the HT cells. Representative forward scatter/side scatter dot plot of one donor for HT WT and HT NM23-KO is shown in Figure 5.19A. (R1) was applied to identify viable cells, (R2) applied for the counting beads. A representative CD19/CD14 dot blot is shown in Figure 5.19B and shows that identify that the whole cell population in the lower part of the transwell is CD19+. The viability of the HT cells in the transwell culture was also not compromised and was >95%.

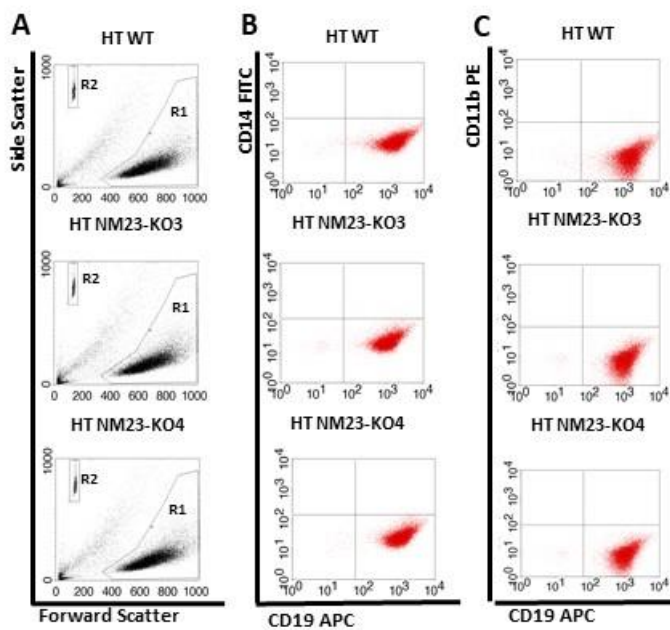


**Figure 5.19 Assessment of HT (WT and Nm23-KO) cells after 48hrs incubation in transwell cell culture.** HT cells and purified monocytes were plated at  $0.5 \times 10^6$  cell/ml with HT cells in the well and monocytes in the transwell inserts. HT (WT or NM23-KO) cells were harvested after 48hrs, stained using anti-CD19 APC, anti-CD14 FITC and anti-CD11b PE antibodies before analysis by flow cytometry. (A) Forward scatter/side scatter dot blot from transwell cultures with one donor is shown, the viable gate (R1) applied to identify the viable cells. (R2) applied to identify the counting beads. (B) CD14/CD19 dot plots depict populations of CD19+ (the lower right quadrant) (C) CD11b/CD19 dot plots depict populations of CD19+ (the lower right quadrant).

### 5.15 CD14+ monocytes from normal donors do not require direct cell to cell contact for improved survival in co-cultures.

The viability and immunophenotype of the monocytes in co-culture and transwells was analysed using flow cytometry after 48hrs of culturing. Monocytes populations were labelled using fluorescent antibodies detecting CD11b and CD14 cell surface markers. Representative side scatter/forward scatter dotplots and representative CD11b/CD14 dotplots for one donor in co-culture are shown in Figure 5.20A and transwells in Figure 5.20B. In co-culture experiments, the monocytes cultured in combination with HT WT cells did not showed better survival than those cultured in combination with HT NM23-KO cells. The same was



also true in transwell cell culture indicating the role of soluble factors in mediating this improved survival (Figure 5.20B). Since this experiment was performed with monocytes from only 2 donors, it is difficult to determine whether there was a survival advantage for monocytes grown in either co-culture or transwell conditions.

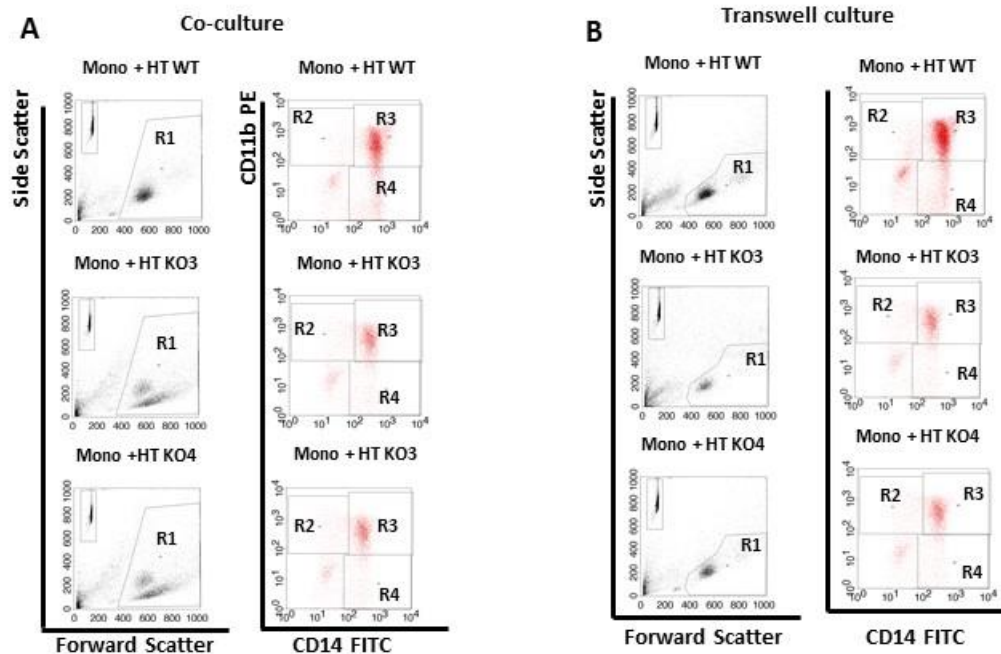


**Figure 5.20 CD11b<sup>+</sup>, CD14 and CD11b<sup>+</sup> CD14<sup>+</sup> population response to extracellular NM23-H1** Purified monocytes from two donors were cultured in combination with HT cells (WT or NM23-KO) cells in either co-culture or in transwells. cells were harvested after 48hrs, stained using PE-conjugated CD11b and FITC- conjugated CD14 antibodies before using flow cytometry for cell analysis. Representative data from one donor is shown. Forward scatter versus side scatter and CD14 versus CD11b staining are shown for cells in ((A) Co-culture and (B) Transwell culture. Gate R1 identifies the viable cells. Gate R2 are CD11b<sup>+</sup> viable cells, R3 CD11<sup>+</sup>CD14<sup>+</sup> viable cells and R4 CD14<sup>+</sup> viable cells. Mono: Monocytes. HT KO3: HT NM23-H1 KO3 clone, HT KO4: HT NM23-H1 KO4 clone

## 5.16 Addition of exogenous rNM23-H1 promotes survival of CD14<sup>+</sup> monocytes in transwell culture conditions.

The above data is for 48hr cultures in the absence of exogenously added rNM23-H1. For one normal donor for whom we had enough monocytes, the transwell experiment was performed with HT KO3 and KO4 cells with the addition of rNM23-H1 protein to the media. This improved overall survival of monocytes. Flow cytometry side scatter/forward scatter and CD11b/CD14 dotplots are shown for this donor in Figure 5.21. This experiment needs repeating for more donors.

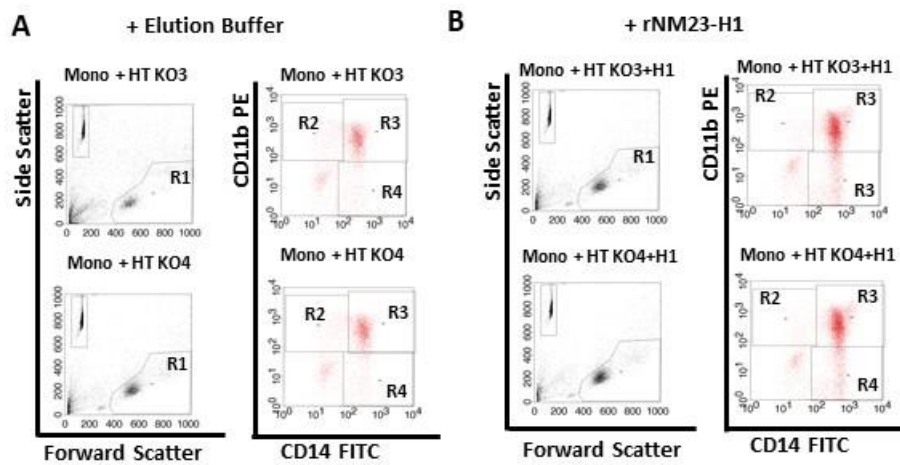


**Figure 5.21 CD11b+, CD14 and CD11b+ CD14+population response to exogenous rNM23-H1.** Purified monocytes from two donors were cultured in combination with HT cells (WT or NM23-KO) cells with either elution buffer or 2µg/ml of exogenous rNM23-H1 in transwells. cells were harvested after 48hrs, stained using PE-conjugated CD11b and FITC- conjugated CD14 antibodies before using flow cytometry for cell analysis. Data is shown for one donor (A) Elution buffer, (B) +rNM23-H1 with forward scatter/ side scatter dotplots and CD14-FITC versus CD11b-PE. A viable gate (R1) was applied to identify viable cells in the total purified monocytes. Gate R2 applied to identify CD11b+ viable cells, Gate R3 applied to identify CD11+CD14+ viable cells and Gate R4 applied to identify CD14+ viable cells. Mono: Monocytes. H1: NM23-H1.

### **5.17 Co-culture of monocytes with HT WT and HT KO cells differentially stimulates the production of certain pro-inflammatory cytokines**

The data with the co-culture and transwell cultures demonstrated that, whilst there was clustering of cells in co-culture experiments, cell-cell contact was not necessary between HT DLBCL cells and monocytes for promoting survival of monocytes. The role of cytokines such as IL-6 and IL-1 $\beta$  had been demonstrated to be important in mediating survival of leukaemia cells by NM23-H1 (Lilly et al., 2015). Therefore, the media from co-cultured cells were harvested and analysed for cytokine levels. Primary monocytes purified from five healthy donors were co-cultured in serum-free conditions (ITS+ media) at  $0.5 \times 10^6$  cell/ml in a 1:1 ratio with HT WT or HT NM23-KO cells and supernatants were harvested after 48hrs. The Bio-Plex Pro™ Human Cytokine 27-plex Assay was used to measure the levels of 27 human cytokines in the samples. Cytokine standard serial dilutions were used to generate standard curves that were used to calculate the concentrations of the samples. The latter was normalised per  $1 \times 10^6$  monocytes (CD19<sup>neg</sup> cells) to give cytokine concentrations as pg/ml/ $1 \times 10^6$  monocytes. Cytokine concentrations were measured in the absence (Elution buffer) and the presence of exogenously added rNM23-H1.

Of the 27 cytokines analysed in this assay, the concentration of 5 cytokines; IL-1 $\beta$ , IL-6, IL-8, MCP-1 $\alpha$  and MIP-1 $\beta$  were significantly decreased in co-cultures with HT cells when NM23-H1 was knocked out (Figure 5.22). For the remaining cytokines measured in this assay, no significant changes in cytokine concentration were detected in any supernatant samples when comparing HT WT to NM23-KO cells (Figure 5.23).

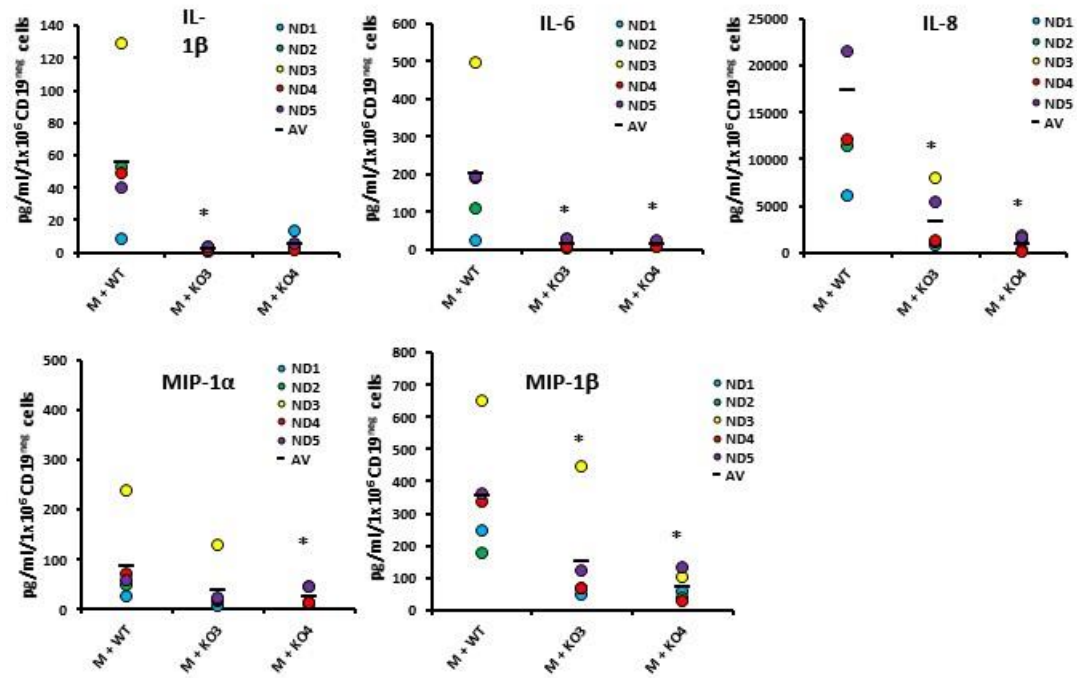


**Figure 5.22 Monocyte - HT cell line co-culture stimulates the production of some pro-inflammatory cytokines.** Supernatants from monocytes-HT cells (WT or Nm23-H1KO) co-culture samples were harvested after 48 hrs and a 27-plex Luminex-based assay was used to measure cytokine levels. Data shown is cytokine concentrations (pg/ml/1x10<sup>6</sup> monocytes) for five donors for cytokines that were significantly altered between WT versus NM23-H1 KO cells (IL-1 $\beta$ , IL-6, IL-8, MIP-1 $\alpha$  and MIP-1 $\beta$ ). M: Monocytes. H1: rNm23-H1. KO3: Nm23-KO3 and KO4: Nm23-KO4. \*p < 0.05 (ANOVA with Dunnett's test). N=5. IL-8: CXCL8, MIP1 $\alpha$ : CCL3, MIP1 $\beta$ : CCL4.

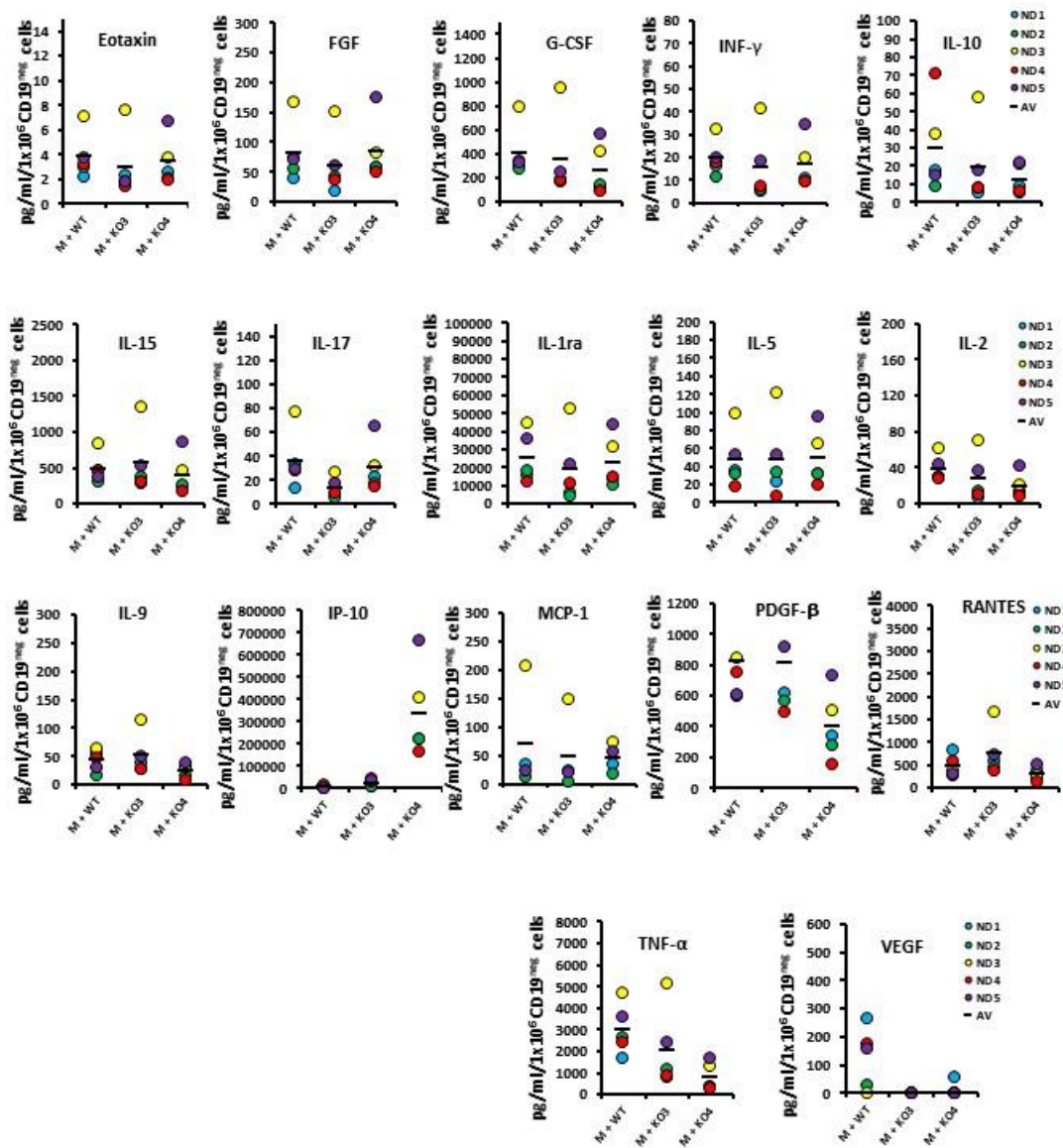


**Figure 5.23 Cytokines not modulated in monocyte co-cultures by knockout of NM23-H1 in HT cells.** Supernatants from monocytes-HT cells (WT or Nm23-H1KO) co-culture samples were harvested after 48 hrs and a 27-plex Luminex-based assay was used to measure cytokine levels. Data shown is cytokine concentrations (pg/ml/1x10<sup>6</sup> monocytes) for five donors. Data showed no differences in the 17 cytokines between WT versus NM23-H1 KO cells. M: Monocytes. H1: rNm23-H1. KO3: Nm23-KO3 and KO4: Nm23-KO4. N=5. \*p<0.05 (ANOVA with Dunnett's test). IL-10: CSIF, IL-5: EDF, IP-10: CXCL10 and MCP-1: CCL2.

### **5.18 KG1a WT cells do not recapitulate the effect of HT WT cells in co-culture with monocytes on pro-inflammatory cytokines.**

The co-culture experiment and cytokine analysis was also performed with KG1a cells. Purified primary monocytes from five healthy donors were co-cultured in ITS+ media at  $0.5 \times 10^6$  cell/ml in a 1:1 ratio with KG1a WT or NM23-H1 KO (both non NM23-H1 secretors) for 48 hrs. No significant differences were observed in any cytokines between monocytes cultured with KG1a WT or KG1a NM23-KO including the 5 pro-inflammatory cytokines altered by knocking out NM23-H1 in HT cells (Figure 5.24). Since KG1a cells do not secrete NM23-H1, the increases in inflammatory cytokines were only detected in co-cultures of HT WT cells that do secrete NM23-H1 and not in co-cultures of four cell lines (HT KO3, HT KO4, KG1a WT & KG1a KO) that do not. This experiment recognises a potential major effect of exogenous NM23-H1 and provides clues to identifying its role in cellular activities due to a direct interaction between secreted NM23-H1 and some pro-inflammatory cytokines levels. For the remaining cytokines measured in this assay, there was no significant changes in cytokine concentration were detected in any supernatant samples when comparing KG1a WT to NM23-KO cells (Figure 5.25).

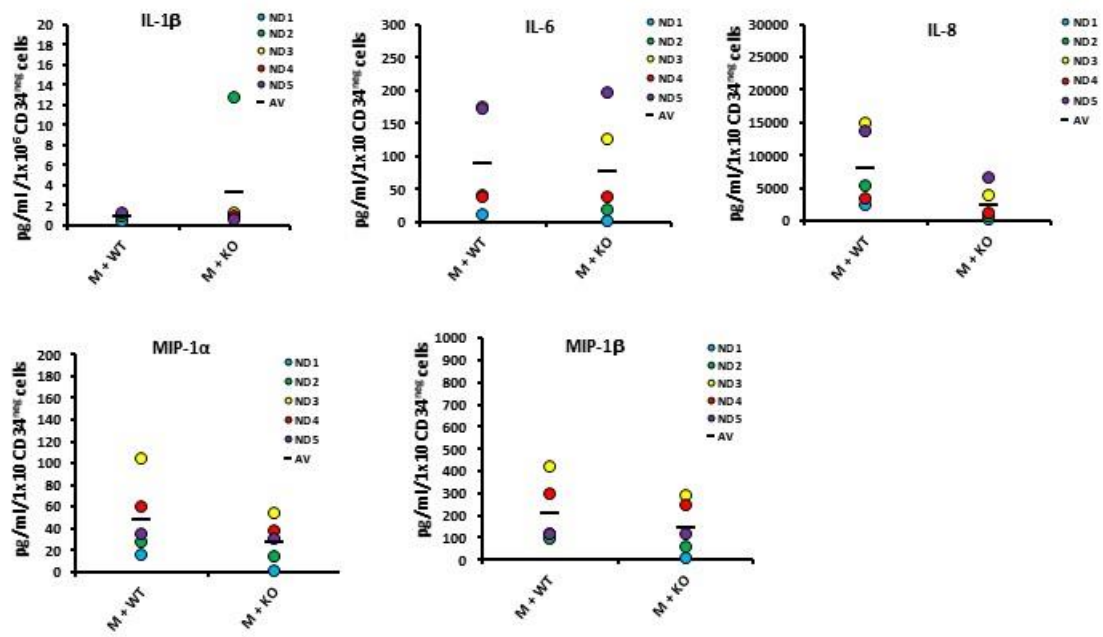


**Figure 5.24 Monocyte–KG1a WT cells co-culture do not recapitulate Monocyte–HT WT cells stimulation effect on pro-inflammatory cytokines.** 27-plex cytokine analysis demonstrates that KG1a WT (non Nm23-H1 secretor) showed no differences in the five cytokines (IL-1b, IL-6, IL-8, MIP-1α and MIP-1b) that enhanced by HT WT cells. Supernatants from monocytes culture only and monocytes-KG1a cells (WT or Nm23-H1) co-culture samples were harvested after 48 hrs. 27-plex Luminex-based assay was used to measure cytokine levels. Data shown is cytokine concentrations (pg/ml/1x10<sup>6</sup> monocytes) for five donors. M: Monocytes. H1: Nm23-H1. and KO: Nm23-KO. \*p<0.05 (ANOVA with Dunnett's test). N=5. IL-8: CXCL8, MIP1α: CCL3, MIP1β: CCL4.

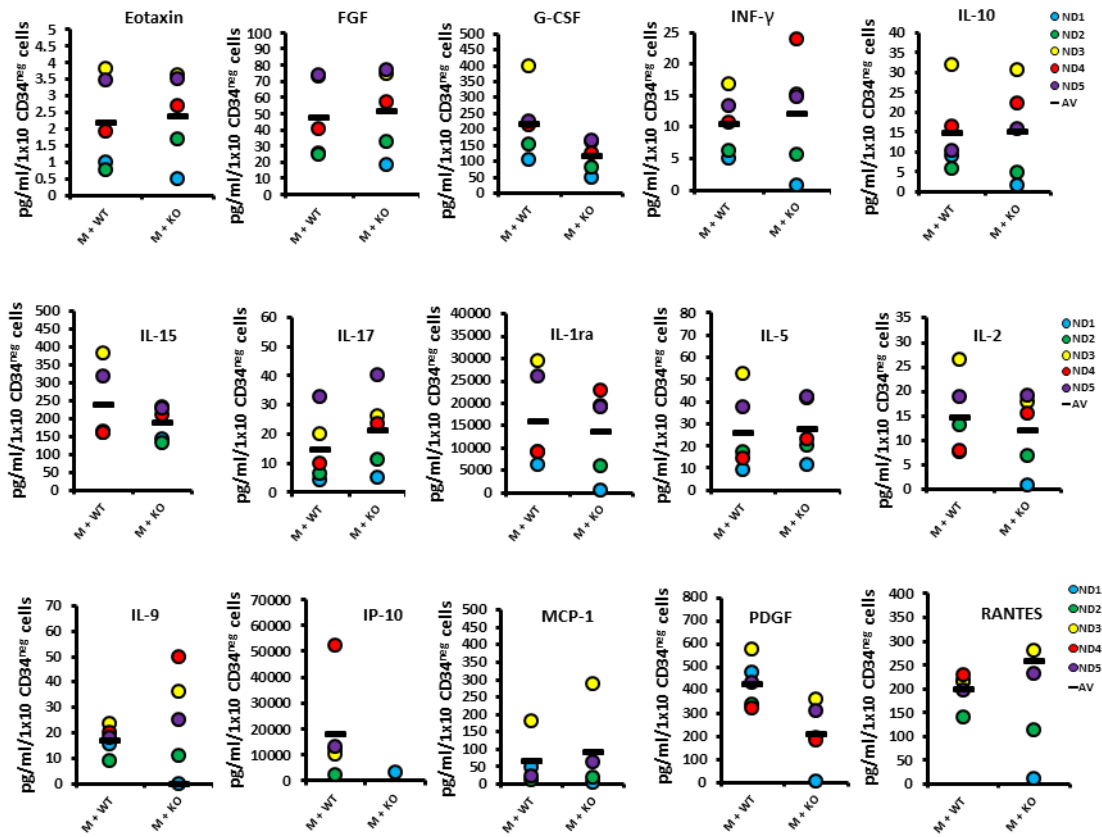
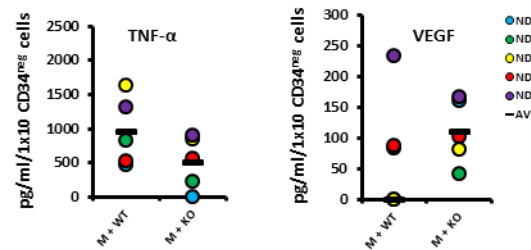


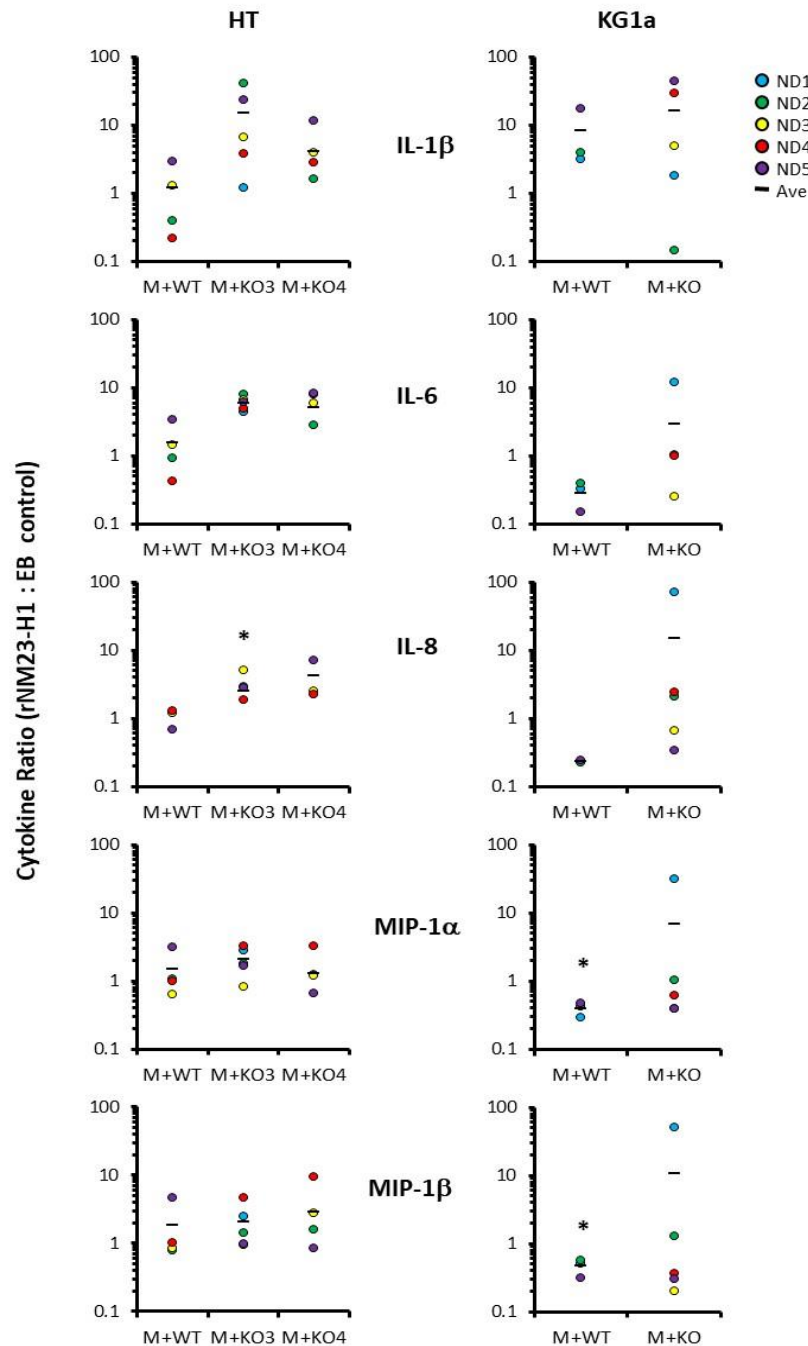
**Figure 5.25. Cytokines not modulated in monocyte co-cultures by knockout of NM23-H1 in KG1a cells.** Supernatants from monocytes culture only and monocytes-KG1a cells (WT or Nm23-H1) co-culture samples were harvested after 48 hrs. The samples were treated with 2  $\mu$ g/ml EB. 27-plex Luminex-based assay was used to measure cytokine levels. Data shown is cytokine concentrations (pg/ml) for five donors. M: Monocytes. and KO:Nm23-KO. \* $p < 0.05$  (ANOVA with Dunnett's test). N=5. IL-10:CSIF, IL-5:EDF, IP-10: CXCL10 and MCP-1: CCL2.



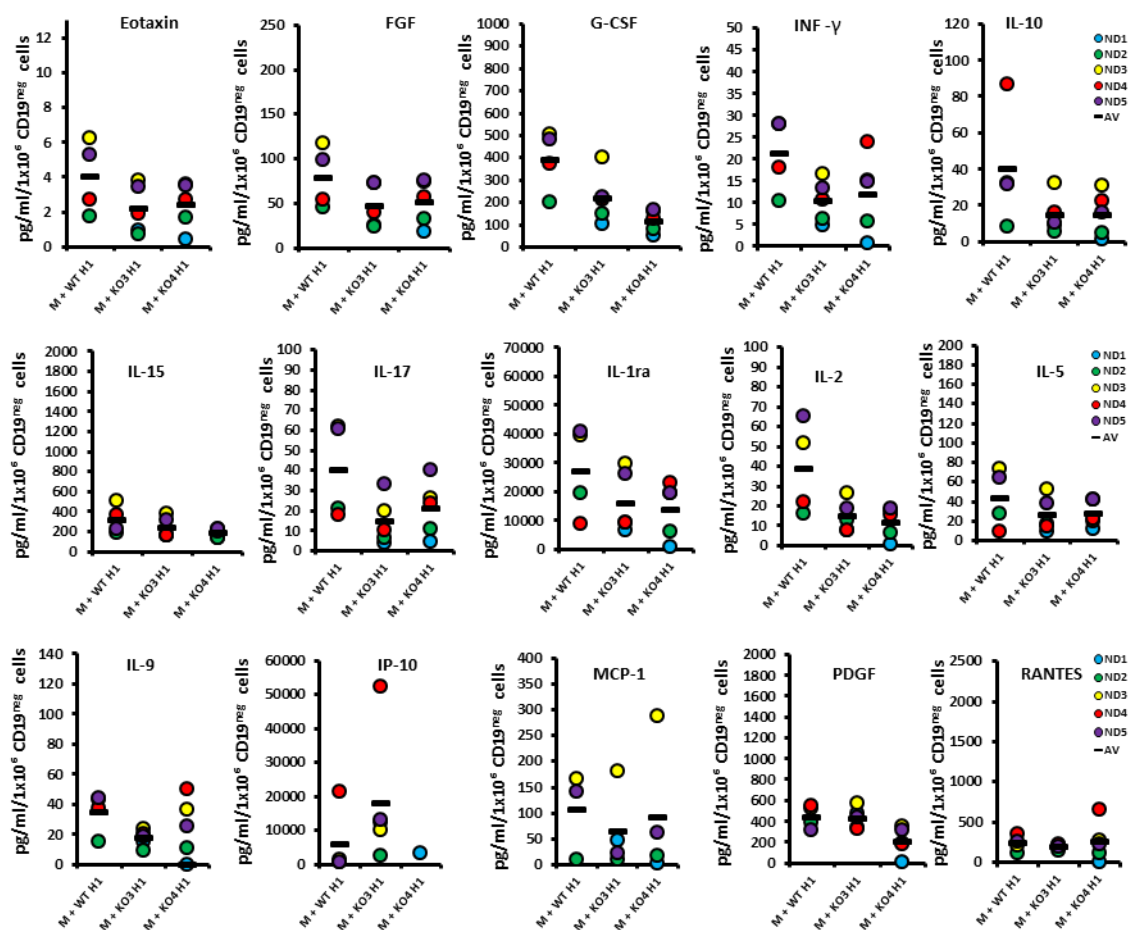


### **5.19 Exogenously added recombinant NM23-H1 promotes the induction of some pro-inflammatory cytokines**

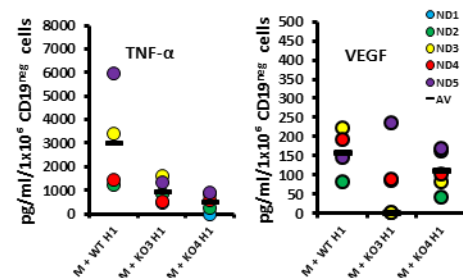
In order to validate that extracellular NM23-H1 is essential for secretion of the 5 pro-inflammatory cytokines, primary monocytes purified from five healthy donors were co-cultured in serum-free conditions (ITS+ media) at  $0.5 \times 10^6$  cell/ml in a 1:1 ratio with HT or KG1a WT or NM23-KO cells for 48 hrs in the presence or absence of 2  $\mu\text{g/ml}$  rNM23-H1. Cytokine levels in the supernatant were measured as described in section 5.18. The mean concentrations of cytokines of samples treated with rNM23-H1 were calculated as a ratio relative to the cytokine levels measured in the same cells treated with EB (Figure 5.26). The data showed that the only cytokines that changed significantly were IL-8 in the HT KO3-monocyte co-cultures where an increase 2-6 fold was observed. MIP1a and MIP-1b were both significantly decreased in monocytes co-cultured with WT KG1a cells after addition of rNM23-H1. Whilst increasing trends could be seen in some of the cytokines after rNM23-H1 treatment, e.g IL-1 $\beta$ , IL-6 and IL-8, there was too much donor-to-donor variability in absolute cytokine concentrations for this to be statistically significant. The remaining cytokines measured in this assay, there was no significant changes in cytokine concentration were detected in any supernatant samples in both cases when comparing HT WT to NM23-KO cells (Figure 5.27), or KG1a WT to NM23-KO cells (Figure 5.28).



**Figure 5.26 Recombinant NM23-H1 protein modulates cytokine expression for some cytokines in co-culture experiments.** Primary CD14<sup>+</sup> monocytes from normal donors were co-cultured with either HT or KG1a cells (WT or Nm23-H1 knockout (KO)) supplemented with either 2  $\mu$ g/ml rNm23-H1 or the equivalent volume of elution buffer (EB). Supernatants were harvested and a 27-plex Luminex-based cytokine assay was used to measure cytokine levels. Cytokine calculations were calculated from standard curves. Data is shown as the amount of cytokine produced following rNM23-H1 treatment as a ration of the corresponding EB treated culture. Data is shown for 3-5 donors + average. M: Monocytes, KO: Nm23-KO. \* $p$ <0.05 (ANOVA with Dunnett's test). IL-8: CXCL8, MIP1 $\alpha$ :CCL3, MIP1 $\beta$ :CCL4.



**Figure 5.27 Cytokines not modulated in monocyte co-cultures in presence of recombinant NM23-H1 protein.** Supernatants from monocytes culture only and monocytes-HT cells (WT or Nm23-H1) co-culture samples were harvested after 48 hrs. The samples were treated with either 2  $\mu$ g/ml of rNm23-H1 or EB. 27-plex Luminex-based assay was used to measure cytokine levels. Data shown is cytokine concentrations (pg/ml) for five donors. M: Monocytes. H1:rNm23-H1. KO3:Nm23-KO3 and KO4:Nm23-KO4. \* $p < 0.05$  (ANOVA with Dunnett's test). N=5. IL-10: CSIF, IL-5:EDF, IP-10: CXCL10 and MCP-1: CCL2.



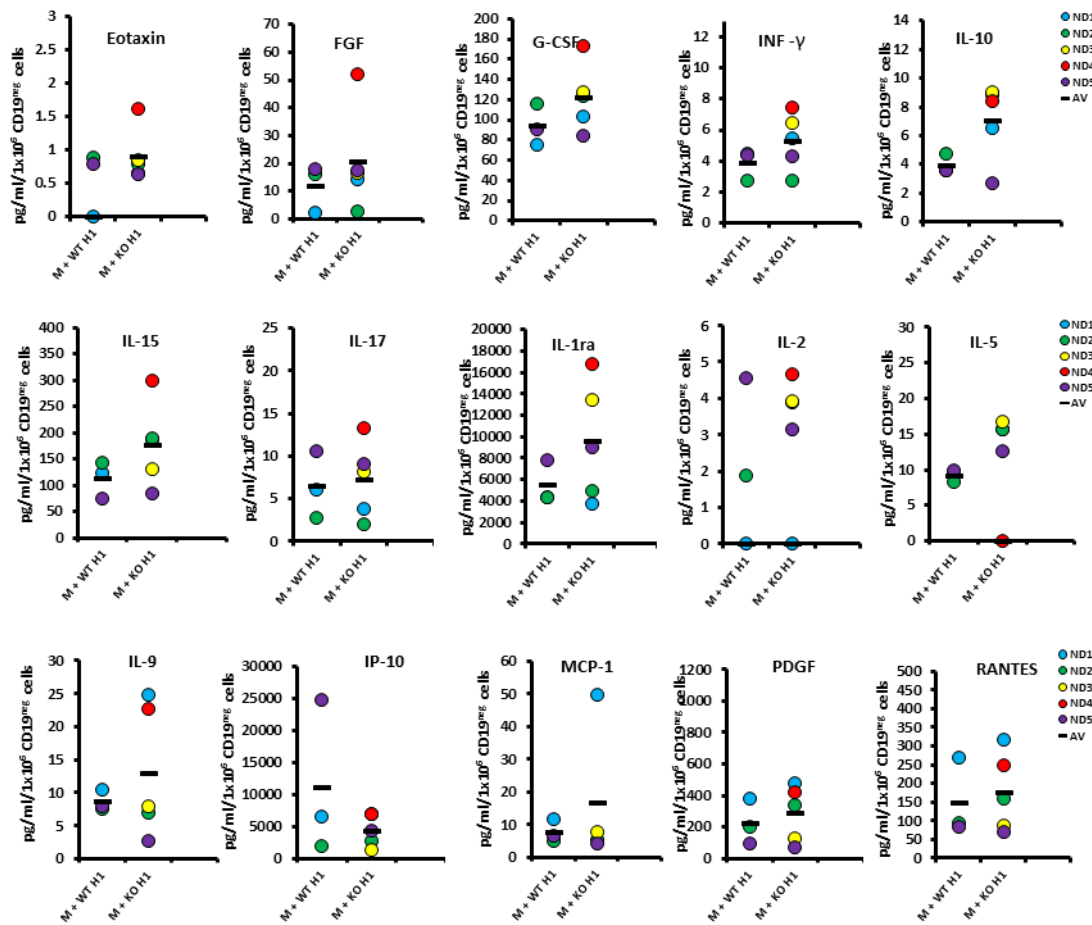
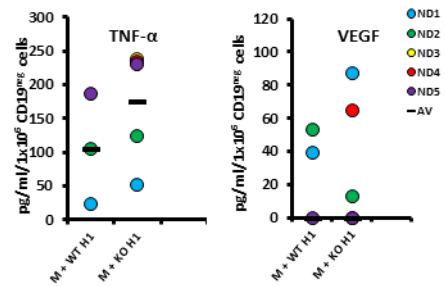


**Figure 5.28 Cytokines not modulated in monocyte co-cultures in presence of recombinant NM23-H1 protein.** Supernatants from monocytes culture only and monocytes-Kg1a cells (WT or Nm23-H1) co-culture samples were harvested after 48 hrs. The samples were treated with either 2  $\mu$ g/ml of rNm23-H1 or EB. 27-plex Luminex-based assay was used to measure cytokine levels. Data shown is cytokine concentrations (pg/ml) for five donors. M: Monocytes. H1:rNm23-H1. and KO:Nm23-KO. \* $p < 0.05$  (ANOVA with Dunnett's test). N=5.



## 5.20 Summary

The experiments described in this chapter aimed to investigate the proposed cross-talk between DLBCL cells and other immune cells via the release of NM23-H1. The experiments were performed under serum-free conditions to avoid any serum components that might bind or interact with cellular secretions and affect the results including bovine NDPKs. The acclimatised cell lines exhibited markedly similar levels of NM23-H1 protein to those grown in serum. It has been previously identified in our lab that peripheral blood monocytes bind exogenously applied NM23-H1 (unpublished). Given the relationships between monocytes/macrophage infiltration in malignant lymph node (Dave et al., 2004, Lenz et al., 2008, Bari et al., 2009) and monocyte /lymphocyte ratios on DLBCL patients' outcome, possible interaction between DLBCL cells and monocytes via the release of NM23-H1 was investigated. Monocytes were cultured alone and in combination with HT-WT and -NM23-KO cells and KG1a WT and NM23-H1 KO cells. Monocyte survival was poor in serum free cultures and the addition of recombinant NM23-H1 improved their viability only slightly. In contrast co-culturing of monocytes with any of the HT or KG1a cell lines regardless of whether they secreted NM23-H1 or not significantly improved their survival. The levels of 27 cytokines were measured in the supernatants of co-cultures via Luminex multiplex technology. Whilst many cytokines showed no variation in their levels, IL-1 $\beta$ , IL-6, IL-8, MIP-1 $\alpha$  and MIP-1 $\beta$  were elevated in co-cultures of WT HT cells and monocytes compared to HT KO cells or KG1a WT or KO cells. Elevated secretion of these cytokines did not require cell-cell contact between HT cells and monocytes. The commonality between HT KO, KG1a WT and KG1a KO cells is that unlike HT WT cells they do not secrete NM23-H1. Thus, it is possible that secreted NM23-H1 drove the elevated secretion of IL-1 $\beta$ , IL-6, IL-8, MIP-1 $\alpha$  and MIP-1 $\beta$ . To test this recombinant NM23-H1 was added HT KO cell/monocyte co-cultures. Addition of NM23-H1 enhanced the secretion of IL-6 and IL1 $\beta$  and to a lesser degree IL-8. However, the addition of recombinant Nm23-H1 had a negligible effect on MIP1 $\beta$  and MIP1 $\alpha$ .

# **CHAPTER SIX**

## **GENERAL DISCUSSION**

## 6 General discussion

Elevated NM23-H1 plasma concentrations have been associated with poor prognosis in myelodysplastic syndromes (MDS) and acute myeloid leukaemia (AML) (Okabe-Kado et al., 2002). Subsequently it was demonstrated that exogenous NM23-H1 provides a survival signal to AML cells and supports the proliferation of malignant blasts (Okabe-Kado et al., 2009b). We studied the survival factors for these malignant blasts and showed that immature cells in the clone release NM23-H1 that binds to more mature AML cells and elicits their release of cytokines including IL-1 $\beta$  and IL-6 that in turn promote the survival of AML blasts (Lilly et al., 2015). These observations indicate that elevated plasma NM23-H1 levels in MDS and AML are not merely a surrogate measure of tumour load but a component of the biology driving disease progression (Lilly et al., 2015).

As for AML, there is evidence of elevated NM23-H1 plasma concentrations in patients with malignant low-grade and high-grade HL and NHL and when compared to healthy controls (Niitsu et al., 1999, Niitsu et al., 2000, Niitsu et al., 2003c, Niitsu et al., 2004, Niitsu et al., 2006). Previous studies also identified elevated cytoplasmic expression of NM23-H1 by immunohistochemistry within lymphoma cells and confirmed a positive correlation between levels of cytoplasmic expression of NM23-H1 and high serum concentrations (Niitsu et al., 2011b). Univariate and multivariate analysis of known prognostic factors in aggressive lymphoma confirmed that the strongest independent factor predicting prognosis was plasma NM23-H1 levels, and that it could be useful in prediction of overall survival (OS) and progression free survival (PFS) (Yokoyama et al., 1998). Elevated NM23-H1 was associated with poor response to treatment and consequently poor prognosis. Taken together, these studies suggest that either extracellular and or intracellular NM23-H1 is potentially mechanistically associated with a poor prognosis in lymphoma (Niitsu et al., 2001a, Niitsu et al., 2003b, Niitsu et al., 2011a). However, in the absence of a biological understanding of this mechanism NM23-H1 expression has not featured in guidelines for the management and treatment of lymphoma patients.

The association of NM23-H1 expression and serum levels with prognosis in lymphoma include studies that have focused on DLBCL (Niitsu et al., 1999, Okabe-Kado, 2002, Niitsu et

al., 2001b, Niitsu et al., 2004). It was confirmed that the serum and cytoplasmic levels of NM23-H1 in DLBCL are significant prognostic factors (Niitsu et al., 2004). In a phase II trial of combination therapy in diffuse large B-cell lymphoma (DLBCL), patients with NM23-H1 serum levels higher than 80ng/ml before the treatment showed poorer outcomes. However, the serum levels of NM23-H1 fell significantly specifically in those patients that obtained a complete remission following treatment (Niitsu et al., 2006). This observation suggested that elevated serum NM23-H1 levels in DLBCL, as in AML, are derived from the malignant cells. Observations reported in this thesis support that hypothesis, however, as yet the role of NM23-H1 in the biology of DLBCL has been entirely unknown. The experiments performed in this study aimed to address this question and considered possible cell extrinsic and intrinsic actions of NM23-H1 in DLBCL

The experiments presented in Chapter 3 studied the expression of NM23-H1 and NM23-H2 in DLBCL cell lines Farage, HT, U2932, SUDHL -4, -5 & -6 and OCILY-1, -3 & -7. Quantitative RT-PCR and western blotting identified expression of NM23-H1 in all cell lines tested and western blotting identified expression of NM23-H2 and in same panel of cell lines. There was apparently greater variation in NM23-H1 protein level than NM23-H2. Comparison of intracellular NM23-H1 and NM23-H2 expression by HT and Farage DLBCL cell lines, the KG1a AML cell line, normal donor B-cells driven into cell cycle by CD40L and IL6 and three Epstein Barr virus (EBV) derived lymphoblastic cell lines (LCLs), showed that expression in HT and Farage is greater than KG1a and much greater than in either normal donor B-cells or LCLs. These observations indicated that DLBCL cell lines recapitulate *in vitro* the elevated expression of NM23-H1 observed in poor risk DLBCL observed *in vivo*. As such DLBCL cell lines provide legitimate models for the study of the role of NM23-H1 and -H2 in the pathogenesis of DLBCL.

Western blotting of supernatant proteins identified extracellular release of NM23-H1. However, release of NM23-H2 was not observed from any of the DLBCL cell lines tested. This was unexpected and indicates that DLBCL selectively release NM23-H1 but not NM23-H2 into their environment. NM23-H1 release was variable between DLBCL cell lines with HT, Farage and U2932 cell lines releasing highest protein levels and SUDHL-4, -5, -6, OCILY-1, -3



and -7 cell lines releasing less. However, extracellular NM23-H1 was detected in all conditioned medium of tested DLBCL cell lines and accumulated over the time.

The observation that DLBCL cells release NM23-H1 into their environment is one of the important findings of this study given the association of circulating level of NM23-H1 and prognosis in DLBCL. The data are consistent with the fall in circulating NM23-H1 observed in patients responding to anti-DLBCL therapy. These results also align with previous studies that reported extracellular expression of NM23-H1, in the conditioned medium of several mouse and human myeloid, lymphoid and breast cancer cell lines (Okabe-Kado et al., 1992, Niitsu et al., 1999, Rumjahn et al., 2007). However, the mechanism of Nm23-H1 secretion mechanism into the extracellular environment is unclear. There is no secretion signalling peptide in NM23-H1. It has been argued that NM23H1 could be secreted in the same fashion as  $\beta$ -catenin through exosomes, or could be overexpressed and then released as a consequence of dying tumour cells (Okabe-Kado et al., 2012, Keller et al., 2008, Chairoungdua et al., 2010).

The findings in these studies are perhaps inconsistent with the argument that extracellular NM23-H1 emanates from dying tumor cells. If this were the case it would be expected that both NM23-H1 and NM23-H2 would be released simultaneously especially as they are known to oligomerise (Postel, 1998) and therefore would be expected to be released together. It is therefore more likely that either, NM23-H1 passively exits from DLBCL cells and NM23-H2 is actively retained by some yet to be understood mechanism, or alternatively NM23-H1 is actively and selectively exported. This study did not address whether the release of NM23-H1 by DLBCL cells was exosomal. The western blotting based detection of extracellular used here would most likely detect both free NM23-H1 and/or NM23-H1 contained within exosomes. Ultracentrifugation of conditioned medium could be used to determine whether NM23-H1 released form DLBCL cell lines was contained within exosomes or other cell derived vesicles. Nonetheless we and others have demonstrated that soluble NM23-H1 is biologically active and can selectively bind to and be taken up by certain cells.

The lack of export of NM23-H2 further suggests that its activity is intracellular. It has been demonstrated that NM23-H2 is a transcriptional regulator of c-myc expression via binding the G-quadruplex in the c-myc promoter (Thakur et al., 2008). Recent studies have described small molecule disrupters of the NM23-H2/G-quadruplex that down-regulate c-MYC transcription, induce cell cycle arrest and apoptosis in cancer cell lines in vitro, and inhibit tumor growth in mouse xenografts (Wang et al., 2017b).

Cell binding studies were undertaken in order to learn more about the mechanism by which NM23-H1 may affect the behavior of DLBCL cells. Flow cytometry using  $\alpha$ NM23-H1 FITC labelled antibody and a negative matched isotype control antibody identified low levels of surface staining for all DLBCL cell lines tested. Low binding of NM23-H1 was also confirmed using fluorescently labeled rNm23-H1. In contrast exposure of myeloid KG1a cells to recombinant NM23-H1 led to significant increase in NM23-H1 staining.

Together these data support the hypothesis that although the elevated serum NM23-H1 levels seen in DLBCL patients are derived from the tumour it may be that the protein does not act directly on the tumour cells. Since we had previously demonstrated that r-NM23-H1 binds non-malignant mononuclear cells and elicits a cytokine response supportive of AML cells, we hypothesised that DLBCL cells exploit a similar mechanism, with important and novel implications for cross talk between the innate and adaptive immune systems in health and disease.

As pre-requisites for co-culture experiments of DLBCL cells with primary mononuclear cells, designed to investigate this potential cross talk, it was first necessary to acclimatise cell lines to serum free conditions and to perform knockdown of the *NME1* gene responsible for producing NM23-H1, using the CRISPR/Cas9 approach.

In DLBCL, poorer prognosis is correlated with both elevated intracellular NM23-H1 as identified by immunohistology (Niitsu et al., 2004) and high levels of protein in the blood (Niitsu et al., 1999, Niitsu et al., 2001b, Okabe-Kado, 2002); which suggests NM23-H1 may affect cell performance either intrinsically and/or extrinsically. The CRISPR/Cas9 approach taken in these studies allowed the investigation of both possibilities.

Although CRISPR/Cas9 knockouts were attempted in other cell lines, the approach was only successful in HT cells. Western blotting showed NM23-H1 knockout or near total knock down in several clones. As expected NM23-H1 could not be detected in the conditioned medium of these NM23-H1 KO clones. Although negative for Nm23-H1 expression these KO clones retained normal expression of Nm23-H2. There was no apparent compensatory increase in Nm23-H2 expression. CRISPR-Cas9 KO of Nm23-H1 was also achieved in KG1a cells which served as an additional control in a number of experiments.

It was identified (in Figure 4.9) that in routine tissue culture conditions NM23-H1 KO HT cells grew similarly to WT and Cas9 cells. Since many lymphomas will have hypoxic areas, the growth of WT and NM23-KO HT cells was compared in both normoxia (21% O<sub>2</sub>) and hypoxia (1% O<sub>2</sub>). However, lack of Nm23-H1 expression had little impact on the growth or viability of HT DLBCL cells in either culture condition. Similarly, KG1a Nm23-h1 cells were viable and grew normally. The lack of impact on viability and cell growth in NM23-H1 KO DLBCL cell clones identified in this study strongly suggested the possibility that DLBCL cells release Nm23-H1 as an exocrine factor to influence the immediate tumour cell environment or the wider host environment.

Previous studies in NHL based on gene expression profiling (GEP) and immunohistochemistry emphasized on the role of host immune cells and tumour microenvironment in lymphoma development (Jelicic et al., 2016, Oki et al., 2008). Absolute monocyte count (AMC), absolute lymphocyte count (ALC) at diagnosis, and lymphocyte-to-monocyte ratio (ALC/AMC) have been classified as important diagnostic and prognostic factors (Dave et al., 2004, Lenz et al., 2008a, Bari et al., 2009). Furthermore it is recognised that across cancer that the microenvironment plays an essential role in initiation tumour (Wang et al., 2017a), its progression (Yuan et al., 2016), and metastasis (Gout and Huot, 2008). Macrophages and extracellular matrix (ECM) have been described as two crucial components. Indeed have showed that tumor-associated macrophages (TAMs) are a macrophage subset that contribute directly to tumour angiogenesis (Salvesen and Akslen, 1999, Gregory and Paterson, 2018) and tumour invasion (Voss et al., 2017). Thus, the studies in this thesis addressed the hypothesis that the association of elevated NM23-H1 with poor

prognosis in DLBCL may be mediated by crosstalk between tumour cells and monocyte/macrophages either in the immediate tumour environment or beyond. Nm23-H1 secretion and its action on monocyte/macrophages could hence be the connecting link between the poorer prognosis seen with high serum and intracellular levels of Nm23-H1 and with high monocyte/lymphocyte ratio.

The studies previously described by Lilly et al (2015) and those in this thesis raise the question of how NM23-H1 mediates cytokine secretion when co-cultured with monocytes. Toll-like receptor (TLR) family upon ligation, activate signal transduction pathways such as NF- $\kappa$ B and MAPK, triggering a pro-inflammatory innate immune response. This includes the release of IL-6, IL-1 $\beta$  and IL-8 which correlates with the data in this study. Thus, future studies should investigate the role of TLRs in NM23-H1 mediated cytokine release.

Peripheral blood monocytes were isolated using immune-magnetic beads and negative selection. Then the purified monocyte populations were co-cultured with HT WT and HT NM23-H1 KO cells in the absence and presence of added exogenous rNM23 H1. As a control, KG1a WT and NM23-H1 KO cells also co-cultured with monocytes. The presence and levels of different cytokines in the supernatant of these cultures was screened using Luminex multiplex technology. The results identified greater induction of TNF $\alpha$ , MIP1 $\alpha$ , MIP1 $\beta$ , IL8, IL1 $\beta$  and IL6 when WT HT cells were co-cultured with monocytes when compared to NM23-H1 KO cells. IL6 and IL1 $\beta$  were largely undetected in co-cultures of monocytes with non-Nm23-H1 releasing KG1a WT or NM23-H1 KO cells. Exogenous rNm23-H1 restored detectable IL6 and IL1 $\beta$  in co-cultures of monocytes with HT NM23-H1 KO cells. IL8 was detectable in supernatants of both co-cultures with HT WT and NM23-H1 KO cells. However, in co-cultures with HT WT cells IL8 levels as high as 18,000pg/ml were obtained as compared to 5,000pg/ml or less in co cultures with HT NM23-H1 KO cells. Fold changes in MIP1 $\beta$ , MIP1 $\alpha$  and TNF $\alpha$  were smaller between co-cultures of monocytes with HT WT cells when compared to co-cultures with NM23-H1 KO cells. However, the levels were consistently higher in the HT WT co-cultures. Co-culture of monocytes with HT NM23-H1 KO cells generated higher levels of MIP1 $\beta$ , MIP1 $\alpha$  and TNF $\alpha$  than co-cultures with either KG1a WT or NM23-H1 KO cells. In summary of this cytokine data, accumulation of TNF $\alpha$ , MIP1 $\alpha$ , MIP1 $\beta$ ,

IL8, IL1 $\beta$  and IL6 in co-cultures of monocytes with HT WT cells which release NM23 outweighed the accumulation seen in co-cultures with non-Nm23-H1 releasing HT NM23-H1 KO cells. The profile of these cytokines in supernatants from co-cultures of monocytes with HT NM23-H1 KO cells more closely resembled those seen in supernatants of co-cultures with KG1a WT and KG1a NM23-H1 KO cells, which do not release NM23-H1, than the profile of the same cytokines in co-cultures with HT WT cells.

There are not a great number of reports associating these cytokines with DLBCL. However, one report has identified high levels of IL6 and TNF $\alpha$  to be associated with worse clinical outcome. High serum levels of soluble interleukin-2 receptor (sIL2-R), interleukin-6 (IL-6) and tumor necrosis factor alpha (TNF) are associated with adverse clinical features and predict poor outcome in diffuse large B-cell lymphoma (Dlouhy et al., 2017). A second study that investigated pre-treatment circulating serum cytokines found higher levels of IL6 IL8 and MIP1 $\alpha$  to be associated with DLBCL (Charbonneau et al., 2012). Previous study identified that the NF- $\kappa$ B1 - 94ATTG deletion was associated with increased IL-6 and DLBCL and that high IL-6 concentration is an independent prognostic factor for responses to rituximab therapy (Giachelia et al., 2012). Nacinović-Duletić et al (2008) performed a targeted analysis of serum levels of IL-6, IL-8 and IL-10 and identified their levels were higher in DLBCL patients than in controls. Their elevation correlated a lower response to therapy (NAČINOVIĆ-DULETIĆ et al., 2008). Serum levels of IL-6 and tumour necrosis factor alpha (TNF-alpha) have been reported to be significantly lower in patients with a germinal centre (GC) phenotype non-GC DLBCL phenotypes (Pedersen et al., 2005).

## Future work

All the work and experiments in this project have been *in vitro*. It will be crucial to also investigate the response to extracellular NM23-H1 *in vivo*. A pilot xenograft study experiment has been performed by Tracey Perry (Institute of Cancer and Genomic Sciences) both HT WT and HT NM23-H1 KO4 cells were injected subcutaneously in NOD scid gamma mice (NSG). After 29 days due to the tumour dimension, the mice were culled and the tumours dissected.

The results showed that tumours in the HT NM23-H1 KO4 transplanted mice started earlier and displayed an unexpected linear-like growth rather than exponential growth. The HT WT tumours developed later than HT KO, but grew exponentially and reached the same volume as KO within two weeks.

It was really interesting that the KO mice had a visible tumour earlier than the WT which took 10 extra days to show any form of tumour. This would suggest that Nm23-H1 could slow down the engraftment of wild type tumour cells, at least in an NSG animal, which is not likely to produce the same microenvironment as an immunocompetent animal/human. The experiment was done once with four animals and more repeats will be needed to confirm the results. Many questions need to think about and answer for example if the mice should humanise and then inject the tumour cells, would that give the same result? Did the tumours/tumour cells look different?

## References

- AALIPOUR, A. & ADVANI, R. H. 2014. Bruton's tyrosine kinase inhibitors and their clinical potential in the treatment of B-cell malignancies: focus on ibrutinib. *Therapeutic advances in hematology*, 5, 121-133.
- AKIRA, S. & HEMMI, H. 2003. Recognition of pathogen-associated molecular patterns by TLR family. *Immunology letters*, 85, 85-95.
- ALIZADEH, A. A., EISEN, M. B., DAVIS, R. E., MA, C., LOSSOS, I. S., ROSENWALD, A., BOLDRICK, J. C., SABET, H., TRAN, T. & YU, X. 2000. Distinct types of diffuse large B-cell lymphoma identified by gene expression profiling. *Nature*, 403, 503.
- ALIZADEH, A. A., GENTLES, A. J., ALENCAR, A. J., LIU, C. L., KOHRT, H. E., HOUOT, R., GOLDSTEIN, M. J., ZHAO, S., NATKUNAM, Y. & ADVANI, R. H. 2011. Prediction of survival in diffuse large B-cell lymphoma based on the expression of two genes reflecting tumor and microenvironment. *Blood*, blood-2011-03-345272.
- ANDERSON, G. & JENKINSON, E. J. 2001. Lymphostromal interactions in thymic development and function. *Nature Reviews Immunology*, 1, 31.
- ANDORSKY, D. J., YAMADA, R., SAID, J. W., PINKUS, G. S., BETTING, D. J. & TIMMERMAN, J. M. 2011. Programmed death ligand 1 (PD-L1) is expressed by non-Hodgkin lymphomas and inhibits the activity of tumor-associated T cells. *Clinical cancer research*, clincanres. 2660.2010.
- ARYEE, D., SIMONITSCH, I., MOSBERGER, I., KOS, K., MANN, G., SCHLÖGL, E., PÖTSCHGER, U., GADNER, H., RADASZKIEWICZ, T. & KOVAR, H. 1996. Variability of nm23-H1/NDPK-A expression in human lymphomas and its relation to tumour aggressiveness. *British journal of cancer*, 74, 1693.
- AURITI, C., PRENCIPE, G., MORIONDO, M., BERSANI, I., BERTAINA, C., MONDÌ, V. & INGLESE, R. 2017. Mannose-binding lectin: biologic characteristics and role in the susceptibility to infections and ischemia-reperfusion related injury in critically ill neonates. *Journal of immunology research*, 2017.
- BACHY, E. & SALLES, G. Treatment approach to newly diagnosed diffuse large B-cell lymphoma. *Seminars in hematology*, 2015. Elsevier, 107-118.
- BARI, A., MARCHESELLI, L., SACCHI, S., MARCHESELLI, R., POZZI, S., FERRI, P., BALLEARI, E., MUSTO, P., NERI, S. & ALOE SPIRITI, M. 2009. Prognostic models for diffuse large B-cell lymphoma in the rituximab era: a never-ending story. *Annals of Oncology*, 21, 1486-1491.
- BERGER, R., ROTEM-YEHUDAR, R., SLAMA, G., LANDES, S., KNELLER, A., LEIBA, M., KOREN-MICHOWITZ, M., SHIMONI, A. & NAGLER, A. 2008. Phase I safety and pharmacokinetic study of CT-011, a humanized antibody interacting with PD-1, in patients with advanced hematologic malignancies. *Clinical Cancer Research*, 14, 3044-3051.
- BESSER, M. J., SHAPIRA-FROMMER, R., ITZHAKI, O., TREVES, A. J., ZIPPEL, D. B., LEVY, D., KUBI, A., SHOSHANI, N., ZIKICH, D. & OHAYON, Y. 2013. Adoptive transfer of tumor-infiltrating lymphocytes in patients with metastatic melanoma: intent-to-treat analysis and efficacy after failure to prior immunotherapies. *Clinical Cancer Research*.
- BILITOU, A., WATSON, J., GARTNER, A. & OHNUMA, S.-I. 2009. The NM23 family in development. *Molecular and cellular biochemistry*, 329, 17-33.
- BIRCAN, S., INAMDAR, K. V., RASSIDAKIS, G. Z. & MEDEIROS, L. 2008. nm23-H1 expression in non-Hodgkin and Hodgkin lymphomas. *Applied Immunohistochemistry & Molecular Morphology*, 16, 207-214.
- BOGUSZ, A. M., KOVACH, A. E., LE, L. P., FENG, D., BAXTER, R. H. & SOHANI, A. R. 2017. Diffuse large B-cell lymphoma with concurrent high MYC and BCL2 expression shows evidence of active B-cell receptor signaling by quantitative immunofluorescence. *PloS one*, 12, e0172364.

- BOISSAN, M., DABERNAT, S., PEUCHANT, E., SCHLATTNER, U., LASCU, I. & LACOMBE, M.-L. 2009. The mammalian Nm23/NDPK family: from metastasis control to cilia movement. *Molecular and cellular biochemistry*, 329, 51-62.
- BOISSAN, M. & LACOMBE, M.-L. 2006. Nm23/NDP kinases in hepatocellular carcinoma. *Journal of bioenergetics and biomembranes*, 38, 169-175.
- BOLLER, T. & FELIX, G. 2009. A renaissance of elicitors: perception of microbe-associated molecular patterns and danger signals by pattern-recognition receptors. *Annual review of plant biology*, 60, 379-406.
- BRAHMER, J. R., TYKODI, S. S., CHOW, L. Q., HWU, W.-J., TOPALIAN, S. L., HWU, P., DRAKE, C. G., CAMACHO, L. H., KAUH, J. & ODUNSI, K. 2012. Safety and activity of anti-PD-L1 antibody in patients with advanced cancer. *New England Journal of Medicine*, 366, 2455-2465.
- CALIGO, M. A., CIPOLLINI, G., FIORE, L., CALVO, S., BASOLO, F., COLLECCHI, P., CIARDIELLO, F., PEPE, S., PETRINI, M. & BEVILACQUA, G. 1995. NM23 gene expression correlates with cell growth rate and S-phase. *International journal of cancer*, 60, 837-842.
- CARBONE, A. & GAIDANO, G. 2001. Acquired immunodeficiency syndrome-related cancer. A study model for the mechanisms contributing to the genesis of cancer. *European Journal of Cancer*, 37, 1184-1187.
- CARRERAS, J., LOPEZ-GUILLERMO, A., FOX, B. C., COLOMO, L., MARTINEZ, A., RONCADOR, G., MONTSERRAT, E., CAMPO, E. & BANHAM, A. H. 2006. High numbers of tumor-infiltrating FOXP3-positive regulatory T cells are associated with improved overall survival in follicular lymphoma. *Blood*, 108, 2957-2964.
- CHAIROUNGDU, A., SMITH, D. L., POCHARD, P., HULL, M. & CAPLAN, M. J. 2010. Exosome release of  $\beta$ -catenin: a novel mechanism that antagonizes Wnt signaling. *The Journal of cell biology*, 190, 1079-1091.
- CHANDRASEKHARAPPA, S. C., GROSS, L. A., KING, S. E. & COLLINS, F. S. 1993. The human NME2 gene lies within 18kb of NME1 in chromosome 17. *Genes, Chromosomes and Cancer*, 6, 245-248.
- CHARBONNEAU, B., MAURER, M. J., ANSELL, S. M., SLAGER, S. L., FREDERICKSEN, Z. S., ZIESMER, S. C., MACON, W. R., HABERMANN, T. M., WITZIG, T. E. & LINK, B. K. 2012. Pretreatment circulating serum cytokines associated with follicular and diffuse large B-cell lymphoma: a clinic-based case-control study. *Cytokine*, 60, 882-889.
- CHERUKURI, A., CHENG, P. C. & PIERCE, S. K. 2001. The role of the CD19/CD21 complex in B cell processing and presentation of complement-tagged antigens. *The Journal of Immunology*, 167, 163-172.
- CHOW, N.-H., LIU, H.-S. & CHAN, S.-H. 2000. The role of nm23-H1 in the progression of transitional cell bladder cancer. *Clinical cancer research*, 6, 3595-3599.
- CIPOLLINI, G., BERTI, A., FIORE, L., RAINALDI, G., BASOLO, F., BEVILACQUA, G. & CALIGO, M. A. 1997. Down-regulation of the nm23. h1 gene inhibits cell proliferation. *International journal of cancer*, 73, 297-302.
- COLOMO, L., LÓPEZ-GUILLERMO, A., PERALES, M., RIVES, S., MARTINEZ, A., BOSCH, F., COLOMER, D., FALINI, B., MONTSERRAT, E. & CAMPO, E. 2003. Clinical impact of the differentiation profile assessed by immunophenotyping in patients with diffuse large B-cell lymphoma. *Blood*, 101, 78-84.
- CRAIG, F. E. & FOON, K. A. 2008. Flow cytometric immunophenotyping for hematologic neoplasms. *Blood*, 111, 3941-3967.
- CUELLO, F., SCHULZE, R. A., HEEMEYER, F., MEYER, H. E., LUTZ, S., JAKOBS, K. H., NIROOMAND, F. & WIELAND, T. 2003. Activation of Heterotrimeric G Proteins by a High Energy Phosphate Transfer via Nucleoside Diphosphate Kinase (NDPK) B and G $\beta$  Subunits COMPLEX FORMATION OF NDPK B WITH G $\beta$  DIMERS AND PHOSPHORYLATION OF His-266 IN G $\beta$ . *Journal of Biological Chemistry*, 278, 7220-7226.



- DAVE, S. S., WRIGHT, G., TAN, B., ROSENWALD, A., GASCOYNE, R. D., CHAN, W. C., FISHER, R. I., BRAZIEL, R. M., RIMSZA, L. M. & GROGAN, T. M. 2004. Prediction of survival in follicular lymphoma based on molecular features of tumor-infiltrating immune cells. *New England Journal of Medicine*, 351, 2159-2169.
- DE JONG, D., XIE, W., ROSENWALD, A., CHHANABHAI, M., GAULARD, P., KLAPPER, W., LEE, A., SANDER, B., THORNS, C. & CAMPO, E. 2009. Retracted: Immunohistochemical prognostic markers in diffuse large B-cell lymphoma: validation of tissue microarray as a prerequisite for broad clinical applications (a study from the Lunenburg Lymphoma Biomarker Consortium). BMJ Publishing Group.
- DE LA ROSA, A., STEEG, P. S. & WILLIAMS, R. L. 1995. Nm23/nucleoside diphosphate kinase: toward a structural and biochemical understanding of its biological functions. *Bioessays*, 17, 53-62.
- DEAROLF, C. R., TRIPOULAS, N., BIGGS, J. & SHEARN, A. 1988. Molecular consequences of awdb3, a cell-autonomous lethal mutation of *Drosophila* induced by hybrid dysgenesis. *Developmental biology*, 129, 169-178.
- DELVES, P. J., MARTIN, S. J., BURTON, D. R. & ROITT, I. M. 2017. *Essential immunology*, John Wiley & Sons.
- DESVIGNES, T., PONTAROTTI, P., FAUVEL, C. & BOBE, J. 2009. Nme protein family evolutionary history, a vertebrate perspective. *BMC evolutionary biology*, 9, 256.
- DEXHEIMER, T. S., CAREY, S. S., ZUOHE, S., GOKHALE, V. M., HU, X., MURATA, L. B., MAES, E. M., WEICHSEL, A., SUN, D. & MEUILLET, E. J. 2009. NM23-H2 may play an indirect role in transcriptional activation of c-myc gene expression but does not cleave the nuclease hypersensitive element III1. *Molecular cancer therapeutics*, 1535-7163. MCT-08-1093.
- DING, Z.-C., HUANG, L., BLAZAR, B. R., YAGITA, H., MELLOR, A. L., MUNN, D. H. & ZHOU, G. 2012. Polyfunctional CD4+ T cells are essential for eradicating advanced B-cell lymphoma after chemotherapy. *Blood*, blood-2011-12-398321.
- DLOUHY, I., FILELLA, X., ROVIRA, J., MAGNANO, L., RIVAS-DELGADO, A., BAUMANN, T., MARTÍNEZ-TRILLOS, A., BALAGUÉ, O., MARTÍNEZ, A. & GONZÁLEZ-FARRE, B. 2017. High serum levels of soluble interleukin-2 receptor (sIL2-R), interleukin-6 (IL-6) and tumor necrosis factor alpha (TNF) are associated with adverse clinical features and predict poor outcome in diffuse large B-cell lymphoma. *Leukemia research*, 59, 20-25.
- DUDLEY, M. E., YANG, J. C., SHERRY, R., HUGHES, M. S., ROYAL, R., KAMMULA, U., ROBBINS, P. F., HUANG, J., CITRIN, D. E. & LEITMAN, S. F. 2008. Adoptive cell therapy for patients with metastatic melanoma: evaluation of intensive myeloablative chemoradiation preparative regimens. *Journal of Clinical Oncology*, 26, 5233.
- DUNLEAVY, K., ERDMANN, T. & LENZ, G. 2018. Targeting the B-cell receptor pathway in diffuse large B-cell lymphoma. *Cancer treatment reviews*.
- DUNLEAVY, K., PITTALUGA, S., CZUCZMAN, M. S., DAVE, S. S., WRIGHT, G., GRANT, N., SHOVLIN, M., JAFFE, E. S., JANIK, J. E. & STAUDT, L. M. 2009. Differential efficacy of bortezomib plus chemotherapy within molecular subtypes of diffuse large B-cell lymphoma. *Blood*, 113, 6069-6076.
- DURSUN, A., AKYÜREK, N., GÜNEL, N. & YAMAÇ, D. 2002. Prognostic implication of nm23-H1 expression in colorectal carcinomas. *Pathology*, 34, 427-432.
- ENGEL, M., VÉRON, M., THEISINGER, B., LACOMBE, M. L., SEIB, T., DOOLEY, S. & WELTER, C. 1995. A novel serine/threonine-specific protein phosphotransferase activity of Nm23/nucleoside-diphosphate kinase. *European journal of biochemistry*, 234, 200-207.
- FANALE, M. A. & YOUNES, A. 2007. Monoclonal antibodies in the treatment of non-Hodgkin's lymphoma. *Drugs*, 67, 333-350.
- FERLAY, J., STELIAROVA-FOUCHER, E., LORTET-TIEULENT, J., ROSSO, S., COEBERGH, J.-W. W., COMBER, H., FORMAN, D. & BRAY, F. 2013. Cancer incidence and mortality patterns in Europe: estimates for 40 countries in 2012. *European journal of cancer*, 49, 1374-1403.

- FREIJE, J. M., BLAY, P., MACDONALD, N. J., MANROW, R. E. & STEEG, P. S. 1997. Site-directed mutation of Nm23-H1 mutations lacking motility suppressive capacity upon transfection are deficient in histidine-dependent protein phosphotransferase pathways in vitro. *Journal of Biological Chemistry*, 272, 5525-5532.
- FRIDMAN, W. H., PAGÈS, F., SAUTES-FRIDMAN, C. & GALON, J. 2012. The immune contexture in human tumours: impact on clinical outcome. *Nature Reviews Cancer*, 12, nrc3245.
- FUJIMOTO, M., FUJIMOTO, Y., POE, J. C., JANSEN, P. J., LOWELL, C. A., DEFRANCO, A. L. & TEDDER, T. F. 2000. CD19 regulates Src family protein tyrosine kinase activation in B lymphocytes through processive amplification. *Immunity*, 13, 47-57.
- FURMAN, R. R., MARTIN, P., RUAN, J., CHEUNG, Y. K. K., VOSE, J. M., LACASCE, A. S., ELSTROM, R., COLEMAN, M. & LEONARD, J. P. 2010. Phase 1 trial of bortezomib plus R-CHOP in previously untreated patients with aggressive non-Hodgkin lymphoma. *Cancer*, 116, 5432-5439.
- GAGRO, A., MCCLOSKEY, N., CHALLA, A., HOLDER, M., GRAFTON, G., POUND, J. D. & GORDON, J. 2000. CD5-positive and CD5-negative human B cells converge to an indistinguishable population on signalling through B-cell receptors and CD40. *Immunology*, 101, 201-9.
- GARBER, K. 2001. Lymphoma rate rise continues to baffle researchers. *Journal of the National Cancer Institute*, 93, 494-496.
- GARCÍA-SUÁREZ, J., BAÑAS, H., ARRIBAS, I., DE MIGUEL, D., PASCUAL, T. & BURGALETA, C. 2007. Dose-adjusted EPOCH plus rituximab is an effective regimen in patients with poor-prognostic untreated diffuse large B-cell lymphoma: results from a prospective observational study. *British journal of haematology*, 136, 276-285.
- GARCÍA-SUÁREZ, J., FLORES, E., CALLEJAS, M., ARRIBAS, I., GIL-FERNÁNDEZ, J. J., OLMEDILLA, G., CURTO, N., GUILLÉN, H., CASCO, C. R. & MARTÍN, Y. 2013. Two-weekly dose-adjusted (DA)-EPOCH-like chemotherapy with high-dose dexamethasone plus rituximab (DA-EDOCH14-R) in poor-prognostic untreated diffuse large B-cell lymphoma. *British journal of haematology*, 160, 510-514.
- GATALICA, Z., BILALOVIC, N., VRANIC, S., ARGUELLO, D., REDDY, S. & GHOSH, N. 2015. PD-L1 and PD1 Expression in Lymphomas. *Am Soc Hematology*.
- GIACHELIA, M., VOSO, M. T., TISI, M. C., MARTINI, M., BOZZOLI, V., MASSINI, G., D'ALÓ, F., LAROCCA, L. M., LEONE, G. & HOHAUS, S. 2012. Interleukin-6 plasma levels are modulated by a polymorphism in the NF- $\kappa$ B1 gene and are associated with outcome following rituximab-combined chemotherapy in diffuse large B-cell non-Hodgkin lymphoma. *Leukemia & lymphoma*, 53, 411-416.
- GILLES, A.-M., PRESECAN, E., VONICA, A. & LASCU, I. 1991. Nucleoside diphosphate kinase from human erythrocytes. Structural characterization of the two polypeptide chains responsible for heterogeneity of the hexameric enzyme. *Journal of Biological Chemistry*, 266, 8784-8789.
- GINHOX, F. & JUNG, S. 2014. Monocytes and macrophages: developmental pathways and tissue homeostasis. *Nature Reviews Immunology*, 14, 392-404.
- GOUT, S. & HUOT, J. 2008. Role of cancer microenvironment in metastasis: focus on colon cancer. *Cancer Microenvironment*, 1, 69-83.
- GREGORY, C. D. & PATERSON, M. 2018. An apoptosis-driven 'onco-regenerative niche': roles of tumour-associated macrophages and extracellular vesicles. *Phil. Trans. R. Soc. B*, 373, 20170003.
- GUCALP, A. & NOY, A. 2010. Spectrum of HIV lymphoma 2009. *Current opinion in hematology*, 17, 362-367.
- HAABETH, O. A. W., LORVIK, K. B., HAMMARSTRÖM, C., DONALDSON, I. M., HARALDSEN, G., BOGEN, B. & CORTHAY, A. 2011. Inflammation driven by tumour-specific Th1 cells protects against B-cell cancer. *Nature communications*, 2, 240.
- HAILAT, N., KEIM, D., MELHEM, R., ZHU, X.-X., ECKERSKORN, C., BRODEUR, G., REYNOLDS, C. P., SEEGER, R., LOTTSPEICH, F. & STRAHLER, J. 1991. High levels of p19/nm23 protein in

- neuroblastoma are associated with advanced stage disease and with N-myc gene amplification. *The Journal of clinical investigation*, 88, 341-345.
- HIGASHI, M., TOKUHIRA, M., FUJINO, S., YAMASHITA, T., ABE, K., ARAI, E., KIZAKI, M. & TAMARU, J. 2016. Loss of HLA-DR expression is related to tumor microenvironment and predicts adverse outcome in diffuse large B-cell lymphoma. *Leukemia & lymphoma*, 57, 161.
- HIPPE, H.-J., LUEDDE, M., LUTZ, S., KOEHLER, H., ESCHENHAGEN, T., FREY, N., KATUS, H. A., WIELAND, T. & NIROOMAND, F. 2007. Regulation of cardiac cAMP synthesis and contractility by nucleoside diphosphate kinase B/G protein  $\beta\gamma$  dimer complexes. *Circulation research*, 100, 1191-1199.
- HOFFBRAND, A. V. & MOSS, P. A. 2011. *Essential haematology*, John Wiley & Sons.
- HOFFMAN, R., BENZ, E. J., SHATTIL, S. J., FURIE, B., SILBERSTEIN, L.E., M., P. & HESLOP, H. 2009. *Haematology : Basic principles and practice*. 5TH Edn.
- HORAK, C. E., LEE, J. H., ELKAHLOUN, A. G., BOISSAN, M., DUMONT, S., MAGA, T. K., ARNAUD-DABERNAT, S., PALMIERI, D., STETLER-STEVENSON, W. G. & LACOMBE, M.-L. 2007. Nm23-H1 suppresses tumor cell motility by down-regulating the lysophosphatidic acid receptor EDG2. *Cancer research*, 67, 7238-7246.
- HOUOT, R., GOLDSTEIN, M. J., KOHRT, H. E., MYKLEBUST, J. H., ALIZADEH, A. A., LIN, J. T., IRISH, J. M., TORCHIA, J. A., KOLSTAD, A. & CHEN, L. 2009. Therapeutic effect of CD137 immunomodulation in lymphoma and its enhancement by Treg depletion. *Blood*, 114, 3431-3438.
- IGAWA, M., RUKSTALIS, D. B., TANABE, T. & CHODAK, G. W. 1994. High levels of nm23 expression are related to cell proliferation in human prostate cancer. *Cancer research*, 54, 1313-1318.
- ISNARDI, I., NG, Y.-S., SRDANOVIC, I., MOTAGHEDI, R., RUDCHENKO, S., VON BERNUTH, H., ZHANG, S.-Y., PUEL, A., JOUANGUY, E. & PICARD, C. 2008. IRAK-4-and MyD88-dependent pathways are essential for the removal of developing autoreactive B cells in humans. *Immunity*, 29, 746-757.
- JAFFE, E. S. 2009. The 2008 WHO classification of lymphomas: implications for clinical practice and translational research. *ASH Education Program Book*, 2009, 523-531.
- JANKU, F., WHELER, J. J., NAING, A., FALCHOOK, G. S., HONG, D. S., STEPANEK, V. M., FU, S., PIHA-PAUL, S. A., LEE, J. J. & LUTHRA, R. 2013. PIK3CA mutation H1047R is associated with response to PI3K/AKT/mTOR signaling pathway inhibitors in early-phase clinical trials. *Cancer research*, 73, 276-284.
- JELICIC, J., BALINT, M. T., JOVANOVIC, M. P., BORICIC, N., MICEV, M., STOJSIC, J., ANTIC, D., ANDJELIC, B., BILA, J. & BALINT, B. 2016. The role of lymphocyte to monocyte ratio, microvessel density and HiGH CD44 tumor cell expression in non Hodgkin lymphomas. *Pathology & Oncology Research*, 22, 567-577.
- JETTEN, A. M. 2009. Retinoid-related orphan receptors (RORs): critical roles in development, immunity, circadian rhythm, and cellular metabolism. *Nuclear receptor signaling*, 7.
- JIN, H.-T., AHMED, R. & OKAZAKI, T. 2010. Role of PD-1 in regulating T-cell immunity. *Negative Co-Receptors and Ligands*. Springer.
- KAETZEL, D. M., ZHANG, Q., YANG, M., MCCORKLE, J. R., MA, D. & CRAVEN, R. J. 2006. Potential roles of 3'-5' exonuclease activity of NM23-H1 in DNA repair and malignant progression. *Journal of bioenergetics and biomembranes*, 38, 163.
- KANZLER, H., KÜPPERS, R., HANSMANN, M.-L. & RAJEWSKY, K. 1996. Hodgkin and Reed-Sternberg cells in Hodgkin's disease represent the outgrowth of a dominant tumor clone derived from (crippled) germinal center B cells. *Journal of Experimental Medicine*, 184, 1495-1505.
- KAWAI, T. & AKIRA, S. 2010. The role of pattern-recognition receptors in innate immunity: update on Toll-like receptors. *Nature immunology*, 11, 373.

- KEIM, D., HAILAT, N., MELHEM, R., ZHU, X., LASCU, I., VERON, M., STRAHLER, J. & HANASH, S. 1992. Proliferation-related expression of p19/nm23 nucleoside diphosphate kinase. *The Journal of clinical investigation*, 89, 919-924.
- KELLER, M., RÜEGG, A., WERNER, S. & BEER, H.-D. 2008. Active caspase-1 is a regulator of unconventional protein secretion. *Cell*, 132, 818-831.
- KIENZLE, G. & VON KEMPIS, J. 2000. CD137 (ILA/4-1BB), expressed by primary human monocytes, induces monocyte activation and apoptosis of B lymphocytes. *International immunology*, 12, 73-82.
- KIM, H. D., YOUN, B., KIM, T.-S., KIM, S.-H., SHIN, H.-S. & KIM, J. 2009. Regulators affecting the metastasis suppressor activity of Nm23-H1. *Molecular and cellular biochemistry*, 329, 167-173.
- KIM, Y.-I., PARK, S., JEOUNG, D.-I. & LEE, H. 2003. Point mutations affecting the oligomeric structure of Nm23-H1 abrogates its inhibitory activity on colonization and invasion of prostate cancer cells. *Biochemical and biophysical research communications*, 307, 281-289.
- KRAMMER, P. H. 2000. CD95's deadly mission in the immune system. *Nature*, 407, 789.
- KUMAR, P. & CLARK, M. L. 2012. *Kumar and Clark's Clinical Medicine E-Book*, Elsevier health sciences.
- KÜPPERS, R. 2005. Mechanisms of B-cell lymphoma pathogenesis. *Nature Reviews Cancer*, 5, 251.
- LACOMBE, M.-L., SASTRE-GARAU, X., LASCU, I., VONICA, A., WALLET, V., THIERY, J. P. & VÉRON, M. 1991. Overexpression of nucleoside diphosphate kinase (Nm23) in solid tumours. *European Journal of Cancer and Clinical Oncology*, 27, 1302-1307.
- LACOMBE, M.-L. L., MUNIER, A., MEHUS, J. G. & LAMBETH, D. O. 2000a. The human Nm23/nucleoside diphosphate kinases. *Journal of bioenergetics and biomembranes*, 32, 247-258.
- LACOMBE, M. L., MILON, L., MUNIER, A., MEHUS, J. G. & LAMBETH, D. O. 2000b. The human Nm23/nucleoside diphosphate kinases. *J Bioenerg Biomembr*, 32, 247-58.
- LAM, K.-P., KÜHN, R. & RAJEWSKY, K. 1997. In vivo ablation of surface immunoglobulin on mature B cells by inducible gene targeting results in rapid cell death. *Cell*, 90, 1073-1083.
- LEBIEN, T. W. & TEDDER, T. F. 2008. B lymphocytes: how they develop and function. *Blood*, 112, 1570-1580.
- LEE, A. I. & LACASCE, A. S. 2009. Nodular lymphocyte predominant Hodgkin lymphoma. *The Oncologist*, 14, 739-751.
- LEE, A. M., CLEAR, A. J., CALAMINICI, M., DAVIES, A. J., JORDAN, S., MACDOUGALL, F., MATTHEWS, J., NORTON, A. J., GRIBBEN, J. G. & LISTER, T. A. 2006a. Number of CD4+ cells and location of forkhead box protein P3-positive cells in diagnostic follicular lymphoma tissue microarrays correlates with outcome. *Journal of Clinical Oncology*, 24, 5052-5059.
- LEE, H.-Y. & LEE, H. 1999. Inhibitory activity of nm23-H1 on invasion and colonization of human prostate carcinoma cells is not mediated by its NDP kinase activity. *Cancer letters*, 145, 93-99.
- LEE, J.-H., CHO, S. J., ZHANG, X., ZHENG, Z., LEE, E. S., KIM, A., KIM, Y.-S., CHAE, Y.-S. & KIM, I. 2006b. nm23-H1 protein expression and gene mutation in 150 patients with non-Hodgkin's lymphomas. *Journal of Korean medical science*, 21, 645-651.
- LENZ, G. & STAUDT, L. M. 2010. Aggressive lymphomas. *New England Journal of Medicine*, 362, 1417-1429.
- LENZ, G., WRIGHT, G., DAVE, S., XIAO, W., POWELL, J., ZHAO, H., XU, W., TAN, B., GOLDSCHMIDT, N. & IQBAL, J. 2008a. Stromal gene signatures in large-B-cell lymphomas. *New England Journal of Medicine*, 359, 2313-2323.
- LENZ, G., WRIGHT, G. W., EMRE, N. T., KOHLHAMMER, H., DAVE, S. S., DAVIS, R. E., CARTY, S., LAM, L. T., SHAFFER, A. & XIAO, W. 2008b. Molecular subtypes of diffuse large B-cell lymphoma arise by distinct genetic pathways. *Proceedings of the National Academy of Sciences*, 105, 13520-13525.

- LEONE, A., FLATOW, U., KING, C. R., SANDEEN, M. A., MARGULIES, I. M., LIOTTA, L. A. & STEEG, P. S. 1991. Reduced tumor incidence, metastatic potential, and cytokine responsiveness of nm23-transfected melanoma cells. *Cell*, 65, 25-35.
- LI, Z.-M., HUANG, J.-J., XIA, Y., SUN, J., HUANG, Y., WANG, Y., ZHU, Y.-J., LI, Y.-J., ZHAO, W. & WEI, W.-X. 2012. Blood lymphocyte-to-monocyte ratio identifies high-risk patients in diffuse large B-cell lymphoma treated with R-CHOP. *PloS one*, 7, e41658.
- LILLY, A. J., KHANIM, F. L. & BUNCE, C. M. 2015. The case for extracellular Nm23-H1 as a driver of acute myeloid leukaemia (AML) progression. *Naunyn-Schmiedeberg's archives of pharmacology*, 388, 225-233.
- LILLY, A. J., KHANIM, F. L., HAYDEN, R. E., LUONG, Q. T., DRAYSON, M. T. & BUNCE, C. M. 2011. Nm23-h1 indirectly promotes the survival of acute myeloid leukemia blast cells by binding to more mature components of the leukemic clone. *Cancer research*, 71, 1177-1186.
- LOMBARDI, D., LACOMBE, M. L. & PAGGI, M. G. 2000. nm23: unraveling its biological function in cell differentiation. *Journal of cellular physiology*, 182, 144-149.
- MAAS, A. & HENDRIKS, R. W. 2001. Role of Bruton's tyrosine kinase in B cell development. *Clinical and Developmental Immunology*, 8, 171-181.
- MACDONALD, N., LA ROSA, D. & STEEG, P. 1995. The potential roles of nm23 in cancer metastasis and cellular differentiation. *European Journal of Cancer*, 31, 1096-1100.
- MACKAY, I., ROSEN, F. S., DELVES, P. & ROITT, I. 2000. The immune system. *N Engl J Med*, 343, 37-49.
- MARINO, N., NAKAYAMA, J., COLLINS, J. W. & STEEG, P. S. 2012. Insights into the biology and prevention of tumor metastasis provided by the Nm23 metastasis suppressor gene. *Cancer and Metastasis Reviews*, 31, 593-603.
- MARKET, E. & PAPAVALIOU, F. N. 2003. V (D) J recombination and the evolution of the adaptive immune system. *PLoS biology*, 1, e16.
- MARTINEZ, A., CARRERAS, J. & CAMPO, E. 2008. The follicular lymphoma microenvironment: from tumor cell to host immunity. *Current hematologic malignancy reports*, 3, 179.
- MICHLANE, J. F., VAN GENT, D. C., RAMSDEN, D. A., ROMEO, C., CUOMO, C. A., GELLERT, M. & OETTINGER, M. A. 1995. Cleavage at a V (D) J recombination signal requires only RAG1 and RAG2 proteins and occurs in two steps. *Cell*, 83, 387-395.
- MEI, Z., LIU, Y., LIU, C., CUI, A., LIANG, Z., WANG, G., PENG, H., CUI, L. & LI, C. 2014. Tumour-infiltrating inflammation and prognosis in colorectal cancer: systematic review and meta-analysis. *British journal of cancer*, 110, 1595.
- MESSINA, J., GILKESON, G. & PISETSKY, D. 1991. Stimulation of in vitro murine lymphocyte proliferation by bacterial DNA. *The Journal of Immunology*, 147, 1759-1764.
- MIN, K., SONG, H. K., CHANG, C., KIM, S. Y., LEE, K. J. & SUH, S. W. 2002. Crystal structure of human nucleoside diphosphate kinase A, a metastasis suppressor. *Proteins: Structure, Function, and Bioinformatics*, 46, 340-342.
- MUNHOZ, R. R. & POSTOW, M. A. 2016. Recent advances in understanding antitumor immunity. *F1000Research*, 5.
- MURPHY, K. M. 2012. Comprar Janeway's Immunobiology 8th Ed. | Kenneth M. Murphy | 9780815342434 | Garland Science. *Janeway's Immunobiology 8th Ed.*-9780815342434-6678000000, 00.
- NAČINOVIĆ-DULETIĆ, A., ŠTIFTER, S., DVORNIK, Š., ŠKUNCA, Ž. & JONJIĆ, N. 2008. Correlation of serum IL-6, IL-8 and IL-10 levels with clinicopathological features and prognosis in patients with diffuse large B-cell lymphoma. *International journal of laboratory hematology*, 30, 230-239.
- NESE, G., PALLI, D., PERNICE, L. M., SAEVA, C., PAGLIERANI, M., KRONING, K. C., CATARZI, S., RUBIO, C. A. & AMOROSI, A. 2001. Expression of nm23 gene in gastric cancer is associated with a poor 5-year survival. *Anticancer research*, 21, 3643-3649.

- NIITSU, N., HONMA, Y., IJIMA, K., TAKAGI, T., HIGASHIHARA, M., SAWADA, U. & OKABE-KADO, J. 2003a. Clinical significance of nm23-H1 proteins expressed on cell surface in non-Hodgkin's lymphoma. *Leukemia*, 17, 196-202.
- NIITSU, N., KOHURI, M., HIGASHIHARA, M. & BESSHO, M. 2006. Phase II study of the CPT-11, mitoxantrone and dexamethasone regimen in combination with rituximab in elderly patients with relapsed diffuse large B-cell lymphoma. *Cancer science*, 97, 933-937.
- NIITSU, N., NAKAMINE, H. & OKAMOTO, M. 2011a. Expression of nm23-H1 is associated with poor prognosis in peripheral T-cell lymphoma, not otherwise specified. *Clinical Cancer Research*, clincanres. 2999.2010.
- NIITSU, N., NAKAMINE, H., OKAMOTO, M., AKAMATSU, H., HIGASHIHARA, M., HONMA, Y., OKABE-KADO, J. & HIRANO, M. 2004. Clinical significance of intracytoplasmic nm23-H1 expression in diffuse large B-cell lymphoma. *Clin Cancer Res*, 10, 2482-90.
- NIITSU, N., NAKAMINE, H., OKAMOTO, M., AKAMATSU, H., HONMA, Y., HIGASHIHARA, M., OKABE-KADO, J., HIRANO, M. & ADULT LYMPHOMA TREATMENT STUDY GROUP, A. 2003b. Expression of nm23-H1 is associated with poor prognosis in peripheral T-cell lymphoma. *Br J Haematol*, 123, 621-30.
- NIITSU, N., OKABE-KADO, J., KASUKABE, T., YAMAMOTO-YAMAGUCHI, Y., UMEDA, M. & HONMA, Y. 1999. Prognostic implications of the differentiation inhibitory factor nm23-H1 protein in the plasma of aggressive non-Hodgkin's lymphoma. *Blood*, 94, 3541-50.
- NIITSU, N., OKABE-KADO, J., NAKAYAMA, M., WAKIMOTO, N., SAKASHITA, A., MASEKI, N., MOTOYOSHI, K., UMEDA, M. & HONMA, Y. 2000. Plasma levels of the differentiation inhibitory factor nm23-H1 protein and their clinical implications in acute myelogenous leukemia. *Blood*, 96, 1080-6.
- NIITSU, N., OKABE-KADO, J., OKAMOTO, M., TAKAGI, T., YOSHIDA, T., AOKI, S., HIRANO, M. & HONMA, Y. 2001a. Serum nm23-H1 protein as a prognostic factor in aggressive non-Hodgkin lymphoma. *Blood*, 97, 1202-10.
- NIITSU, N., OKAMOTO, M., HONMA, Y., NAKAMINE, H., TAMARU, J. I., NAKAMURA, S., YOSHINO, T., HIGASHIHARA, M., HIRANO, M., OKABE-KADO, J. & ADULT LYMPHOMA TREATMENT STUDY, G. 2003c. Serum levels of the nm23-H1 protein and their clinical implication in extranodal NK/T-cell lymphoma. *Leukemia*, 17, 987-90.
- NIITSU, N., OKAMOTO, M., OKABE-KADO, J., TAKAGI, T., YOSHIDA, T., AOKI, S., HONMA, Y. & HIRANO, M. 2001b. Serum nm23-H1 protein as a prognostic factor for indolent non-Hodgkin's lymphoma. *Leukemia*, 15, 832-9.
- NIITSU, N., TAMARU, J.-I., YOSHINO, T., NAKAMURA, N., NAKAMURA, S., OHSHIMA, K., NAKAMINE, H. & OKAMOTO, M. 2011b. A study on nm23-H1 expression in diffuse large B-cell lymphoma that was treated with CycLOBEAP plus rituximab therapy. *Annals of hematology*, 90, 185-192.
- NOGAI, H., DÖRKEN, B. & LENZ, G. 2011. Pathogenesis of non-Hodgkin's lymphoma. *Journal of clinical oncology*, 29, 1803-1811.
- NÜRNBERGER, T. & BRUNNER, F. 2002. Innate immunity in plants and animals: emerging parallels between the recognition of general elicitors and pathogen-associated molecular patterns. *Current opinion in plant biology*, 5, 318-324.
- OKABE-KADO, J. 2002. Serum nm23-H1 protein as a prognostic factor in hematological malignancies. *Leuk Lymphoma*, 43, 859-67.
- OKABE-KADO, J., KASUKABE, T. & HONMA, Y. 2002. Expression of cell surface NM23 proteins of human leukemia cell lines of various cellular lineage and differentiation stages. *Leuk Res*, 26, 569-76.
- OKABE-KADO, J., KASUKABE, T., HONMA, Y., HAYASHI, M., HENZEL, W. J. & HOZUMI, M. 1992. Identity of a differentiation inhibiting factor for mouse myeloid leukemia cells with NM23/nucleoside diphosphate kinase. *Biochemical and biophysical research communications*, 182, 987-994.

- OKABE-KADO, J., KASUKABE, T., HONMA, Y., KOBAYASHI, H., MASEKI, N. & KANEKO, Y. 2009a. Extracellular NM23-H1 protein inhibits the survival of primary cultured normal human peripheral blood mononuclear cells and activates the cytokine production. *Int J Hematol*, 90, 143-152.
- OKABE-KADO, J., KASUKABE, T., HONMA, Y., KOBAYASHI, H., MASEKI, N. & KANEKO, Y. 2009b. Extracellular NM23 protein promotes the growth and survival of primary cultured human acute myelogenous leukemia cells. *Cancer Sci*, 100, 1885-94.
- OKABE-KADO, J., KASUKABE, T. & KANEKO, Y. 2012. Extracellular NM23 Protein as a Therapeutic Target for Hematologic Malignancies. *Adv Hematol*, 2012, 879368.
- OKI, Y., YAMAMOTO, K., KATO, H., KUWATSUKA, Y., TAJI, H., KAGAMI, Y. & MORISHIMA, Y. 2008. Low absolute lymphocyte count is a poor prognostic marker in patients with diffuse large B-cell lymphoma and suggests patients' survival benefit from rituximab. *European journal of haematology*, 81, 448-453.
- OTT, G., ZIEPERT, M., KLAPPER, W., HORN, H., SZCZEPANOWSKI, M., BERND, H.-W., THORNS, C., FELLER, A. C., LENZE, D. & HUMMEL, M. 2010. Immunoblastic morphology but not the immunohistochemical GCB/non-GCB classifier predicts outcome in diffuse large B-cell lymphoma in the RICOVER-60 trial of the DSHNHL. *Blood*, blood-2010-03-276766.
- PASQUALUCCI, L., TRIFONOV, V., FABBRI, G., MA, J., ROSSI, D., CHIARENZA, A., WELLS, V. A., GRUNN, A., MESSINA, M. & ELLIOT, O. 2011. Analysis of the coding genome of diffuse large B-cell lymphoma. *Nature genetics*, 43, 830.
- PEDERSEN, L. M., JÜRGENSEN, G. W. & JOHNSEN, H. E. 2005. Serum levels of inflammatory cytokines at diagnosis correlate to the bcl-6 and CD10 defined germinal centre (GC) phenotype and bcl-2 expression in patients with diffuse large B-cell lymphoma. *British journal of haematology*, 128, 813-819.
- PERRY, A. M., CROCKETT, D., DAVE, B. J., ALTHOF, P., WINKLER, L., SMITH, L. M., AOUN, P., CHAN, W. C., FU, K. & GREINER, T. C. 2013. B-cell lymphoma, unclassifiable, with features intermediate between diffuse large B-cell lymphoma and burkitt lymphoma: study of 39 cases. *British journal of haematology*, 162, 40-49.
- PHIPPS-YONAS, H., CUI, H., SEBASTIAO, N., BRUNHOEBER, P. S., HADDOCK, E., DEYMIER, M. J., KLAPPER, W., LYBARGER, L., ROE, D. & HASTINGS, K. T. 2013. Low GILT expression is associated with poor patient survival in diffuse large B-cell lymphoma. *Frontiers in immunology*, 4, 425.
- POSTEL, E. H. 1998. NM23-NDP kinase. *The international journal of biochemistry & cell biology*, 30, 1291-1295.
- POSTEL, E. H. 2003. Multiple biochemical activities of NM23/NDP kinase in gene regulation. *Journal of bioenergetics and biomembranes*, 35, 31-40.
- POSTEL, E. H., ZOU, X., NOTTERMAN, D. A. & LA PERLE, K. M. 2009. Double knockout Nme1/Nme2 mouse model suggests a critical role for NDP kinases in erythroid development. *Molecular and cellular biochemistry*, 329, 45-50.
- QU, C., BRINCK-JENSEN, N.-S., ZANG, M. & CHEN, K. 2014. Monocyte-derived dendritic cells: targets as potent antigen-presenting cells for the design of vaccines against infectious diseases. *International Journal of Infectious Diseases*, 19, 1-5.
- RACHINEL, N. & SALLES, G. 2009. The host-tumor interface in B-cell non-Hodgkin lymphoma: a new world to investigate. *Current hematologic malignancy reports*, 4, 196-201.
- RAJEWSKY, K. 1996. Clonal selection and learning in the antibody system. *Nature*, 381, 751.
- RAN, F. A., HSU, P. D., WRIGHT, J., AGARWALA, V., SCOTT, D. A. & ZHANG, F. 2013. Genome engineering using the CRISPR-Cas9 system. *Nature protocols*, 8, 2281.
- RAO, M. R. M. & GOPAL, S. D. 2015. C-Reactive Protein-A critical Review. *Int. J. Curr. Microbiol. App. Sci*, 4, 55-61.

- RÉCHER, C., COIFFIER, B., HAIOUN, C., MOLINA, T. J., FERMÉ, C., CASASNOVAS, O., THIÉBLEMONT, C., BOSLY, A., LAURENT, G. & MORSCHHAUSER, F. 2011. Intensified chemotherapy with ACVBP plus rituximab versus standard CHOP plus rituximab for the treatment of diffuse large B-cell lymphoma (LNH03-2B): an open-label randomised phase 3 trial. *The Lancet*, 378, 1858-1867.
- REDMAN, M., KING, A., WATSON, C. & KING, D. 2016. What is CRISPR/Cas9? *Archives of Disease in Childhood-Education and Practice*, edpract-2016-310459.
- REECE, J. B., URRY, L. A., CAIN, M. L., WASSERMAN, S. A., MINORSKY, P. V. & JACKSON, R. B. 2011. *Campbell biology*, Pearson Boston.
- REYA, T., MORRISON, S. J., CLARKE, M. F. & WEISSMAN, I. L. 2001. Stem cells, cancer, and cancer stem cells. *nature*, 414, 105.
- RIMSZA, L. M., ROBERTS, R. A., MILLER, T. P., UNGER, J. M., LEBLANC, M., BRAZIEL, R. M., WEISENBERGER, D. D., CHAN, W. C., MULLER-HERMELINK, H. K. & JAFFE, E. S. 2004. Loss of MHC class II gene and protein expression in diffuse large B-cell lymphoma is related to decreased tumor immunosurveillance and poor patient survival regardless of other prognostic factors: a follow-up study from the Leukemia and Lymphoma Molecular Profiling Project. *Blood*, 103, 4251-4258.
- RODRIGUEZ-ABREU, D., BORDONI, A. & ZUCCA, E. 2007. Epidemiology of hematological malignancies. *Annals of oncology*, 18, i3-i8.
- ROSCHESKI, M., STAUDT, L. M. & WILSON, W. H. 2014. Diffuse large B-cell lymphoma—treatment approaches in the molecular era. *Nature reviews Clinical oncology*, 11, 12.
- ROSENWALD, A., WRIGHT, G., CHAN, W. C., CONNORS, J. M., CAMPO, E., FISHER, R. I., GASCOYNE, R. D., MULLER-HERMELINK, H. K., SMELAND, E. B. & GILTNANE, J. M. 2002. The use of molecular profiling to predict survival after chemotherapy for diffuse large-B-cell lymphoma. *New England Journal of Medicine*, 346, 1937-1947.
- RUMJAHN, S., JAVED, M., WONG, N., LAW, W. & BUXTON, I. 2007. Purinergic regulation of angiogenesis by human breast carcinoma-secreted nucleoside diphosphate kinase. *British Journal of Cancer*, 97, 1372.
- SALVESEN, H. B. & AKSLEN, L. A. 1999. Significance of tumour-associated macrophages, vascular endothelial growth factor and thrombospondin-1 expression for tumour angiogenesis and prognosis in endometrial carcinomas. *International journal of cancer*, 84, 538-543.
- SAVAGE, K. J., JOHNSON, N. A., BEN-NERIAH, S., CONNORS, J. M., SEHN, L. H., FARINHA, P., HORSMAN, D. E. & GASCOYNE, R. D. 2009. MYC gene rearrangements are associated with a poor prognosis in diffuse large B-cell lymphoma patients treated with R-CHOP chemotherapy. *Blood*, 114, 3533-3537.
- SAVAGE, K. J., MONTI, S., KUTOK, J. L., CATTORETTI, G., NEUBERG, D., DE LEVAL, L., KURTIN, P., DAL CIN, P., LADD, C. & FEUERHAKE, F. 2003. The molecular signature of mediastinal large B-cell lymphoma differs from that of other diffuse large B-cell lymphomas and shares features with classical Hodgkin lymphoma. *Blood*, 102, 3871-3879.
- SCHMITT, T. M. & ZÚÑIGA-PFLÜCKER, J. C. 2002. Induction of T cell development from hematopoietic progenitor cells by delta-like-1 in vitro. *Immunity*, 17, 749-756.
- SEHN, L. H. & GASCOYNE, R. D. 2015. Diffuse large B-cell lymphoma: optimizing outcome in the context of clinical and biologic heterogeneity. *Blood*, 125, 22-32.
- SEO, A., LEE, H., KIM, E., KIM, H., JANG, M., LEE, H., KIM, Y., KIM, J. & PARK, S. 2013. Tumour-infiltrating CD8+ lymphocytes as an independent predictive factor for pathological complete response to primary systemic therapy in breast cancer. *British journal of cancer*, 109, 2705.
- SHANKLAND, K. R., ARMITAGE, J. O. & HANCOCK, B. W. 2012. Non-hodgkin lymphoma. *The Lancet*, 380, 848-857.
- SIEGEL, R. L., MILLER, K. D. & JEMAL, A. 2017. Cancer statistics, 2017. *CA: a cancer journal for clinicians*, 67, 7-30.



- STAHL, J. A., LEONE, A., ROSENGARD, A. M., PORTER, L., KING, C. R. & STEEG, P. S. 1991. Identification of a second human nm23 gene, nm23-H2. *Cancer research*, 51, 445-449.
- STARR, T. K., JAMESON, S. C. & HOGQUIST, K. A. 2003. Positive and negative selection of T cells. *Annual review of immunology*, 21, 139-176.
- STEEG, P. S., BEVILACQUA, G., KOPPER, L., THORGEIRSSON, U. P., TALMADGE, J. E., LIOTTA, L. A. & SOBEL, M. E. 1988. Evidence for a novel gene associated with low tumor metastatic potential. *JNCI: Journal of the National Cancer Institute*, 80, 200-204.
- STEEG, P. S., ZOLLO, M. & WIELAND, T. 2011. A critical evaluation of biochemical activities reported for the nucleoside diphosphate kinase/Nm23/Awd family proteins: opportunities and missteps in understanding their biological functions. Springer.
- SWERDLOW, S. H., CAMPO, E., PILERI, S. A., HARRIS, N. L., STEIN, H., SIEBERT, R., ADVANI, R., GHIELMINI, M., SALLES, G. A. & ZELENETZ, A. D. 2016. The 2016 revision of the World Health Organization (WHO) classification of lymphoid neoplasms. *Blood*, blood-2016-01-643569.
- TAI, W., CHUNG, J., TANG, P., KOO, Y., HOU, X., TAY, K., QUEK, R., TAO, M. & LIM, S. 2011. Central nervous system (CNS) relapse in diffuse large B cell lymphoma (DLBCL): pre-and post-rituximab. *Annals of hematology*, 90, 809-818.
- THAKUR, R. K., KUMAR, P., HALDER, K., VERMA, A., KAR, A., PARENT, J.-L., BASUNDR, R., KUMAR, A. & CHOWDHURY, S. 2008. Metastases suppressor NM23-H2 interaction with G-quadruplex DNA within c-MYC promoter nuclease hypersensitive element induces c-MYC expression. *Nucleic acids research*, 37, 172-183.
- THIEBLEMONT, C., DELFAU-LARUE, M.-H. & COIFFIER, B. 2012. Lenalidomide in diffuse large B-cell lymphoma. *Advances in hematology*, 2012.
- THOMAS, R. K., RE, D., WOLF, J. & DIEHL, V. 2004. Part I: Hodgkin's lymphoma—molecular biology of Hodgkin and Reed-Sternberg cells. *The lancet oncology*, 5, 11-18.
- TIMMONS, L. & SHEARN, A. 1997. 6. prune/Killar of prune: A Conditional Dominant Lethal Interaction in Drosophila. *Advances in genetics*. Elsevier.
- TOPALIAN, S. L., HODI, F. S., BRAHMER, J. R., GETTINGER, S. N., SMITH, D. C., MCDERMOTT, D. F., POWDERLY, J. D., CARVAJAL, R. D., SOSMAN, J. A. & ATKINS, M. B. 2012. Safety, activity, and immune correlates of anti-PD-1 antibody in cancer. *New England Journal of Medicine*, 366, 2443-2454.
- TORTORA, G. J. & NIELSEN, M. T. 1992. *Principles of human anatomy*, HarperCollins.
- TOWNSEND, W. & LINCH, D. 2012. Hodgkin's lymphoma in adults. *The Lancet*, 380, 836-847.
- TSANG, R. W. & GOSPODAROWICZ, M. K. Low-grade non-hodgkin lymphomas. *Seminars in radiation oncology*, 2007. Elsevier, 198-205.
- URA, H., DENNO, R. & HIRATA, K. 1996. The significance of nm23 protein expression in human gastric carcinomas. *Surgery today*, 26, 957-965.
- VELUTHAKAL, R., SURESH, M. V. & KOWLURU, A. 2009. Down-regulation of expression and function of nucleoside diphosphate kinase in insulin-secreting  $\beta$ -cells under in vitro conditions of glucolipotoxicity. *Molecular and cellular biochemistry*, 329, 121-129.
- VÉRON, M., TEPPER, A., HILDEBRANDT, M., LASCU, I., LACOMBE, M.-L., JANIN, J., MORÉRA, S., CHERFILS, J., DUMAS, C. & CHIADMI, M. 1995. Nucleoside diphosphate kinase: an old enzyme with new functions? *Purine and Pyrimidine Metabolism in Man VIII*. Springer.
- VOSS, J. J., FORD, C. A., PETROVA, S., MELVILLE, L., PATERSON, M., POUND, J. D., HOLLAND, P., GIOTTI, B., FREEMAN, T. C. & GREGORY, C. D. 2017. Modulation of macrophage antitumor potential by apoptotic lymphoma cells. *Cell death and differentiation*, 24, 971.
- WANG, M., ZHAO, J., ZHANG, L., WEI, F., LIAN, Y., WU, Y., GONG, Z., ZHANG, S., ZHOU, J. & CAO, K. 2017a. Role of tumor microenvironment in tumorigenesis. *Journal of Cancer*, 8, 761.
- WANG, Y.-Q., HUANG, Z.-L., CHEN, S.-B., WANG, C.-X., SHAN, C., YIN, Q.-K., OU, T.-M., LI, D., GU, L.-Q. & TAN, J.-H. 2017b. Design, synthesis, and evaluation of new selective NM23-H2 binders as c-

- MYC transcription inhibitors via disruption of the NM23-H2/G-quadruplex interaction. *Journal of medicinal chemistry*, 60, 6924-6941.
- WESTIN, J. R., CHU, F., ZHANG, M., FAYAD, L. E., KWAK, L. W., FOWLER, N., ROMAGUERA, J., HAGEMEISTER, F., FANALE, M. & SAMANIEGO, F. 2014. Safety and activity of PD1 blockade by pidilizumab in combination with rituximab in patients with relapsed follicular lymphoma: a single group, open-label, phase 2 trial. *The lancet oncology*, 15, 69-77.
- WILCOX, R., RISTOW, K., HABERMANN, T., INWARDS, D., MICALLEF, I., JOHNSTON, P., COLGAN, J., NOWAKOWSKI, G., ANSELL, S. & WITZIG, T. 2011. The absolute monocyte and lymphocyte prognostic score predicts survival and identifies high-risk patients in diffuse large-B-cell lymphoma. *Leukemia*, 25, 1502.
- WILKINSON, R. W., ANDERSON, G., OWEN, J. & JENKINSON, E. J. 1995. Positive selection of thymocytes involves sustained interactions with the thymic microenvironment. *The Journal of Immunology*, 155, 5234-5240.
- WILLEMS, R., HENCKAERTS, E., LENJOU, M., NIJS, G., RODRIGUS, I., MOULIJN, A., SLEGGERS, H., BERNEMAN, Z. & VAN BOCKSTAELE, D. 2001. Establishment of serum-free pre-colony forming unit assays for differentiation of primitive hematopoietic progenitors: serum induces early macrophage differentiation and inhibits early erythroid differentiation of CD34++ CD38-cells. *Annals of hematology*, 80, 17-25.
- WILLEMS, R., SLEGGERS, H., RODRIGUS, I., MOULIJN, A. C., LENJOU, M., NIJS, G., BERNEMAN, Z. N. & VAN BOCKSTAELE, D. R. 2002. Extracellular nucleoside diphosphate kinase NM23/NDPK modulates normal hematopoietic differentiation. *Experimental hematology*, 30, 640-648.
- WILLEMS, R., VAN BOCKSTAELE, D. R., LARDON, F., LENJOU, M., NIJS, G., SNOECK, H.-W., BERNEMAN, Z. N. & SLEGGERS, H. 1998. Decrease in nucleoside diphosphate kinase (NDPK/nm23) expression during hematopoietic maturation. *Journal of Biological Chemistry*, 273, 13663-13668.
- XU, J., LIU, L. Z., DENG, X. F., TIMMONS, L., HERSPERGER, E., STEEG, P. S., VERON, M. & SHEARN, A. 1996. The Enzymatic Activity of Drosophila AWD/NDP Kinase Is Necessary but Not Sufficient for Its Biological Function. *Developmental biology*, 177, 544-557.
- XU, Y., KROFT, S. H., MCKENNA, R. W. & AQUINO, D. B. 2001. Prognostic significance of tumour-infiltrating T lymphocytes and T-cell subsets in de novo diffuse large B-cell lymphoma: a multiparameter flow cytometry study. *British journal of haematology*, 112, 945-949.
- YAMAGUCHI, M., NAKAMURA, N., SUZUKI, R., KAGAMI, Y., OKAMOTO, M., ICHINOHASAMA, R., YOSHINO, T., SUZUMIYA, J., MURASE, T. & MIURA, I. 2008. De novo CD5+ diffuse large B-cell lymphoma: results of a detailed clinicopathological review in 120 patients. *Haematologica*, 93, 1195-1202.
- YANG, Z.-Z., NOVAK, A. J., STENSON, M. J., WITZIG, T. E. & ANSELL, S. M. 2006. Intratumoral CD4+ CD25+ regulatory T-cell-mediated suppression of infiltrating CD4+ T cells in B-cell non-Hodgkin lymphoma. *Blood*, 107, 3639-3646.
- YOKOYAMA, A., OKABE-KADO, J., WAKIMOTO, N., KOBAYASHI, H., SAKASHITA, A., MASEKI, N., NAKAMAKI, T., HINO, K., TOMOYASU, S., TSURUOKA, N., MOTOYOSHI, K., NAGATA, N. & HONMA, Y. 1998. Evaluation by multivariate analysis of the differentiation inhibitory factor nm23 as a prognostic factor in acute myelogenous leukemia and application to other hematologic malignancies. *Blood*, 91, 1845-51.
- YUAN, Y., JIANG, Y.-C., SUN, C.-K. & CHEN, Q.-M. 2016. Role of the tumor microenvironment in tumor progression and the clinical applications. *Oncology reports*, 35, 2499-2515.
- ZHANG, Q., MCCORKLE, J. R., NOVAK, M., YANG, M. & KAETZEL, D. M. 2011. Metastasis suppressor function of NM23-H1 requires its 3'-5' exonuclease activity. *International journal of cancer*, 128, 40-50.

- ZHANG, Z., BULUR, P. A., DOGAN, A., GASTINEAU, D. A., DIETZ, A. B. & LIN, Y. 2015. Immune independent crosstalk between lymphoma and myeloid suppressor CD14<sup>+</sup> HLA-DR<sup>low</sup>/neg monocytes mediates chemotherapy resistance. *Oncoimmunology*, 4, e996470.
- ZOU, M., SHI, Y., AL-SEDAIRY, S. & FARID, N. 1993. High levels of Nm23 gene expression in advanced stage of thyroid carcinomas. *British journal of cancer*, 68, 385.

## **Appendix A: Recipes and buffers**

### **A.1. Agarose gel electrophoresis**

#### **1×TBE buffer**

- Dissolve 10.8g Tris and 5.5g Boric acid in 4ml 5M EDTA pH8.
- Make up the volume to 1 litre with dH<sub>2</sub>O.

#### **1% agarose gel**

- Mix 1g of agarose powder in 100ml 1×TBE buffer
- Heat in a microwave to dissolve completely
- When cooled add 3µl ethidium bromide.

### **A.2. Protein extraction**

#### **Ripa buffer**

- 1ml of NP40 (IGEPAL)
- 0.5g sodium deoxycholate
- 1ml 10% SDS
- Then make up the volume to 100ml with dH<sub>2</sub>O.

### **A.3. Western blotting**

#### **10×SDS running buffer**

- 30g Tris (250mM)
- 144g glycine (1.92M)
- 10g SDS (1%)
- Then make up the volume to 1 litre with dH<sub>2</sub>O.
- Diluted 1:10 to make 1x SDS Running Buffer

#### **4× SDS gel loading buffer**

- 2.0mL 1M Tris-HCl, pH 6.8
- 0.8g SDS
- 4.0mL 100% glycerol
- 0.4mL 14.7M β-mercaptoethanol
- 1.0mL 0.5M EDTA
- 8.0mg bromophenol blue
- 2.6mL dH<sub>2</sub>O

- Diluted 1:4 to make 1x SDS gel loading buffer.

### **1.5M Tris (pH 8.8)**

- Dissolve 90.8g Tris in 400ml dH<sub>2</sub>O and adjust pH to 8.8
- Make up to 500ml in dH<sub>2</sub>O
- 0.5M Tris (pH 6.8)
- Dissolve 30.3g Tris in 400ml dH<sub>2</sub>O and adjust pH to 6.8
- Make up to 500ml with dH<sub>2</sub>O

### **Transfer Buffer**

- Dissolve 7.575g Tris and 36g glycine in 500ml methanol
- Make up the volume to 2.5 litres with dH<sub>2</sub>O

### **TBTS-T**

- Dissolve 16g NaCl and 2ml Tween 20 in 40ml 1M Tris HCL pH7.6
- Make up the volume to 2 litres with dH<sub>2</sub>O

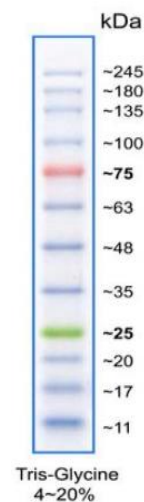
### **TBS**

- Add:20mM Tris HCl, pH 7.5
- 0.8% w/v NaCl
- Make up the volume to 1L with dH<sub>2</sub>O

### **BLUeye Prestained Protein Ladder (Geneflow Ltd)**

A three-colour protein molecular weight standard with

12 pre-stained proteins covering molecular weights 10 - 245 kDa



### Stacking and resolving gel mixes

Ingredients	Stacking	Resolving			
		7.5%	10%	12.5%	15%
dH <sub>2</sub> O	2.03ml	5ml	4.1ml	3.2ml	2.4ml
Acrylamide	440µl	2.5ml	3.3ml	4.2ml	5ml
1.5M Tris pH8.8	-	2.5ml	2.5ml	2.5ml	2.5ml
0.5M Tris pH6.8	830µl	-	-	-	-
10% SDS	33µl	100µl	100µl	100µl	100µl
10% Ammonium Persulphate	16.7µl	50µl	50µl	50µl	50µl
TEMED	1.7µl	3.3µl	3.3µl	3.3µl	3.3µl

### **A.3. Bacterial work**

#### L-broth

- 10g L-Broth (Sigma) dissolved in 500mL dH<sub>2</sub>O and autoclave sterilised
- Supplemented with 100µg/mL ampicillin

#### L-broth agar

- L-broth recipe + 15g/L agar (1.5% w/v)

#### His-Bind® Resin Chromatography Kit (Novagen) Buffers

- 1x Charge Buffer: 50mM NiSO<sub>4</sub>
- 1x Binding Buffer: 0.5M NaCl, 20mM Tris-HCl, 5mM imidazole, pH 7.9
- 1x Wash Buffer: 0.5M NaCl, 60mM imidazole, 20mM Tris-HCl, pH 7.9
- 1x Elute Buffer: 1M imidazole, 0.5M NaCl, 20mM Tris-HCl, pH 7.9
- 1x Strip Buffer: 0.5M NaCl, 100mM EDTA, 20mM Tris-HCl, pH 7.9

#### **A.4. Coomassie staining**

##### **Coomassie Blue Stain Solution**

- 50% v/v methanol
- 10% v/v acetic acid
- 0.05% w/v Coomassie Brilliant Blue stain.
- Made up to 500mL with dH<sub>2</sub>O.

##### **Destain Solution**

- 7% acetic acid
- 5% methanol
- Made up to 1L with dH<sub>2</sub>O.

#### **A.5. Flow cytometry and cell sorting**

##### **FACS Fix**

- 1% formaldehyde
- 2% FBS
- Made up to volume in PBS (Sigma) without calcium chloride and magnesium chloride.

##### **MACS buffer**

PBS with the addition of 2mM EDTA and 1% FBS

## Appendix B: Supplementary figures

### B.1

DLBCL cells were plated at either  $5 \times 10^3$ ,  $1 \times 10^4$  or  $2 \times 10^4$  cells per well in 200 $\mu$ l in 96 well plates, incubated for 72 hours and CellTiter-Blue<sup>®</sup> Reagent was added and cells were incubated for 3 hour before recording fluorescence (560Ex/590Em) a using a FLUO star Omega plate reader. The optimal cell density was determined to be  $5 \times 10^3$  cells/well since the cells were still actively growing and the wells were not confluent.

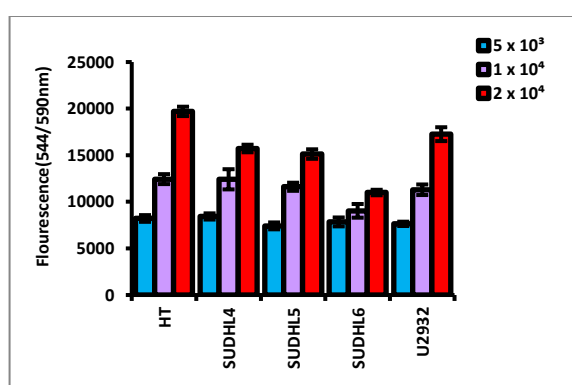


*Figure B.1 Cell density optimising. Cells were plated at 200 $\mu$ l/well with 3 different cell densities,  $5 \times 10^3$ ,  $1 \times 10^4$  and  $2 \times 10^4$  in a 96-well plate and cultured for 72 hours at 37°C. CellTiter-Blue<sup>®</sup> Reagent (10 $\mu$ l/well) was added and cells were incubated for 3 hour before recording fluorescence (560Ex/590Em) using a FLUO star Omega plate reader. Data shown is average geometric mean  $\pm$  SEM of N= 4 replicates.*



## B.2A

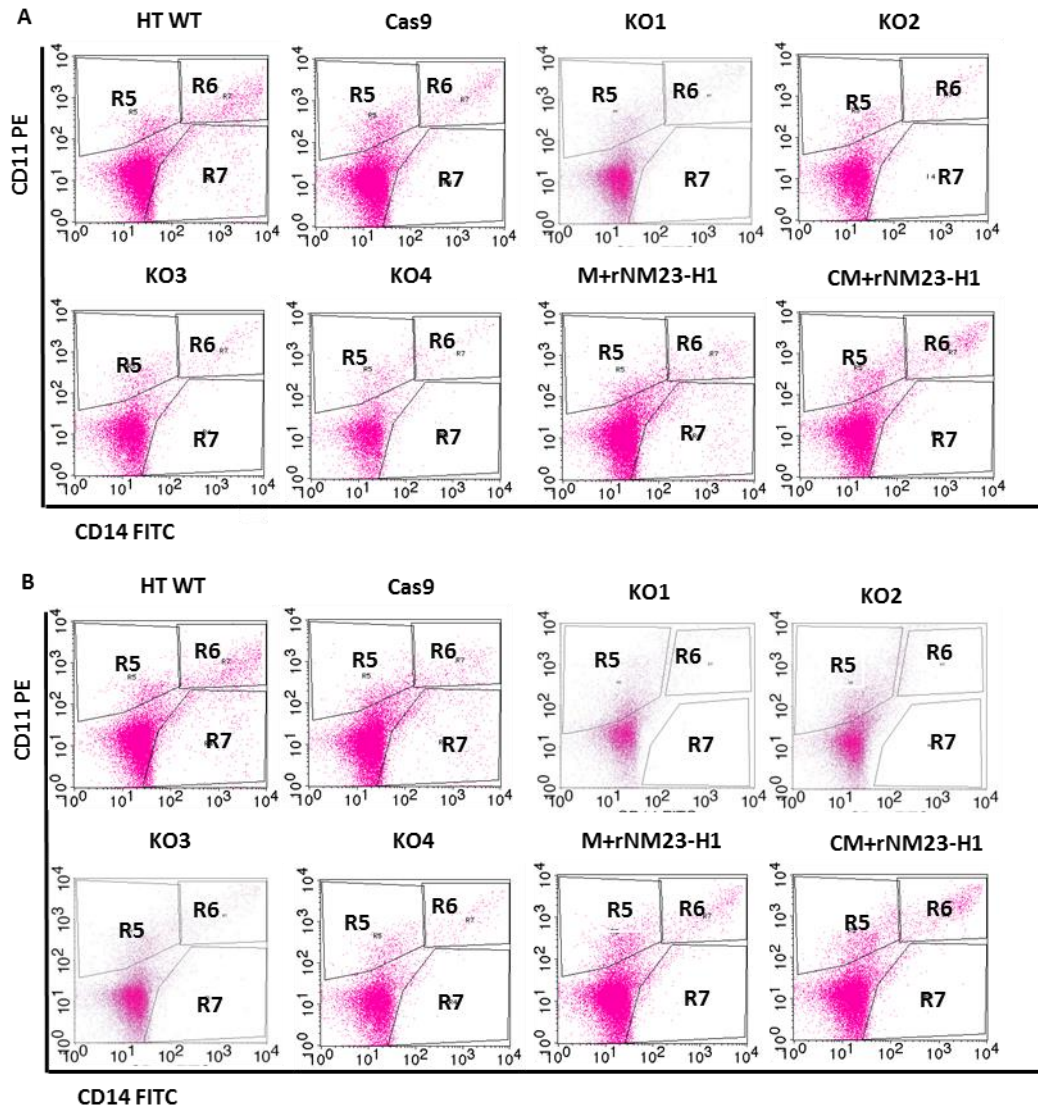


**Figure B.2A Response of CD14<sup>+</sup> monocytes to extracellular NM23-H1 and exogenous rNM23-H1.** PBMCs were purified using density centrifugation and seeded at  $0.5 \times 10^6$  cells/ml in conditioned medium from HT WT, HT Cas9, NM23-KO clones, RPMI 1640 FBS+ media plus  $2 \mu\text{g/ml}$  exogenous rNM23-H1 or WT HT conditioned media plus  $2 \mu\text{g/ml}$  exogenous rNM23-H1. Cells were harvested at day 6 and stained with anti-CD14 FITC and anti-CD11b PE antibodies before analysis by flow cytometry. (A) Representative CD14/CD11b dot plots from ND2 show CD11b<sup>+</sup> cells (R5). CD14<sup>+</sup> cells (R7). CD14<sup>+</sup> CD11b<sup>+</sup> (R6). (B) Representative CD14/CD11b dot plots from ND3 show CD11b<sup>+</sup> cells (R5). CD14<sup>+</sup> cells (R7). CD14<sup>+</sup> CD11b<sup>+</sup> (R6).

## B.2B

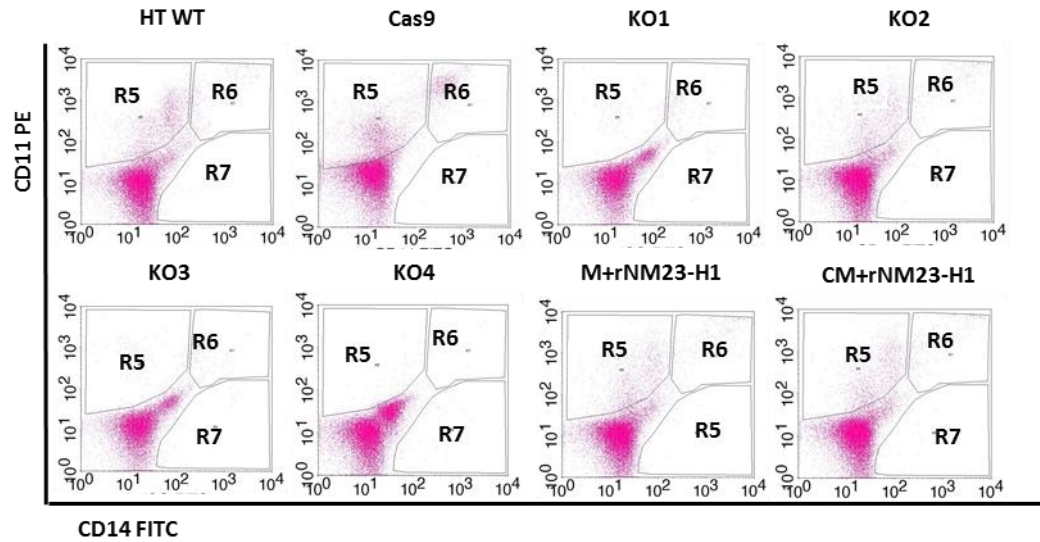


**Figure B.2B Response of CD14<sup>+</sup> monocytes to extracellular NM23-H1 and exogenous rNM23-H1.**

PBMCs were purified using density centrifugation and seeded at  $0.5 \times 10^6$  cells/ml in conditioned medium from HT WT, HT Cas9, NM23-KO clones, RPMI 1640 FBS+ media plus  $2 \mu\text{g/ml}$  exogenous rNM23-H1 or WT HT conditioned media plus  $2 \mu\text{g/ml}$  exogenous rNM23-H1. Cells were harvested at day 6 and stained with anti-CD14 FITC and anti-CD11b PE antibodies before analysis by flow cytometry. Representative CD14/CD11b dot plots from ND2 show CD11b<sup>+</sup> cells (R5). CD14<sup>+</sup> cells (R7). CD14<sup>+</sup> CD11b<sup>+</sup> (R6).

### B.3

Non-classical CD14+CD16++	Intermediate CD14++CD16+
CD14 -CD16 -	Classical CD14++CD16-

**Figure B.3** Gating profile for monocyte subsets based on CD14 and CD16 relative expression. Flow cytometry show the gating strategy of the classical, intermediate and non-classical monocyte subsets. Classical monocytes express high levels of CD14 but no CD16, intermediate monocytes express high levels of CD14 and low CD16, and non-classical monocytes express low CD14 but high CD16.

#### B.4

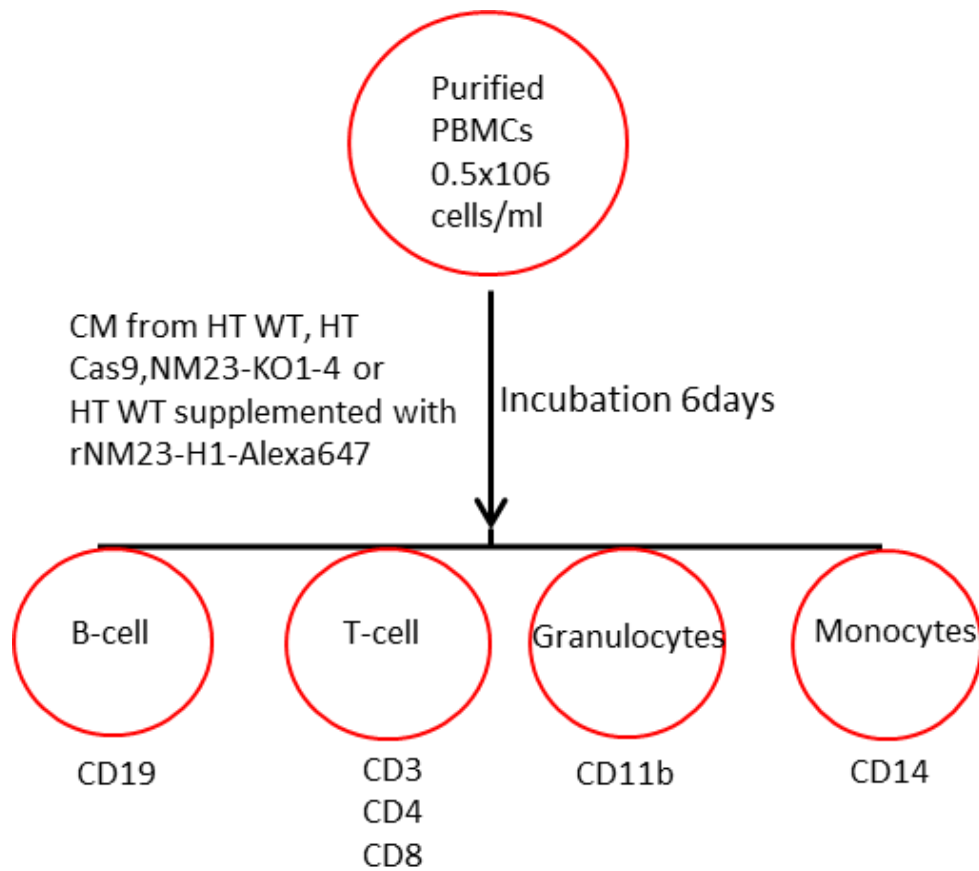


**Figure B.4 Characterising viable PBMCs sup-populations by Immunophenotyping.** Density centrifugation was used to purify PBMCs, cells were cultured at  $0.5 \times 10^6$  cells/ml and treated with conditioned medium of HT WT, HT Cas9,NM23-KO clones, RPMI 1640 FBS+ media plus (2 $\mu$ g/ml) exogenous rNM23-H1 or conditioned media of WT HT plus (2 $\mu$ g/mL) exogenous rNM23-H1 for 6 days. PBMCs cells were harvested at day 6 and stained with anti-CD19 APC, antiCD3-PE, anti-CD4 APC, anti-CD8 FITC, anti-CD14 FITC and anti-CD11b PE antibodies before analysis by flow cytometry.

## **Appendix C: Publications**

- Diffuse Large B Cell Lymphoma (DLBCL)-released NM23-H1 promotes monocyte survival and inflammatory cytokine release (manuscript submitted).